Role of the ribosomal protein RACK1 in translation regulation

Evelyne Einhorn

UNIVERSITÉ DE STRASBOURG

ÉCOLE DOCTORALE DES SCIENCES DE LA VIE ET DE LA SANTÉ

UPR9022 – Modèles insectes d'immunité innée

THÈSE présentée par :

Evelyne EINHORN

soutenue le : **18 juin 2019**

pour obtenir le grade de : **Docteur de l'université de Strasbourg**

Discipline/ Spécialité : Aspects moléculaires et cellulaires de la biologie

Rôle de la protéine ribosomale RACK1 dans la régulation de la traduction

THÈSE dirigée par :

Pr. Jean-Luc IMLER — Professeur des Universités, Institut de biologie moléculaire et cellulaire, université de Strasbourg, France.

RAPPORTEURS :

Pr. Zoya IGNATOVA — Professeur des Universités, Institut de biochimie et de biologie moléculaire, université de Hambourg, Allemagne.

Pr. Nicola GRAY — Professeur des Universités, Centre MRC pour la santé reproductive, université d'Edimbourg, Royaume-Uni.

AUTRES MEMBRES DU JURY :

Pr. Serge POTIER — Professeur des Universités, Génétique moléculaire, Génomique, Microbiologie, université de Strasbourg, France.

Pr. Carine MEIGNIN — Professeur des Universités, Institut de biologie moléculaire et cellulaire, université de Strasbourg, France.

Dr. Rénald DELANOUE — Chargé de Recherche, Institut de biologie Valrose, université de Nice Sophia Antipolis, France.

Acknowledgements

This PhD has been a great experience and it would not have been achieved without the support and guidance I received from many people.

First, I would like to express my sincere gratitude to my PhD advisors, Jean-Luc Imler and Carine Meignin. You gave me an opportunity to join the lab first as a Master student, and later as a PhD student. You supported me all along those years and I learned a lot at your side, both scientifically and personally. I would also like to mention the tremendous contribution of Franck Martin to my thesis work. I thank you for all the discussions we had and the valued advices you gave me.

I am deeply thankful to my PhD committee members, Pr. Zoya Ignatova, Pr. Nicola Gray, Dr. Rénald Delanoue and Pr. Serge Potier, who accepted to come to Strasbourg and judge my work. I also thank Dr. Andrea Pauli for the insightful discussions we had during my mid-thesis committee.

As science is not a lonely path, I acknowledge the participation of many persons to the projects: Estelle Santiago for the experimental (and personal) help, Timothée Vincent for the bioinformatics analysis, Laurent Troxler for the help on R scripts and Emilie Lauret for continuing parts of the work. All the people from the IBMC proteomic platform were also always very helpful and considerate. Moreover, I am grateful to Karim Majzoub who initiated the RACK1 project, and Lauriane Gross, with whom I collaborated during these years.

I would like to thank the interns for their contribution to the project: ZaÏane, Romane, Marie, Emmanuel and Matthieu. It was a great pleasure for me to supervise your first weeks as researchers. I also very much enjoyed guiding young students, Livia, Noémie, Jasmin and Amélie, through their discovery of the laboratory life.

I extend my sincere gratitude to my present and former labmates: Steffi for making time fly in the fly room, Laurent and Estelle for their continuous support, Alexandre for his precious help, Nathalie for her great kindness, Assel for her thoughtfulness, all the girls from the office for supporting me during the writing of the manuscript, as well as Loïc, Aurélie, Hua, Shree, Ludivine, Matthieu, Vincent and Samuel for discussions.

Last but not least, words cannot express how grateful I am to my friends and family, for their understanding and continuous support. You are all very dear to me and I feel lucky to be surrounded by such great persons.

Abbreviations

2'O-Me: 2'-O Methylation
4E-BP: eukaryotic initiation factor 4E binding protein
Ago2: Argonaute 2
AMP: anti-microbial peptide
AMPK: Adenosine mono phosphate-activated protein kinase
ARCA: Anti-reverse cap analogue
ATF4: Activating Transcription factor 4
ATF6: Activating Transcription factor 6
Att: Attacin
Bcl-2: B-cell lymphoma 2
BiP: Binding immunoglobulin protein
Cat: Catalase
CDK1: Cyclin-dependent kinase 1
cDNA: complementary desoxyribonucleic acid
Cec: Cecropin
CHOP: C/EBP homologous protein
CHOP: CCAAT-enhancer-binding proteins homologous protein
CReP: Constitutive repressor of eukaryotic initiation factor 2α phosphorylation
CRISPR/Cas9: Clustered Regularly Interspaced Short Palindromic Repeats /CRISPR associated 9
CrPV: Cricket paralysis virus
Cyp18a1: Cytochrome P450-18a1
DAA: direct-acting antivirals
DBA: Diamond Blackfan anemia
Dcr-2: Dicer-2
DENV: Dengue virus
Dpt: Diptericin
dsRNA: double stranded ribonucleic acid
DTT: Dithiothreitol
E. coli: Escherichia coli
eIF: eukaryotic initiation factor
EMCV: encephalomyocarditis virus
ER: Endoplasmic Reticulum
ERAD: Endoplasmic reticulum-associated protein degradation
FGF1: Fibroblast growth factor 1
FHV: Flock House virus
GADD34: growth arrest and DNA damage-inducible protein 34
GAIT: Interferon-γ-Activated Inhibitor of Translation
GAPDH: Glyceraldehyde-3-phosphate dehydrogenase
GCN2: General Control non-derepressible 2
GDP: guanosine diphosphate
GO: Gene ontology
GTP: guanosine tri-phosphate
H_2O_2: hydrogen peroxide
HCC: Hepatocellular carcinoma
HCV: hepatitis C virus
HEK293T: human embryonic kidney 293T
HIV: Human immunodeficiency virus
HRI: Heme-regulated eIF2α kinase
HSV-1: Herpes simplex virus 1
HTA: host-targeted antivirals
IFN: interferon
IGF-1R: insulin-like growth factor 1 receptor
IGR: intergenic
IKK: IκB kinase
IL: Interleukin
IMD: immune deficiency
IMDM: Iscove's Modified Dulbecco's Media
Ird5: Immune response-deficient 5
IRE1: inositol requiring enzyme 1
IRES: internal ribosome entry sites
IRF-7: Interferon regulatory factor 7
ISG15: Interferon stimulated gene 15
ISR: integrated stress response
ISRIB: Integrated stress response inhibitor
ITAF: Internal ribosome entry site trans-acting factors
K63: Lysine 63
KD: knock down
KO: knock out
KSHV: Kaposi's sarcoma-associated herpesvirus
Ksp1: Kinase Suppressing Prp20-10
LRRK2: leucine-rich repeat kinase 2
m^6A: N6 methyladenosine

MAPK: Mitogen-activated protein kinase
MDM2: murine double minute 2
MERS-CoV: Middle East Respiratory Syndrome Coronavirus
mESC: mouse embryonic stem cells
Met-tRNAi: initiator methionyl transfer RNA
Mnk: Mitogen-activated protein kinase interacting kinase
mRNA: messenger ribonucleic acid
mRNP: messenger ribonucleoprotein
Mtk: Metchnikovin
mTOR: mechanistic target of rapamycin
nc-RNA: non-coding ribonucleic acid
NF-κB: nuclear factor-kappa B
O-GlcNAc*: O*-linked β-d-N-acetylglucosamine
PABP: polyA binding protein
PCA: Principal component analysis
PCR: polymerase chain reaction
PD: Parkinson's disease
PERK: double-stranded RNA-activated protein kinase–like ER kinase
PGRP-SB1: Peptidoglycan recognition protein SB1
PIC: pre-initiation complex
Pirk: Poor imd response upon knock-in
PKC: protein kinase C
PKR: double-stranded RNA-activated protein kinase
polyA: polyadenylated
PP1C: protein phosphatase 1 catalytic subunit
PTM: post-translational modification
PV: poliovirus
RACK1: Receptor for activated protein C kinase 1
RANTES: Regulated upon Activation, Normal T cell Expressed, and Secreted
Rel: Relish
RIG-I: retinoic acid-inducible gene I
RNAi: Ribonucleic acid interference
RP: ribosomal protein
RpL: Ribosomal protein of the large subunit
RpS: Ribosomal protein of the small subunit
RpS6: Ribosomal protein S6
rRNA: ribosomal RNAs
RT-qPCR: Reverse transcription followed by quantitative polymerase chain reaction
S. cerevisiae*: Saccharomyces cerevisiae*
S. pombe*: Schizosaccharomyces pombe*
S2: Schneider 2
S6K1: p70S6 kinase
Ser/Thr: Serine/Threonine
sgRNA: Single guide ribonucleic acid
shRNA: small hairpin ribonucleic acid
snoRNA: small nucleolar ribonucleic acid
TC: ternary complex
TF: Transcription factor
TNF-R: tumor necrosis factor receptor
TNF: tumor necrosis factor
TRAF6: Tumor necrosis factor associated factor 6
TRiP: Transgenic RNAi Project
tRNA: transfer ribonucleic acid
Trx-1: Thioredoxin reductase 1
UAS: Upstream activating sequence
uORF: upstream open reading frame
UPR: Unfolded Protein Response
UTR: untranslated region
VacV: Vaccinia virus
VISA: Virus-induced signaling adapter
VSV: Vesicular stomatitis virus
WD: tryptophane and aspartic acid
WNV: West Nile Virus
WT: wild-type
X-DC: X-linked Dyskeratosis Congenita
XBP-1: X-box binding protein 1
ZIKV: Zika virus

Table of contents

INTRODUCTION

I. Cellular adaptation through gene expression

A. The cellular response to stress

1. Towards a definition of stress

The concept of stress emerged from studies of famous scientists, who have shaped the way we understand biology today (inspired from Goldstein and Kopin, 2007; Szabo et al., 2012). In 1865, Claude Bernard first postulated in his book "*Introduction to experimental medicine*", that the ability of an organism to maintain a constant fluid environment bathing cells of the body (the internal environment) is essential for life, and independent of the external environment. Later, Walter Cannon appropriated the idea and defined the term "homeostasis", which consists in the maintenance of several physiological variables within a certain range, in other words, the stability of the internal environment. In 1936, Hans Selye defined the "general adaptation syndrome" as a generalized effort of the organism to adapt itself to new conditions (Selye, 1936). Based on experiments using rats, he observed that when the organism is severely damaged by acute non-specific harmful agents, the adaptation syndrome is composed of:

(i) an initial alarm reaction, when the organism is suddenly confronted to a critical situation,

(ii) a stage of adaptation, where the organism adapts to this imbalance, and the appearance and function of the tissues returns practically to normal,

(iii) and eventually a stage of exhaustion and death of the organism if it did not manage to cope with the critical situation.

Later, he coined the term "stress" to define this general adaptation syndrome, which was to him a nonspecific response of the body. He started to use the word "stressor" as the factor or agent that triggers the stress response. Stressor may be physical (e.g. cold, heat), chemical (e.g. paraquat, DTT), psychologic or biologic (e.g. infection). We can also add infection as a stressor, as it leads to the same stages of adaptation response.

Years later, experiments showed that the stress response is not unique, but has a degree of specificity, depending on many factors such as the type of challenge to homeostasis, the organism's perception of the stressor and the ability to cope with it. Hans Selye thus popularized the term of stress, not without difficulties, as it was hard for these concepts to get acceptance in the 1940s. Nowadays, this area of research is still active, as impaired stress response is related to many pathologies, such as cancer or chronic inflammation (Dandekar et al., 2015). We will discuss further one example of stress response in light of Hans Selye definition of stress response.

2. Case study: gene expression in the unfolded protein response

The endoplasmic reticulum (ER) is a cellular organelle in which the majority of secreted proteins folds and assembles. When unfolded proteins accumulate in the lumen of the ER (for instance as a result of stress induced by chemicals perturbing the function of chaperones or by virus infection), the unfolded protein response (UPR) pathway is activated (**Figure 1**) (for precise information, please refer to Frakes and Dillin, 2017; Walter and Ron, 2011). The UPR response is classically divided into three branches, each resulting from the activation of an ER-resident protein, the initial alarm reaction. The first branch involves the activation of inositol requiring enzyme 1 (IRE1), which is conserved in all eukaryotes. When activated, IRE1 induces the splicing of the mRNA encoding X-box binding protein 1 (XBP1), a transcription factor (TF) that regulates the expression of enzymes involved in lipid synthesis and of components of the ER-associated protein degradation (ERAD) pathway. The second branch involves a eukaryotic initiation factor 2α (eIF2α) kinase known as double-stranded RNA-activated protein kinase (PKR)–like ER kinase (PERK). Activation of PERK leads to the inhibition of translation through activation of the integrated stress response (ISR), which will be discussed later. This reduction in protein production alleviates ER stress. In parallel, activating transcription factor 4 (ATF4) escapes this inhibition and is preferentially translated. In the nucleus, this TF leads to the expression of other UPR target genes such as the apoptosis modulator C/EBP homologous protein (CHOP). In the last UPR branch, the Activating Transcription Factor 6 (ATF6) is transported from the ER into the Golgi upon UPR activation, where it is cleaved by Golgi-resident proteases. The N-terminal part of ATF6 then translocates into the nucleus, where it activates the transcription of UPR

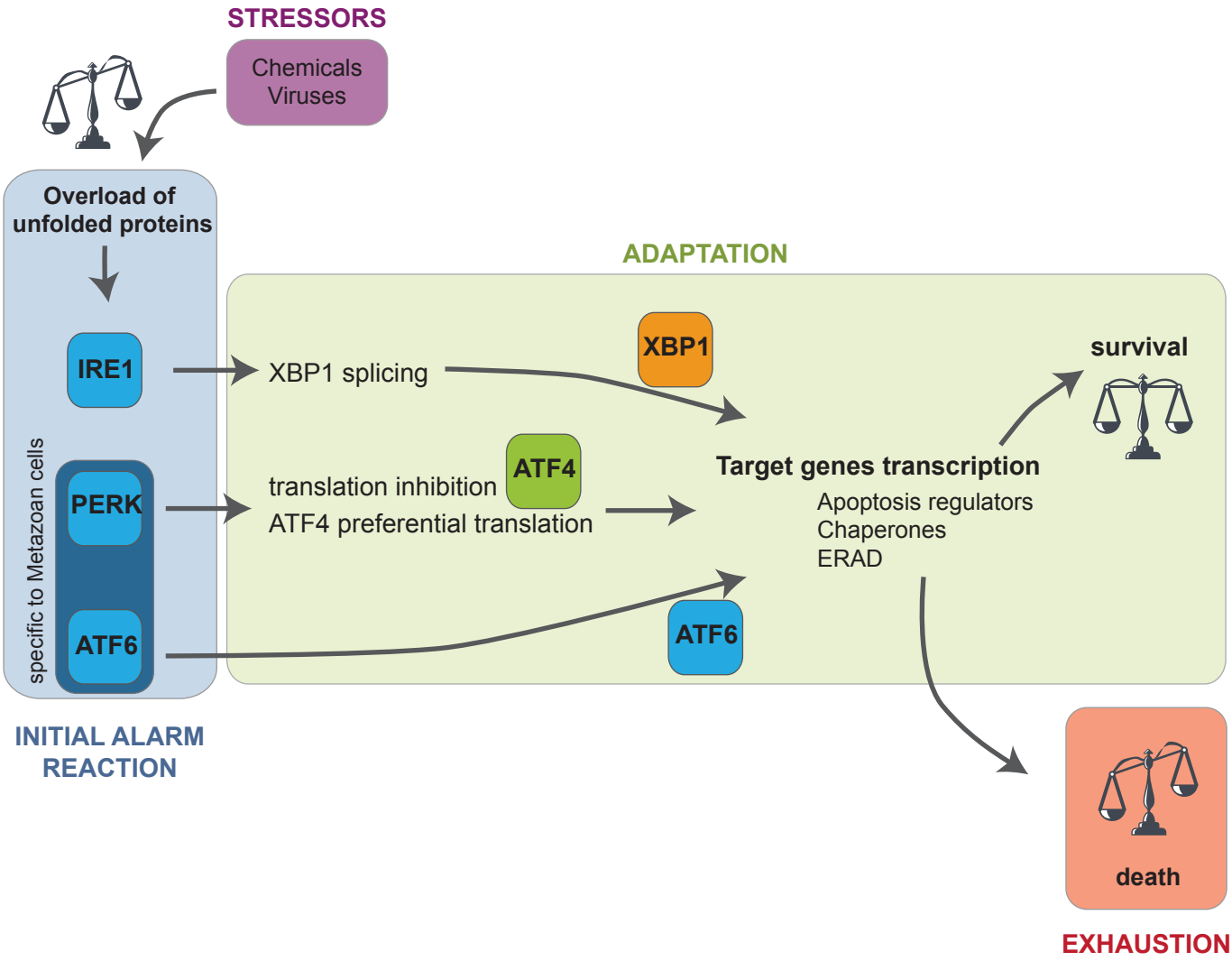

Figure 1: Overview of the unfolded protein response. Stressors such as chemicals or virus infection induce an overload of proteins in the ER. The initial alarm reaction consists in the activation of the three ER sensors: IRE1, PERK and ATF6. PERK and ATF6 are specific to Metazoan cells, whereas IRE1 is present in all eukaryotes. This leads to a cellular response, mainly consisting in gene transcription through the main transcription facors (XBP1, ATF4 and ATF6). It is the phase of adaptation, which eventually end in a return to an apparent homeostasis. In the case where the cell can not recover from the stress, it leads to cell death, the exhaustion phase.

target genes such as Chaperones. Of note, the two latter branches of UPR are specific to Metazoan.

All these pathways converge towards the transcription of genes required to restore the protein balance of the ER. Together, they compose the adaptation phase. Prolonged activity of the UPR, when homeostasis cannot be restored, leads to cell death, the exhaustion phase. Of note, although the transcriptional responses are the best understood aspects of the UPR, this response also involves critical post-transcriptional steps, such as preferential translation of ATF4, IRE1-mediated splicing of XBP-1 mRNA and ERAD. Indeed, only few studies assessed the role and the precise mechanism of translation regulation in the UPR until recently (Young and Wek, 2016). It now appears that preferentially translated proteins play a major role in the maintenance of homeostasis, as revealed by the characterization of transcription factors (ATF4), amino acid transporters (CAT1), negative regulators of the pathway (GADD34) and apoptotic modulators (CHOP). This highlights the importance of considering any cellular processes (including stress response) as a whole, comprised of transcriptional and post-transcriptional regulations. We will now describe the latter.

B. From mRNA to protein levels

1. Post-transcriptional control of gene expression

Gene expression has historically been measured by mRNA levels, as shown by the exponential increase in the number of transcriptome studies published since 1997 (**Figures 2A, 2B**). It is only in the early 2000 that translatome studies were also published. This lag is mainly due to the emergence of polysome profiling and ribosome profiling techniques in 2001 and 2009 respectively (Piccirillo et al., 2014). Studies coupling transcriptomes and translatomes also arise since 2001. These studies allow assessing of the post-transcriptional control of gene expression. Indeed, messenger ribonucleic acids (mRNAs) are subjected to many regulated steps in the nucleus and the cytosol before being translated (**Figure 2A**) (reviewed in Corbett, 2018). Nuclear steps include 5'-end capping, splicing of introns by the spliceosome, 3'-end cleavage and polyadenylation. Once the mature mRNA is produced, it is exported to the cytoplasm through nuclear pores. There, it can be

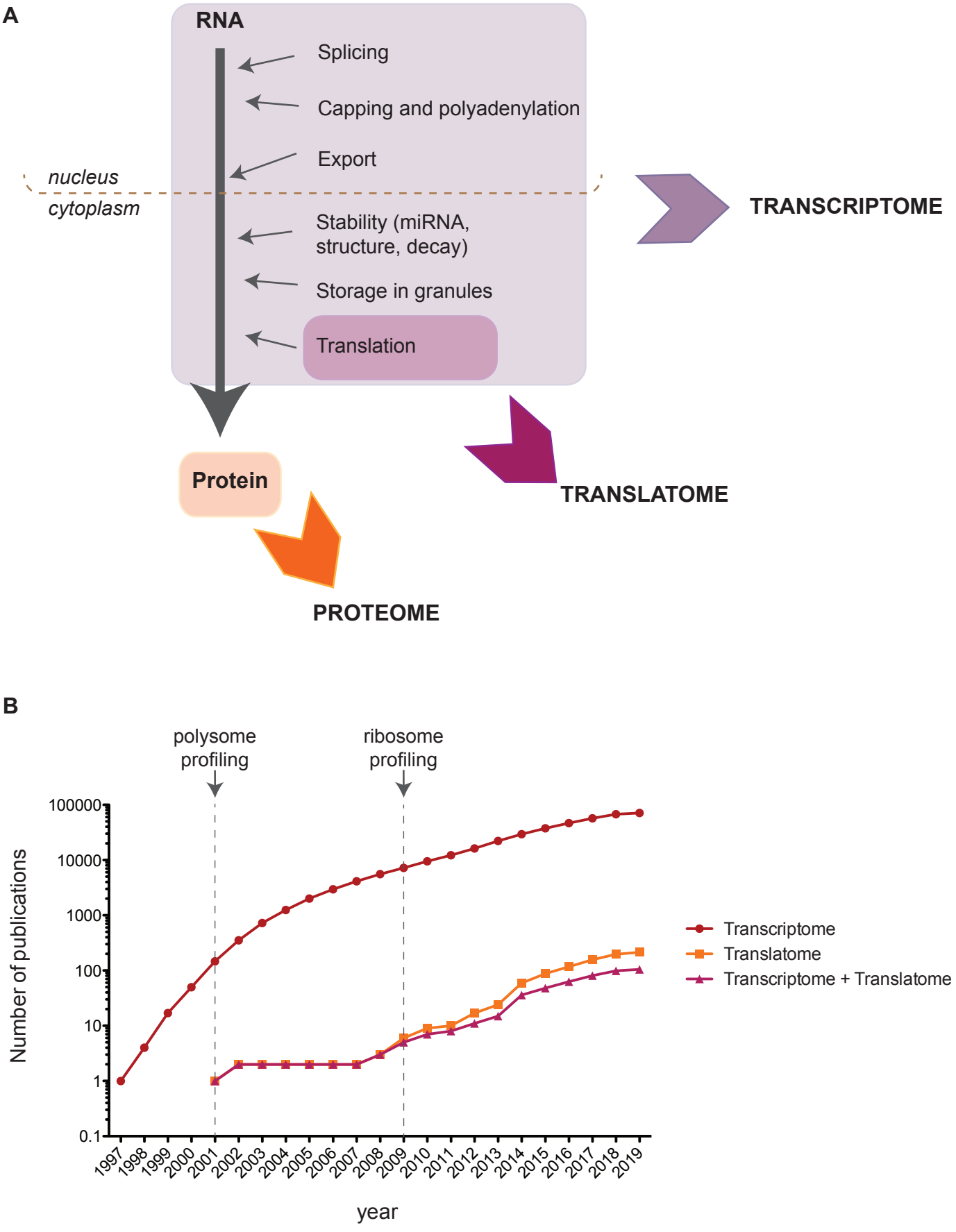

Figure 2: Post transcriptional control of gene expression. **A**. Post-transcriptional gene regulation from RNA to proteins. The molecules analyzed by each high througput analysis are indicated by colored boxes (Transcriptome, Translatome and Proteome). **B**. Number of publication from the PubMed database across the years.

either translated into proteins, stored in cytoplasmic bodies, or subjected to decay. Of note, the dynamics of RNA and protein production are different. It is estimated that a mammalian cell produces two copies of a given mRNA per hour, whereas one mRNA leads to the production of dozens of the corresponding protein per hour. Moreover, the average half-life of mRNAs is 2.6–7 hours whereas that of proteins is around 46 hours (Vogel and Marcotte, 2012). These data suggest that protein levels are highly controlled, as they are the long lasting players of any biological response.

2. mRNA levels do not entirely explain protein abundance

At steady-state, mRNA level is a poor predictor of protein abundance

Simultaneous measure of 96 mRNAs and proteins quantity in a single cell show a poor correlation between protein and mRNA levels, with a correlation between 0 and 35% (Darmanis et al., 2016). In early *Drosophila* embryos, where the amount of RNA is maternally-supplied and stable, mRNA abundance predicts only a third of the variance of protein synthesis (Dunn et al., 2013). Simultaneous measurement of absolute mRNA and protein abundance and turnover in mammalian cells showed that only around 40% of the variance in protein amounts is explained by the level of the corresponding mRNAs (Schwanhausser et al., 2011). Genes with stable mRNAs and proteins are enriched in constitutive metabolic cellular processes, whereas genes with unstable mRNAs and/or proteins are enriched in signal responsive genes, such as components of signaling pathways or chromatin-modifying enzymes. Of note however, the estimation of the correlation between mRNA and protein levels seem to depend on the statistical model used. Indeed, re-analysis of the same dataset led to the conclusion that up to 56-84% of the protein variation can be explained by mRNA levels (Li et al., 2014). These opposing results show the difficulty of establishing models of mRNA/protein dependency. Of note, comparison of neural tubes and forelimb buds of mouse embryo showed that around 16% of mRNAs are differentially translated between the two tissues, even if mRNA levels are comparable between both tissues (Fujii et al., 2017). This indicates that cellular differentiation is driven mainly by differential translation of genes.

Overall, steady state transcript abundances only partially predict protein abundances in almost every condition that has been tested, with correlations depending on the gene considered and on the status of the cell. This highlights the

importance of considering the dynamic relationship between protein and mRNAs in a physiological context (for a complete review, please refer to Liu et al., 2016).

Correlation of RNA and protein levels in stressed systems

Comparison between ribosome associated mRNAs and transcript levels in yeast shows that severe stress, such as amino acid depletion or osmotic shock, induces a highly correlated response between mRNAs and proteins (around 80%) (Halbeisen and Gerber, 2009). On the contrary, mild stresses have a minor and variable impact on translatome and transcriptome, with a correlation of 1-56%. These numbers were confirmed in other studies, where 80% of changes in protein expression could be explained by mRNA level after osmotic or oxidative stress in yeast (Liu et al., 2016). A more precise study assessed protein production as well as RNA amounts in dendritic cells stimulated with lipopolysaccharides (Jovanovic et al., 2015). In this system, mRNA levels contribute to 59-68% of protein expression levels before stimulation, a percentage that increases to 87-92% after 12 hours of stimulation. Thus, mRNA dynamics is the major driver of protein expression after immune stimulation of these cells.

In perturbed systems, it seems that mRNA levels are more correlated to protein abundance. However, the relationship between mRNA and protein levels depends on the cell type and the conditions. Overall, it seems that the interplay between levels of protein and mRNA levels is much subtle than previously expected. As stress response is a conjugated effect of transcription and translation, we now need deeper insight into the translation response.

II. Modulation of translation by stresses

A. The role of initiation factors in translation initiation

1. Canonical cap-dependent translation initiation

Protein synthesis is an energetically expensive process that is tightly regulated. Translation is divided into four steps: initiation, elongation, termination and recycling. Regulation takes place mainly at the initiation step (reviewed in Hershey et al., 2012; Hinnebusch and Lorsch, 2012). In eukaryotes, initiation requires the formation of the ternary complex (TC) composed of the initiator methionyl transfer RNA (Met-tRNAi) and the eIF2 protein bound to guanosine tri-phosphate (GTP) (**Figure 3**). The TC binds to the small subunit of the ribosome (40S), giving rise to the 43S pre-initiation complex (PIC). This binding is promoted by initiation factors such as eIF1, eIF1A, eIF5 and eIF3. On the other hand, the capped and polyadenylated (polyA) mRNA interacts with polyA binding protein (PABP) and eIFs such as eIF4F and eIF4B. This forms the activated messenger ribonucleoprotein (mRNP). The eIF4F complex is composed of 3 eIFs, namely eIF4A (an RNA helicase, which unwinds RNA structures in the 5'untranslated region (5'UTR) of mRNAs with the help of eIF4B), eIF4E (a cap binding protein) and eIF4G (a scaffolding protein). The interaction between PABP and eIF4G allows the circularization of the mRNA to form the so-called "closed-loop structure". This structure is thought to increase the efficiency of translation by favoring the recycling and re-initiation of ribosomes on the mRNA. However, whether the formation of this structure is stable over time is still a matter of debate, as single molecule end-to-end measurements recently revealed that translating mRNAs rarely show co-localizing 5' and 3' ends (Adivarahan et al., 2018). The 43S complex binds the mRNP near the cap and initiates scanning until an AUG initiation codon (or a near-cognate initiation codon) is recognized. Base-pairing between the anticodon of Met-tRNAi and the AUG in the peptidyl site of the 40S subunit triggers the conversion of eIF2-GTP into eIF2-GDP by the GTPase-activating factor eIF5 and the release of initiation factors (eIF4F, eIF4B, eIF3, eIF1A and eIF1). The precise timing of events leading to eIF4F release is still unknown and seems to depend on the mRNA (Gross et al., 2018). Finally, eIF5B catalyzes the joining of the large subunit of the ribosome (60S) to form the 80S initiation complex that will enter into the elongation phase. eIF2-GDP is

recycled into eIF2-GTP by eIF2B, thus allowing assembly of a new TC and translation initiation on another mRNA.

2. Viral IRES-dependent translation initiation

Many viruses hijack the host translation system by the use of alternative ways of translation initiation such as internal ribosome entry sites (IRES) (reviewed in Lee et al., 2017; Plank and Kieft, 2012). IRES-mediated translation occurs when cap-dependent translation is inhibited, allowing the virus to replicate within the cell. The first IRES element was identified in the 1980s in poliovirus (PV) and encephalomyocarditis virus (EMCV) RNAs. Many viral IRESs were discovered since and classified according to the number of eIFs required for initiation and the use of IRES trans-acting factors (ITAFs). Type I IRESs are found in Enteroviruses (e.g. PV) and require almost all eIFs for initiation except eIF4E. Moreover, by contrast with other IRESs, type I IRESs necessitate a scanning step. Type II IRESs are mainly found in *Picornaviridae* (e.g. EMCV) and necessitate the recruitment of eIF3, eIF4G, eIF4B, eIF4A, eIF2 and ITAFs for IRES activity. Type III IRES are carried by members of the *Flaviviridae* (e.g. HCV) and only require eIF2 and eIF3. The last class of IRES, type IV class, contains IRESs that do not require any cellular factors for translation initiation, such as the intergenic (IGR) IRES of Cricket paralysis virus (CrPV). IRES elements are also found in cellular mRNAs and a recent study estimated that up to 10% of human 5'UTRs regulate translation in a cap-independent way (Weingarten-Gabbay et al., 2016).

During the initiation process, the recruitment of the mRNA to the 40S ribosomal subunit is thought to be the rate-limiting step, and is often modulated. This involves mainly phosphorylation of eIF2α and regulation of the eIF4F complex availability, two examples which we will discuss further below.

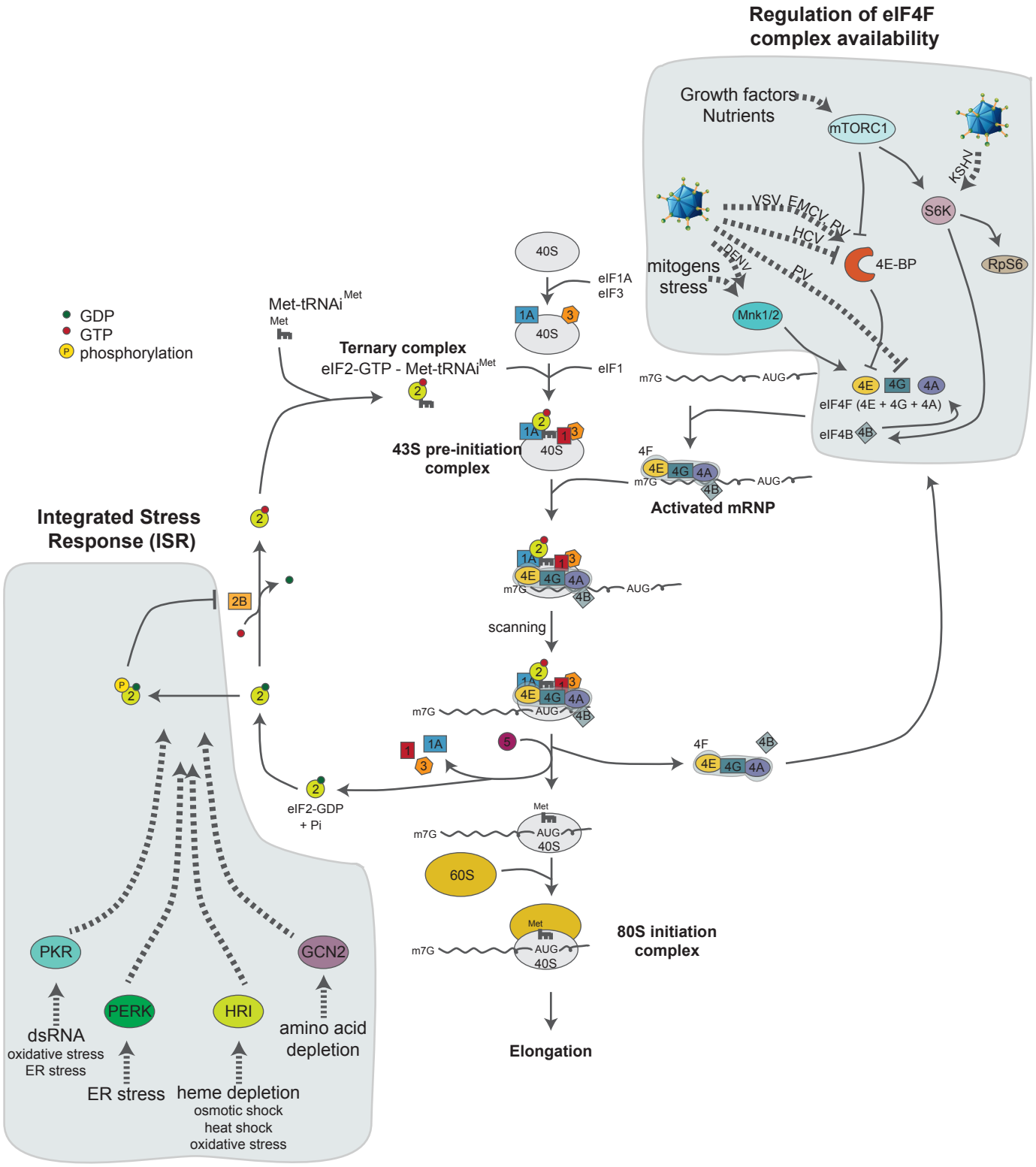

Figure 3: Model of canonical cap-dependent translation initiation (adapted from Sonenberg *et al.*, 2005). Translation initiation is composed of many steps involving initiation factors (eIFs), indicated here by their numbers.The 40S ribosomal subunit, together with eIF1A, eIF3 and the ternary complex, forms the 43S pre-initiation complex. The activated messenger Ribonucleoprotein (mRNP) is composed of the mRNA bound to the eIF4F complex and other eIFs. Binding of this activated mRNP to the 43S initiation complex initiates scanning. Upon AUG recognition, most of the eIFs are released and the 60S subunits joins the 40S, leading to an active 80S nitiation complex that can enter into the elongation phase. Extra- or intracellular stimuli modulate translation initiation by sequestering or inducing phosphorylations of eIFs. The integrated stress response (ISR) converges in the phosphorylation of eIF2α by kinases, rendering the eIF2 complex unavailable for recycling and ternary complex formation. The activation of mRNP is also modulated by signals, which aim at the modulation of eIF4F activity.

B. Modulation of initiation factors activity by homeostasis disruption

1. eIF2α is a key factor of ternary complex formation

Activation of the Integrated Stress Response pathway

A wide range of stimuli triggers the ISR. Stress signals activating this pathway are either cell extrinsic (hypoxia, amino acid starvation, viral or bacterial infections) or cell intrinsic (ER stress or oncogene activation). Sensing of these stresses is performed by four conserved Serine/Threonine (Ser/Thr) kinases, named PERK, general control non-derepressible 2 (GCN2), double-stranded RNA (dsRNA)-dependent protein kinase (PKR) and heme-regulated eIF2α kinase (HRI), which phosphorylate one component of the eIF2 complex, the eIF2α protein (**Figure 3**) (Pakos-Zebrucka et al., 2016).

PERK is an ER-resident kinase activated by the accumulation of misfolded proteins in the ER lumen. It is part of the UPR pathway discussed above. Two mechanisms of PERK activation are described. In the classic model, PERK is bound to Binding immunoglobulin protein (BiP), a chaperone protein. Upon accumulation of misfolded proteins, BiP dissociates from PERK, allowing its activation. Other evidences suggest that the binding of misfolded proteins could directly activate PERK. GCN2 kinase is activated by the binding of deacylated transfer RNA (tRNA), which is a sign of amino acid deprivation (Pakos-Zebrucka et al., 2016). Activation of this kinase prevents translation initiation if some amino acids are absent or rare in the cell. While PERK expression seem to be restricted to Metazoan, GCN2 is found in all eukaryotes (Taniuchi et al., 2016). PKR is an interferon-inducible protein activated by the presence of double stranded RNAs (dsRNAs) from viruses such as human immunodeficiency virus (HIV) and hepatitis C virus (HCV) or synthetic dsRNA such as polyI:C. Endogenous RNAs such as Tumor necrosis factor (TNF)α or interferon (IFN)γ mRNAs also activate PKR (Bou-Nader et al., 2019). Activation of PKR shuts down translation, thus blocking expression of viral mRNAs. Interestingly, some viruses have evolved mechanisms to counteract this recognition such as Middle East Respiratory Syndrome Coronavirus (MERS-CoV). Protein 4a of this virus is a dsRNA binding protein, which prevents the activation of the stress response

pathway, possibly by sequestering dsRNAs (Rabouw et al., 2016). Other stimuli such as oxidative or ER stress have been shown to activate PKR in a dsRNA-independent manner. Upon RNA recognition, PKR dimerizes, autophosphorylates and becomes active to phosphorylate eIF2α. The last Ser/Thr kinase involved in the UPR pathway, HRI, is expressed in erythroid cells and is activated by low heme levels. HRI is involved in the coupling of globin mRNA translation with heme levels, avoiding accumulation of toxic globin aggregates upon iron deficiency. HRI can also be activated by oxidative stress, heat shock, 26S proteasome inhibition and osmotic stress (Pakos-Zebrucka et al., 2016). Both PKR and HRI kinases seem to be restricted to vertebrates (Taniuchi et al., 2016).

All the four eIF2α kinases have overlapping functions and might be activated by a wide range of stress. For instance, bacterial infection induces the ISR through activation of several eIF2α kinases (Rodrigues et al., 2018).

eIF2α phosphorylation and downstream effects

Activation of all the eIF2α kinases leads to the phosphorylation of the initiation factor eIF2α. Phosphorylated eIF2α stabilizes the eIF2-guanosine diphosphate (GDP)-eIF2B complex and blocks the exchange of GDP to GTP by eIF2B protein, thus preventing the recycling of eIF2-GDP to eIF2-GTP. This inhibits the generation of a new TC, 43S PIC formation and cap-dependent translation.

In this context, alternative translation mechanisms are favored, such as upstream open reading frame (uORF) translation. ATF4, one of the main effector of the ISR pathway is translated through an uORF-dependent mechanism. Indeed, upon ISR activation, the ribosome re-initiation is slower and allows initiation at alternative start codons. Moreover, ribosome scanning is slowed down by N6 methylation of adenosine residues (m^6A) in the mRNA 5'UTR. This methylation is reduced in ATF4 5'UTR upon amino acid deprivation, which favors its translation (Zhou et al., 2018). Of note, oxidative stress induces m^6A modifications in mRNA 5'UTR and leads to the triaging of these mRNAs into stress granules (Anders et al., 2018). Here, translationally stalled mRNAs are waiting for translation to resume, showing that m^6A modifications have dual roles towards translation regulation. In addition to ATF4, translation of uORFs allows expression of proteins important for ISR recovery such growth arrest and DNA damage-inducible protein 34 (GADD34).

Recent data show that the diversity of human leukocyte antigen peptides is in part due to 5'UTR uORFs (Starck et al., 2016). These results suggest that uORF translation might be a way to signal stressed cells to neighboring cells through immune pathways.

Resolution of signaling, return to normal conditions and regulation

Dephosphorylation of eIF2α is the key step in the termination of the ISR pathway. It is mediated by a complex containing the protein phosphatase 1 catalytic subunit (PP1c) and one of two different regulatory subunits. GADD34 is induced through ATF4 transcription factor in a negative feedback loop. The second regulatory subunit is the constitutively expressed constitutive repressor of eIF2α phosphorylation (CReP). The PP1c-CReP complex is responsible for the maintenance of low levels of eIF2α phosphorylation in basal condition (Pakos-Zebrucka et al., 2016). Interestingly, partial translational recovery upon chronic stress is mediated by an eIF3d-dependent mechanism of mRNA recruitment, indicating that even upon stress, translation re-starts to sustain cell viability (Guan et al., 2017). Cellular recovery depends on the nature and the intensity of the stress stimuli. The decreased in translation favors the recovery from different stresses and prevents the expression of pro-apoptotic molecules. In conditions where homeostasis cannot be restored, the transcriptional ATF4-target gene C/EBP homologous protein (CHOP) induces cell death by the expression of pro-apoptotic factors such as B-cell lymphoma 2 (Bcl-2) family members for instance (Pakos-Zebrucka et al., 2016).

Activation of the ISR is responsible, at least in part, for the memory deficits associated with traumatic brain injury in mice. Inhibition of the ISR by the potent ISR inhibitor (ISRIB) drug reverses memory defects associated with brain injury such as spatial learning and memory consolidation (Chou et al., 2017). This shows the importance of ISR regulation and its potential use as a therapeutic target.

2. Modulation of eIF4F activity influences messenger ribonucleoprotein recruitment to the ribosome

Upstream signaling pathways

Recruitment of the mRNP to the 43S pre-initiation complex is mainly regulated through the modulation of eIF4F complex components (**Figure 3**). One of the best-known regulators of translation is the mechanistic target of rapamycin (mTOR) pathway. It links cell growth and metabolism with environmental inputs such as nutrients availability and growth factors. mTOR is a Ser/Thr kinase, which is part of two complexes with different molecules, mTORC1 and mTORC2. Protein synthesis is stimulated by mTORC1 through the phosphorylation of two main effectors: the p70S6 kinase (S6K1) and eIF4E binding protein (4E-BP). 4E-BP sequesters eIF4E from the eIF4F complex. 4E-BP phosphorylation lowers its affinity for eIF4E, thus making the latter available for cap binding and downstream translation initiation (reviewed in Saxton and Sabatini, 2017). S6K has many different phosphorylation targets, among them eIF4B and Ribosomal protein S6 (RpS6).

Signals such as mitogens and stresses modulate eIF4E activity through phosphorylation. Indeed, Mitogen-activated protein kinase interacting kinase (Mnk) 1 and 2 phosphorylate eIF4E at Serine 209 (S209) after activation of the Mitogen-activated protein kinase (MAPK) pathway by mitogens or stresses (Waskiewicz et al., 1997). This phosphorylation is dependent on the interaction of Mnk with the scaffold protein eIF4G (Shveygert et al., 2010). Interestingly, Dengue virus (DENV) induces MAPK-Mnk1/2 signaling, which results in the phosphorylation of eIF4E (Roth et al., 2017). This phosphorylation is essential for efficient production of virus particles. On the other hand, Influenza virus, Adenoviruses, EMCV and PV dephosphorylate eIF4E, showing that the effect of viral infection on eIF4E is virus-specific. Furthermore, 4E-BP1 is dephosphorylated in Vesicular stomatitis virus (VSV), EMCV and PV infected cells, which increases its affinity for eIF4E and results in subsequent shutoff of cap-dependent translation. By contrast, HCV infection increases the phosphorylation of 4E-BP1, thus up-regulating host translation (reviewed in Piccirillo et al., 2014).

Effect of eIF4F modulation on translation

eIF4E phosphorylation increases the oncogenic activity of cells through preferential translation of pro-tumorigenic genes such as matrix metalloproteases and chemokines (Furic et al., 2010). Moreover, mice expressing a non-phosphorylatable eIF4E (S209A) are resistant to the formation of lung metastases in a mouse syngeneic mammary tumor model (Robichaud et al., 2018). eIF4E phosphorylation also confers resistance to stresses induced by DNA damaging agents or oxidative stress (Martínez et al., 2015). Although 50% reduction in eIF4E expression is viable in mice, translation of genes involved in the regulation and response to reactive oxygen species is significantly reduced in these cells upon cellular transformation (Truitt et al., 2015). The 5'UTR of eIF4E-dependent mRNAs confers translational sensitivity to eIF4E levels. These results show a clear involvement of eIF4E in cancer progression. In the same way, 4E-BPs inhibit cell proliferation by blocking the translation of proliferation-promoting proteins or proteins involved in cell cycle regulation (Dowling et al., 2010). Of note, 4E-BPs also inhibits the translation of Interferon regulatory factor-7 (IRF-7) and thus type-I IFN production (Colina et al., 2008). Mice knock out (KO) for 4E-BPs are resistant to VSV infection. It is still unknown whether the role of 4E-BPs in the translation of specific mRNAs is through modulation of eIF4E activity.

In mammalian cells, protein kinase C isoform βII (PKCβII) phosphorylates eIF4G and eIF3a and controls eIF4G:eIF3 assembly (Dobrikov et al., 2018a). This modulates translation initiation possibly by facilitating dissociation and recycling of the eIF4F complex (Dobrikov et al., 2018b). In yeast, TORC1 and Adenosine monophosphate-activated protein kinase (AMPK) signaling converge on the Kinase Suppressing Prp20-10 (Ksp1), which phosphorylate eIF4G under glucose deprivation conditions (Chang and Huh, 2018). This phosphorylation regulates the degradation of ribosomal proteins (RPs) mRNAs for instance, likely through the recruitment of an mRNA decay activator to the target mRNA. Viruses also use the eIF4G protein to shape translation initiation. PV infection leads to the cleavage of eIF4G, which renders the eIF4F inactive (reviewed in Piccirillo et al., 2014). On the opposite, ICP27 RNA binding protein of Herpes simplex virus 1 (HSV-1) interacts with PABP in a eIF4G-dependent, but cap-independent manner, stimulating the recruitment of the small subunit of the ribosome (Smith et al., 2017). Some cellular RNA binding proteins share this mechanism.

Triggering of mTOR pathway induces the activation of S6K and phosphorylation of eIF4B (Raught et al., 2004). This phosphorylation stimulates the helicase activity of eIF4A. It also increases eIF4B affinity for eIF3 and translation initiation (Shahbazian et al., 2006). Inhibition of eIF4A reveals that 284 genes rely on eIF4A for efficient translation in breast cancer cells (Rubio et al., 2014). Complexity of the 5'UTR is a major determinant of eIF4A sensitivity and altering the 5'UTR structure modifies this dependency. In the same way, depletion of eIF4B decreases translation of mRNAs harboring complex structures in their 5'UTR such as the pro-apoptotic factor Bcl-2 in HeLa cells (Shahbazian et al., 2010).

3. The particular and intriguing case of RpS6 phosphorylation

Disruptions in homeostasis or external stimuli converge on the modulation of initiation factors to coordinate translation with the cellular state. Apart from initiation factors, one of the targets of the S6K is the ribosomal protein S6 (RpS6). Its phosphorylation controls cell size, malignant transformation and glucose homeostasis among others (Meyuhas, 2015). Viruses also take advantage of this pathway. Indeed, the viral protein kinase of Kaposi's sarcoma-associated herpesvirus (KSHV) phosphorylates RpS6 and upregulates protein synthesis (Bhatt et al., 2016). These results reveal that the ribosome itself might have a regulatory capacity towards mRNA translation.

III. The ribosome and its regulatory capacity

In 1950, George Pallade discovered the existence of "small particulate component of the cytoplasm'', that will be later called "ribosomes". He uncovered that proteins are synthesized by ribosomes, a discovery that awarded him a Nobel Price in 1974. In 1959, Francis Crick hypothesized that ribosomes are carriers of the genetic information, and thus each ribosome in the cell is customized for the expression of only one protein: the "one gene – one ribosome – one protein" hypothesis. Experiments performed by Sydney Brenner, François Jacob, and Mathew Meselson in 1961 showed that infection of *Escherichia coli (E. coli)* with bacteriophages results in viral protein expression by a bacterial ribosome. Thus, ribosomes were then described as non-specialized structures which synthetize at a given time the protein encoded by the mRNA they contain. Consequently, the vision

of the ribosome radically changed over a few years from an extremely specialized molecular machine to a passive machine without any regulatory function (reviewed in Genuth and Barna, 2018a, 2018b). The eukaryotic ribosome is composed of 4 ribosomal RNAs (rRNAs) (18S, 5.8S, 28S and 5S) and 79 ribosomal proteins (RPs). Among these, 46 are unique to eukaryotes, such as RpS6, RACK1 and RpL40 (Ban et al., 2014). These eukaryote-specific RPs often have important roles. Indeed, in addition to a function in the stabilization of the rRNA architecture, they appear to be important for binding of eukaryotic-specific regulatory factors (Wilson and Doudna Cate, 2012). Of note, a new nomenclature of RPs has been suggested in 2014, where homologous RPs are assigned the same name, regardless of species (Ban et al., 2014). The letters “e” and “u” precede the name of eukaryote-specific RPs and universal RPs respectively.

A. Heterogeneity of the ribosome

1. Hints for a ribosome heterogeneity

Patterns of ribosomal proteins expression

It is only since the 1980s that studies suggested again the existence of a ribosomal heterogeneity. The social amoeba *Dictyostelium discoideum* undergoes cell differentiation, which is accompanied by changes in the cell RP content (Ramagopal and Ennis, 1981). Two RPs are specific of the vegetative form, and three RPs are specific of the spore. Seven additional RPs are enriched in one cell type or the other, showing that cellular differentiation is related with ribosomal heterogeneity. More recent studies *in vivo* in mouse showed that the expression of 72 RPs depends on the tested tissue (Kondrashov et al., 2011). This was confirmed at the protein level, by proteomic profiling of human samples (**Figure 4**) (Kim et al., 2014). Some tissues such as the adult pancreas and fetal liver express an overall high but homogeneous level of RPs. By contrast, hematopoietic cells exhibit a high variability of RP level of expression, where all RPs are not expressed at the same level within one cell type. These data suggest a ribosomal heterogeneity in which each cell type has its own ribosome subset.

RPs expression level is also modulated by external signals. Neuronal differentiation in human cultured cells induces changes in RPs expression levels. In

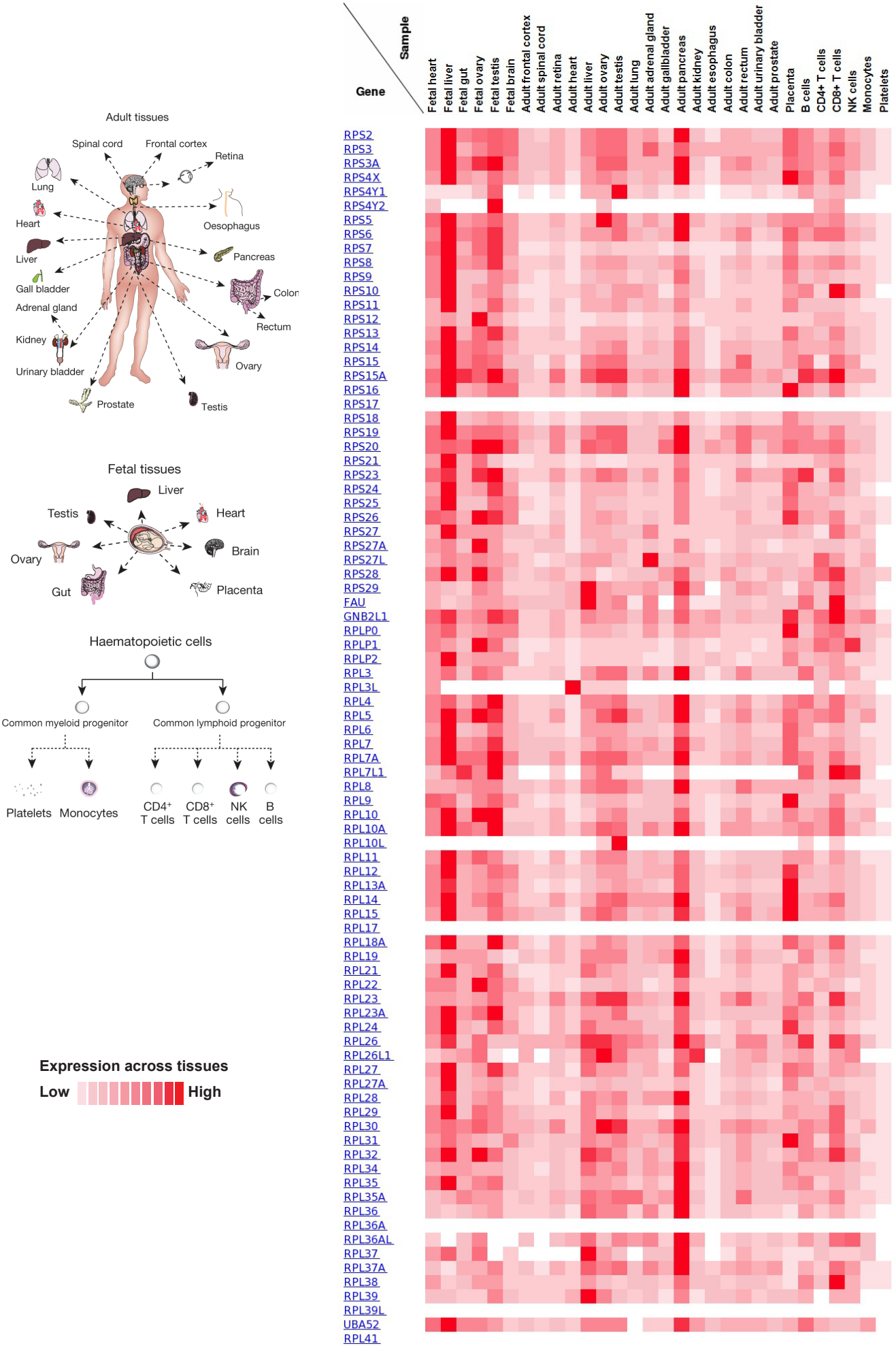

Figure 4: Expression level of human ribosomal proteins. The list of human ribosomal protein was obtained from the the HUGO gene nomenclature committee. Protein levels were quantified by in-depth proteomic of human samples including 17 adult tissues, 7 fetal tissues and 6 purified primary haematopoietic cells (data extracted from Kim *et al.*, 2014).

this study, the majority of RPs are down regulated from the start to the end of differentiation (Bévort and Leffers, 2000). Infection by adenovirus induces a depletion of RpL29/eL29 from the nucleolus of infected cells, whereas RpS15a/uS8 is enriched (Lam et al., 2010). The biological significance of RP levels modulation is still unknown, but one intriguing hypothesis is that the ribosome adapts to the environmental conditions.

In mammals, most functional RPs are encoded by a single gene. In the contrary, RPs are encoded by more than one gene in *Drosophila,* yeast and plants. Heterogeneity in RP paralogue expression exists in fruit fly. For example, RpL22-like, RpS5b, RpS19a, RpL10Aa and RpL37b have an enhanced expression in the testes compared to their paralogues (Xue and Barna, 2012). The yeast *Saccharomyces cerevisiae* (*S. cerevisiae*) genome carries two genomic copies of 59 out of 78 RPs. Deletion of one paralogue or the other induces the expression of different genes. For instance, the absence of Rpl12a induces the expression of genes involved in amino acid metabolism and biosynthesis, while the absence of Rpl12b induces the expression of nuclear proteins and represses genes involved in cell wall and RNA modification (Komili et al., 2007). These results show a differential expression of paralogues, as well as a functional specialization of some RPs.

Dysfunctions in ribosomal components

In *Drosophila*, mutations in RPs were initially identified by the *Minute* phenotype, which consists in a prolonged development, low fertility and viability, altered body size and short bristles on the body (Marygold et al., 2007). In mice, mutations in RpS7/eS7, RpS19/eS19, RACK1 and RpL24/eL24 lead to a white belly spot phenotype among other defects (Shi and Barna, 2015).

Ribosomopathies are a group of human pathologies caused by RP haploinsufficiency or defects in ribosome biosynthesis (reviewed in McCann and Baserga, 2013; Mills and Green, 2017). One of the most studied is Diamond Blackfan anemia (DBA), in which around 60% of cases are caused by heterozygous mutations in one of 12 RPs, leading to bone marrow failure. Isolated congenital asplenia results from a haploinsuffiency of RpSA/uS2, which impairs splenic development. Thus, patients are very prone to severe infections. The 5q-syndrome is a pathology resulting in macrocytic anemia, erythroblastopenia and hypolobulated megakaryocytes in the bone marrow and is linked to a predisposition to leukemia.

5q-syndrome is often associated with haploinsufficiency of RpS14/uS11. Ribosomopathies do not only depend on RPs, but also on rRNAs. Mutations in Dyskerin, an enzyme involved in rRNA modifications, lead to the development of X-linked Dyskeratosis Congenita (X-DC). This pathology is characterized by nail dystrophy and changes in skin pigmentation, as well as a high risk of developing bone marrow disorders. For a complete list of all ribosomopathies and the associated gene mutations, please refer to Armistead and Triggs-Raine, 2014. Mutations in RPs are correlated with increased cancer incidence in humans (Stumpf and Ruggero, 2011). For instance, DBA, X-DC and 5q-syndrome patients have an increased risk of developing hematological tumors.

It is surprising that mutations in such a ubiquitous complex as the ribosome lead to tissue specific defects (Mills and Green, 2017). One possible explanation is that a mutation in RPs would affect the concentration of ribosome, and consequently reduce the translation of mRNAs with low-efficiency of initiation. Therefore, these mRNAs are highly sensitive to ribosome defects. Another explanation is that the composition of ribosomes may be different depending on cell types, leading to a variable sensitivity among tissues towards the loss of a specific ribosomal component. Altogether, these results point to an heterogeneity of the ribosome.

2. Ribosomal RNA modifications

A study based on the 1000 Genomes project estimated that each human individual expresses on average 32 distinct rRNA alleles, which are differentially expressed between organs (Parks et al., 2018). The *Plasmodium* parasite carries two classes of rRNA genes. One form is predominantly expressed when the parasite is in the sporozoite form in the mosquito, whereas the other form is found when it is in the gametocyte form in the bloodstream of the mammalian host (Xue and Barna, 2012). Multiple rRNA sequence variants have also been identified in mice, with some of them having tissue-specific expression. This diversity leads to the presence of ribosome varying by their rRNA sequence among and between individuals.

In addition to sequence variation, the rRNA nucleotides themselves can be modified, creating further diversity. Indeed, approximately 2% of rRNA nucleotides are modified, corresponding to over 100 sites of modification in yeast and over 200 sites in humans. Most of these modifications are 2'-O Methylation (2'O-Me) of the

sugar and pseudouridylation. Both modifications are made by enzymes guided by small nucleolar RNAs (snoRNAs) and are thought to occur co-transcriptionally or in early stages of ribosome biogenesis. These modifications are made at very conserved positions and cluster around functional sites in the rRNA, including the decoding site and the peptidyl transfer center. Nevertheless, some rRNA modifications are inducible by stress. How those modifications are induced and regulated is not yet fully understood (Roundtree et al., 2017).

3. Modulation of ribosomal proteins

In addition to the differential expression of RPs, recent evidences suggest that ribosome heterogeneity exists within a single cell type. Studies in mouse embryonic stem cells (mESC) showed that RpL10A/uL1, RpL38/eL38, RpS7/eS7 and eS25/RpS25 are substoichiometric in polysomes (Shi et al., 2017). However, quantification of 76 RPs showed a similar abundance across monosomes and polysomes fractions in both human embryonic kidney (HEK)293T and HeLa cells (Imami et al., 2018). This might suggest that heterogeneity of the ribosome is cell-type specific or specie-specific.

RPs can be subjected to post-translational modifications (PTM). As previously mentioned, the first RP PTM identified was the phosphorylation of RpS6/eS6 as a consequence of mTOR pathway activation. A recent study in human cells identified 46 phosphorylation sites in RPs (Imami et al., 2018). In addition, many RPs are modified at Ser and Thr residues by the addition of *O*-linked β-d-N-acetylglucosamine (O-GlcNAc). In yeast, at least 16 ribosomal proteins are either methylated or acetylated (reviewed in Xue and Barna, 2012). RPs can also be Lysine 63 (K63)-ubiquitinated. Indeed, experiments performed in yeast showed that RPs were ubiquitinated in response to hydrogen peroxide stress (Silva et al., 2015). Another stress, induction of the UPR, has been shown to induce ubiquitylation in RPs of the small subunit in human, Drosophila and yeast (Higgins et al., 2015). Defective ubiquitylation resulted in an elevated sensibility to UPR-induced cell death. RpL28/eL28 of *S. cerevisiae* is heavily ubiquitylated during the S phase of the cell cycle, and less ubiquitylated in the G1 phase, modulating the speed of translation at different steps of the cell cycle (Spence et al., 2000). Thus, we start to have a better view of the diversity of RPs PTM, although the functional consequences of these modifications are rarely addressed.

Altogether, these results reveal an heterogeneity of the ribosome, which can be modulated by extracellular signals (**Figure 5**). If we consider that all variations can be superimposed, this gives rise to millions of possibilities within a single cell (Dinman, 2016). Therefore, understanding the functional consequences of ribosome heterogeneity is now a major challenge in the field. Indeed, as early as 2007, Vincent Mauro and Gerald Edelman proposed their ribosome filter hypothesis, which postulates that ribosomes are not simply monolithic translation machines but also function as regulatory elements that differentially affect or filter the translation of particular mRNAs (Mauro and Edelman, 2007).

B. The ribosome filter: a ribosome code

1. A role of the ribosome in the regulation of gene expression

In the past 10 years, evidences for the existence of a ribosome selectivity (or ribosome filter) have accumulated. For example, RpS25/eS25 is required for the translation of the IGR IRES of CrPV as well as for the HCV IRES, but not for cap-dependent translation (Landry et al., 2009); RpL40/eL40 is necessary for *Mononegavirales* cap-dependent translation (VSV, Measles virus, Newcastle disease virus and rabies virus) as well as for the translation of some cellular mRNAs such as the stress-related DDR2 gene (Lee et al., 2013). Deletion of RpL13a/uL13 inhibits cellular IRES activity of p53, p27 and SNAT2 mRNAs by inhibiting rRNA methylation (Chaudhuri et al., 2007). Treatment of cells with cycloleucine, a methylation inhibitor, blocks cellular IRES activity whereas it does not affect viral IRES-dependent translation. Inhibition of the rRNA methyltransferase Fibrillarin modifies the 2'-O-Me repertoire and induces a decrease in translation initiation from CrPV IGR IRES, EMCV IRES and cellular IRESs of fibroblast growth factor 1 (FGF1), insulin-like growth factor 1 receptor (IGF-1R), but not Globin and Glyceraldehyde-3-phosphate dehydrogenase (GAPDH) 5'UTRs (Erales et al., 2017).

In response to osmotic and high-pH stress, yeast form ribosomes depleted from RpS26/eS26 (Ferretti et al., 2017). RpS26/eS26 deficient ribosomes bind to different mRNAs than WT ribosomes do. Indeed, Rps26/eS26-containing ribosome transcripts are enriched in genes coding for highly regulated processes, including transcriptional control, phosphorylation, cell cycle and DNA repair. This modulation of

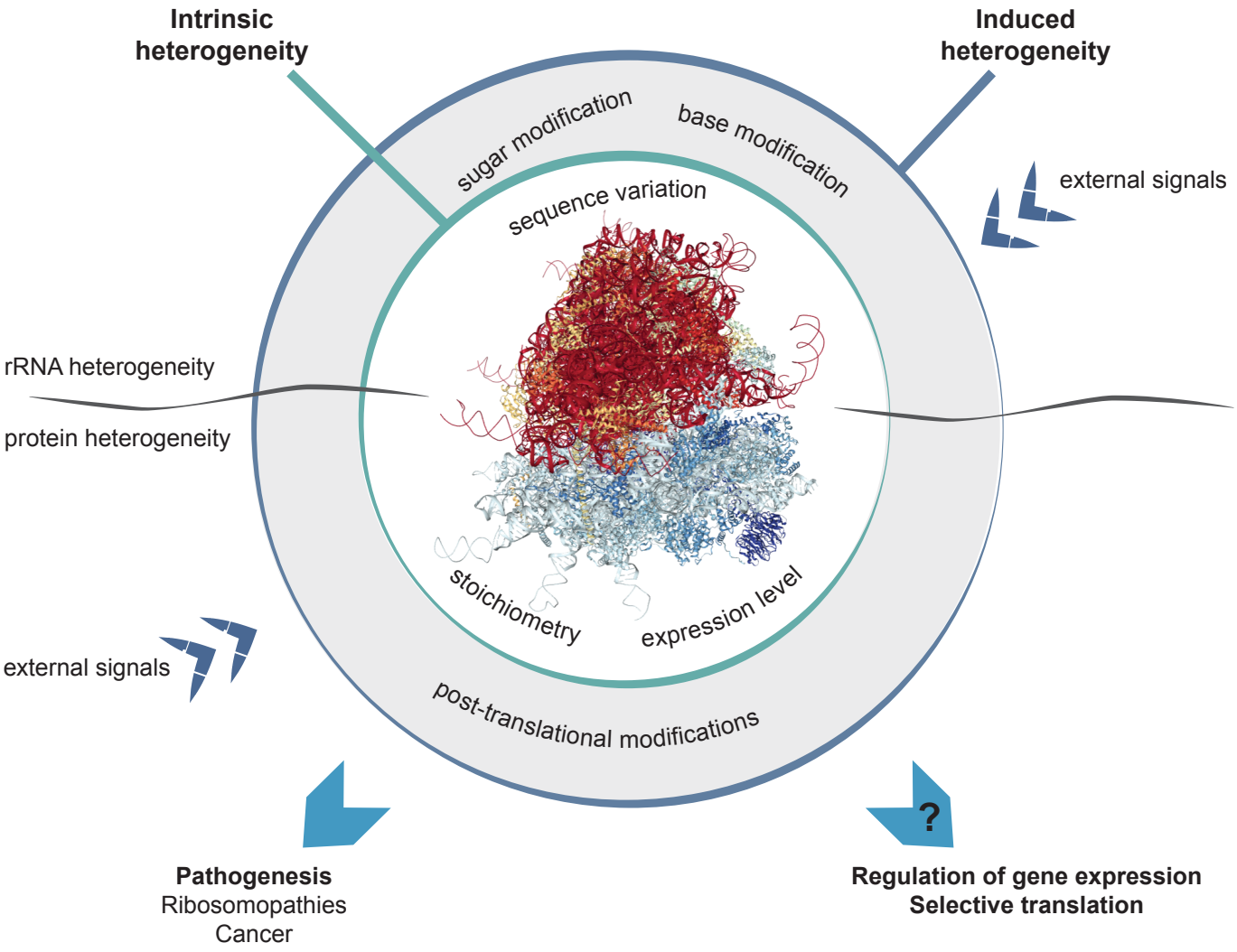

Figure 5: The heterogeneity of the ribosome. The different layers of heterogeneity are indicated, for both ribosomal proteins and ribosomal RNAs. Intrinsic heterogeneity is achieved through differences in the expression levels or stoichiometry of ribosomal proteins, as well as ribosomal RNA sequence variation. External signals can lead to the modification of both ribosomal proteins and ribosomal RNA. Heterogeneity or mutations in ribosomal components can lead to pathologies, and might lead to selective translation. The structure of the human 80S ribosome is extracted from the PDB ID 4V6X with NGL Viewer (AS Rose *et al.*,2018).

RpS26/eS26 levels could be part of an adaptive response to extracellular stimuli. Hemizygous mice for RpL38/eL38 show tissue-patterning defects, as expression of only one copy of RpL38/eL38 led to the formation of 14 instead of 13 ribs associated with vertebrae (Kondrashov et al., 2011). This phenotype is due to an impaired translation of a specific subset of *Hox* mRNAs. Interestingly, these mRNAs are translated by an IRES cap-independent mechanism, which require RpL38/eL38 for translation (Xue et al., 2015). RpL10A/uL1 is substoichiometric in mESC and its presence at the ribosome directs it towards the translation of specific cellular and viral mRNAs. Interestingly, RpL10A/uL1-enriched transcripts show a higher sensitivity towards RpL10A/uL1 loss (Shi et al., 2017). Recently, is has been shown that RPs can modulate antigen peptide presentation, thus shaping surveillance by the immune system (Wei et al., 2019). For instance, depleting RpL6/eL6 or RpL28/eL28 decreases or increases peptide presentation respectively.

Altogether, these results suggest that ribosome heterogeneity is accompanied by a regulatory capacity of the ribosome. As translation modulation is a fast response to environmental signals, the ribosome could be a player in this adaptation.

2. The involvement of post-translational modifications of ribosomal components in selective translation

An obvious way to modulate ribosome function in response to environmental changes is through the use of reversible PTMs. RpL12/uL11 is phosphorylated at Serine 38 by the Cyclin-dependent kinase 1 (CDK1) during mitosis (Imami et al., 2018). This phosphorylation does not impact global protein synthesis, but regulates the translation of mitosis-related mRNAs. Interestingly, expression of a modified RpL12/uL11, which cannot be phosphorylated, induces the preferential translation of mRNAs that are more actively translated in S phase. Hence, phosphorylation of RpL12/uL11 appears to shape the cell cycle progression. RpL13a/uL13 is phosphorylated after a prolonged IFN-γ treatment, leading to its removal from the ribosome (Mazumder et al., 2003). Phosphorylated RpL13a/uL13 then binds to the 3'UTR of the *Ceruloplasmin* mRNA containing an IFN-γ-Activated Inhibitor of Translation (GAIT) element and represses its translation. This mechanism is common to a subset of genes, which are mainly pro-inflammatory genes (Rauscher and Ignatova, 2015). Finally, RpS15/uS19 is phosphorylated by the leucine-rich repeat kinase 2 (LRRK2) (Martin et al., 2014). Mutations in this kinase are a common

cause of familial and sporadic Parkinson's disease (PD) and stimulate cap-dependent and cap-independent translation, which is reverted by the expression of a RpS15/uS19 mutant that cannot be phosphorylated. Of note, RpS11/uS17, RpS15/uS19, and Rps27/eS27 are the major interactors of LRRK2 and 19 of 67 RPs tested can be phosphorylated directly by this kinase (Simsek and Barna, 2017). These results suggest that RPs modifications could be part of the PD pathogenesis.

In summary, accumulating evidences suggest the existence of a basal ribosomal heterogeneity, which can be increased by reversible modifications and participates in the preferential translation of specific subsets of mRNAs. The analysis of this ribosome code is still in its infancy and more in-depth molecular studies are required to understand this novel layer of regulation in gene expression.

C. RACK1 in the ribosome code

1. RACK1, a ribosomal protein and a signaling hub

Receptor for activated protein C kinase 1 (RACK1) is a 36 kDa protein identified as an anchoring protein for activated Ser/Thr kinase PKC βII. It is encoded by the human gene *gnb2l1* (Adams et al., 2011; Ron et al., 1994)**.** This protein is evolutionarily conserved throughout eukaryotes, suggesting it carries important physiological functions (McCahill et al., 2002). In 2004, RACK1 has also been described as a RP, located at the small ribosomal subunit near to the mRNA exit channel (Nilsson et al., 2004). In mESC, RACK1 is stoichiometric in polysomes and free subunits (Shi et al., 2017). RACK1 is composed of tryptophane and aspartic acid (WD)-repeats that adopt a seven bladed propeller structure, facilitating protein-protein interaction (Adams et al., 2011). In its ribosome-bound form, one face of RACK1 exposes its WD-repeats as a docking platform (**Figure 6**). Interestingly, RACK1 is subjected to various PTMs such as phosphorylation, O-GlcNAc or K63 ubiquitination in response to various stimuli (e.g. viral infection, oxidative and ER stress), suggesting it may modulate ribosome activity in response to the cellular state (Higgins et al., 2015; Jha et al., 2017; Ohn et al., 2008; Silva et al., 2015).

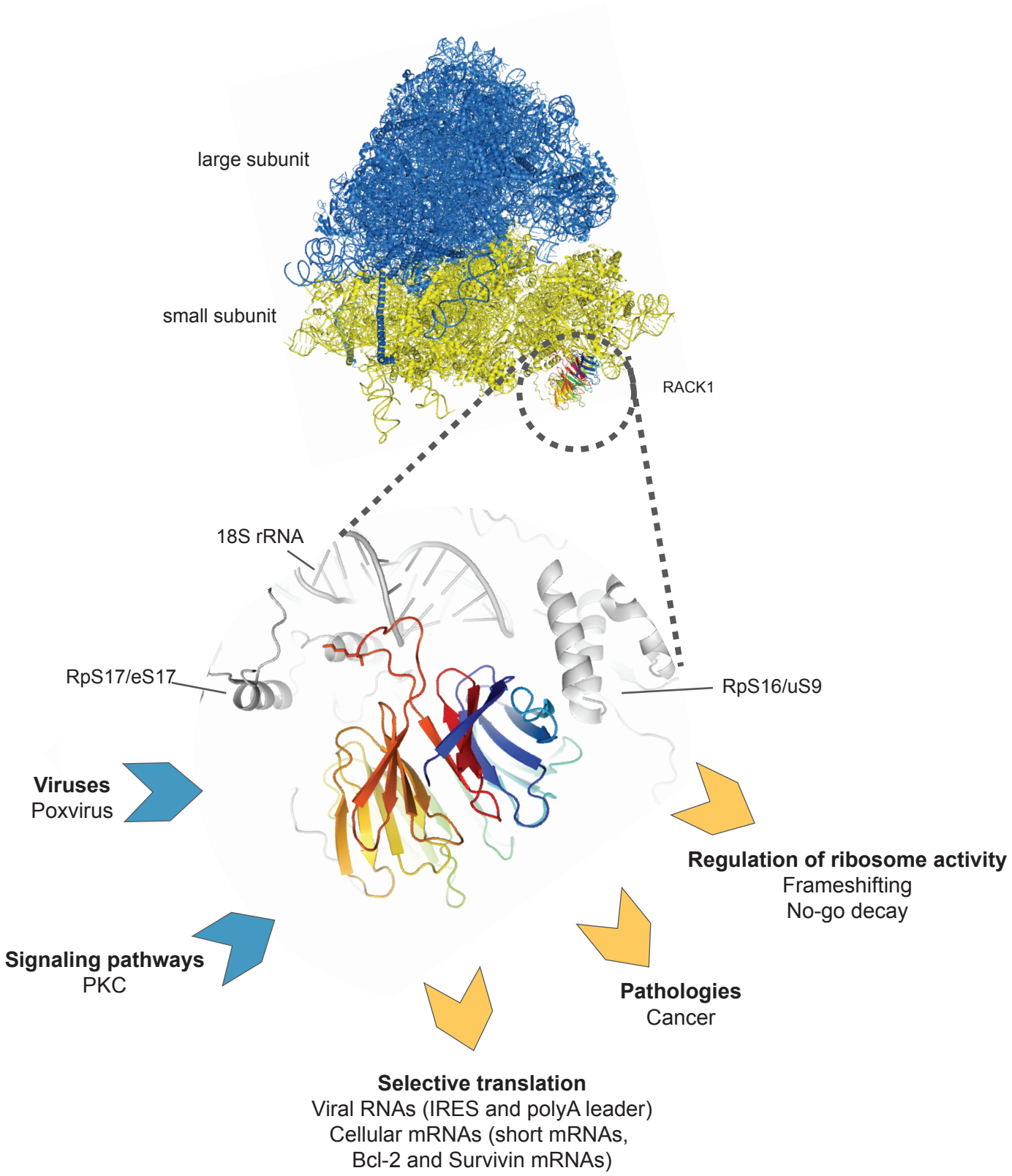

Figure 6: RACK1 function at the ribosome. RACK1 is a ribosomal protein from the small subunit. It is located close to the 18S rRNA and in close proximity with other ribosomal proteins such as RpS17/eS17 and RpS16/uS9. RACK1 is a good candidate to integrate signals to the ribosome. It can be post-translationnally modified by viruses, and is a signaling platform for many signaling proteins (inputs, indicated by blue arrows). RACK1 plays a role in many cellular processes related to translation (yellow arrows). For instance, RACK1 is involved in the selective translation of viral and cellular mRNAs and in the regulation of ribosome activity. Its expression is deregulated in many cancers. The ribosome and RACK1 structures are adapted from Anger *et al.*, 2013.

RACK1 function was assessed in many model organisms. Deletion of RACK1 orthologue in *Saccharomyces cerevisiae,* Asc1/RACK1, is not lethal but leads to a shift towards a hypoxic energy metabolism (Rachfall et al., 2012). Moreover, Asc1/RACK1 mutants show an increased fermentation and a lack of respiration, suggesting a role in metabolism regulation. In the contrary, depletion of RACK1 in multicellular organisms is lethal. For instance, fruit flies depleted from RACK1 never develop into adults (Kadrmas et al., 2007). In mice, homozygous mutation is lethal at the gastrulation stage but RACK1 heterozygous mutants are viable and have skin pigmentation defects, a phenotype similar to other RPs mutation (Shi and Barna, 2015; Volta et al., 2013). However, even if RACK1 is known to be a RP, most of the knowledge on this protein is focused on its function in signaling pathways. Many studies have pointed a role of RACK1 in signaling pathways related to cell growth, apoptosis, proliferation… (reviewed in Adams et al., 2011; Li and Xie, 2015). Moreover, RACK1 expression is often deregulated in cancers, suggesting it might play a role in oncogenesis. Whether these signaling pathways depend on the localization of RACK1 at the ribosome is still debated and poorly studied (Gibson, 2012; Nielsen et al., 2017). Nevertheless, from yeast studies, it seems that Asc1/RACK1 has both ribosome-dependent and independent functions (Coyle et al., 2009).

2. RACK1 role in ribosome function

During translation initiation, eIF6 maintains both ribosomal subunits dissociated. Its removal from the 60S subunit leads to subsequent 80S initiation complex formation (Brina et al., 2015). Activation of PKCβII leads to eIF6 phosphorylation, release and subsequent joining of the two ribosomal subunits, thus increasing translation rate (Ceci et al., 2003). RACK1 acts as a platform for PKCβII recruitment at initiating ribosomes and this recruitment increases translation rates (Grosso et al., 2008). As RACK1 interacts with both eIF6 and activated PKCβII, it was proposed that RACK1 is the bridge between both proteins, allowing PKC-mediated translation initiation. Moreover, RACK1 is also required for the recruitment of the initiation factor eIF4E to the ribosome and subsequent translation initiation of capped mRNAs (Gallo et al., 2018). Furthermore, RACK1 localization at the ribosome is necessary for the association of the mRNA binding protein Scp160 with polysomes, which is thought to direct specific translation of mRNAs (Coyle et al., 2009). These studies suggest that RACK1 could act as a ribosomal scaffold protein

for specific mRNA-RNA binding protein complexes, or initiation factors, to tightly regulate the translation of specific mRNAs.

Translation elongation is subjected to quality control, where sensing of stalled ribosomes leads to ribosome subunits dissociation and degradation of both nascent peptide and associated mRNA, the no-go decay (Karamyshev and Karamysheva, 2018). RACK1 participates in stalling regulation by controlling translation arrest and facilitating mRNA cleavage (Ikeuchi and Inada, 2016; Kuroha et al., 2010). In the same way, RACK1 plays a role in ribosome quality control by helping in the resolution of stalling on polyA sequences through ubiquitination of RPs (Sundaramoorthy et al., 2017). In addition, yeast Asc1/RACK1 prevents frameshifts during translation of mRNAs containing CGA codon repeats (Wolf and Grayhack, 2015). Altogether, these results point to RACK1 as an important factor in ribosome quality control.

3. RACK1 in selective translation

RACK1 position at the small subunit of the ribosome suggests it might assemble signaling complexes at the ribosome, allowing translation regulation in response to cell stimuli (Nilsson et al., 2004). As Asc1/RACK1 yeast mutants show elevated levels of some proteins, one of Asc1/RACK1 functions may be gene repression (Gerbasi et al., 2004). Other data suggest on the contrary that *Schizosaccharomyces pombe* (*S. pombe*) Cpc2/RACK1 promotes the efficient translation of some mRNAs (Shor et al., 2003). In condition of peroxide stress, Cpc2/RACK1 regulates positively the translation of specific gene products involved in key biological processes such as MAPK cascade, defense against oxidative stress, and cell cycle progression (Núñez et al., 2009). More recently, Asc1/RACK1 has been suggested to enhance the translation of short mRNAs that form a closed-loop complex (Thompson et al., 2016). Indeed, yeast depleted from Asc1/RACK1 show a decreased translation of mRNAs coding for cytoplasmic and mitochondrial RPs. It was also shown that Asc1/RACK1 controls the translation of some transcription factor mRNAs through their 5'UTR (Rachfall et al., 2012). Moreover, overexpression of WT RACK1 in hepatocellular carcinoma (HCC) cells promotes cell survival and increases the 5'UTR activity of *Cyclin D1*, *Myc*, *Survivin* and *Bcl-2* mRNAs (Ruan et al., 2012).

Our group came across RACK1 path by an unexpected discovery. The interest of our team is *Drosophila* antiviral immunity[1], which is mainly composed by the nucleic acid-based RNA interference (RNAi) pathway among others (Mussabekova et al., 2017). Interactome study of the main RNAi components Argonaute 2 (Ago2), Dicer-2 (Dcr-2) and R2D2 in S2 cells led to the identification of 103 partners (unpublished results). The most represented group was RPs (16 proteins out of 103). Among them, RACK1 was found to interact with Ago2 and R2D2 but only in cells infected with Drosophila C virus (DCV), a virus from the *Dicistroviridae* family. Depletion of RACK1 from S2 cells impaired the replication of DCV and CrPV, but not Flock House virus (FHV) or VSV (Majzoub et al., 2014). The team showed that RACK1 is required for the translation mediated by the 5'IRES of these *Dicistroviridae*, and that this function is dependent on RACK1 localization at the ribosome. Interestingly, RACK1 was found to be also required in human hepatocytes for the IRES-dependent translation of HCV. Finally, depletion of one subunit of the eIF3 complex, eIF3j, had a similar effect than RACK1 depletion towards CrPV and HCV replication. This raised the possibility that RACK1 and eIF3j might act together in viral selective translation. Of note, a proviral role for RACK1 was subsequently confirmed. Indeed, RACK1 is required for the translation of Vaccinia virus (VacV), while it does not affect HSV-1 translation (Jha et al., 2017). Upon VacV infection, RACK1 is phosphorylated and favors the translation of polyA-leader mRNAs of the virus. RACK1 is also required for *Flaviviridae* replication such as DENV, Zika virus (ZIKV) and West Nile Virus (WNV) replication (Hafirassou et al., 2017). However, this dependency does not seem to depend on the viral translation.

These results open possibilities for the use of RACK1 as a target for host-targeted antivirals (HTAs), active against a broad range of viral infections, including viruses for which treatments are still missing such as ZIKV. Indeed, the design of HTAs aim to target host cell factors that are required for a pathogen replication or persistence, to enhance protective immune response or reduce exacerbated inflammation (Kaufmann et al., 2017). The advantage of these treatments is the lower risk of resistance, as it implies for the pathogen to use another cell host factor or to evade defense mechanisms. However, given that HTAs interfere with host proteins, one theoretical caveat is the possibly greater risk of cellular toxicity as compared to direct-acting antivirals (DAAs). Data obtained in cell culture did not reveal any major toxicity linked to RACK1 inhibition in laboratory cell culture

[1] A review on the cellular and molecular mechanism of insect immunity can be found in Annex.

conditions, but the role of RACK1 in perturbed systems was not assessed (Majzoub et al., 2014). Hence, we need to get deeper insight into the molecular function of RACK1 apart from its proviral role. In the context of selective translation, RACK1 is a promiscuous protein, as this signaling hub is an ideal candidate to integrate environmental signals to the ribosome. In this regard, the use of a multicellular organism such as *Drosophila* is an advantage. My PhD project focuses on the role of RACK1 in selective translation, which I tried to decipher through three main questions:

1. Which are the structural features of the RACK1-dependent IRES? (Chapter 1)
2. Are there cofactors of RACK1 in selective translation? (Chapters 2 and 3)
3. Are there cellular mRNAs for which translation is RACK1-dependent? (Chapter 4)

CHAPTER I

CHARACTERIZATION OF A RACK1-DEPENDENT VIRAL IRES

The CrPV RNA genome contains two IRES and translation of the 5'IRES requires RACK1 (Majzoub et al., 2014). In contrast to the extensively studied IGR IRES, the 5'IRES remained largely unexplored. The aim of the project was to get deeper insight into how CrPV 5'IRES mediates translation. Structural studies showed that the 5'IRES contains a pseudoknot structure. I tested the importance of its structure integrity *ex vivo* by generating point mutations in reporter plasmids and assessing the translation efficiency of the mutants by luciferase assay in cell culture (**Figure 4E**). Mass spectrometry analysis revealed that the 5'IRES recruits eIF3, showing that it belongs to type III class of IRES elements (like HCV). I performed immunoprecipitation of CrPV IRES with eIF3b antibody in *Drosophila* S2 cells and showed that although the pseudoknot is essential for the 5'IRES activity, it is not required for eIF3 recruitment (Figure 5C). Altogether, these results show that the 5'IRES of CrPV belong to the type III class of IRES and that the pseudoknot structure is essential for proper folding of the RNA and subsequent ribosome recruitment. This work was done in collaboration with Dr. F. Martin (UPR9002, IBMC, Strasbourg) and was published in 2017 in *Nucleic Acid Research* (NAR) journal.

Published online 18 July 2017

Nucleic Acids Research, 2017, Vol. 45, No. 15 ***8993–9004***
doi: 10.1093/nar/gkx622

The $IRES_{5'UTR}$ of the dicistrovirus cricket paralysis virus is a type III IRES containing an essential pseudoknot structure

Lauriane Gross[1], Quentin Vicens[1], Evelyne Einhorn[2], Audrey Noireterre[1], Laure Schaeffer[1], Lauriane Kuhn[3], Jean-Luc Imler[2], Gilbert Eriani[1], Carine Meignin[2] and Franck Martin[1,*]

[1]Université de Strasbourg, CNRS, Architecture et Réactivité de l'ARN, UPR 9002, F-67000 Strasbourg, France, [2]Université de Strasbourg, CNRS, Réponse Immunitaire et Développement chez les Insectes, UPR 9022, F-67000 Strasbourg, France and [3]Université de Strasbourg, CNRS, Plateforme Protéomique Strasbourg—Esplanade, F-67000 Strasbourg, France

Received November 03, 2016; Revised June 30, 2017; Editorial Decision July 06, 2017; Accepted July 07, 2017

ABSTRACT

Cricket paralysis virus (CrPV) is a dicistrovirus. Its positive-sense single-stranded RNA genome contains two internal ribosomal entry sites (IRESs). The 5′ untranslated region (5′UTR) $IRES_{5'UTR}$ mediates translation of non-structural proteins encoded by ORF1 whereas the well-known intergenic region (IGR) $IRES_{IGR}$ is required for translation of structural proteins from open reading frame 2 in the late phase of infection. Concerted action of both IRES is essential for host translation shut-off and viral translation. $IRES_{IGR}$ has been extensively studied, in contrast the $IRES_{5'UTR}$ remains largely unexplored. Here, we define the minimal IRES element required for efficient translation initiation in drosophila S2 cell-free extracts. We show that $IRES_{5'UTR}$ promotes direct recruitment of the ribosome on the cognate viral AUG start codon without any scanning step, using a Hepatitis-C virus-related translation initiation mechanism. Mass spectrometry analysis revealed that $IRES_{5'UTR}$ recruits eukaryotic initiation factor 3, confirming that it belongs to type III class of IRES elements. Using Selective 2′-hydroxyl acylation analyzed by primer extension and DMS probing, we established a secondary structure model of 5′UTR and of the minimal $IRES_{5'UTR}$. The $IRES_{5'UTR}$ contains a pseudoknot structure that is essential for proper folding and ribosome recruitment. Overall, our results pave the way for studies addressing the synergy and interplay between the two IRES from CrPV.

INTRODUCTION

Viruses use various strategies to hijack the host cellular translational machinery in order to produce their viral proteins. Among these, positive-stranded RNA viruses down-regulate host translation while increasing viral translation (1). For example, during poliovirus infection, an RNA structural element on the viral genome, also named internal ribosome entry site (IRES), is able to recruit the host ribosome while cap-dependent cellular translation is shut-off upon cleavage of essential canonical translation factors such as eukaryotic initiation factor eIF4G and PolyA Binding Protein (2–4). IRES has been classified into four main types according to their structural organization and their eIF requirement (5,6). Type I and II are large IRES that need most of the eIF except cap-binding protein eIF4E. Type I IRES recruits the ribosome upstream of the AUG start codon and then undergoes a scanning step to localize the AUG. In contrast, type II IRES loads the ribosome directly on the start codon without any scanning step. Type III IRES needs only eIF2 and eIF3 in order to bind directly to the 40S ribosomal subunit and to load the ribosome on the start codon without scanning. Finally, type IV IRES is the most compact: they usually contains pseudoknots, do not need any eIFs at all and can initiate translation on a non-AUG start codon.

The genome of *Dicistroviridae* consists of an ∼9 kb monopartite positive-stranded RNA containing two open reading frames, ORF1 and ORF2, which encode respectively non-structural and structural proteins. Cricket paralysis virus (CrPV) is a prototype member of this family that has been thoroughly investigated. Translation of viral proteins is exclusively driven by two IRES: the 5′UTR contains $IRES_{5'UTR}$ for ORF1 translation, while a type IV IRES is located in the intergenic region (IGR) $IRES_{IGR}$ between the two ORFs and controls expression of structural proteins from ORF2 (7–10). Both IRES act in synergy to pro-

*To whom correspondence should be addressed. Tel: +33 388417042; Fax: +33 388602218; Email: f.martin@ibmc-cnrs.unistra.fr

duce the viral proteins required for rapid shut-off host protein translation to favor preferential viral protein synthesis. Whereas expression of non-structural proteins driven by $IRES_{5'UTR}$ is constant during the whole infectious process, the expression of structural proteins from the $IRES_{IGR}$ begins during the late phase of infection, with concentrations gradually increasing until reaching supramolar concentration at the end of infection (8–10). The dramatic increase in structural protein expression from the $IRES_{IGR}$ is directly dependent on the expression of non-structural proteins from $IRES_{5'UTR}$, although the details of the underlying mechanisms remain elusive (11).

Translation initiation mediated by $IRES_{IGR}$ has been extensively studied in the last two decades (12–17). Briefly, a pseudoknot structure named PKI mimics a codon–anticodon interaction in the P-site of the ribosome, therefore allowing direct ribosome recruitment without any translation factors and translation initiation from a non-AUG codon (12,13,18–20). It was recently observed by Cryo-electron microscopy (Cryo-EM) that PKI enters the ribosome in the A-site of the ribosome and is then further translocated into the P-site by eEF2, leaving the A-site free to accept the first aminoacyl-tRNA in order to proceed to elongation (18,19,21). In contrast to $IRES_{IGR}$, translation mediated by $IRES_{5'UTR}$ has been much less studied. The $IRES_{5'UTR}$ of the related dicistrovirus *Rhapdosilum padi* virus requires the scanning factors eIF1, eIF2 and eIF3 for efficient translation in a reconstituted cell-free translation extract (22). However, while the $IRES_{IGR}$ sequences of dicistroviruses are highly conserved (23), $IRES_{5'UTR}$ elements are largely variable and do not share any common consensus sequence suggesting the existence of different organizations among the *Dicistroviridae* family (24). Although it was discovered in early 2000, the CrPV $IRES_{5'UTR}$ remains largely uncharacterized (10). Recently, it was demonstrated that $IRES_{5'UTR}$-driven translation requires the ribosomal protein RACK1 while the $IRES_{IGR}$ can still promote efficient translation initiation with RACK1-depleted ribosomes (25). Therefore, CrPV $IRES_{5'UTR}$ and $IRES_{IGR}$ are using fundamentally different strategies to initiate translation. In order to better understand the translational events leading to viral propagation, a better understanding of the structure and function of the CrPV $IRES_{5'UTR}$ is needed.

Here, we have characterized structurally and functionally the CrPV $IRES_{5'UTR}$. We have mapped the IRES to the 760 nt-long 5′UTR and, using selective 2′-hydroxyl acylation analyzed by primer extension (SHAPE) and dimethyl sulfate (DMS) probing, established a secondary structure model of the entire 5′UTR. Then, we have determined the minimal IRES element, and shown that it contains a pseudoknot structure. The existence of the pseudoknot was validated by mutational analysis. Finally, we have shown that this structure is essential for proper folding and activity of the $IRES_{5'UTR}$ *in vitro* in *drosophila* cell-free translation extracts and *in vivo* in S2 cells.

MATERIALS AND METHODS

RNA transcription

Renilla reporter mRNAs were synthesized from DNA template by *in vitro* transcription using recombinant T7 RNA polymerase. After transcription, unincorporated nucleotides were trapped on a G-25 column and RNA transcripts were phenol-extracted and precipitated. RNA pellets were resuspended in water and their concentration was determined by absorbance measurements.

RNA translation in cell-free translation extract

In vitro translation competent extracts from *Drosophila melanogaster* S2 cells were prepared as previously described (25,26). Cells were lysed in 40 mM HEPES–KOH [pH8], 100 mM potassium acetate, 1 mM magnesium acetate, 1 mM DTT at a density of 10^9 ml^{-1} using a Cell Disruption Bomb (Parr Instrument Company). The lysate was then cleared by centrifugations at 4°C and supplemented with creatine kinase at 0, 24°C, aliquoted and stored at −80°C. *In vitro* translation experiments were performed as previously described under subsaturating conditions to avoid substrates titration (25,26). Translation efficiency was determined by Renilla Luciferase assay. RNA integrity of translated reporter mRNAs was checked by polyacrylamide gel electrophoresis (PAGE) on denaturing 4% acrylamide gels.

RNA translation in S2 cells

The pACT5C–$IRES_{5'CrPV}$–Renilla Luciferase was mutated by site-directed mutagenesis to obtain the m1–m4 plasmids (25). *Drosophila* S2 cells were transfected with reporter plasmid DNAs by the $CaPO_4$ precipitation method (adapted from (27)). Twenty-four hours later, medium was changed and copper was added to the culture medium (0.5 mM) to induce the expression of the capped Firefly construct (pMT-Firefly). Forty-eight hours later, cells were lysed and luciferase activity was measured with the Promega Dual-Luciferase assay, using a Berthold luminometer.

SHAPE analysis

Full-length RNA was designed to comprise the following elements: a leader sequence (19 nt), the entire CrPV 5′UTR (709 nt), the beginning of the ORF1 (47 nt), a 3′ linker and a generic reverse transcription primer-binding site (28). Mutants comprising the 357–754 sequence did not possess any leader or 3′ linker and generic primer-binding site. RNA was transcribed and purified on 4% acrylamide denaturing gels.

RNA folding assays. For the full-length wt RNA, 18 pmoles RNA in 11 μl of a buffer containing 25 mM NaCl, 15 mM MgCl2, 25 mM Na cacodylate pH 6.5, were incubated at 60°C for 2 min, except for the no-refolding (NR) control, which was not heated. Then, 'R_a' samples underwent 1-h long cool down to 37°C. A total of 10 pmoles of NR RNA were used for SHAPE modification (see below). A total of 8 pmoles of NR and refolded RNA were added to an equivalent volume (5 μl) of loading buffer (50% glycerol, 2.5 mM Na cacodylate pH 6.5). Native PAGE was performed at 4°C on 4% acrylamide, 10 mM glycine, 10 mM Tris base. RNA were detected with toluidine blue.

For each wt or mutant RNA (m1–m4), 15 pmoles RNA in 10 μl of translation buffer and incubated at 50°C for 5

min, except for NR controls. Then, 'R_b' samples were kept at 25°C for 10 min, while 'R_c' samples underwent a 15 min-long cool down to 25°C. A total of 4–8 pmoles of R_b RNA were used for SHAPE modification.

SHAPE. SHAPE was performed in 10 μl containing 2 pmoles RNA (0.5 μM final concentration), 6.5 mM 1-methyl-7-nitroisatoic anhydride (1M7) or 80 mM benzoyl cyanide (BzCN; for full length wt RNA dataset only), 10% dimethylsulfoxyde (DMSO), 90 mM Na HEPES pH 8.0. Modification is complete after 10 min at RT (∼23°C). The modified RNA was precipitated, washed, dried and resuspended in 0.5X TE.

Reverse transcription was performed in 20 μl containing 2 pmoles RNA (except for BzCN dataset: 3 pmoles RNA), 0.9 pmoles of a fluorescently labeled primer (except for BzCN dataset: 6 pmoles; primers used: cr-rev421: 5′-GACCACGCGAGTCGTAATC-3′; cr-rev529: 5′-CAAGGGCTAACTAATCAGGTGTAC-3′; cr-rev769: 5′-GAGTTGATGTTGTTGGTTGCGTTG-3′; 3′gen: 5′-GAACCGGACCGAAGCCCG-3′), 160 U SuperScript III reverse transcriptase, 83 mM KCl, 56 mM Tris–HCl (pH 8.3), 0.56 mM each deoxynucleotides (dNTP), 5.6 mM DTT and 3 mM $MgCl_2$. Denaturing occurred at 95°C for 2 min, followed by annealing at 65°C for 5 min and incubation on ice for 2 min. RT extension parameters were: 42°C for 2 min, 50°C for 30 min and 65°C for 5 min. Sequencing reactions were performed in parallel in similar conditions, but containing 0.5 mM dideoxythymidine triphosphate (ddTTP). Reactions were stopped by the addition of 4 μl 50 mM EDTA pH 8.0, phenol–chloroform extracted, precipitated, washed, dried and resuspended in 10 μl deionized formamide. Samples were loaded on a 96-well plate for sequencing on an Applied Biosystems 3130xl genetic analyzer.

The resulting electropherograms were analyzed using QuSHAPE (29), which aligns signal within and across capillaries, as well as to the dideoxy references and corrects for signal decay. Normalized reactivities range from 0 to ∼2, with 1.0–1.2 being the average reactivity for highly reactive positions. For the sake of simplicity, the final *.shape file contains reactivities for the full length RNA (752 nt) that were combined from reactivities for nucleotides 1–353 from primer cr-rev421, reactivities for nucleotides 354–711 from primer cr-rev769 (three datasets with 1M7 modification) and reactivities for nucleotides 712–752 from primer 3′-gen (two datasets with BzCN modification, for which 75% of the residues have reactivities either >1.2 or undetermined, which suggest that the region is highly unstructured).

Structure prediction. Secondary structure prediction was obtained using the Fold and ShapeKnots algorithms available in RNAStructure v. 5.7 (30). The recommended parameters for pseudoknot and probing-based prediction were used, using the *.shape file as input. A value of −500 was given to nucleotides for which reactivities were not determined. The output 2D models were rendered using VARNA (31). The secondary structure of the region 357–466 region was used as input for automated three-dimensional (3D) modeling using the web-based RNAComposer server (32), using default parameters.

DMS probing

Like the SHAPE experiments, the DMS probing reactions were performed on 2 pmoles of the minimal $IRES_{5'UTR}$. Briefly, the RNA is incubated for 10 min in dimethylsufate (DMS) buffer (50 mM Na cacodylate, pH 7.5, 5 mM $MgCl_2$ and 100 mM KCl). The RNA was modified in the presence of 1.25% DMS. The reaction is performed for 10 min at 20°C and terminated on ice. Then, the modified RNA are precipitated in ethanol. The modification sites were detected by primer extension with two fluorescent primers complementary to nucleotides 732–755 and 517–707, respectively. The resulting electropherograms were analyzed by the same method as previously described for SHAPE analysis.

CMCT probing

The 1-cyclohexyl-3-(2-morpholinoethyl)carbodiimide met ho-p-toluene sulfonate (CMCT) experiments were performed on 4 pmoles RNA. The RNA is incubated for 10min in CMCT buffer (Na borate 50 mM pH 8, 5; $MgCl_2$ 5 mM; KCl 100 mM added with 1 μg of total tRNA). The modifications were done with 10, 5 g/l; final CMCT. The reaction is completed in 30 min at 20°C, then the RNA is precipitated. The primer extension and capillary electrophoresis steps are the same as for the DMS probing.

Sucrose gradients

Pre-initiation complexes were assembled on 3′ 32P-labeled RNA transcript by incubation in S2 cell-free extracts in the presence of 2 mM of a non hydrolysable GTP analog (GMP-PNP). The complexes are then resolved on sucrose gradients 7–47% and centrifuged in a SW41 rotor for 2 h 30 min at 37K at 4°. After centrifugation, the gradient is collected into 45 distinct fractions, then the positions of pre-initiation complexes were monitored by detection of radiolabeled RNA transcripts by Cerenkov counting of each fraction.

Mass spectrometry analysis and data processing.

Protein extracts were digested with sequencing-grade trypsin (Promega) as described previously (33). Resulting peptides were analyzed by nanoLC-MS/MS and MS data were searched by the Mascot algorithm against the UniProtKB *D. melanogaster* database. Identifications were validated with a protein False Discovery Rate (FDR) < 1% using a decoy database strategy. The total number of MS/MS fragmentation spectra was used to quantify each protein from three independent biological replicates. This spectral count was submitted to a negative-binomial test using an edgeR GLM regression through the R-package. For each identified protein, an adjusted *P*-value corrected by Benjamini–Hochberg was calculated, as well as a protein fold-change (FC = average spectral count in IRES/average spectral count in Domain I). The results are presented in a Volcano plot using protein $\log_2$ fold changes and their corresponding adjusted $\log_{10}$ *P*-values highlighted proteins up-regulated in each condition (Domain I and IRES).

RNA immunoprecipitation

The reporter plasmids containing the Wt $IRES_{5'UTR}$, mut2, mut4 upstream of Renilla coding sequence were transfected into drosophila S2 cells (Invitrogen) by the Effectene method following manufacturer's instructions (Qiagen). Forty-eight hours later, cells were lysed and immunoprecipitated with an eIF3b antibody (gift from M. Hentze) coupled to Dynabeads Protein G (Life technologies). After overnight incubation, RNA and proteins were extracted with TriZol reagent (MRC). For reverse transcriptase-quantitative polymerase chain reaction (RT-qPCR), 500 ng RNA were used to perform reverse transcription (iScript cDNA Synthesis Kit from BioRad) followed by qPCR (BioRad SYBR-Green). Primers qPCR Renilla: Fw 5′-GGATGATAACTGGTCCGCAG-3′, Rev 5′-TTGCCTGATTTGCCCATACC-3′.

RESULTS AND DISCUSSION

The 712-nt long 5′UTR of CrPV contains an IRES that mediates translation of ORF1 polyprotein (7). In order to characterize the minimal IRES element, we inserted nucleotides 1–761 from the 5′UTR or truncated versions upstream of the reporter gene Renilla luciferase which leads to the production of a fusion protein containing the first 17 viral N-terminal amino acids fused to Renilla luciferase peptide sequence. These constructs were *in vitro* transcribed and used for *in vitro* translation assays using S2 cell-free translation extracts. Renilla luciferase activity was used to measure the IRES translational activity driven by each RNA construct.

First, we demonstrated that capped and uncapped RNA constructs are stable in S2-cell extracts and have identical translational activity (Supplementary Figure S1). We only used uncapped RNA in subsequent experiments. We then proceeded to map the location of the IRES. Truncations from the 5′ end revealed that the 5′ distal half of the 5′UTR is not required for IRES activity, but that the 5′ proximal half is essential (Figure 1A). More precise 5′ and 3′ truncations revealed that the minimal IRES element is located between nucleotides 357 and 761 (Figure 1B).

Translation efficiency was not modified when the N-terminal viral sequence coding for the first 17 amino acids was deleted, indicating that the minimal $IRES_{5'UTR}$ is located precisely between nucleotides 357 and 709 (see construct 0 aa in Figure 2A). We next investigated whether the $IRES_{5'UTR}$ is able to recruit the ribosome and promote scanning for a downstream AUG start codon. We mutated the viral AUG start codon at position 709 to ACG and observed a dramatic decrease of translation activity. This indicates that $IRES_{5'UTR}$ is not able to promote scanning to reach the Renilla luciferase AUG codon further downstream and that it needs a genuine AUG start codon in its immediate vicinity (Figure 2A). To further analyze the ability of $IRES_{5'UTR}$ to drive efficient ribosomal scanning, we re-introduced in-frame AUG start codons (at codon number 5 and 8) downstream of the cognate AUG start codon mutated to ACG. In order to avoid AUG context effects, we kept the wt AUG flanking sequence, namely A at position −3 and U at position +4 for these AUGs. (Figure 2B). When the start codon was placed at codon 5, the translation efficiency was already dramatically reduced (∼4-fold reduction), and when it was placed at codon 8 the $IRES_{5'UTR}$ was almost totally inactive.

Interestingly, when a stop codon is introduced between the two in-frame AUGs, translation is less severely affected. This suggests that the ribosome cannot undergo a shunting mechanism to bypass the stop codon but rather terminates at the UAA codon and then proceed to partial re-initiation on the next Renilla AUG codon. This probably explains the better translation efficiency with the variant containing the UAA codon (Figure 2A). These experiments confirmed that $IRES_{5'UTR}$ drives efficient ribosome assembly on the genuine viral start codon but is not able to promote scanning for another AUG start codon further downstream. The observation that $IRES_{5'UTR}$ was able to drive translation initiation with the same efficiency for three other constructs containing frame shifting of the coding sequence by inserting 1, 2 and 3 nts upstream of the first AUG supports this interpretation (Figure 2C).

Altogether, our data show that $IRES_{5'UTR}$ recruits ribosomes to its cognate viral AUG start codon, and is not able to scan for an alternative AUG start codon further downstream. This is evocative of type III IRES (5), and contrasts with the model proposed for the related discistrovirus *Rhapdopsilum padi* virus (RhPV). Reconstitution experiments revealed that the $IRES_{5'UTR}$ from RhPV requires the scanning factor eIF1 in addition to eIF2 and eIF3 for translation and belongs to the type I category of IRES (22). Similarly, the $IRES_{5'UTR}$ from another positive-strand unclassified virus, Halastavi arva virus (34), behaves like a type I IRES and allows the recruited ribosome to perform retrograde scanning (35). The cadicivirus $IRES_{5'UTR}$ from the picornavirus family, which shares a similar dicistronic genome structure (36), is also a type I IRES that promotes normal 5′ scanning (37). These differences in the translation mechanism are consistent with the large differences both in size and sequence between the $IRES_{5'UTR}$ from members of this virus family, which contrast with the high conservation of the $IRES_{IGR}$ (10,23,24). They suggest that $IRES_{5'UTR}$ from dicistroviruses might use different strategies to recruit the host translational machinery, reflecting evolution of distinct host adaptation strategies among members of this virus family.

We next determined the secondary structure of the whole 5′UTR using the SHAPE method (28), after checking that the 709-nt long RNA was homogeneously folded (Supplementary Figure S2A). The resulting predicted 2D model shows that the overall 5′UTR contains three highly structured domains that are separated by flexible linkers (Figure 3). Domain I encompasses nucleotides 1–263 and contains five stem-loops. Domain II (302–466) and III (505–689) present a more sophisticated secondary structure with hairpins and three- and four-way junctions. Based on our deletion experiments (Figures 1 and 2), we mapped the minimal $IRES_{5'UTR}$ to nucleotides 357–709, which is in good agreement with our predicted secondary structure model. Indeed, construct 365 in which the first-half of P1 in domain II is deleted has a 4-fold reduction of its translation activity compared with constructs 360 and 357. Therefore, the minimal $IRES_{5'UTR}$ requires domains II and III to be fully active.

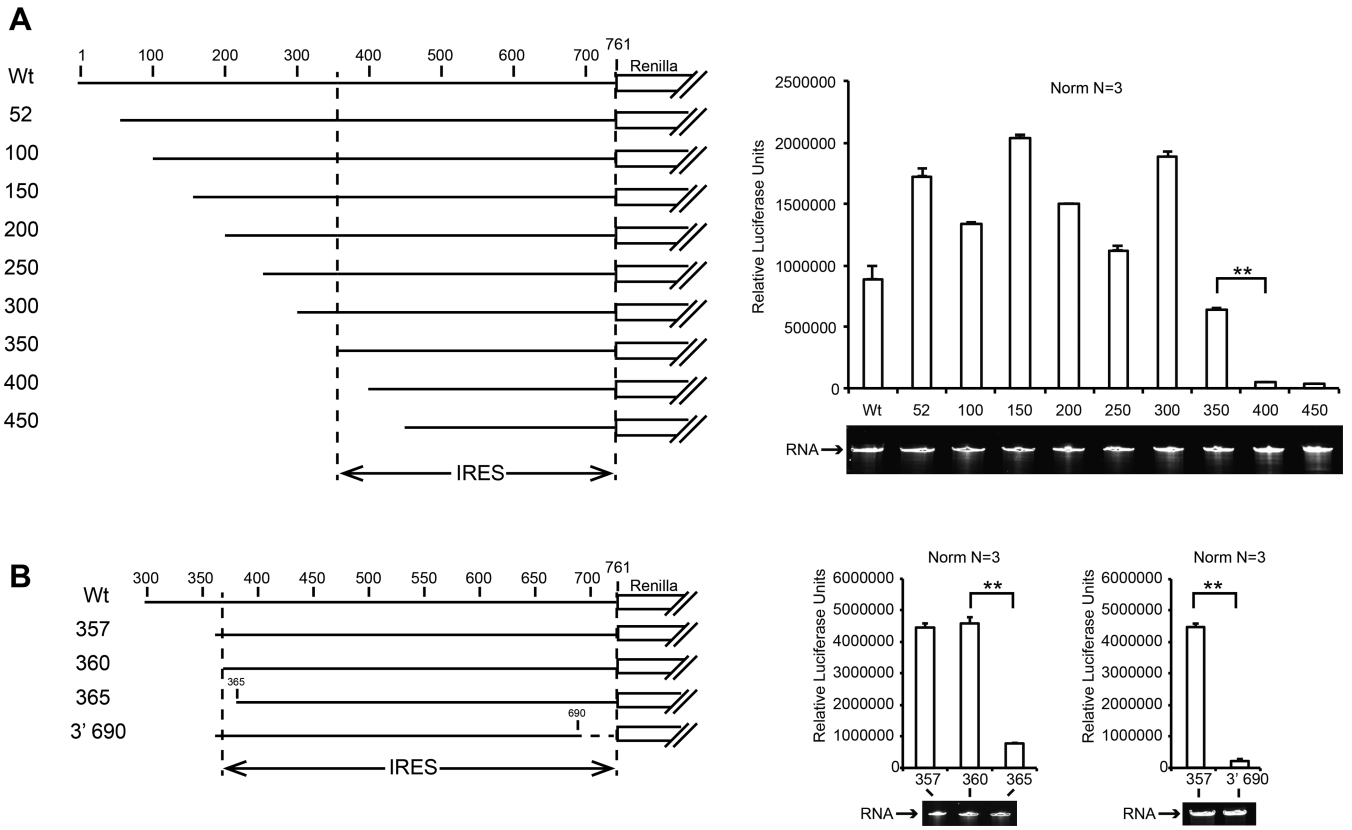

Figure 1. Mapping of the minimal IRES sequence in the 5′UTR of CrPV by 5′ and 3′ truncation. On the left panels, a cartoon representation of Renilla luciferase reporter transcripts used in S2 cell-free translation extracts is shown. On the right panels, translation efficiencies are represented as raw bioluminescence activity (Relative Light Units or RLU) for each transcript. Standard deviations or translational activity for each transcript are shown and calculated from three independent experiments. $^{**}P < 0.005$ based on Student's *t*-test. RNA integrity was controlled by 4% denaturing polyacrylamide gel electrophoresis (PAGE) and Ethidium Bromide staining. (**A**) IRES mapping within the entire CrPV 5′UTR and (**B**) precise mapping of 5′ and 3′ ends of the $IRES_{5'UTR}$ from CrPV.

Domains II and III from $IRES_{5'UTR}$ are separated by a flexible region, which contains a 7-nt loop and 6 bp stem. Since domains II and III are sufficient for $IRES_{5'UTR}$ activity, we also determined the secondary structure of the minimal $IRES_{5'UTR}$ construct isolated from the full-length 5′UTR. The SHAPE analysis revealed highly similar reactivities between the full length and minimal IRES construct (Supplementary Figure S3) indicating that domain II and III retain their structure in an RNA fragment containing residues 357–754 (Pearson correlation coefficient $R_{Pearson} = 0.8$). Therefore, domains II and III can fold independently from domain I.

A closer look at the SHAPE reactivity in domain II revealed that loops J3/3a (382GGGA385) and L5 (436UCCC439) are completely inaccessible to the SHAPE reagent (Figure 4A; Supplementary Figure S2B and C). Moreover, the J3/3a and L5 loops contain complementary sequences suggesting long-range base pairs mediated by a pseudoknot structure, as the ShapeKnots algorithm helped us pinpoint (30). To strengthen this observation, we performed DMS and CMCT probing. The pattern of DMS/CMCT reactivities supports the 2D structure predicted on the basis of the SHAPE data (Figure 3, see insert). The absence of DMS/CMCT reactivity for the nucleotides involved in the putative pseudoknot structure confirms the SHAPE analysis and further supports the existence of a long-range interaction between these residues.

To demonstrate the presence of the pseudoknot structure, we constructed minimal $IRES_{5'UTR}$ fragments containing mutations in J3/3a and L5. Mutants m1 and m2 contained non-complementary sequences in the two loops, whereas mutants m3 and m4 contained compensatory mutations that are complementary but different from the wt sequence (Figure 4A). In compensatory mutant m3, 3 nts in the loops of the putative pseudoknot have been swapped whereas in m4, the 4 nts have been swapped. To assess the impact of these mutations on the $IRES_{5'UTR}$ secondary structure, we determined the SHAPE reactivity profiles of the four mutants in the buffer used for translation assays (see 'Materials and Methods' section; Supplementary Figure S4) and compared it with the wt $IRES_{5'UTR}$. As expected, the loops J3/3a and L5 are more reactive to the SHAPE reagent in the non-complementary mutants m1 and m2 than in the wt sequence indicating an increased flexibility (Figure 4B, green boxes). On the contrary, compensatory mutants m3 and m4 have reduced accessibility to the SHAPE reagent in loops J3/J3a and L5, as observed for the wt $IRES_{5'UTR}$, suggesting that these loops are indeed involved in a pseudoknot interaction. Moreover, mutations m1 and m2 not only destabilize the long-range interaction but also affect

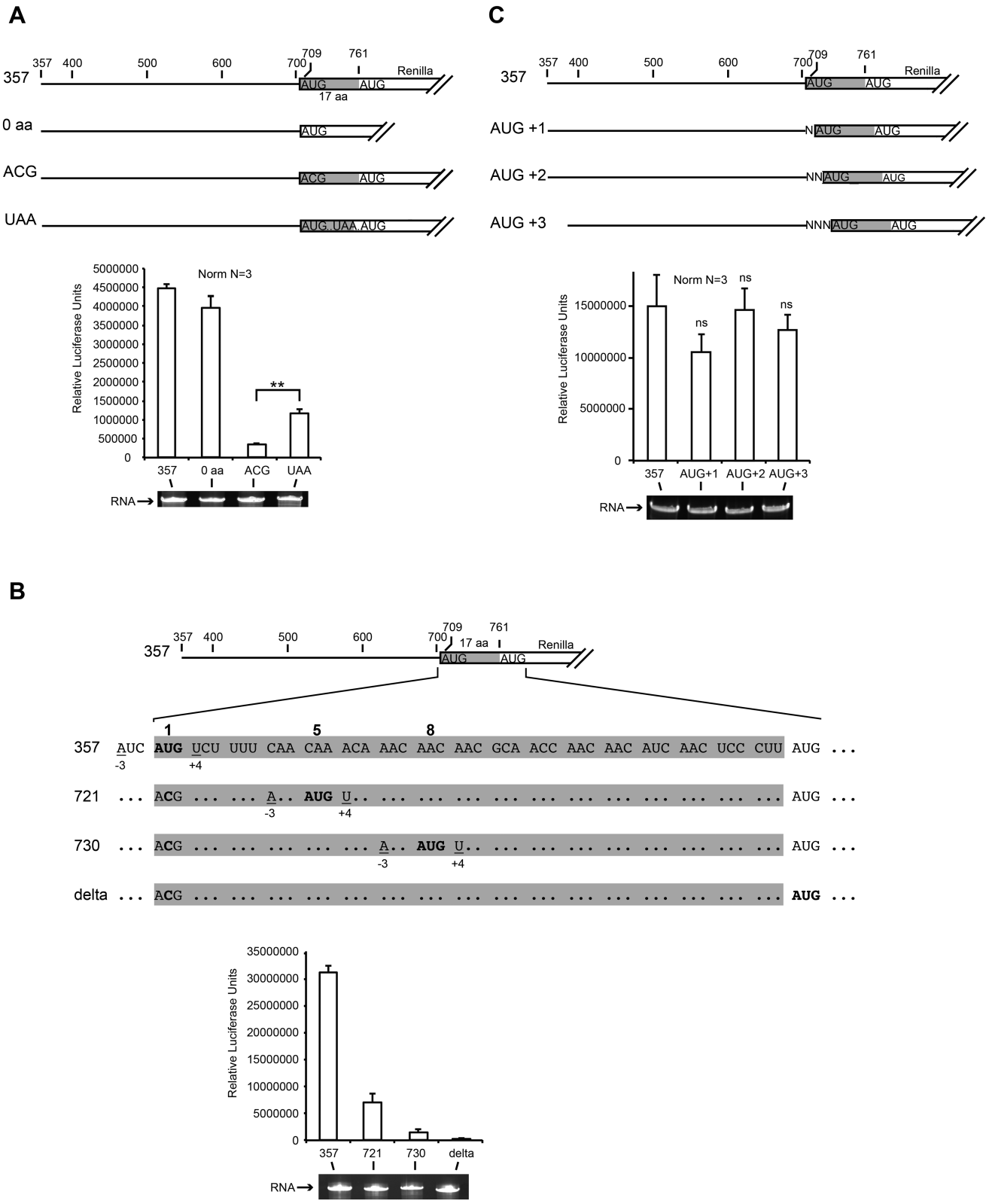

Figure 2. AUG start codon recognition during CrPV $IRES_{5'UTR}$-driven translation initiation Renilla luciferase reporter transcripts used in S2 cell-free translation are represented as raw bioluminescence activity (RLU) for each transcript. Standard deviations or translational activity for each transcript are shown and calculated from three independent experiments. $^{**}P < 0.005$ based on Student's *t*-test; ns, nonsignificant. RNA integrity was controlled by 4% denaturing PAGE and Ethidium Bromide staining. Viral coding sequences are shown in gray and fused to Renilla luciferase coding sequence. (**A**) $IRES_{5'UTR}$ drives translation initiation on viral cognate AUG start codon but does not promote scanning further downstream to find the Renilla AUG when the viral AUG is mutated to ACG (**B**) In these transcripts, the cognate viral AUG start codon is mutated to ACG. In addition in-frames AUGs were inserted at codon position 5 and 8 with the same context than the wt viral AUG. The 5′ proximal AUG codons are shown in bold. (**C**) In these transcripts the cognate viral AUG is shifted by 1, 2 or 3 nts.

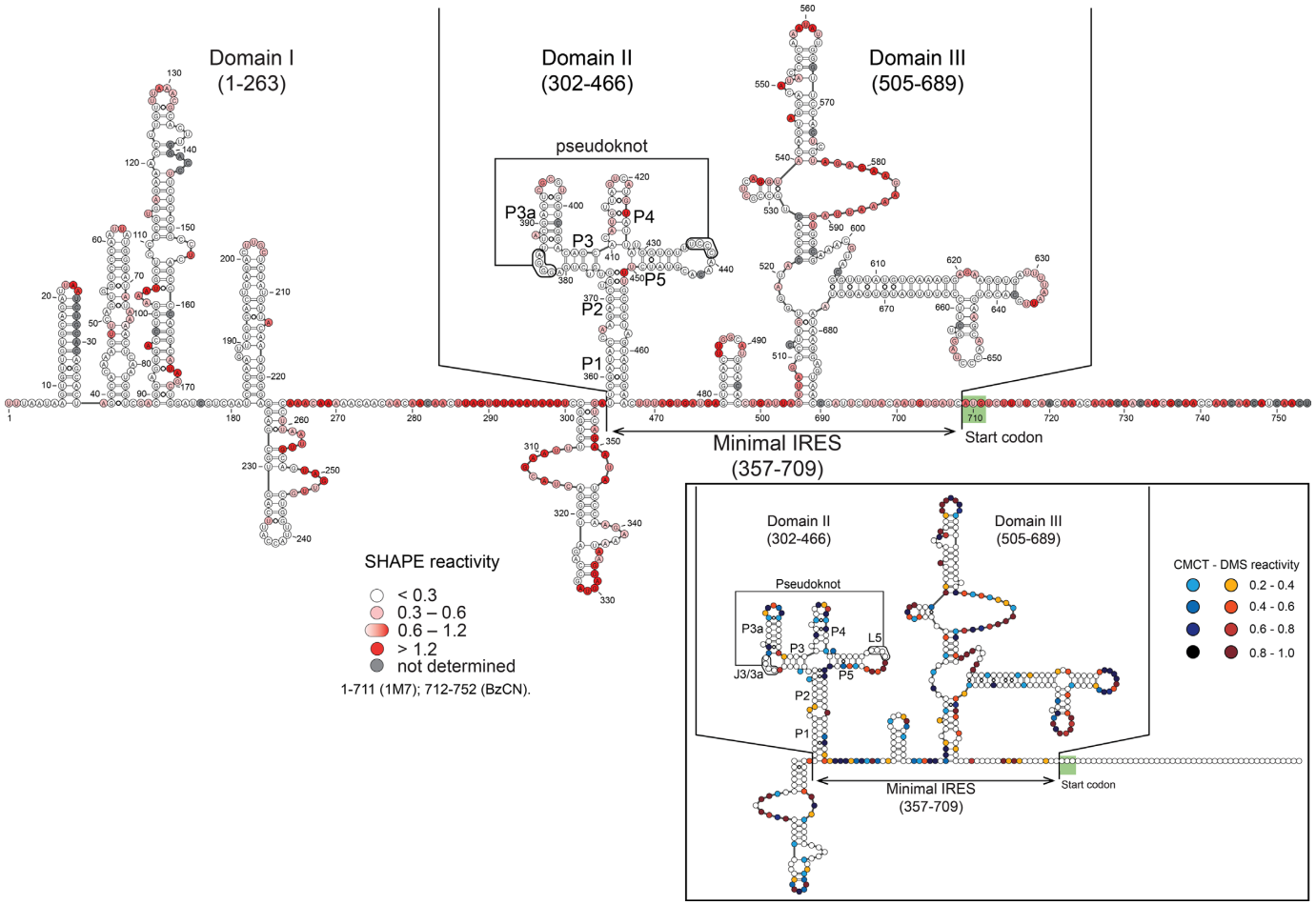

Figure 3. The predicted secondary structure of the $IRES_{5'UTR}$ of CrPV reveals three highly structured domains named I, II and III separated by flexible linkers. Selective 2′-hydroxyl acylation analyzed by primer extension (SHAPE) data are overlaid on the structure prediction for the full-length 5′UTR RNA. Reactivities are shown as averages from three independent experiments (except for region 711–754: average from two experiments). Position of the minimal IRES is indicated (375–709). DMS and CMCT reactivity data for the minimal IRES domain (357–710). Reactivities are represented as averages from three independent experiments in the box of the right part of the figure. Nucleotides from J3/3a and L5 involved in long-distance interaction to form the pseudoknot are boxed. Reactivity values with standard deviations are listed in Supplementary Tables S1–4.

the overall folding of domain II when compared with the wt $IRES_{5'UTR}$ as shown by the Pearson correlation coefficients for both m1 and m2 mutants with the wt structure ($R_{Pearson} = 0.2$) (Alternative folds for m1 and m2 are presented in Supplementary Figure S5). Both compensatory mutants m3 and m4 present an overall folding of domains II and III very close to that of the wt $IRES_{5'UTR}$ ($R_{Pearson} = 0.9$) (Figure 4B). Altogether, these data demonstrate that loops J3/3a and L5 are involved in a pseudoknot structure and that this long-range interaction is essential to reach the native folding of domain II.

We next addressed the requirement of the pseudoknot structure for the $IRES_{5'UTR}$ translation activity. Mutants m1–m4 were inserted upstream of Renilla luciferase coding sequences in reporter constructs and the IRES activity was tested in *in vitro* translation assays with S2 cell-free extracts. The mutants m1 and m2 were inactive and unable to drive efficient translation, whereas mutants m3 and m4 showed partial or even fully restored $IRES_{5'UTR}$ activity (60 and 90% respectively) (Figure 4C). We conclude that the pseudoknot structure is essential for the $IRES_{5'UTR}$ activity, indicating that these long-range distances are required for proper folding and translation initiation. In addition, a 3 bp inversion in mutant m3 is less efficient than a full 4 bp inversion as shown by the near wt IRES activity driven by mutant m4.

In order to determine the precise role of the pseudoknot structure, we performed translation initiation complex assembly and analyzed these complexes by sucrose gradient analysis. We first checked that the mutations did not affect RNA stability in S2-cell extracts (Supplementary Figure S6). Then, in the presence of GMP-PNP (a non-hydrolysable GTP-analog), the wt IRES showed accumulation of the 48S pre-initiation complexes (Figure 4D and Supplementary Figure S7). As expected the null mutants m1 and m2 showed a significant decrease in the 48S complex formation. The compensatory mutant m3 and m4 restored 48S complex assembly although with different efficiencies. The most efficient mutant was m4 as already observed in previous *in vitro* translation experiments with S2 cell-free extracts (Figure 4C). Taken together, these experiments indicate that the pseudoknot structure in domain II

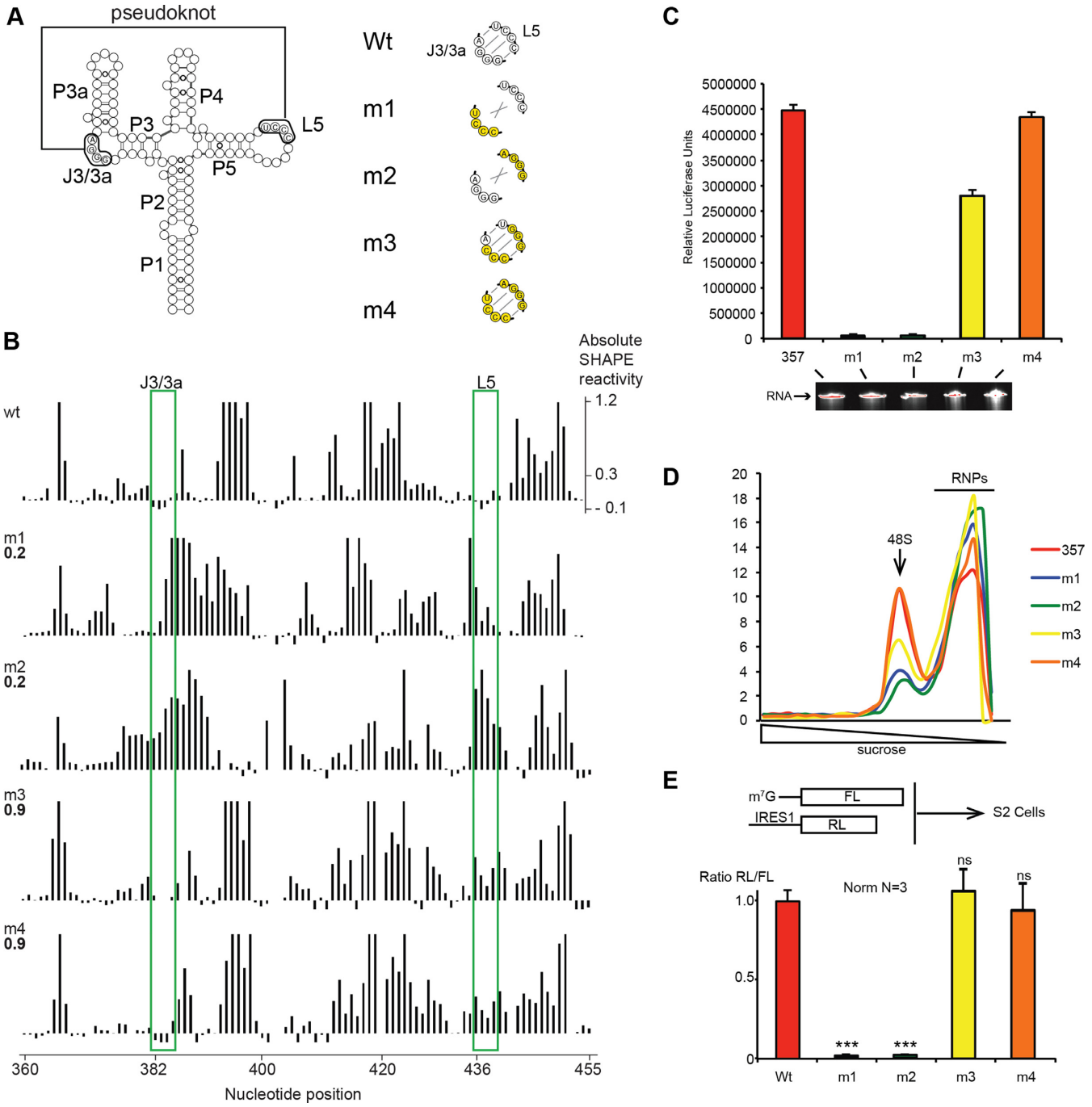

Figure 4. A pseudoknot is required for correct folding and efficient $IRES_{5'UTR}$ -driven translation. (**A**) Mutants in the J3/3a and/or L5 regions used in this study, mutated nucleotides are shown in yellow. (**B**) Absolute SHAPE reactivities for 357–754 RNA transcripts with either wt or m1–m4 mutant sequence. Reactivities are shown as averages from two independent experiments (reactivity values with standard deviation are given in Supplementary Table S2). The Pearson correlation coefficients ($R_{Pearson}$) with the 357–754 wt dataset are shown on the left of each histogram. J3/3a and L5 are boxed in green. (**C**) Translation activity of IRES 357–754 wt and mutants m1–m4 when placed upstream of Renilla luciferase coding region. RNA integrity control by denaturing 4% sodium dodecyl sulphate-PAGE is shown under the histogram. (**D**) Pre-initiation complex assembly and analysis on 7–47% sucrose gradient with P^{32} radio-labeled wt and mutant m1–m4 IRES. (**E**) *In vivo* translation assay using monocistronic reporters transfected in S2 cells. The mutants m1–m4 are compared with wt $IRES_{5'UTR}$ activity. $*P < 0.05$ and $**P < 0.005$, $***P < 0.0005$ based on Student's *t*-test.

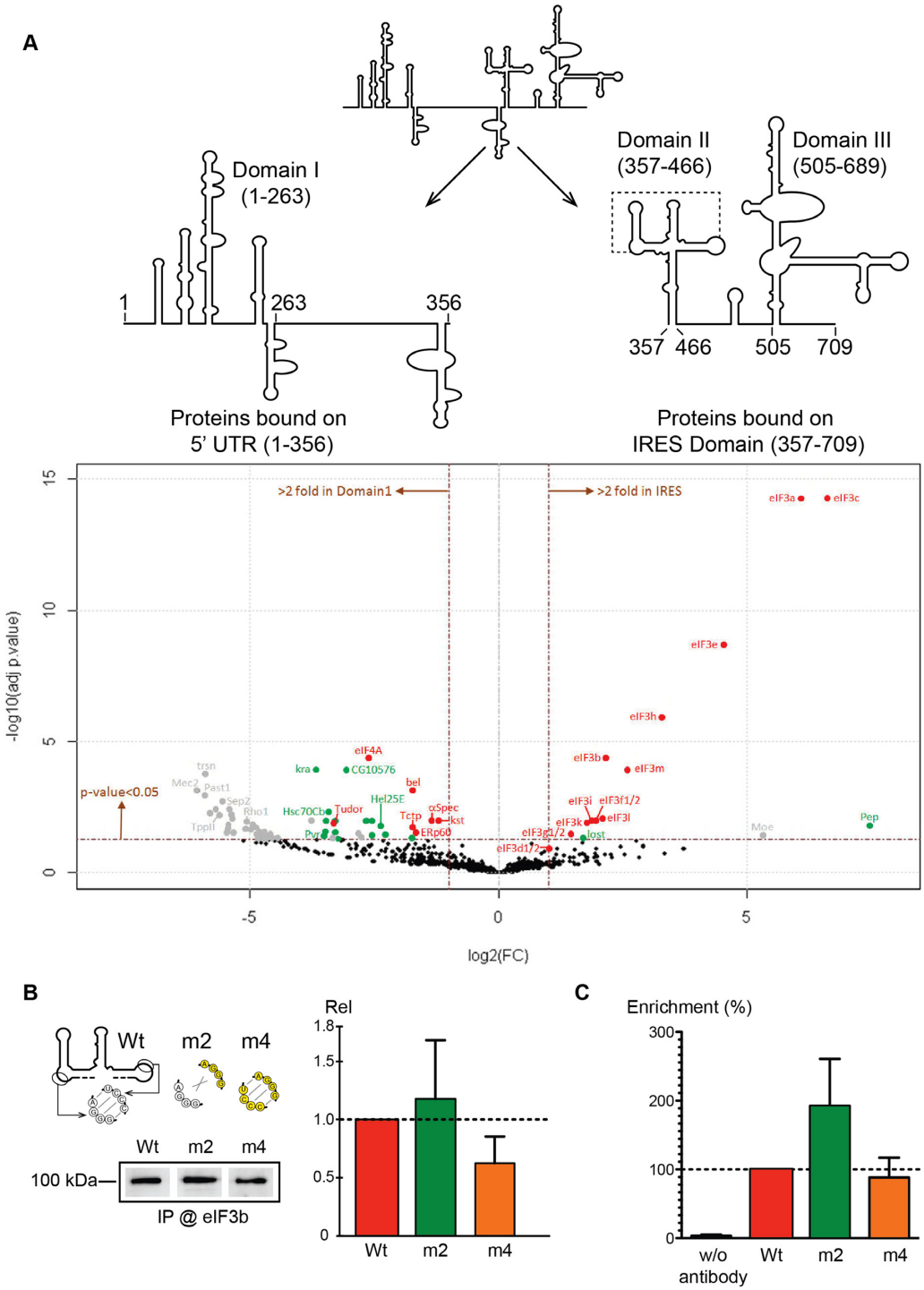

Figure 5. Eukaryotic initiation factor (eIF)3 is recruited specifically by the $IRES_{5'UTR}$ in a pseudoknot-independent manner. (**A**) Mass spectrometry analysis of edeine-blocked translation initiation complexes on the 5′ proximal fragment (1–356) and the minimal IRES (357–709). Graphical representation of proteomics data: protein $\log_2$ spectral count fold changes (on the *x*-axis) and the corresponding adjusted $\log_{10}$ *P*-values (on the *y*-axis) are plotted in a pairwise volcano plot**.** The significance thresholds are represented by a horizontal dashed line (*P*-value = 0.05, negative-binomial test with Benjamini–Hochberg adjustment) and two vertical dashed lines (−2.0-fold on the left and +2.0-fold on the right). Data points in the upper left and upper right quadrants indicate significant negative and positive changes in protein abundance. Protein names are labeled next to the off-centered spots and they are depicted according to the following color code: proteins represented by a red spot are identified by more than 30 MS/MS spectra, by a green spot when identified by 11–30 spectra and by a gray spot when identified by <10 spectra. Data points are plotted on the basis of average spectral counts from triplicate analysis. For an exhaustive list of hits, see Supplementary Table S5. (**B**) Western blots analysis with drosophila eIF3b antibody of edeine-blocked translation initiation complexes programmed with Wt and m2 and m4 mutants. The complexes were assembled *in vitro* in S2-cell extracts. The histogram represents the quantification of three independent experiments. (**C**) *In vivo* RNA immunoprecipitation of $IRES_{5'UTR}$-Renilla reporter mRNA in S2 cells. Wt, m2 and m4 mRNA were immunoprecipitated using drosophila eIF3b antibody and quantified by RT-qPCR. The histogram represents the quantification of three independent experiments. The enrichment fold was calculated by the ratio between immunoprecipitated and the input and was set to 100% for the Wt.

is essential for 48S pre-initiation complex formation and is therefore essential at an early step of translation initiation.

Finally, mutants m1–m4 were tested for IRES activity *in vivo* using monocistronic reporters transfected in S2 cells (Figure 4E). Here again, m1 and m2 mutants were totally inactive, whereas the IRES activity was restored to the same extent for m3 and m4 mutants. Taken together, this demonstrates that the pseudoknot structure is essential for $IRES_{5'UTR}$ activity *in vivo* as well.

To further characterize the CrPV $IRES_{5'UTR}$, we performed mass spectrometry analysis on translation initiation complexes in order to determine the factors that bind specifically to the IRES. To do so, translation initiation complexes were assembled on a biotinylated CrPV $IRES_{5'UTR}$ in S2-cell extracts. Translation initiation complexes were then first immobilized on magnetic streptavidin beads and subsequently eluted by DNAse treatment as previously described (33,38). The composition of the purified translation initiation complex was then determined by mass spectrometry. To determine the factors required at the initial step of the translational process, translation initiation was blocked by addition of edeine, which prevents initiator $tRNA^{Met}$ codon–anticodon interaction in the P-site of the ribosome (39–41). As a negative control, we performed the same experiments with the 5′ proximal part of the 5′UTR that is not essential for IRES activity. Interestingly, 12 of the 13 subunits of eIF3 are specifically found on the IRES fragment, indicating that $IRES_{5'UTR}$ recruits this factor (Figure 5A and Supplementary Table S5), the only missing factor being eIF3j. However, we have previously shown that eIF3j is required for the activity of $IRES_{5'UTR}$ (25). In yeast, eIF3j/hcr1 has been shown to participate in efficient AUG recognition during the scanning process by directly interacting with eIF1A for canonical cap-dependent translation (42). A similar function has also been proposed for mammalian eIF3j (43,44). Since we have shown that $IRES_{5'UTR}$ does not promote scanning for initiation on the viral AUG, our data show that eIF3j has a different function for $IRES_{5'UTR}$. We propose that eIF3j is essential for ribosome recruitment to the $IRES_{5'UTR}$ and that it dissociates after complex formation prior to AUG recognition.

In order to determine whether the pseudoknot is necessary for eIF3 recruitment, pre-initation complexes were programmed *in vitro* with S2-cell extracts with Wt, m2 and m4 and were purified as previously described. Western blot analysis with an antibody specific for drosophila eIF3b subunit showed that mutant m2 (which has no pseudoknot) is also able to recruit eIF3 suggesting that eIF3 interaction does not require the pseudoknot (Figure 5B). To further corroborate this statement *in vivo*, Renilla reporter mRNAs containing the Wt $IRES_{5'UTR}$ and mutants m2 and m4 were transfected in S2 cells. Then we performed RNA immunoprecipication with an antibody raised against drosophila eIF3b subunit, we quantified the Renilla reporter mRNA by RT-qPCR. Indeed, mutant m2 is also able to interact with eIF3 *in vivo* confirming that the pseudoknot is not required for eIF3 recruitment (Figure 5C). The interaction between the $IRES_{5'UTR}$ and eIF3 is transient during the translation initiation process. In both experiments, mutant m2 seems to interact more efficiently than Wt and m4, this might be explained by the fact that mutant m2 is inactive and therefore accumulates more complexes with eIF3 than Wt and m4.

The $IRES_{5'UTR}$ is preceded by domain I which is dispensable for translational activity. A few other proteins bind specifically to this domain (Figure 5A and Supplementary Table S5). These secondary structures might be involved in other steps required for viral propagation such as initiation of replication or encapsidation. Our data are in good agreement with previous observations made while constructing an infectious molecular clone of CrPV (45). The authors isolated a clone containing a duplication of fragment 75–271, which inhibits viral infectivity. In our secondary structure model, this duplication is located in domain I, away from the minimal IRES sequence. The duplication however has no effect on viral translation and RNA accumulation during CrPV infection suggesting it impacts viral entry and/or viral packaging (46).

In addition, the structured arrangements of domains II and III with several helices connected by three- and four-way junctions and loops is reminiscent of those in the classical swine fever virus (CSFV), the Hepatitis-C virus (HCV), the foot-and-mouth disease virus (FMDV) and other IRESes (6). These structured domains were shown to be important for IRES function, through binding to eIF3 (47), promoting long-range interactions (48,49), or binding to IRES-*trans* acting factors (50,51). The secondary structure of the apical domain II in CrPV $IRES_{5'UTR}$ that harbors a pseudoknot bears some resemblance to that of residues 153–255 in CSFV and residues 134–249 in FMDV (Supplementary Figure S8). Automatic 2D-based 3D-RNA modeling suggests that, because of the pseudoknot, the four-way junction would adopt a topology closer to that of the L-shaped CSFV (52), than to the topology modeled for FMDV (49). Future studies using X-ray crystallography or cryo-EM will be needed to pinpoint the similarities and differences in how type III IRES domains fold, and what role they play in IRES function.

In summary, the $IRES_{5'UTR}$ contains a three-way junction structure with a pseudoknot that recruits the ribosome on the cognate viral AUG start codon without any scanning step. Moreover $IRES_{5'UTR}$ specifically recruits eIF3. This is reminiscent of translation driven by the HCV–IRES, the prototypic type III IRES (5). This similarity between CrPV $IRES_{5'UTR}$ and HCV–IRES is in agreement with the fact that both IRES are strictly dependent on the ribosomal protein RACK1. On the contrary $IRES_{IGR}$-driven translation efficiency does not require the presence of RACK1 on the ribosome, suggesting fundamentally distinct molecular mechanisms for ribosome recruitment (53). The structural characterization of the $IRES_{5'UTR}$ from CrPV will facilitate the investigation of the role played by RACK1 in cap-independent translation. During CrPV infection, the $IRES_{5'UTR}$ promotes translation from ORF1 in a constitutive manner during the whole infectious process, whereas $IRES_{IGR}$-driven translation starts in the second half of infection and is boosted in the late phase of infection (11). The molecular basis for this differential expression pattern, which is essential for the progression of the viral infection, remains unexplored. Our data on the $IRES_{5'UTR}$ represent a first step toward a better understanding of the concerted ac-

tion of the two structurally and functionally different IRES active in dicistroviruses.

SUPPLEMENTARY DATA

Supplementary Data are available at NAR Online.

ACKNOWLEDGEMENTS

We thank Claire Batisse and Adeline Renaud for S2-cell extracts preparation. We are thankful to Matthias Hentze for *drosophila* eIF3 antibodies. We also thank Redmond P. Smyth for critical reading of the manuscript.

FUNDING

Centre National de la Recherche Scientifique (CNRS); Université de Strasbourg; Investissement d'Avenir program [NetRNA ANR-10-LABX-36, ANR ANR-11-SVSE802501]. Funding for open access charge: Centre National de la Recherche Scientifique.
Conflict of interest statement. None declared.

REFERENCES

1. Walsh,D. and Mohr,I. (2011) Viral subversion of the host protein synthesis machinery. *Nat. Rev. Microbiol.*, **9**, 860–875.
2. Joachims,M., Van Breugel,P.C. and Lloyd,R.E. (1999) Cleavage of poly(A)-binding protein by enterovirus proteases concurrent with inhibition of translation in vitro. *J. Virol.*, **73**, 718–727.
3. Etchison,D., Milburn,S.C., Edery,I., Sonenberg,N. and Hershey,J.W. (1982) Inhibition of HeLa cell protein synthesis following poliovirus infection correlates with the proteolysis of a 220, 000-dalton polypeptide associated with eucaryotic initiation factor 3 and a cap binding protein complex. *J. Biol. Chem.*, **257**, 14806–14810.
4. Kuyumcu-Martinez,N.M., Joachims,M. and Lloyd,R.E. (2002) Efficient cleavage of ribosome-associated poly(A)-binding protein by enterovirus 3C protease. *J. Virol.*, **76**, 2062–2074.
5. Jackson,R.J., Hellen,C.U.T. and Pestova,T. V (2010) The mechanism of eukaryotic translation initiation and principles of its regulation. *Nat. Rev. Mol. Cell Biol.*, **11**, 113–127.
6. Filbin,M.E. and Kieft,J.S. (2009) Toward a structural understanding of IRES RNA function. *Curr. Opin. Struct. Biol.*, **19**, 267–276.
7. Bonning,B.C. and Miller,W.A. (2010) Dicistroviruses. *Annu. Rev. Entomol.*, **55**, 129–150.
8. Garrey,J.L., Lee,Y.-Y., Au,H.H.T., Bushell,M. and Jan,E. (2010) Host and viral translational mechanisms during cricket paralysis virus infection. *J. Virol.*, **84**, 1124–1138.
9. Moore,N.F., Kearns,A. and Pullin,J.S. (1980) Characterization of cricket paralysis virus-induced polypeptides in Drosophila cells. *J. Virol.*, **33**, 1–9.
10. Wilson,J.E., Powell,M.J., Hoover,S.E. and Sarnow,P. (2000) Naturally occurring dicistronic cricket paralysis virus RNA is regulated by two internal ribosome entry sites. *Mol. Cell. Biol.*, **20**, 4990–4999.
11. Khong,A., Bonderoff,J.M., Spriggs,R. V, Tammpere,E., Kerr,C.H., Jackson,T.J., Willis,A.E. and Jan,E. (2016) Temporal regulation of distinct internal ribosome Entry sites of the dicistroviridae cricket paralysis virus. *Viruses*, **8**, doi:10.3390/v8010025.
12. Wilson,J.E., Pestova,T. V, Hellen,C.U. and Sarnow,P. (2000) Initiation of protein synthesis from the A Site of the Ribosome. *Cell*, **102**, 511–520.
13. Costantino,D.A, Pfingsten,J.S., Rambo,R.P. and Kieft,J.S. (2008) tRNA-mRNA mimicry drives translation initiation from a viral IRES. *Nat. Struct. Mol. Biol.*, **15**, 57–64.
14. Spahn,C.M.T., Jan,E., Mulder,A., Grassucci,R.A., Sarnow,P. and Frank,J. (2004) Cryo-EM visualization of a viral internal ribosome entry site bound to human ribosomes: The IRES functions as an RNA-based translation factor. *Cell*, **118**, 465–475.
15. Pestova,T. V. and Hellen,C.U.T. (2003) Translation elongation after assembly of ribosomes on the Cricket paralysis virus internal ribosomal entry site without initiation factors or initiator tRNA. *Genes Dev.*, **17**, 181–186.
16. Jan,E., Kinzy,T.G. and Sarnow,P. (2003) Divergent tRNA-like element supports initiation, elongation, and termination of protein biosynthesis. *Proc. Natl. Acad. Sci. U.S.A.*, **100**, 15410–15415.
17. Jan,E. and Sarnow,P. (2002) Factorless ribosome assembly on the internal ribosome entry site of cricket paralysis virus. *J. Mol. Biol.*, **324**, 889–902.
18. Fernàndez,I.S., Bai,X.C., Murshudov,G., Scheres,S.H.W. and Ramakrishnan,V. (2014) Initiation of translation by cricket paralysis virus IRES requires its translocation in the ribosome. *Cell*, **157**, 823–831.
19. Muhs,M., Hilal,T., Mielke,T., Skabkin,M.A., Sanbonmatsu,K.Y., Pestova,T. V. and Spahn,C.M.T. (2015) Cryo-EM of ribosomal 80s complexes with termination factors reveals the translocated cricket paralysis virus IRES. *Mol. Cell*, **57**, 422–433.
20. Pfingsten,J.S., Costantino,D.A. and Kieft,J.S. (2006) Structural basis for ribosome recruitment and manipulation by a viral IRES RNA. *Science*, **314**, 1450–1454.
21. Murray,J., Savva,C.G., Shin,B.-S., Dever,T.E., Ramakrishnan,V. and Fernández,I.S. (2016) Structural characterization of ribosome recruitment and translocation by type IV IRES. *Elife*, **5**, doi:10.7554/eLife.13567.
22. Terenin,I.M., Dmitriev,S.E., Andreev,D.E., Royall,E., Belsham,G.J., Roberts,L.O. and Shatsky,I.N. (2005) A cross-kingdom internal ribosome entry site reveals a simplified mode of internal ribosome entry. *Mol. Cell. Biol.*, **25**, 7879–7888.
23. Kanamori,Y. and Nakashima,N. (2001) A tertiary structure model of the internal ribosome entry site (IRES) for methionine-independent initiation of translation. *RNA*, **7**, 266–274.
24. Roberts,L.O. and Groppelli,E. (2009) An atypical IRES within the 5′ UTR of a dicistrovirus genome. *Virus Res.*, **139**, 157–165.
25. Majzoub,K., Hafirassou,M.L., Meignin,C., Goto,A., Marzi,S., Fedorova,A., Verdier,Y., Vinh,J., Hoffmann,J.A., Martin,F. *et al.* (2014) RACK1 controls IRES-mediated translation of viruses. *Cell*, **159**, 1086–1095.
26. Wakiyama,M., Kaitsu,Y. and Yokoyama,S. (2006) Cell-free translation system from Drosophila S2 cells that recapitulates RNAi. *Biochem. Biophys. Res. Commun.*, **343**, 1067–1071.
27. Green,M.R. and Sambrook,J. (2012) *Molecular cloning: a laboratory manual*. Cold Spring Harbor Laboratory Press, NY.
28. Wilkinson,K.A., Merino,E.J. and Weeks,K.M. (2006) Selective 2'-hydroxyl acylation analyzed by primer extension (SHAPE): quantitative RNA structure analysis at single nucleotide resolution. *Nat. Protoc.*, **1**, 1610–1616.
29. Karabiber,F., McGinnis,J.L., Favorov,O.V and Weeks,K.M. (2013) QuShape: rapid, accurate, and best-practices quantification of nucleic acid probing information, resolved by capillary electrophoresis. *RNA*, **19**, 63–73.
30. Hajdin,C.E., Bellaousov,S., Huggins,W., Leonard,C.W., Mathews,D.H. and Weeks,K.M. (2013) Accurate SHAPE-directed RNA secondary structure modeling, including pseudoknots. *Proc. Natl. Acad. Sci. U.S.A.*, **110**, 5498–5503.
31. Darty,K., Denise,A. and Ponty,Y. (2009) VARNA: Interactive drawing and editing of the RNA secondary structure. *Bioinformatics*, **25**, 1974–1975.
32. Popenda,M., Szachniuk,M., Antczak,M., Purzycka,K.J., Lukasiak,P., Bartol,N., Blazewicz,J. and Adamiak,R.W. (2012) Automated 3D structure composition for large RNAs. *Nucleic Acids Res.*, **40**, e112.
33. Chicher,J., Simonetti,A., Kuhn,L., Schaeffer,L., Hammann,P., Eriani,G. and Martin,F. (2015) Purification of mRNA-programmed translation initiation complexes suitable for mass spectrometry analysis. *Proteomics*, **15**, 2417–2425.
34. Boros,Á., Pankovics,P., Simmonds,P. and Reuter,G. (2011) Novel positive-sense, single-stranded RNA (+ssRNA) virus with di-cistronic genome from intestinal content of freshwater carp (Cyprinus carpio). *PLoS One*, **6**, e29145.
35. Abaeva,I.S., Pestova,T.V and Hellen,C.U.T. (2016) Attachment of ribosomal complexes and retrograde scanning during initiation on the Halastavi árva virus IRES. *Nucleic Acids Res.*, **44**, 2362–2377.

36. Woo,P.C.Y., Lau,S.K.P., Choi,G.K.Y., Huang,Y., Teng,J.L.L., Tsoi,H.-W., Tse,H., Yeung,M.L., Chan,K.-H., Jin,D.-Y. *et al.* (2012) Natural occurrence and characterization of two internal ribosome entry site elements in a novel virus, Canine Picodicistrovirus, in the Picornavirus-like superfamily. *J. Virol.*, **86**, 2797–2808.
37. Asnani,M., Pestova,T.V and Hellen,C.U.T. (2016) Initiation on the divergent Type I cadicivirus IRES: factor requirements and interactions with the translation apparatus. *Nucleic Acids Res.*, **44**, 3390–3407.
38. Prongidi-Fix,L., Schaeffer,L., Simonetti,A., Barends,S., Ménétret,J.-F., Klaholz,B.P., Eriani,G. and Martin,F. (2013) Rapid purification of ribosomal particles assembled on histone H4 mRNA: a new method based on mRNA-DNA chimaeras. *Biochem. J.*, **449**, 719–728.
39. Odon,O.W., Kramer,G., Henderson,A.B., Pinphanichakarn,P. and Hardesty,B. (1978) GTP hydrolysis during methionyl-tRNAf binding to 40 S ribosomal subunits and the site of edeine inhibition. *J. Biol. Chem.*, **253**, 1807–1816.
40. Garreau de Loubresse,N., Prokhorova,I., Holtkamp,W., Rodnina,M.V., Yusupova,G. and Yusupov,M. (2014) Structural basis for the inhibition of the eukaryotic ribosome. *Nature*, **513**, 517–522.
41. Kozak,M. and Shatkin,A.J. (1978) Migration of 40 S ribosomal subunits on messenger RNA in the presence of edeine. *J. Biol. Chem.*, **253**, 6568–6577.
42. Aylett,C.H.S., Boehringer,D., Erzberger,J.P., Schaefer,T. and Ban,N. (2015) Structure of a yeast 40S-eIF1-eIF1A-eIF3-eIF3j initiation complex. *Nat. Struct. Mol. Biol.*, **22**, 269–271.
43. ElAntak,L., Wagner,S., Herrmannova,A., Karaskova,M., Rutkai,E., Lukavsky,P.J. and Valasek,L. (2010) The indispensable n-terminal half of eIF3j/hcr1 cooperates with its structurally conserved binding partner eIF3b/prt1-rrm and with eiF1A in stringent aug selection. *J. Mol. Biol.*, **396**, 1097–1116.
44. Sokabe,M. and Fraser,C.S. (2014) Human eukaryotic initiation factor 2 (eIF2)-GTP-Met-tRNAi ternary complex and eIF3 stabilize the 43 S preinitiation complex. *J. Biol. Chem.*, **289**, 31827–31836.
45. Kerr,C.H., Wang,Q.S., Keatings,K., Khong,A., Allan,D., Yip,C.K., Foster,L.J. and Jan,E. (2015) The 5′ untranslated region of a novel infectious molecular clone of the dicistrovirus cricket paralysis virus modulates infection. *J. Virol.*, **89**, 5919–5934.
46. Kerr,C.H., Wang,Q.S., Keatings,K., Khong,A., Allan,D., Yip,C.K., Foster,L.J. and Jan,E. (2015) The 5′ untranslated region of a novel infectious molecular clone of the dicistrovirus cricket paralysis virus modulates infection. *J. Virol.*, **89**, 5919–5934.
47. Hashem,Y., des Georges,A., Fu,J., Buss,S.N., Jossinet,F., Jobe,A., Zhang,Q., Liao,H.Y., Grassucci,R.A., Bajaj,C. *et al.* (2013) High-resolution cryo-electron microscopy structure of the Trypanosoma brucei ribosome. *Nature*, **494**, 385–389.
48. Fernández-Miragall,O. and Martínez-Salas,E. (2003) Structural organization of a viral IRES depends on the integrity of the GNRA motif. *RNA*, **9**, 1333–1344.
49. Jung,S. and Schlick,T. (2013) Candidate RNA structures for domain 3 of the foot-and-mouth-disease virus internal ribosome entry site. *Nucleic Acids Res.*, **41**, 1483–1495.
50. Pacheco,A. and Martinez-Salas,E. (2010) Insights into the biology of IRES Elements through riboproteomic approaches. *J. Biomed. Biotechnol.*, **2010**, 1–12.
51. Lozano,G. and Martínez-Salas,E. (2015) Structural insights into viral IRES-dependent translation mechanisms. *Curr. Opin. Virol.*, **12**, 113–120.
52. Hashem,Y., des Georges,A., Dhote,V., Langlois,R., Liao,H.Y., Grassucci,R.A., Pestova,T. V, Hellen,C.U.T. and Frank,J. (2013) Hepatitis-C-virus-like internal ribosome entry sites displace eIF3 to gain access to the 40S subunit. *Nature*, **503**, 539–543.
53. Majzoub,K., Hafirassou,M.L., Meignin,C., Goto,A., Marzi,S., Fedorova,A., Verdier,Y., Vinh,J., Hoffmann,J.A., Martin,F. *et al.* (2014) Ribosomal protein RACK1 is a specific host factor required for IRES-mediated translation of fly and human viruses. *Cell*, **159**, 1086–1095.

CHAPTER II

CHARACTERIZATION OF A RACK1 INTERACTOME

RACK1 is known to interact with many signaling partners including PKC, transmembrane receptors and receptor tyrosine kinases (reviewed in Adams et al., 2011; Nielsen et al., 2017). However, none of the studies concerning RACK1 interactome had been performed in *Drosophila*. Moreover, we wanted to uncover proteins acting together with RACK1 in CrPV translation. Thus, we used *Drosophila* S2 cells overexpressing tagged versions of RACK1 to uncover RACK1 partners. These cells were infected or not with the virus CrPV to decipher whether the RACK1 network was affected by infection. Mass spectrometry after RACK1 pull-down identified 52 interacting partners of RACK1. These molecules include several proteins involved in translation (structural components of the ribosome, factors regulating translation initiation or elongation and RNA binding proteins) and some proteins involved in stress response such as chaperones (e.g. Hsc70-3 and Hsp26), Thioredoxin reductase 1 (Trxr-1) and a catalase (Cat).

I performed a RNA interference screen in S2 cells and showed that among these 52 interactants, 10 were restricting viral replication, and only Lark (RBM4 in mammals) was a proviral factor like RACK1. However, although Lark knock down (KD) impaired CrPV replication, it did not affect translation driven by the 5' IRES of the virus (Figure 5 of the article). We concluded that Lark promotes CrPV replication by a mechanism different from RACK1. This work was published in 2017 in the journal *Genes Genomes Genetics* (G3).

G3 Genes | Genomes | Genetics

INVESTIGATION

Definition of a RACK1 Interaction Network in *Drosophila melanogaster* Using SWATH-MS

Lauriane Kuhn,*,[1] Karim Majzoub,†,[1] Evelyne Einhorn,† Johana Chicher,* Julien Pompon,†,[2] Jean-Luc Imler,† Philippe Hammann,*,[3] and Carine Meignin†,[3]

*Plateforme Protéomique Strasbourg-Esplanade FRC 1589 and †RIDI UPR 9022, Université de Strasbourg, Centre National de la Recherche Scientifique, F-67000, France

ABSTRACT Receptor for Activated protein C kinase 1 (RACK1) is a scaffold protein that has been found in association with several signaling complexes, and with the 40S subunit of the ribosome. Using the model organism *Drosophila melanogaster*, we recently showed that RACK1 is required at the ribosome for internal ribosome entry site (IRES)-mediated translation of viruses. Here, we report a proteomic characterization of the interactome of RACK1 in *Drosophila* S2 cells. We carried out Label-Free quantitation using both Data-Dependent and Data-Independent Acquisition (DDA and DIA, respectively) and observed a significant advantage for the Sequential Window Acquisition of all THeoretical fragment-ion spectra (SWATH) method, both in terms of identification of interactants and quantification of low abundance proteins. These data represent the first SWATH spectral library available for *Drosophila* and will be a useful resource for the community. A total of 52 interacting proteins were identified, including several molecules involved in translation such as structural components of the ribosome, factors regulating translation initiation or elongation, and RNA binding proteins. Among these 52 proteins, 15 were identified as partners by the SWATH strategy only. Interestingly, these 15 proteins are significantly enriched for the functions translation and nucleic acid binding. This enrichment reflects the engagement of RACK1 at the ribosome and highlights the added value of SWATH analysis. A functional screen did not reveal any protein sharing the interesting properties of RACK1, which is required for IRES-dependent translation and not essential for cell viability. Intriguingly however, 10 of the RACK1 partners identified restrict replication of Cricket paralysis virus (CrPV), an IRES-containing virus.

KEYWORDS
Drosophila melanogaster
mass spectrometry
translation
RACK1
ribosome
virus
IRES
Lark
AGO2

Infectious diseases represent a major cause of death for animals, including humans. Among them, viral infections are particularly hard to treat because viruses replicate inside host cells. Many cellular proteins are hijacked by viruses to complete their replication cycle and represent putative targets for host-targeted antiviral drugs. Using the model organism *Drosophila melanogaster*, we recently showed that RACK1 is an essential host factor for the replication of fly and human viruses (Majzoub *et al.* 2014). More specifically, we demonstrated that RACK1, a component of the 40S subunit of the ribosome, is required for translation driven by the 5′ IRES element of two members of the Dicistroviridae family in flies, *Drosophila* C virus (DCV) and CrPV. Related to Picornaviridae, these viruses are used as models to decipher the genetic basis of host–virus interactions in flies. Importantly, RACK1 is also essential for translation driven by the IRES of human hepatitis C virus in human hepatocytes. By contrast, RACK1 is not required for general 5′ cap-dependent translation, indicating that this factor regulates selective translation at the level of the ribosome (Majzoub *et al.* 2014). Thus, RACK1 could be used as target for the development of new host-targeted antiviral drugs (Martins *et al.* 2016). The ribosomal proteins RpS25 (Landry *et al.* 2009), RpL40 (Lee *et al.* 2013), and RpL38 (Kondrashov *et al.* 2011) are also required for selective translation, bringing support for the

doi: https://doi.org/10.1534/g3.117.042564
Manuscript received March 7, 2017; accepted for publication May 9, 2017; published Early Online May 18, 2017.

Supplemental material is available online at www.g3journal.org/lookup/suppl/doi:10.1534/g3.117.042564/-/DC1
[1]These authors contributed equally to this work.
[2]Present address: MIVEGEC (IRD 224 CNRS 5290-UM1-UM2) Maladies Infectieuses et Vecteurs: Écologie, Génétique, Évolution et Contrôle, Centre IRD de Montpellier, F-34394, France
[3]Corresponding authors: Institut de Biologie Moléculaire et Cellulaire, CNRS FRC1589, Université de Strasbourg, Plateforme Protéomique Strasbourg-Esplanade, 15 rue René Descartes, 67084 Strasbourg Cedex, France. E-mail: proteomic-esplanade@unistra.fr; and Institut de Biologie Moléculaire et Cellulaire, CNRS UPR9022, Université de Strasbourg, Plateforme Protéomique Strasbourg-Esplanade, 15 rue René Descartes, 67084 Strasbourg Cedex, France. E-mail: c.meignin@unistra.fr

existence of a ribosomal code (Mauro and Edelman 2002; Topisirovic and Sonenberg 2011; Barna 2015).

RACK1 is a 36 kDa protein containing seven WD40 β-propeller domains, evolutionarily conserved throughout eukaryotes (Wang *et al.* 2003; Kadrmas *et al.* 2007). RACK1 was also identified as an interacting partner of many proteins, including kinases, phosphatases, and adhesion molecules, suggesting that it functions as a scaffold protein (Gibson 2012; Long *et al.* 2014; Li and Xie 2015). Of note, we identified RACK1 as a factor pulled down with Argonaute (AGO) 2, a key component of the *Drosophila* antiviral RNA interference (RNAi) pathway, in virus-infected cells (Majzoub *et al.* 2014). Independent studies confirmed that RACK1 can interact with components of the RISC complex and impacts microRNA (miRNA) function (Jannot *et al.* 2011; Speth *et al.* 2013). In summary, RACK1 appears to be the central node of a molecular hub at the interface of the ribosome and signaling complexes. Hence, a comprehensive characterization of the RACK1 interactome is of central importance to gain insight into the function of this molecule.

Affinity purification followed by mass spectrometry (AP-MS) is a popular strategy for identifying interactions between an affinity-purified bait and its copurifying partners (Rinner *et al.* 2007; Gingras *et al.* 2007; Wepf *et al.* 2009; Collins *et al.* 2013; Lambert *et al.* 2013). This approach is particularly appreciated because experiments can be performed under near physiological conditions and because dynamic changes can be assessed by quantitative techniques operated under DDAs, with or without labeling strategies (Gavin *et al.* 2006, 2011; Krogan *et al.* 2006; Kühner *et al.* 2009). In the past few years, targeted proteomics as well as techniques derived from DIAs, such as sequential windowed acquisition termed MS/MS^{ALL} with SWATH acquisition (Gillet *et al.* 2012), have emerged as a complement to these more widely used discovery proteomic methods. DIA results in comprehensive high resolution data with qualitative confirmation and no tedious method development (Bisson *et al.* 2011; Chang *et al.* 2012; Picotti and Aebersold 2012; Picotti *et al.* 2013; Selevsek *et al.* 2015). Moreover, one can acquire useful information for all analytes in a single run, thus enabling retrospective *in silico* interrogation to explore unexpected biological pathways for example (Gillet *et al.* 2012). Here, we applied these techniques to define the RACK1 interactome in tissue culture *Drosophila* S2 cells infected or not by the dicistrovirus CrPV.

MATERIALS AND METHODS

Cell culture and immunoaffinity purification

Drosophila S2 cells were grown in Schneider medium complemented with 10% fetal bovine serum, 1% glutamax, and 1% Penicillin/Streptomycin. RACK1 immunoprecipitation (IP) was performed after the transient transfection (Effectene, QIAGEN) of RACK1 tagged with the 3xHA or 3xFLAG versions in 30 million cells in triplicate. Cells were either mock-infected or infected with DCV or CrPV at multiplicity of infection (MOI) 1 for 16 hr. Protein purification and identification was performed as previously described (Fukuyama *et al.* 2013). Next, 1 ml of TNT lysis buffer (50 mM Tris-HCl pH 7.5, 150 mM NaCl, 10% Glycerol, 1% Triton X-100, 100 mM NaF, 5μM $ZnCl_2$, 1 mM Na_3VO_4, 10 mM EGTA pH 8.0, and Complete Protease Inhibitor Cocktail containing EDTA from Roche) was used and kept on ice for 30 min before centrifugation at 13,000 rpm for 30 min at 4°. Supernatants were mixed with 150 μl of either prewashed anti-DYKDDDDK (Clontech #635686) or anti-HA (Sigma #A2095) beads and incubated for 1 hr at 4°. Beads were washed three times with 1 ml wash buffer I (50 mM Tris-HCl pH 7.5, 150 mM NaCl, 10% Glycerol, 0.1% Triton X-100, 100 mM NaF, 5 μM $ZnCl_2$, 1 mM Na_3VO_4, and 10 mM EGTA pH 8.0), one time with 1 ml wash buffer II (wash buffer I without Triton X-100), and suspended in 1 ml wash buffer II plus Complete Protease Inhibitor Cocktail containing EDTA. The elution was performed with Laemmli 1 × buffer. Eluates from RACK1 and control cell lines were separated by SDS-PAGE: a precast gradient 4–12% acrylamide gel was used followed by Coomassie Blue staining. Each gel lane was cut into 48 consecutive bands, with the exception of the two bands containing the light and heavy chains of immunoglobulins, and submitted to proteomic analysis.

Label-free quantification using DDAs and DIAs

A Spectral Counting (SpC) strategy was carried out using the Mascot identification results and Proteinscape 3.1 package. A total number of MS/MS spectra (including modified and shared peptides) was attributed to each protein in each of the 18 conditions. The partner quality was positively assessed if Ratio(RACK-Cter/Control) > 2 and/or Ratio(RACK-Nter/Control) > 2. The MS1 label-free strategy was carried out using the PeakView v1.2 and MarkerView v1.2 software from Sciex. Resulting tables were then submitted to a Student's *t*-test: peptides and proteins validated with a *P*-value < 0.05 were considered statistically significant. The SWATH strategy was carried out using an AB Sciex informatics package to extract the quantitative information from the files acquired in Data-Independent mode (MS/MS^{ALL} with SWATH acquisition). The Paragon results file (group) was imported into PeakView v1.2 to create an experimental in-house *Drosophila* spectral library. Data were further evaluated in MarkerView using a Principal Component Analysis (PCA) (Pareto) and a Student's *t*-test. The same significance criteria were applied to the ion, peptide, and protein tables. More detailed presentation of the mass spectrometry data analysis can be found in the supplemental information (File S1).

Functional classification and network analysis of RACK1 identified partners

Gene Ontology (GO) annotations were retrieved from the PANTHER classification system (v10.0 Released 2015-05-15) with the following parameters: (i) Enter IDs: UniProtKB accession numbers; (ii) Organism: *D. melanogaster*; and (iii) Analysis: functional classification viewed in pie chart. GO enrichment analysis was performed using the same classification system with the following parameters: (i) Enter IDs: UniProtKB accession numbers; (ii) Organism: *D. melanogaster*; and (iii) Analysis: statistical overrepresentation test release 20160302. The network of RACK1-interacting proteins was further constructed by STRING (http://string-db.org/,v10.0) while considering the following active interaction sources: "Coexpression," "Databases," "Experiments," and "Textmining."

RNAi screen and RT-qPCR

Target genes were amplified by PCR with specific primers containing the T7 RNA polymerase binding site in their 5′-end. After PCR product purification by GE Illustra GFX PCR DNA purification kit and verification on agarose gels for correct sizes, 1 μg of DNA template was used to generate dsRNA with the MEGAscript T7 Ambion kit. After overnight incubation, dsRNA was precipitated with 0.3 M NaAc and absolute ethanol and resuspended in nuclease-free water. Then, 3 μg of dsRNA was mixed with 2×10^4 S2 cells in serum-free medium for 2–3 hr in 96-well plates, allowing the penetration of dsRNA into the cells. Four replicates of the same dsRNA were tested. Afterward, complete medium was added. After 1 wk incubation, cells were infected for 1 d with DCV (MOI 1) and CrPV (MOI 0.1). Cell lysis, retrotranscription, and qPCR against the target virus genome were performed using

the Cell-To-Ct Ambion kit. Cells were lysed in 50 μl lysis buffer for 5 min. Reverse transcription was performed on 10 μl lysate in SYBR RT buffer and enzyme mix in a final volume of 50 μl. Quantitative PCR on 4 μl cDNA samples was done in 20 μl final volumes with 10 μl SYBR Green power master mix and 0.5 mM of each primer. An unpaired two-tailed *t*-test was then performed, comparing control dsRNA against GFP with all tested dsRNA. At least three independent biological replicates were performed for each experiment. All primers used are presented in the supplemental information.

Cell viability upon dsRNA treatment was tested with CellTiter 96 AQueous One Solution Cell Proliferation Assay (MTS) reagent (Promega) or assessed on the genome RNAi database (http://www.genomernai.org).

Luciferase assay

Drosophila S2 cells (Invitrogen) were soaked with dsRNA. Four days later, reporter plasmids (CrPV5′ IRES-Renilla and Cap-Firefly) were transfected using an Effectene kit (QIAGEN). After 48 hr, cells were lysed and luciferase activity was measured with the Promega dual-luciferase assay, using a Berthold Luminometer.

Data availability

Datasets have been deposited to the ProteomeXchange Consortium with identifiers PXD002965 (http://proteomecentral.proteomexchange.org) via the PRIDE partner repository.

RESULTS

Identification of 37 RACK1-interacting proteins using data-dependent acquisition

In order to define the RACK1 interactome in *D. melanogaster*, N- or C-terminal FLAG-tagged RACK1 was transiently expressed in *Drosophila* S2 cells, in mock- or virus-infected conditions (Figure 1). A vector expressing RACK1 with a hemagglutinin (HA) tag was used as control, which is not recognized by the anti-FLAG antibody, so that cells expressing similar levels of RACK1 were compared. Biological triplicates were analyzed for each of the six samples. We first optimized the AP-MS protocol at three critical steps to improve specificity (type of tag, incubation time and salt concentration in the washing buffer, and type of virus, see Supplemental Material, in Figure S1 in File S1). We also ran a quality control sample in triplicate (500 ng of a trypsin-digested HeLa lysate) to ascertain the technical reproducibility of the MS instrument. As expected, the variability of the affinity purification replicates is higher than that of the technical replicates of injection (Table S1 in File S2). Purified complexes were eluted from the beads with Laemmli buffer and separated by SDS-PAGE. Proteins bands were in-gel digested with trypsin before being submitted to liquid chromatography MS analysis. DDA was used in the first instance to estimate relative changes between all conditions via SpC (Table S2 in File S2). After normalization, we calculated the ratio RACK1/control for the N- and C-terminally tagged protein in mock- and virus-infected cells, to assess the quality of the partners. A protein was considered as a RACK1 partner if it was enriched in the condition where RACK1 was overexpressed and pulled-down, using the following criterion: ratio (IP/Ctrl) > 2 and P-value < 0.05 (t-test). The P-values were not corrected by multiple testing in this initial step, in which the goal was to identify a list of putative partners for RACK1. This criterion identified 34 potential interacting proteins (Figure 2A), having either an "on/off" behavior or being enriched by a factor of ≥ 2 when RACK1 was pulled-down. The same DDA data were then submitted to an MS1 label-free analysis, using the vendor's processing package and composed from PeakView v1.2 and MarkerView v1.2 software (Sciex). This identified 19 RACK1 partners in either mock- or virus-infected samples (Figure 2, A and B and Table S2 in File S2). Of note, the average coefficient of variation (CV) of the 18 samples is 25% higher than the average CV of the nine noninfected samples. Altogether, close to 75% of the partners were identified with both tagged versions of RACK1. This highlights the overall good reproducibility and attests to the reliability of the approach, even if the position of the tag appears to influence the recovery of some partners, possibly reflecting their interaction with the extremities of RACK1.

SWATH-MS quantification reveals an additional 15 RACK1-interacting proteins

We next used the MS/MS spectra obtained with the DDA mode to build a spectral library to be used for 18 consecutive DIA injections. Up to 10 peptides per protein and 5 transitions per peptide were considered for SWATH-MS quantification leading a total of 3368 transitions. A careful adaptation of the retention time window reduced the sensitivity of peak picking interferences, as reflected by the very low chromatographic shift observed all along the separation (1.48 min). Each protein detected as being a RACK1 partner was manually inspected and validated or corrected (Figure S2 in File S1). As in the MS1 label-free quantification, the CV of the SWATH data decreases by 21% when only the nine noninfected samples are taken into account. The PCA analysis revealed a clear-cut difference between the control and the co-IP samples (Figure 2C). A total of 48 RACK1 partners were identified, which included 17 out of the 19 partners identified using the MS1 quantification method. This indicates that SWATH quantification is as reliable as the standard MS1 label-free approach, yet more sensitive (Figure 2A and Table S2 in File S2). The IP bait, RACK1, identified both by MS1 and SWATH, was enriched by an average factor of 27.7 with SWATH, which is significantly higher than with the MS1 quantification (average fold change of 8.4, Figure S3 in File S2). Most of the partners identified by SWATH (53.5%) were validated with both C- and N-terminally tagged constructions.

The selective requirement for RACK1 in IRES-dependent translation suggests that infection by an IRES-containing virus, such as CrPV, may involve an association with specific cofactors. However, our approach did not reveal specific factors recruited to RACK1 in the context of CrPV infections. As the infection can affect the post-translational status of RACK1 and its partners (*e.g.*, Valerius *et al.* 2007), an extended Mascot search was performed using an "Error Tolerant Search" strategy. This did not lead to the identification of novel interactants. Despite the fact that RACK1 is a phosphoprotein itself and that ubiquitination has been demonstrated for the orthologs in yeast and human cells (Starita *et al.* 2012; Yang *et al.* 2017), the only modifications we detected were: (i) the acetylation of the second residue (S2) with the loss of the initiation methionine, and (ii) deamidation on N24 and N52. Regarding the involvement of RACK1 in cell signaling, we did identify some signaling proteins, such as the serine/threonine kinase Polo, but we did not isolate the kinases previously reported to interact with RACK1, such as protein kinase C β (PKCβ) or Src. We note that these proteins were also not detected in the RACK1 interactome in *Aedes albopictus* cells, in which the endogenous protein was pulled down (González-Calixto *et al.* 2015).

Characteristics of the RACK1 interactome in Drosophila S2 cells

The PANTHER classification system (http://www.pantherdb.org) was used to assess the GO annotations of the 52 different proteins retrieved

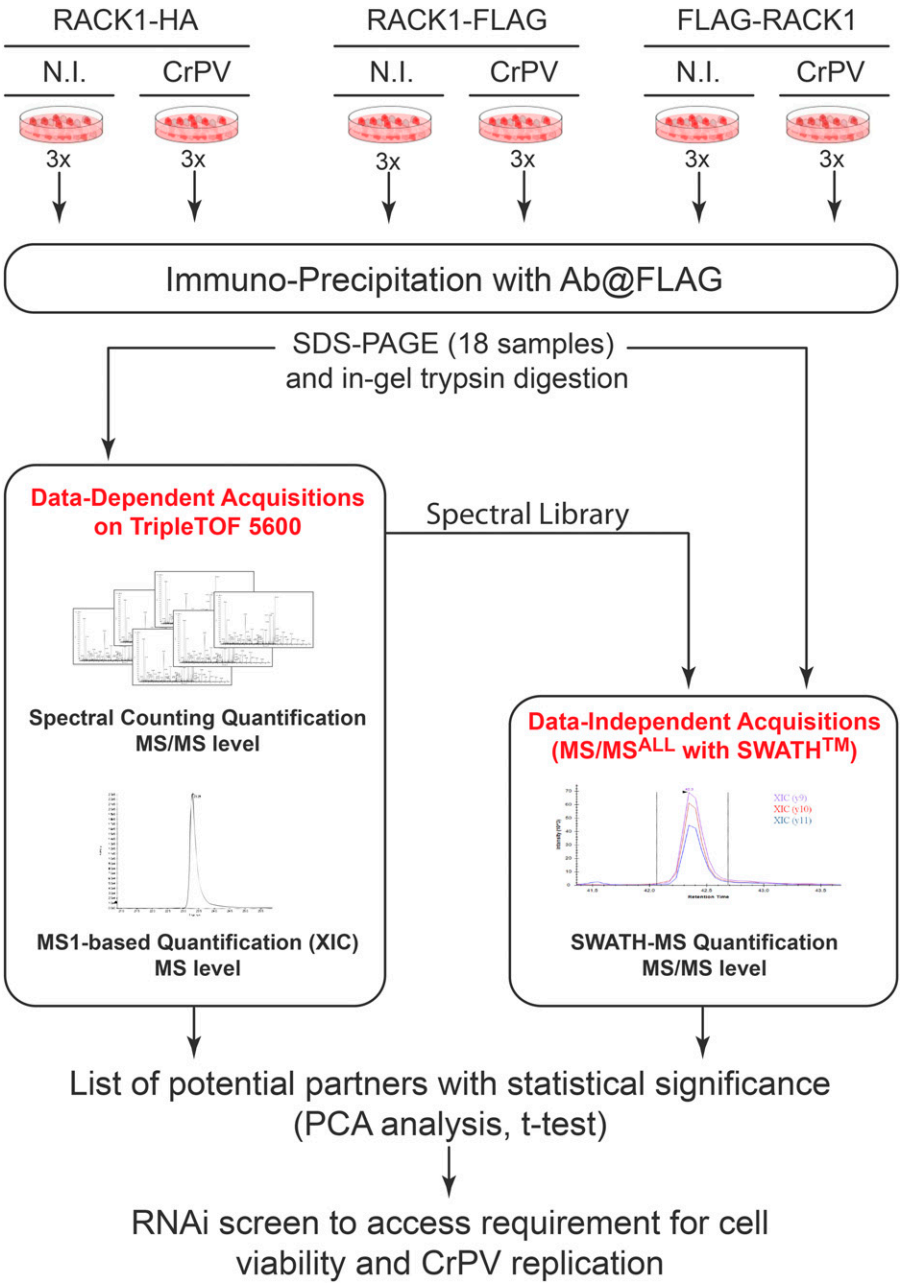

Figure 1 Immunoprecipitation and proteomic workflows used to identify RACK1 partners. Thirty million *D. melanogaster* S2 cells were transiently transfected with RACK1, tagged either at the N- or C-terminus with the indicated peptide epitopes. Cells were then left uninfected or challenged with CrPV MOI 0.1 for 24 hr and co-IP experiments were performed using an anti-FLAG antibody. Following SDS-PAGE, in-gel trypsin digestion was performed, before nanoLC-MS/MS analyses. Quantification was made under either Data-Dependent Acquisition mode, thus enabling Spectral Counting and MS1 label-free methods, or Data-Independent Acquisition mode, dedicated to MS/MS^{ALL} with SWATH-MS quantification method. The biological relevance of potential RACK1 partners, identified and statistically validated by these three quantification methods, was finally tested using RNAi. co-IP, co-immunoprecipitation; CrPV, Cricket paralysis virus; MOI, multiplicity of infection; MS, mass spectrometry; N.I., noninfected; RACK1, Receptor for Activated protein C kinase 1; RNAi, RNA interference; SDS-PAGE, sodium dodecyl sulfate polyacrylamide gel electrophoresis; SWATH, Sequential Window Acquisition of all THeoretical fragment-ion spectra.

(Figure 3 and Table S3 in File S2). The PANTHER overrepresentation test used a reference list of 13624 *D. melanogaster* accessions, as well as adjusted *P*-values (correction for multiple testing using the Benjamini–Hochberg method). Of note, the PANTHER Protein Classes "Nucleic Acid Binding proteins" and "Chaperones" were well represented, and 37.5% of the proteins were annotated as "Macromolecular complexes." Interestingly, when considering each of the three quantitative methods independently, the SWATH approach identified more proteins involved in nucleic acid binding ($n = 13$) than the SpC or MS1 approaches ($n = 5$ for each). It also recognized eight proteins involved in RNA interaction or translation regulation, including several ribosomal proteins (Table S3 in File S2). Thus, the SWATH analysis appears to best reflect the known cellular functions of RACK1 in regulation of mRNA translation.

The whole set of 52 RACK1-interacting partners was further submitted to a PANTHER overrepresentation test, which was subsequently run with the 37 RACK1 partners identified by the SpC and MS1 methods only (Table S4 in File S2). Figure 4A displays the fold enrichment returned by PANTHER with or without the SWATH-specific RACK1 partners for each of the three GO terms, as well as the significance of the fold enrichment (P-value < 0.05). Nine GO annotations exhibit increased fold enrichment when the 16 additional SWATH-specific interactors are included. Eight of them are related to translation, RNA helicase activity, and nucleic acid binding. Moreover, the fold enrichment systematically becomes significant for the nine GO terms when including the SWATH dataset. To further elucidate the relationships between the set of 52 RACK1-interacting proteins and to identify functional complexes, the STRING interaction database was used to map

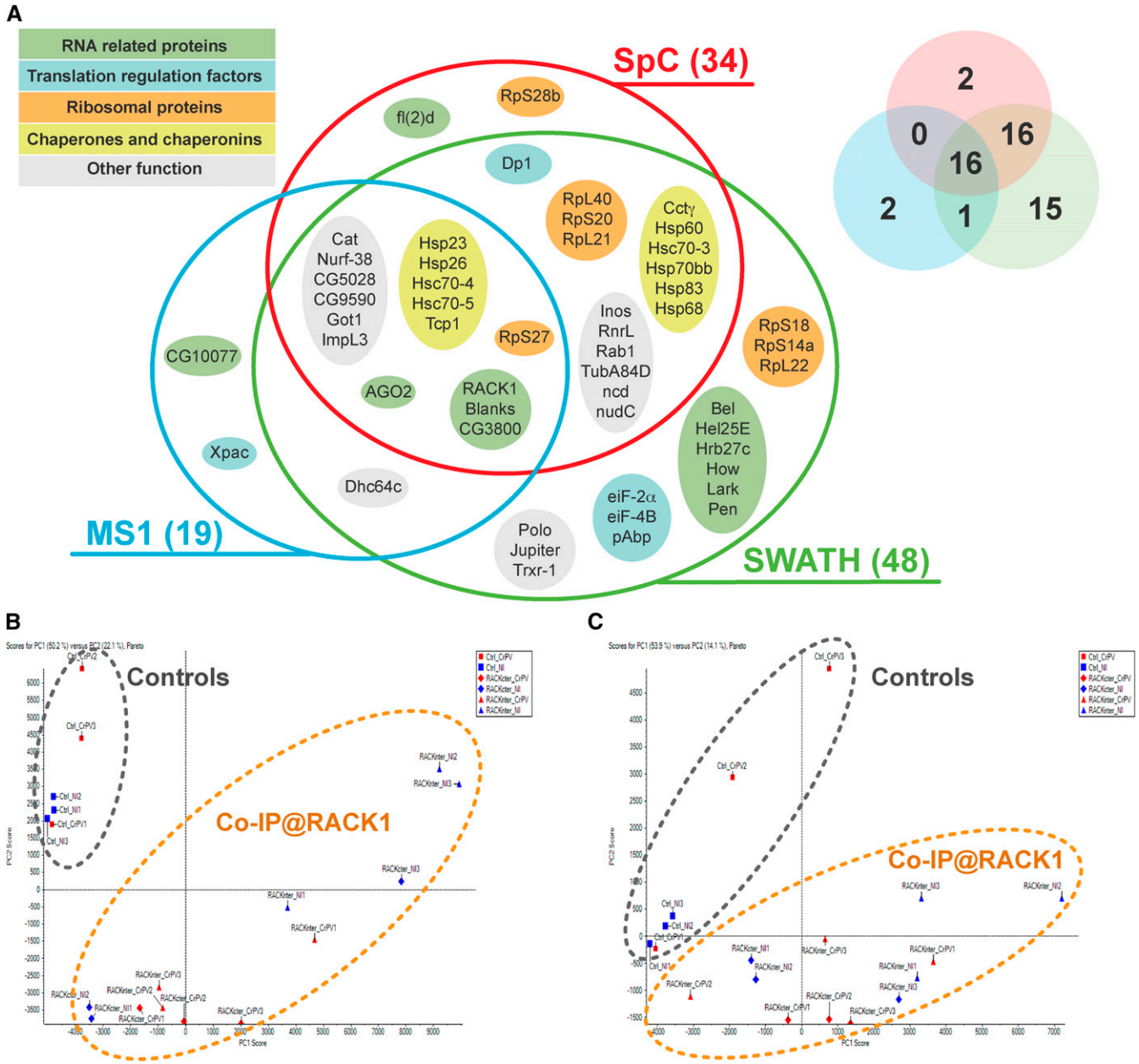

Figure 2 RACK1 partners identified by either the DDA (Spectral Counting = SpC, MS1 label-free = MS1) or DIA approach (MS/MS^{ALL} with SWATH = SWATH). (A) Proteins identified as RACK1 partners by the three types of quantitative methods. The Venn diagram shows the global overlap between the three strategies. Five functional categories are represented. (B) Principle Component Analysis for the MS1 label-free dataset: 231 proteins were identified by Paragon algorithm and further quantified after the automatic reconstruction of peptide features at the MS level (XIC). (C) Principle Component Analysis for the SWATH dataset: proteins were quantified by interrogation of a home-made spectral library at the MS/MS level. co-IP, co-immunoprecipitation; DDA, Data-Dependent Acquisition; DIA, Data-Independent Acquisition; MS, mass spectrometry; RACK1, Receptor for Activated protein C kinase 1; SWATH, Sequential Window Acquisition of all THeoretical fragment-ion spectra.

the RACK1 network (Figure 4B). This analysis reveals that the vast majority of the protein nodes are connected together. It also shows a high connectivity with a total of 21 protein nodes between the group of ribosomal proteins, to which RACK1 belongs, and three other groups: (i) RNA-related proteins; (ii) chaperones and chaperonins; and (iii) translation regulation factors.

One family of molecules reported to interact with RACK1 and possessing interesting properties in the context of the regulation of translation and the control of viral infections are members of the AGO family. Indeed, RACK1 is involved in miRNA function in the plant *Arabidopsis thaliana* (Speth *et al.* 2013), the nematode *Caenorhabditis elegans* (Jannot *et al.* 2011), and humans (Otsuka *et al.* 2011). In *Drosophila* as well, we previously reported that RACK1 participates in silencing triggered by miRNAs, although its impact was stronger for some miRNAs than others (Majzoub *et al.* 2014). In *Drosophila*, most miRNAs are loaded onto AGO1, with only a small subset loaded onto AGO2. Interestingly, we recovered AGO2, but not AGO1, in the RACK1 interactome (Figure 2A). The functional significance of the

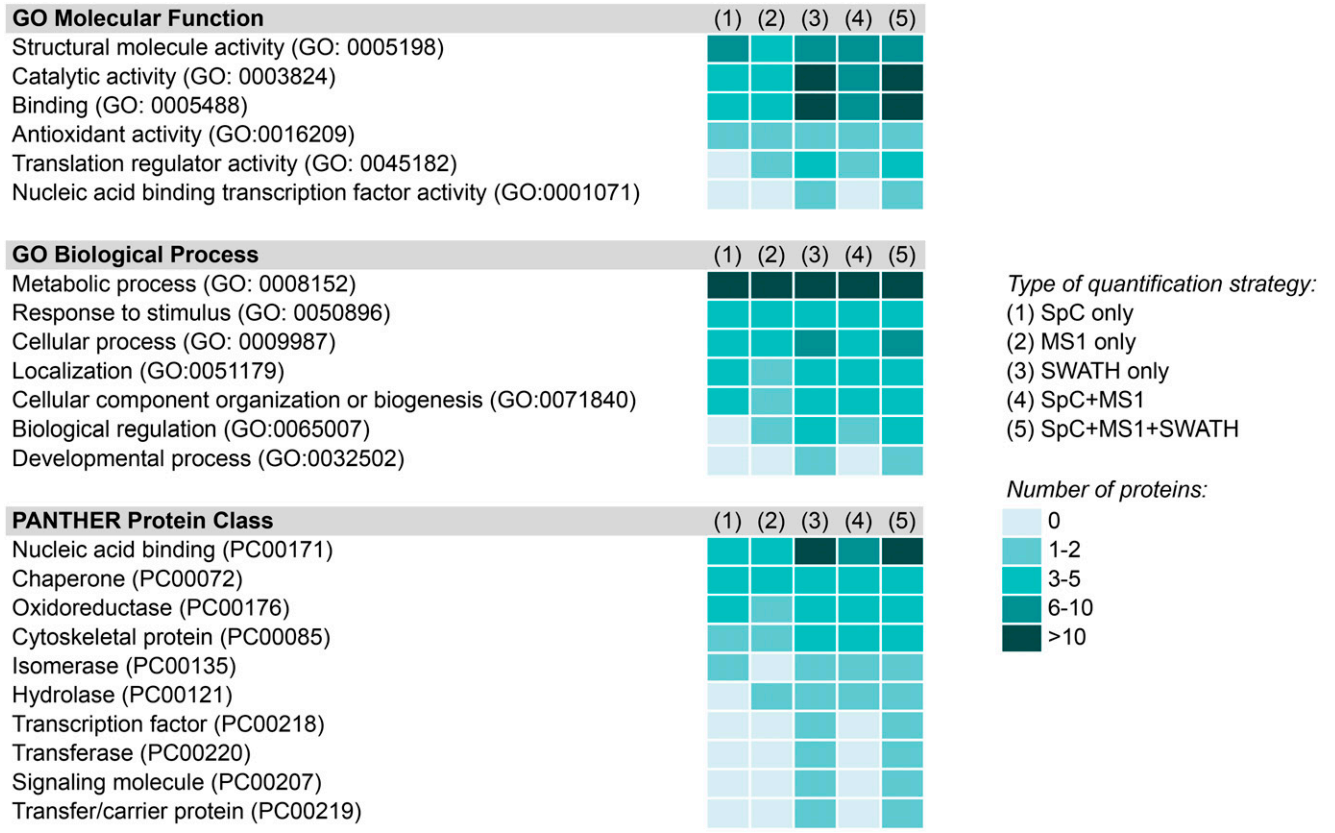

Figure 3 Heat map displaying the Gene Ontology (GO) annotations of the Molecular Process of the identified proteins. The classification system made by PANTHER (http://www.pantherdb.org). Proteins included in heat map were identified by either one or several of the three quantification methods [Spectral Counting (SpC), MS1 Label-Free (MS1), and MS/MS^{ALL} with SWATH (SWATH, Sequential Window Acquisition of all THeoretical fragment-ion spectra)].

interaction of RACK1, which promotes translation driven by viral IRES elements, and AGO2, a major effector of antiviral immunity in flies, deserves further investigation.

Functional characterization of the RACK1 interactome

To assess the biological significance of the interactions identified in the context of viral infection, we used RNAi in S2 cells to silence expression of the RACK1-interacting proteins (Figure 5A). Silencing of 17 of the 52 identified proteins affected cell viability or proliferation, preventing further characterization. As expected, these included the majority of the ribosomal proteins, with the notable exception of RpS20 and RACK1. We next tested the impact on CrPV replication of the remaining 35 genes. Genes were silenced for 4 d prior to CrPV infection and accumulation of viral RNA was monitored by RT-qPCR 16 hr later. Twenty-three genes (66%) did not significantly impact CrPV replication. Interestingly, 10 genes (28%) led to increased CrPV RNA in infected cells when their expression was knocked-down, suggesting that they encode factors restricting viral infection. Indeed, these include AGO2, a central component of the antiviral siRNA pathway (van Rij *et al.* 2006; Mueller *et al.* 2010) (Figure 5A). The others were not previously associated with the control of viral infections. Besides RACK1, only one other gene, *Lark*, led to decreased CrPV replication when it was silenced (Figure 5A). To rule out off-target effects, we synthesized two dsRNA targeting different regions of the *Lark* gene. Both dsRNAs efficiently silenced *Lark* expression (Figure 5B) and suppressed CrPV replication, although not as efficiently as silencing of RACK1 (Figure 5C). This suggests that Lark, an RNA-binding protein, might participate in selective mRNA translation together with RACK1. Because RACK1 is also required for translation of the related virus DCV, we next tested replication of this virus in *Lark*-silenced cells. However, silencing *Lark* had no significant impact on DCV (not shown). Finally, we tested directly whether Lark had an effect on viral translation, using a CrPV-5′ IRES luciferase reporter (Majzoub *et al.* 2014). As expected, silencing RACK1 had a strong impact on the expression of the reporter. By contrast, silencing of Lark did not affect its activity (Figure 5D). We conclude that Lark and RACK1 promote CrPV replication by different mechanisms.

DISCUSSION

The present study represents a first description in the model organism *Drosophila* of the interactome of RACK1, an intriguing cytoplasmic protein at the interface of the ribosome and cell signaling pathways. In spite of its limitations (transient overexpression of the bait; analysis of a single cell line; interactions not confirmed by alternative techniques; and only one time point analyzed for viral infection), the study confirms the power of SWATH for the establishment of the RACK1 interaction network under the biological conditions described in this study, and reveals some interesting findings. Indeed, 48 out of the 52 RACK1 interactants were identified using SWATH, and 9 of the 15 partners identified only by this method are RNA-related proteins (Bel, Hel25E, How, Lark, Pen, and Hrb27c) or translation regulation factors (eIF-2α, eIF-4B, and pAbp). Overall, our data are consistent

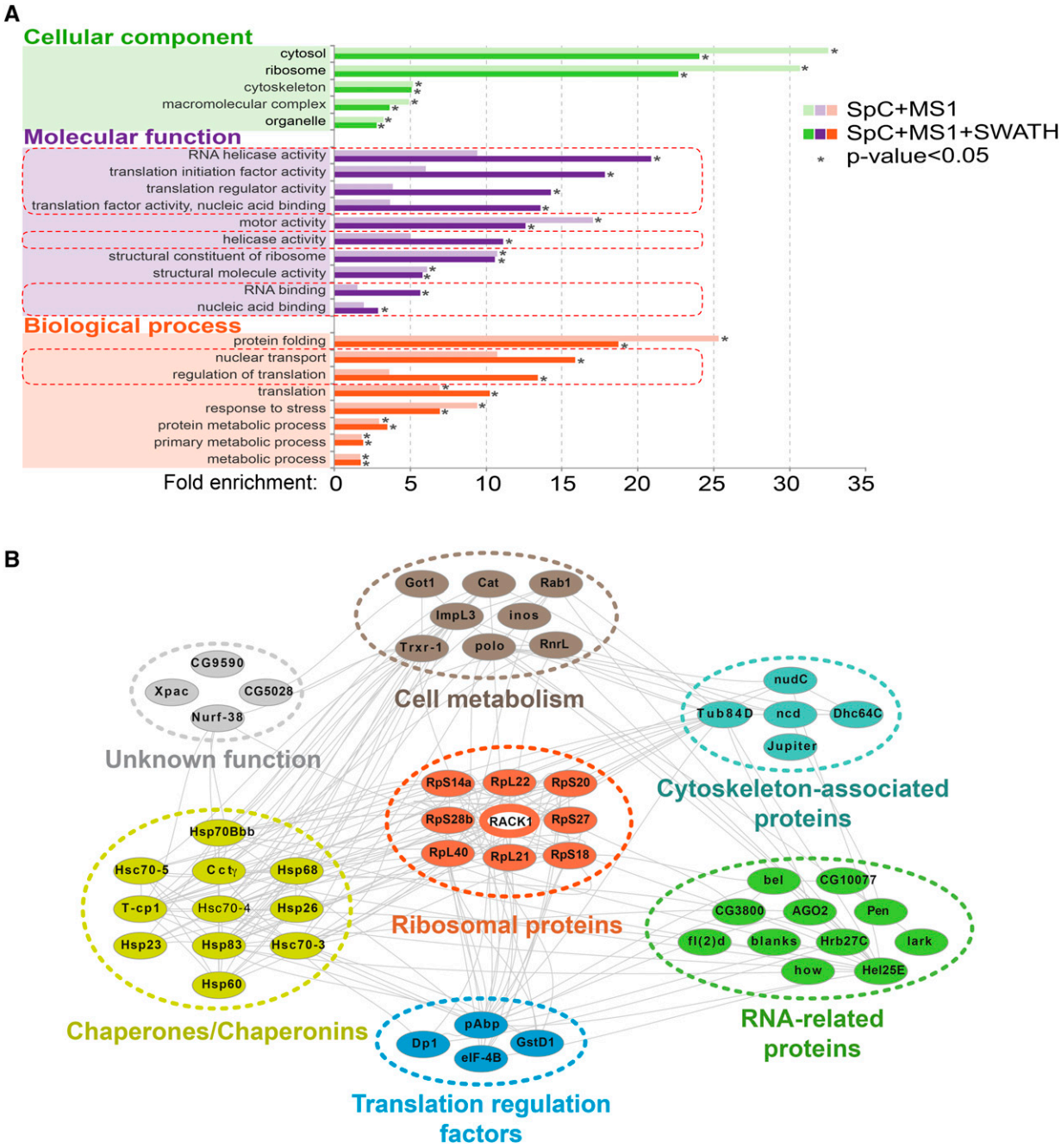

Figure 4 Functional Classification and Enrichment analysis of the RACK1-interacting proteins identified by the three quantification methods. (A) STRING network prediction of the 52 proteins identified as partners by SpC, MS1, and SWATH approaches. (B) Gene Ontology terms overrepresentation analysis by PANTHER: GO terms with an increased fold enrichment when considering SWATH data and for which *P*-value becomes significant (< 0.05) are highlighted by a red box. GO, Gene Ontology; MS1, MS1 Label-Free; RACK1, Receptor for Activated protein C kinase 1; SpC, Spectral Count; SWATH, Sequential Window Acquisition of all THeoretical fragment-ion spectra.

with RACK1 playing a major role at the level of the ribosome on translational control. RACK1 has been proposed to interact with an array of signaling molecules and to act as a scaffold protein (Adams *et al.* 2011; Li and Xie 2015). Indeed, RACK1 was identified as a partner of several kinases (*e.g.*, PKCβ (Ron *et al.* 1994; Sharma *et al.* 2013), Src (Chang *et al.* 1998), p38 MAPK (Belozerov *et al.* 2014), a phosphatase (PP2A, Long *et al.* 2014), and membrane receptors [*e.g.*, Flt1 (Wang *et al.* 2011) and integrins (Liliental and Chang 1998)]. It is intriguing that we only identified a few signaling proteins (*e.g.*, polo kinase, Rab1, and a myo-inositol 1-phosphate synthetase). Interestingly, the interactome of RACK1 in a mosquito cell line also revealed that 25% of the RACK1 partners were annotated as involved in ribosomal structure and/or translation (González-Calixto *et al.* 2015). This study also detected a few signaling proteins, which differ from the ones reported here. Our failure to identify signaling proteins associated with RACK1 could reflect the experimental settings used (*e.g.*, use of cell line, and high detergent and salt concentration in the washing steps to minimize nonspecific interactions, at the risk of elimination of weak interactors).

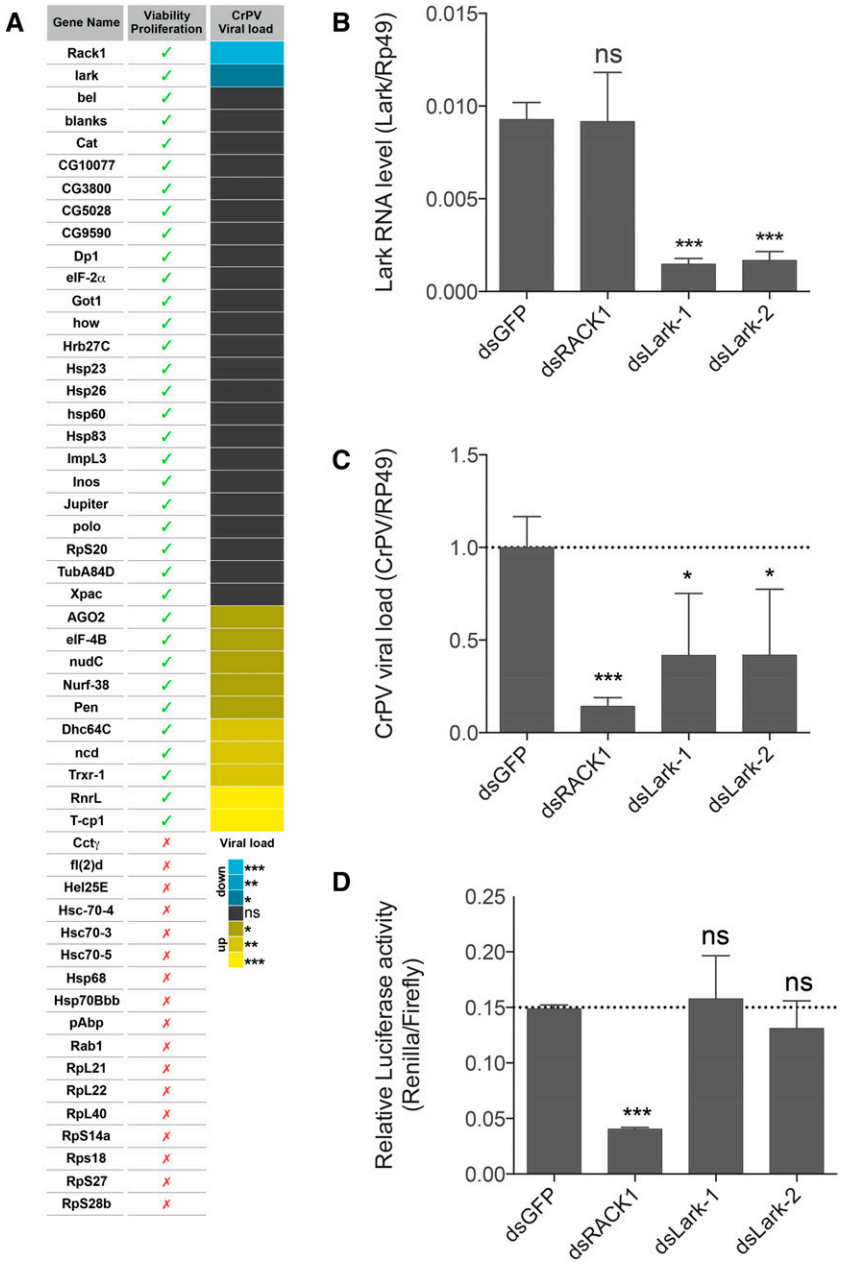

Figure 5 Functional characterization of the 52 RACK1 interactors identified (A). Impact of the silencing of the 52 genes on cell number and CrPV replication. Cell viability/proliferation was monitored by counting nuclei following DAPI staining. Viral load was monitored only on cells not impacted by silencing of the candidate genes (B). Incubation of S2 cells with two dsRNAs targeting different regions of the gene result in efficient *Lark* silencing. (C) Silencing of *Lark* affects CrPV replication in S2 cells. (D) Silencing of *Lark* does not affect translation driven by 5′ IRES from CrPV, unlike silencing RACK1. Statistical analysis with *t*-test: $^{*}P < 0.05$, $^{**}P < 0.01$, $^{***}P < 0.001$ and ns, not significant. CrPV, Cricket paralysis virus; DAPI, 4′,6-diamidino-2-phenylindole; dsRNA, double-stranded RNA; GFP, green fluorescent protein; IRES, internal ribosome entry site; RACK1, Receptor for Activated protein C kinase 1.

It could also reflect a transient, signal-dependent nature of the interaction. This hypothesis could also account for the lack of interaction induced by CrPV infection. Although RACK1 is known to be subject to post-translation modification, we did not detect any (Adams *et al.* 2011; Schmitt *et al.* 2017; Yang *et al.* 2017). Additional experiments in conditions stabilizing these modifications (*e.g.*, in the presence of phosphatase inhibitors) could clarify this issue and confirm that RACK1 acts as a scaffold protein (Adams *et al.* 2011). However, we cannot rule out the possibility that all functions so far attributed to RACK1 indirectly result from its presence at the ribosome (Schmitt *et al.* 2017). This hypothesis is consistent with the fact that RACK1 appears to be exclusively associated with ribosomes and polysomes in *Drosophila* cells (E. Einhorn, F. Martin, C. Meignin and J. Imler., unpublished data).

Our aim was to identify proteins functioning together with RACK1 in IRES-dependent translation. However, none of the 52 interacting proteins identified behaved like RACK1 in our functional assays. Interestingly however, one of them, Lark, appears to be required for CrPV replication, although it is not required for translation driven by the 5′ IRES of the virus. Lark encodes a protein composed of an N-terminal Zinc knuckle domain, followed by two RRM motifs, initially characterized for its role in mRNA splicing and regulation of the circadian rhythm (Huang *et al.* 2007). Interestingly, Lark is evolutionarily conserved, and both Lark and its mammalian homolog RBM4 participate in miRNA-dependent inhibition of translation by AGO proteins (Höck *et al.* 2007; Lin and Tarn 2009). Thus, the functional significance of the interaction between RACK1 and Lark/RBM4 deserves to be tested in other settings (Otsuka *et al.* 2011; Jannot *et al.* 2011; Speth *et al.* 2013). Of note, our functional analysis is limited to the genes not affecting cell viability or proliferation, which could explain our lack of success in identifying functional partners of RACK1.

One unexpected finding of our study was that 20% of the identified interacting proteins (10 out of 52) restrict CrPV replication. This may at

first sight seem surprising in light of the opposite effect of RACK1 on this virus. However, translation control is a critical step in the viral replication cycle, where the viral RNAs are exposed to host cell molecules, including restriction factors. Thus, it is possible that RACK1, a critical molecule for viral IRES-dependent translation, is used as a surveillance platform for proteins participating to cellular intrinsic antiviral responses. Although we cannot rule out that the antiviral effect of some of these genes is indirect at this stage, AGO2 has antiviral functions that have been well characterized *in vitro* and *in vivo* (Wang *et al.* 2006; van Rij *et al.* 2006; Nayak *et al.* 2010; van Mierlo *et al.* 2012). Therefore, this protein represents a prime candidate to elucidate the biological significance of the interaction between factors restricting viral replication and RACK1.

ACKNOWLEDGMENTS

We thank Marjorie Fournier for insightful comments on the manuscript, and Estelle Santiago and Alice Courtin for technical assistance. This work was supported by Centre National de la Recherche Scientifique (CNRS), the National Institutes of Health program grant PO1 AI07167, Investissement d'Avenir Programs (NetRNA ANR-10-LABX-36 and I2MC ANR-11-EQPX-0022), Fondation pour la Recherche Médicale, and Fondation ARC. K.M. was supported by a fellowship from CNRS/Région Alsace.

LITERATURE CITED

Adams, D. R., D. Ron, and P. A. Kiely, 2011 RACK1, A multifaceted scaffolding protein: structure and function. Cell Commun. Signal. CCS 9: 22.

Barna, M., 2015 The ribosome prophecy. Nat. Rev. Mol. Cell Biol. 16: 268.

Belozerov, V. E., S. Ratkovic, H. McNeill, A. J. Hilliker, and J. C. McDermott, 2014 In vivo interaction proteomics reveal a novel p38 mitogen-activated protein kinase/Rack1 pathway regulating proteostasis in Drosophila muscle. Mol. Cell. Biol. 34: 474–484.

Bisson, N., D. A. James, G. Ivosev, S. A. Tate, R. Bonner *et al.*, 2011 Selected reaction monitoring mass spectrometry reveals the dynamics of signaling through the GRB2 adaptor. Nat. Biotechnol. 29: 653–658.

Chang, B. Y., K. B. Conroy, E. M. Machleder, and C. A. Cartwright, 1998 RACK1, a receptor for activated C kinase and a homolog of the beta subunit of G proteins, inhibits activity of src tyrosine kinases and growth of NIH 3T3 cells. Mol. Cell. Biol. 18: 3245–3256.

Chang, C. Y., P. Picotti, R. Hüttenhain, V. Heinzelmann-Schwarz, M. Jovanovic *et al.*, 2012 Protein significance analysis in selected reaction monitoring (SRM) measurements. Mol. Cell. Proteomics 11: M111.014662.

Collins, B. C., L. C. Gillet, G. Rosenberger, H. L. Röst, A. Vichalkovski *et al.*, 2013 Quantifying protein interaction dynamics by SWATH mass spectrometry: application to the 14–3-3 system. Nat. Methods 10: 1246–1253.

Fukuyama, H., Y. Verdier, Y. Guan, C. Makino-Okamura, V. Shilova *et al.*, 2013 Landscape of protein-protein interactions in Drosophila immune deficiency signaling during bacterial challenge. Proc. Natl. Acad. Sci. USA 110: 10717–10722.

Gavin, A.-C., P. Aloy, P. Grandi, R. Krause, M. Boesche *et al.*, 2006 Proteome survey reveals modularity of the yeast cell machinery. Nature 440: 631–636.

Gavin, A.-C., K. Maeda, and S. Kühner, 2011 Recent advances in charting protein-protein interaction: mass spectrometry-based approaches. Curr. Opin. Biotechnol. 22: 42–49.

Gibson, T. J., 2012 RACK1 research - ships passing in the night? FEBS Lett. 586: 2787–2789.

Gillet, L. C., P. Navarro, S. Tate, H. Röst, N. Selevsek *et al.*, 2012 Targeted data extraction of the MS/MS spectra generated by data-independent acquisition: a new concept for consistent and accurate proteome analysis. Mol. Cell. Proteomics 11: O111.016717.

Gingras, A.-C., M. Gstaiger, B. Raught, and R. Aebersold, 2007 Analysis of protein complexes using mass spectrometry. Nat. Rev. Mol. Cell Biol. 8: 645–654.

González-Calixto, C., F. E. Cázares-Raga, L. Cortés-Martínez, R. M. Del Angel, F. Medina-Ramírez *et al.*, 2015 AealRACK1 expression and localization in response to stress in C6/36 HT mosquito cells. J. Proteomics 119: 45–60.

Höck, J., L. Weinmann, C. Ender, S. Rüdel, E. Kremmer *et al.*, 2007 Proteomic and functional analysis of Argonaute-containing mRNA-protein complexes in human cells. EMBO Rep. 8: 1052–1060.

Huang, Y., G. Genova, M. Roberts, and F. R. Jackson, 2007 The LARK RNA-binding protein selectively regulates the circadian eclosion rhythm by controlling E74 protein expression. PLoS One 2: e1107.

Jannot, G., S. Bajan, N. J. Giguère, S. Bouasker, I. H. Banville *et al.*, 2011 The ribosomal protein RACK1 is required for microRNA function in both C. elegans and humans. EMBO Rep. 12: 581–586.

Kadrmas, J. L., M. A. Smith, S. M. Pronovost, and M. C. Beckerle, 2007 Characterization of RACK1 function in Drosophila development. Dev. Dyn. Off. Publ. Am. Assoc. Anat. 236: 2207–2215.

Kondrashov, N., A. Pusic, C. R. Stumpf, K. Shimizu, A. C. Hsieh *et al.*, 2011 Ribosome-mediated specificity in Hox mRNA translation and vertebrate tissue patterning. Cell 145: 383–397.

Krogan, N. J., G. Cagney, H. Yu, G. Zhong, X. Guo *et al.*, 2006 Global landscape of protein complexes in the yeast Saccharomyces cerevisiae. Nature 440: 637–643.

Kühner, S., V. van Noort, M. J. Betts, A. Leo-Macias, C. Batisse *et al.*, 2009 Proteome organization in a genome-reduced bacterium. Science 326: 1235–1240.

Lambert, J.-P., G. Ivosev, A. L. Couzens, B. Larsen, M. Taipale *et al.*, 2013 Mapping differential interactomes by affinity purification coupled with data-independent mass spectrometry acquisition. Nat. Methods 10: 1239–1245.

Landry, D. M., M. I. Hertz, and S. R. Thompson, 2009 RPS25 is essential for translation initiation by the Dicistroviridae and hepatitis C viral IRESs. Genes Dev. 23: 2753–2764.

Lee, A. S.-Y., R. Burdeinick-Kerr, and S. P. J. Whelan, 2013 A ribosome-specialized translation initiation pathway is required for cap-dependent translation of vesicular stomatitis virus mRNAs. Proc. Natl. Acad. Sci. USA 110: 324–329.

Li, J.-J., and D. Xie, 2015 RACK1, a versatile hub in cancer. Oncogene 34: 1890–1898.

Liliental, J., and D. D. Chang, 1998 Rack1, a receptor for activated protein kinase C, interacts with integrin beta subunit. J. Biol. Chem. 273: 2379–2383.

Lin, J.-C., and W.-Y. Tarn, 2009 RNA-binding motif protein 4 translocates to cytoplasmic granules and suppresses translation via Argonaute2 during muscle cell differentiation. J. Biol. Chem. 284: 34658–34665.

Long, L., Y. Deng, F. Yao, D. Guan, Y. Feng *et al.*, 2014 Recruitment of phosphatase PP2A by RACK1 adaptor protein deactivates transcription factor IRF3 and limits type I interferon signaling. Immunity 40: 515–529.

Majzoub, K., M. L. Hafirassou, C. Meignin, A. Goto, S. Marzi *et al.*, 2014 RACK1 controls IRES-mediated translation of viruses. Cell 159: 1086–1095.

Martins, N., J.-L. Imler, and C. Meignin, 2016 Discovery of novel targets for antivirals: learning from flies. Curr. Opin. Virol. 20: 64–70.

Mauro, V. P., and G. M. Edelman, 2002 The ribosome filter hypothesis. Proc. Natl. Acad. Sci. USA 99: 12031–12036.

Mueller, S., V. Gausson, N. Vodovar, S. Deddouche, L. Troxler *et al.*, 2010 RNAi-mediated immunity provides strong protection against the negative-strand RNA vesicular stomatitis virus in Drosophila. Proc. Natl. Acad. Sci. USA 107: 19390–19395.

Nayak, A., B. Berry, M. Tassetto, M. Kunitomi, A. Acevedo *et al.*, 2010 Cricket paralysis virus antagonizes Argonaute 2 to modulate antiviral defense in Drosophila. Nat. Struct. Mol. Biol. 17: 547–554.

Otsuka, M., A. Takata, T. Yoshikawa, K. Kojima, T. Kishikawa *et al.*, 2011 Receptor for activated protein kinase C: requirement for efficient

microRNA function and reduced expression in hepatocellular carcinoma. PLoS One 6: e24359.
Picotti, P., and R. Aebersold, 2012 Selected reaction monitoring-based proteomics: workflows, potential, pitfalls and future directions. Nat. Methods 9: 555–566.
Picotti, P., M. Clément-Ziza, H. Lam, D. S. Campbell, A. Schmidt *et al.*, 2013 A complete mass-spectrometric map of the yeast proteome applied to quantitative trait analysis. Nature 494: 266–270.
Rinner, O., L. N. Mueller, M. Hubálek, M. Müller, M. Gstaiger *et al.*, 2007 An integrated mass spectrometric and computational framework for the analysis of protein interaction networks. Nat. Biotechnol. 25: 345–352.
Ron, D., C. H. Chen, J. Caldwell, L. Jamieson, E. Orr *et al.*, 1994 Cloning of an intracellular receptor for protein kinase C: a homolog of the beta subunit of G proteins. Proc. Natl. Acad. Sci. USA 91: 839–843.
Schmitt, K., N. Smolinski, P. Neumann, S. Schmaul, V. Hofer-Pretz *et al.*, 2017 Asc1p/RACK1 connects ribosomes to eukaryotic phosphosignaling. Mol. Cell. Biol. 37: e00279-16.
Selevsek, N., C.-Y. Chang, L. C. Gillet, P. Navarro, O. M. Bernhardt *et al.*, 2015 Reproducible and consistent quantification of the Saccharomyces cerevisiae proteome by SWATH-mass spectrometry. Mol. Cell. Proteomics MCP 14: 739–749.
Sharma, G., J. Pallesen, S. Das, R. Grassucci, R. Langlois *et al.*, 2013 Affinity grid-based cryo-EM of PKC binding to RACK1 on the ribosome. J. Struct. Biol. 181: 190–194.
Speth, C., E.-M. Willing, S. Rausch, K. Schneeberger, and S. Laubinger, 2013 RACK1 scaffold proteins influence miRNA abundance in Arabidopsis. Plant J. Cell. Mol. Biol. 76: 433–445.
Starita, L. M., R. S. Lo, J. K. Eng, P. D. von Haller, and S. Fields, 2012 Sites of ubiquitin attachment in Saccharomyces cerevisiae. Proteomics 12: 236–240.
Topisirovic, I., and N. Sonenberg, 2011 Translational control by the eukaryotic ribosome. Cell 145: 333–334.
Valerius, O., M. Kleinschmidt, N. Rachfall, F. Schulze, S. López Marín *et al.*, 2007 The Saccharomyces homolog of mammalian RACK1, Cpc2/Asc1p, is required for FLO11-dependent adhesive growth and dimorphism. Mol. Cell. Proteomics MCP 6: 1968–1979.
van Mierlo, J. T., A. W. Bronkhorst, G. J. Overheul, S. A. Sadanandan, J.-O. Ekström *et al.*, 2012 Convergent evolution of Argonaute-2 slicer antagonism in two distinct insect RNA viruses. PLoS Pathog. 8: e1002872.
van Rij, R. P., M.-C. Saleh, B. Berry, C. Foo, A. Houk *et al.*, 2006 The RNA silencing endonuclease Argonaute 2 mediates specific antiviral immunity in Drosophila melanogaster. Genes Dev. 20: 2985–2995.
Wang, F., M. Yamauchi, M. Muramatsu, T. Osawa, R. Tsuchida *et al.*, 2011 RACK1 regulates VEGF/Flt1-mediated cell migration via activation of a PI3K/Akt pathway. J. Biol. Chem. 286: 9097–9106.
Wang, S., J.-Z. Chen, Z. Zhang, S. Gu, C. Ji *et al.*, 2003 Cloning, expression and genomic structure of a novel human GNB2L1 gene, which encodes a receptor of activated protein kinase C (RACK). Mol. Biol. Rep. 30: 53–60.
Wang, X.-H., R. Aliyari, W.-X. Li, H.-W. Li, K. Kim *et al.*, 2006 RNA interference directs innate immunity against viruses in adult Drosophila. Science 312: 452–454.
Wepf, A., T. Glatter, A. Schmidt, R. Aebersold, and M. Gstaiger, 2009 Quantitative interaction proteomics using mass spectrometry. Nat. Methods 6: 203–205.
Yang, S.-J., Y. S. Park, J. H. Cho, B. Moon, H.-J. Ahn *et al.*, 2017 Regulation of hypoxia responses by flavin adenine dinucleotide-dependent modulation of HIF-1α protein stability. EMBO J. 36(8): 1011–1028.

Communicating editor: E. R. Gavis

CHAPTER III

FUNCTIONAL CHARACTERIZATION OF POST-TRANSLATIONAL MODIFICATION SITES IN RACK1

I. INTRODUCTION

RACK1 was initially identified as a protein interacting with the signaling protein PKC (Ron et al., 1994). Several studies also reported RACK1 as a signaling hub interacting with a plethora of signaling proteins (Adams et al., 2011; Nielsen et al., 2017). This protein is present in all eukaryotes (Dresios et al., 2006) and is a stoichiometric component of the 40S subunit of the ribosome and thus a core ribosomal protein (Sengupta et al., 2004; Slavov et al., 2015). These properties make RACK1 an ideal candidate to integrate inputs from distinct signaling pathways at the level of the ribosome. Curiously however, the relation between the signaling and translation functions of RACK1 has not been addressed so far (Gibson, 2012). The available the fly genetic tools provide a powerful system to explore this question in a multicellular organism.

RACK1 mutants unable to associate with the ribosome do not support translation and replication of CrPV (Majzoub et al., 2014). We wondered whether RACK1 residues reported to associate with signaling molecules (Chang et al., 2001; Kiely et al., 2009), adhesion molecules (Kiely et al., 2008), or components of the autophagy pathway (Zhao et al., 2015) in mammalian cell culture were also involved in the translation of CrPV in *Drosophila* cells. We mutated the corresponding residues in *Drosophila* RACK1 to test their function (**Figure 7A**). We also deleted the knob region of RACK1 (Δknob), a conserved loop (amino acids 275-283) pointing to

the ribosome, although its presence is not required for RACK1 binding to the ribosome (**Figure 7B**) (Coyle et al., 2009). A closer analysis of the structure of the RACK1 knob at the ribosome made us suspect that Threonine 279 (T279) could interact with Aspartic acid 283 (D283). We thus modified both amino acids into Alanine to prevent this potential interaction. The orientation of the Serine 280 (Ser280) and Lysine 281 (Lys281) suggested they might interact with the 18S rRNA and RpS17/eS17 protein respectively. We thus modified these amino acids into Alanine to prevent a potential interaction. Moreover, a recent study showed that poxviruses phosphorylate RACK1 knob upon infection (Jha et al., 2017). These phosphorylations confer a negative charge to the knob, which favors translation of viral late mRNAs that contain polyA leaders. To see whether the phosphorylation of the conserved Threonine 279 (Thr279) and the region containing Serine 277 - Proline 278 - Threonine 279 – Glutamic acid 280 (SPTE) were also involved in viral IRES translation, we decided to include the equivalent phosphomimetics modifications in our study by replacing the potentially phosphorylated amino acids by Glutamic acids (T279E and SPTE-EPEE).

II. RESULTS

A. The knob region of RACK1 is required for translation and replication of *Dicistroviridae*

To assess the role of the modified versions of RACK1 in viral IRES translation, we used a modified S2 cell line (S2_shRACK1) that stably expresses a small hairpin RNA (shRNA) targeting the 5'UTR of RACK1 mRNA expressed under the control of the metallothionein promoter (Majzoub et al., 2014). We rescued the expression of RACK1 in these cells by transfection of plasmids coding for different versions of tagged-RACK1 complementary (cDNA) under the *actin42A* promoter. These cells were also transfected with a CrPV 5'IRES-Renilla reporter plasmid and a standard capped-Firefly reporter plasmid (**Figure 8A**). Expression of a FLAG-tagged wild-type (WT) version of RACK1 allowed the translation of the CrPV 5'IRES whereas expression of RACK1 versions unable to bind to the ribosome (D108Y) did not allow CrPV 5'IRES translation (**Figure 8B**). Both WT *Drosophila* and human RACK1 proteins were able to support CrPV 5'IRES translation, showing that the function of RACK1 towards viral replication is conserved across species.

To rule out an influence of the peptide tag used, we also expressed HA-tagged RACK1. Expression of a HA-tagged WT version of RACK1 allowed the translation of the CrPV 5'IRES whereas expression of two RACK1 versions unable to bind to the ribosome (R36D-K38E and D108Y) did not allow CrPV 5'IRES translation (**Figure 8C**). We showed by western-blot that all the signaling mutants (T51A, Y53F, Y229F, Y247F and Y303F) were expressed in S2 cells. Furthermore, all these modified versions of RACK1 were able to support translation driven by the 5'IRES of CrPV, like the WT protein. This suggests that the interaction of RACK1 with the tested cofactors (Vps15, Atg14, Beclin, FAK, Src, β-integrin, PP2A) is not necessary for its role in the selective translation of viral IRES.

Interestingly however, a complete deletion of the knob (Δknob) affected CrPV translation similarly to cells depleted of RACK1 (**Figure 8D**). The T279A and T279E substitutions also showed an impaired CrPV 5'IRES translation, but the proteins were not expressed properly (**Figures 8D, 8E**). In the same way, the SPTS-EPEE mutant showed an impaired translation of the virus, but the SPTS-EPEE protein was less expressed than the WT protein (**Figure 8E**). All the other proteins with point mutations in the knob (S208A, K281A and D283A) were expressed at the same level as the WT protein and behaved like WT RACK1 (**Figure 8D**). Overall, these results reveal that the knob region of RACK1 is necessary for CrPV translation, although the precise residues involved remain to be pinpointed.

We conclude that the interaction of RACK1 with the tested cofactors does not play a crucial role in the regulation of an IRES-containing virus, at least in this tissue culture assay. One caveat is that we did not confirm by co-immunoprecipitation that the interaction between RACK1 and its cofactor is abolished upon mutation of the corresponding residue in our *Drosophila* model. Nevertheless, the knob region of RACK1 appears to play an important role in this process. Finally, we validated these results on the importance of the knob in the context of virus-infected cells. We complemented the S2_shRACK1 cells with different versions of RACK1 and infected the cells with CrPV or DCV (**Figure 9A**). As expected, expression of the WT version of RACK1 allowed replication of both viruses, whereas expression of the two versions of RACK1 unable to bind to the ribosome did not allow viral replication (**Figures 9B, 9C**). By contrast, expression of the RACK1 Δknob did not support the replication of either CrPV or DCV.

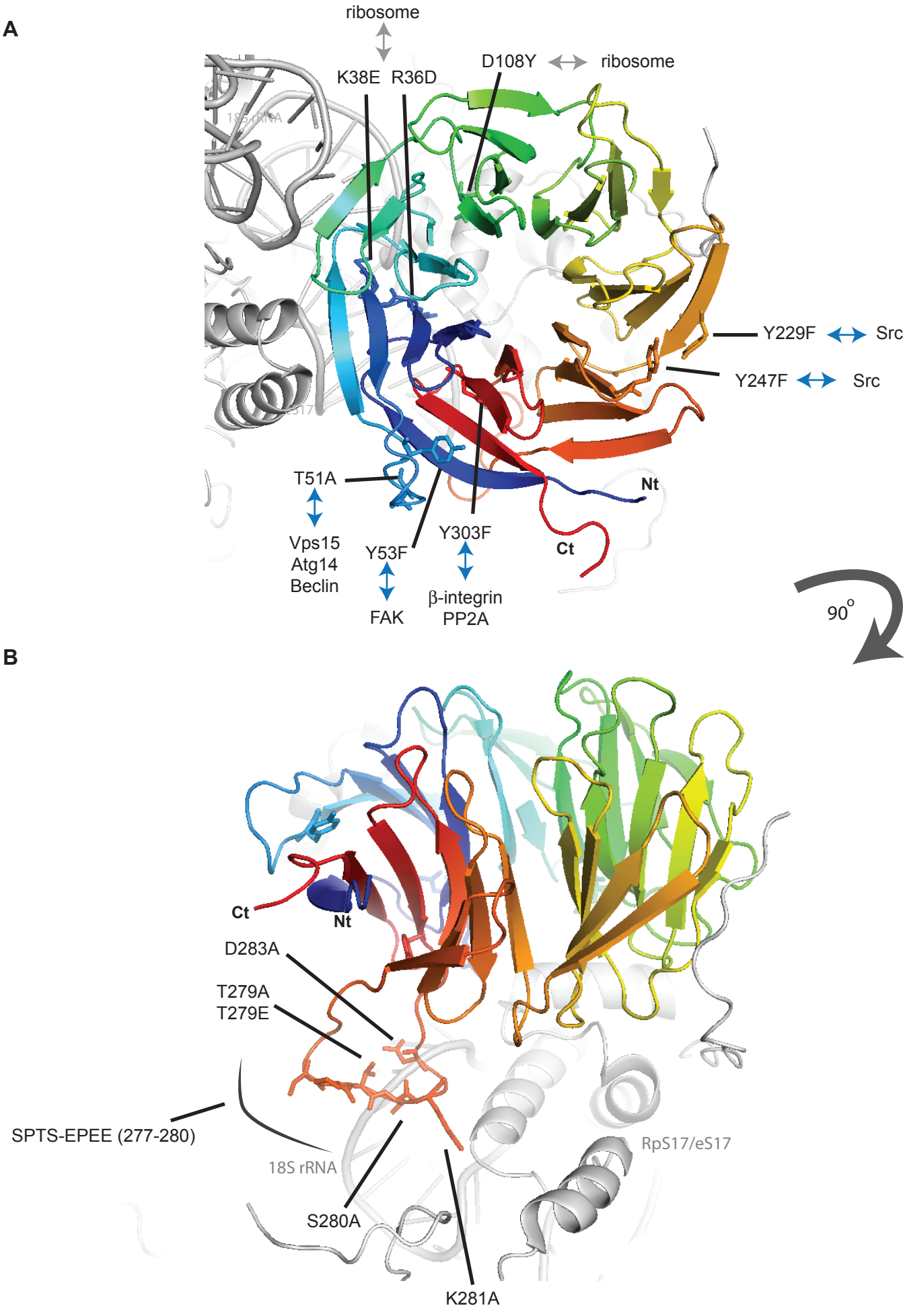

Figure 7: Position of the mutated RACK1 residues. (A-B) RACK1 protein structure is depicted in color, together with the neighbouring RpS17/eS17 and 18S rRNA in grey. **A**. View of RACK1 from the top of the molecule. All the mutated amino acids are indicated, together with the interaction they abolish (in blue: signaling proteins, in grey: ribosome). **B**. View of RACK1 from the side of the molecule. The mutated amino acids position in the knob region are indicated.

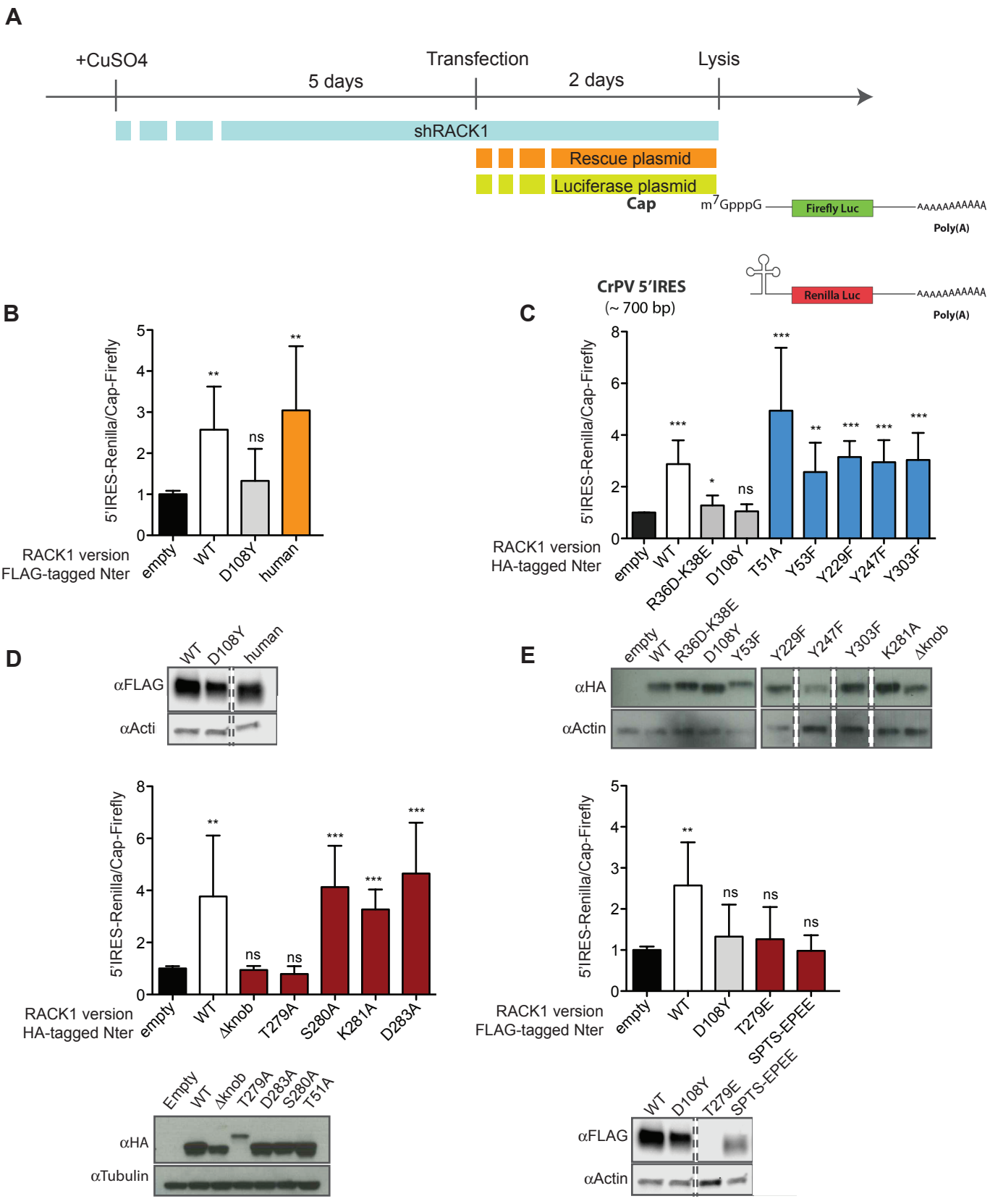

Figure 8: Activity of CrPV 5'IRES in S2 cells expressing modified versions of RACK1. A. Experimental setup. S2 cells expressing a shRNA against RACK1 were complemented with different RACK1 versions together with cap-Firefly and CrPV 5'IRES-Renilla coding plasmids. **B**. CrPV 5'IRES activity measured after expression of a FLAG-tagged WT RACK1 version (white) or versions impairing interaction with the ribosome (grey) or the human protein (orange). **C**. CrPV 5'IRES activity measured after expression of a HA-tagged WT RACK1 version (white), or RACK1 versions impairing interaction with the ribosome (grey) or with signaling partners (blue). **D**. CrPV 5'IRES activity measured after expression of a HA-tagged WT RACK1 version (white) or RACK1 versions modified in the knob region (red). **E**. CrPV 5'IRES activity measured after expression of a FLAG-tagged WT RACK1 version (white) or RACK1 versions modified in the knob region (red). (**B-E**) Western-blotting was performed in parallel (n=1). Statistical analysis was performed using unpaired t-test with Welch correction. Data show the mean + SEM of 3 independent experiments. ns: nonsignificant; *p<0.05; **p < 0.01; ***p<0.001.

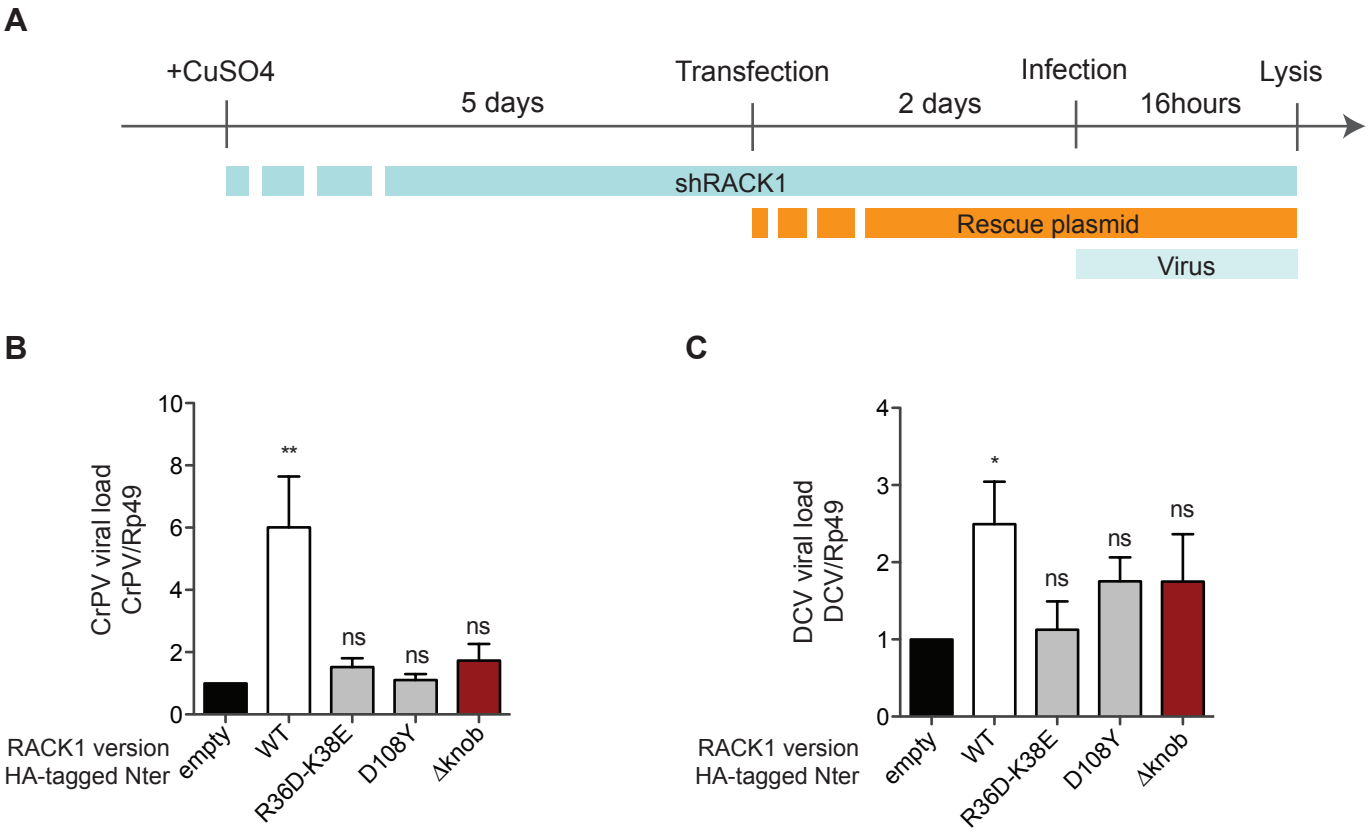

Figure 9: The knob region of RACK1 is required for replication of CrPV and DCV. A. Experimental setup. S2 cells expressing a shRNA against RACK1 were complemented with different RACK1 versions before viral infection. **B-C**. Expression of an empty plasmid, WT version of RACK1, RACK1 versions impairing interaction with the ribosome (grey) or deleted of the knob region (red) in S2_shRACK1 cells. Cells were infected with CrPV (**B**) or DCV (**C**). Statistical analysis was performed using unpaired t-test with Welch correction. Data show the mean + SEM of 3 independent experiments. ns: nonsignificant; *p<0.05; **p < 0.01; ***p<0.001.

These results confirm the importance of the knob for the replication of IRES-containing viruses. This might be explained in two ways: (i) complete deletion of the knob in *Drosophila* RACK1 impairs its integration into the ribosome, or (ii) RACK1 knob is a central region for RACK1 activity as a translational selector.

B. Towards the role of RACK1 interaction with cofactors *in vivo*

Until now, the function of RACK1 remains poorly characterized *in vivo*. Indeed, most functional studies have been carried in yeast, a unicellular eukaryote. We wanted to take advantage of the *Drosophila* model to gain insight on the role of RACK1 in a multicellular organism. *In vivo*, RACK1 deletion is lethal during development in flies and mice (Kadrmas et al., 2007; Volta et al., 2013). To understand whether the interaction of RACK1 with the ribosome and/or cofactors is important during development, we aimed at complementing RACK1 mutant flies with some of the mutant versions of RACK1 described above. We also generated a transgene to see if human RACK1 could substitute to the drosophila protein *in vivo*. We generated transgenic flies expressing under the ubiquitous hsp70 promoter different RACK1 versions, carrying a FLAG-tagged at their N-termini. All transgenes were inserted in the same region of the third chromosome in the *Drosophila* genome using ΦC31-mediated integration at *attP* sites. We first tested the incorporation of RACK1 in the ribosomes *in vivo* (**Figure 10**). Flies overexpressing the modified versions of RACK1 were subjected to sucrose gradient fractionation followed by western-blot. The WT version of RACK1 integrated into the ribosome, as did the human version of the protein. As expected, the two RACK1 versions unable to bind to the ribosome (R36D-K38E and D108Y) were found only in the free fraction. The Y247F and Y303F versions, which were active in the 5'IRES reporter assay in S2 cells, were correctly inserted into the ribosome. Interestingly, the Δknob version, which was inactive in this assay, was also inserted in ribosomes. This confirms the results obtained in yeast (Coyle et al., 2009) and highlights the importance of the knob in the activity of RACK1 at the ribosome. Of note, RACK1 was detected in the free fraction for many constructs (WT, human RACK1, Y247F, Y303F and Δknob) although the endogenous RACK1 protein from CantonS WT flies was restricted to the ribosomal fractions. We hypothesize that the presence of RACK1 in the soluble fraction could result from the overexpression of the protein.

The function of these RACK1 mutants was tested by genetic complementation in a RACK1 null mutant background (**Figure 11**). None of the transgenes, even the WT version of RACK1, could rescue the mutant lethal phenotype. This is surprising, especially because Carine Meignin succeeded in previous unpublished experiments to rescue the RACK1 mutants with a WT transgene, but not with the R36D-K38E or D108Y transgene. We reasoned that the parental mutant line might have acquired other mutations elsewhere in the genome. Therefore, we generated our own Clustered Regularly Interspaced Short Palindromic Repeats (CRISPR)/CRISPR associated (Cas9) knock out (KO) flies. We used the protocol already described in Port and Bullock, 2016, and generated transgenic flies expressing three different single guide RNA (sgRNAs) targeting RACK1 exons (**Figure 12A**). We crossed these flies with females expressing the Cas9 protein in the germline (**Figure 12B**) and screened by PCR the offspring. More than half of the males tested had a deletion in the region of the RACK1 gene (**Figure 12C**). We sequenced the genomic DNA of F2 flies and observed a deletion of 845 nucleotides in the gene region of RACK1, resulting in a premature stop codon at the amino acid 48. After performing all the crosses depicted in **Figure 12B**, we obtained heterozygous mutants of RACK1 using this technique. However, we were not able to maintain the mutation with the *CyO* balancer chromosome and the mutation was lost. Indeed, this balancer chromosome is known to be poorly efficient at maintaining mutations near the chromosome ends (Bloomington Drosophila Stock Center). As a result, we were not able to perform the planned phenotypic rescue experiments with the panel of RACK1 mutants we constructed. Nevertheless, we have introduced the CRISPR/Cas9 system in the team and all the tools are now available to generate new mutants. Other balancer chromosomes such as SM1, SM5, or SM6a will be used to maintain heterozygous RACK1 mutation in future experiments.

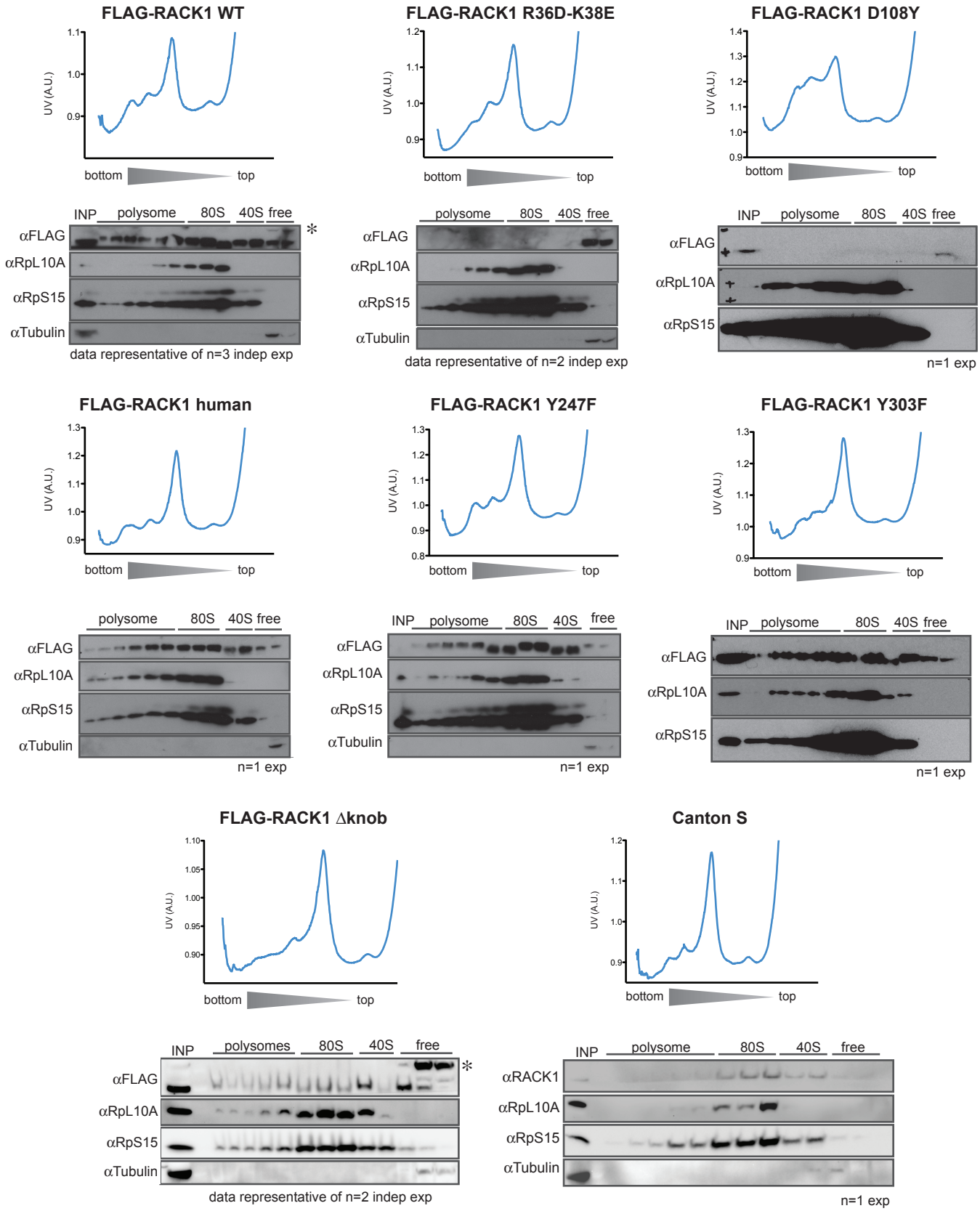

Figure 10: Integration of RACK1 transgenic versions into the ribosome. Drosophila expressing FLAG-RACK1 versions of WT RACK1, R36D-K38E, D108Y, human RACK1, Y247F, Y303F, and Δknob were subjected to sucrose gradient fractionnation to separate between polysome, monosome, 40S and free fractions. Wild-type CantonS flies were also used as a control of the subcellular localization of endogenous RACK1. Fractions were selected and subjected to western-blot.The number of independent experiments is indicated.

* Aspecific band.

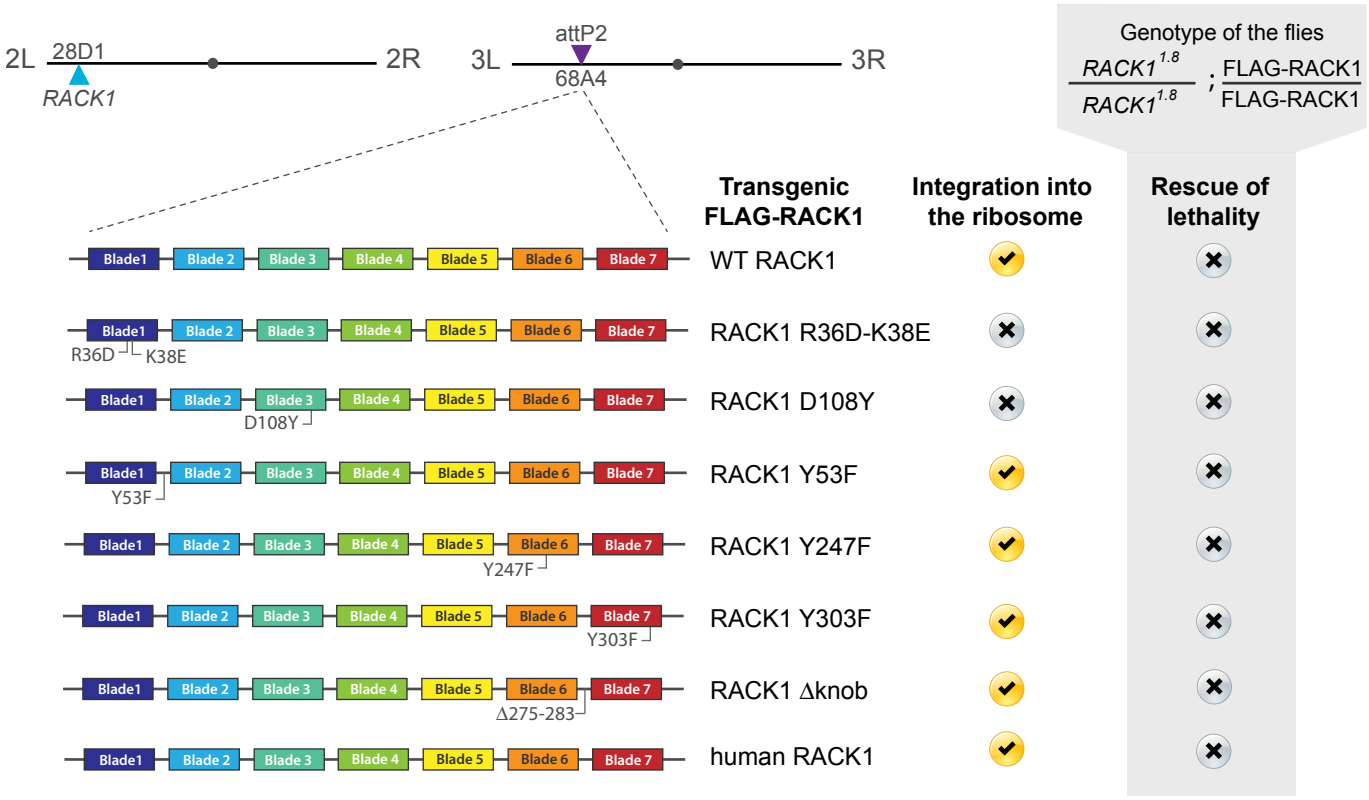

Figure 11: RACK1 transgenic fly lines obtained. Transgenic flies expressing different FLAG-tagged RACK1 versions under the hsp70 promoter were obtained. The integration of RACK1 into ribosome is indicated, as well as the phenotype considering lethality during development.

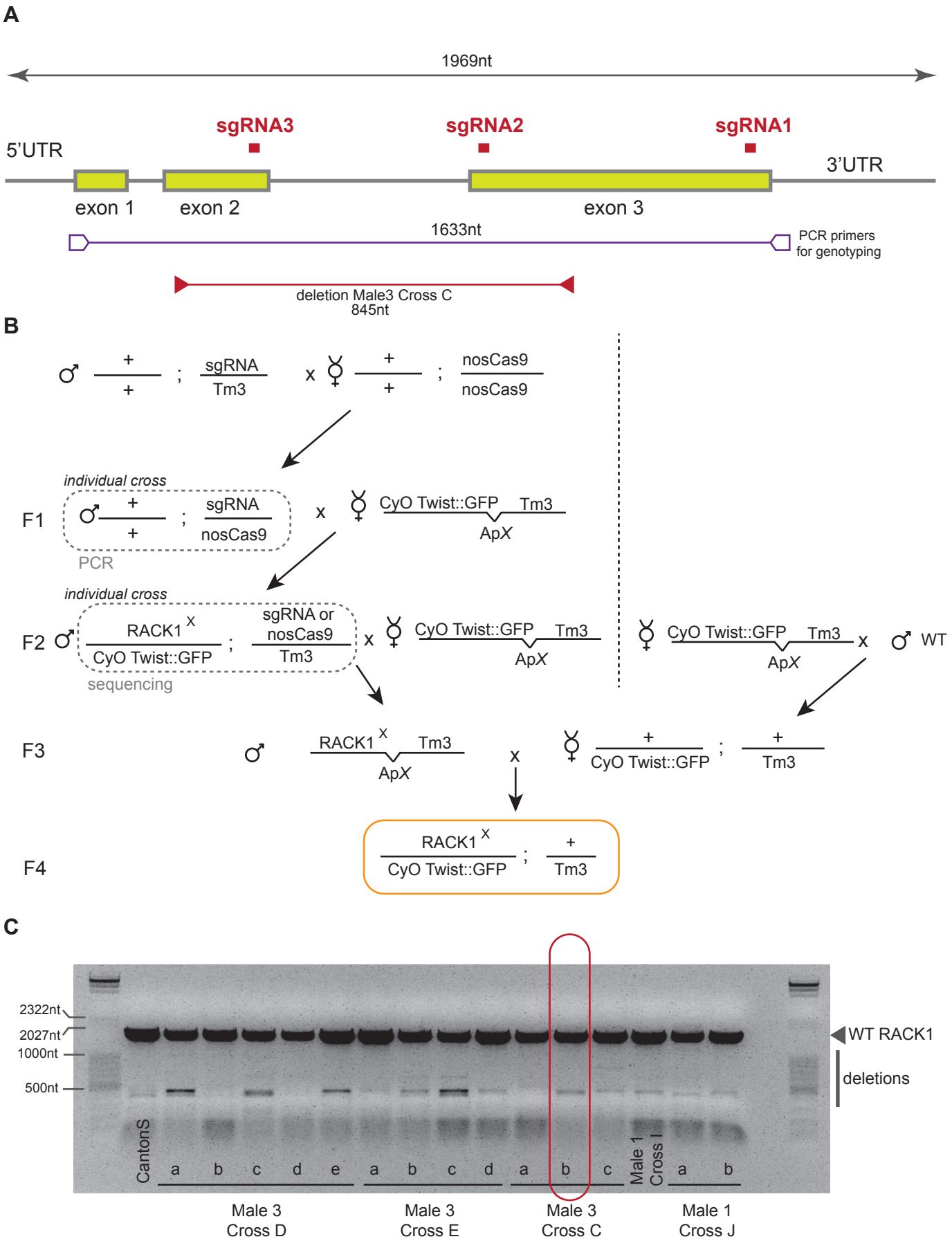

Figure 12: Strategy for the generation of RACK1 mutation *in vivo* by CRISPR/Cas9. A. Annotated RACK1 gene region showing the position of the 3 sgRNA used, the PCR primers used for screening of mutants and the position of one of the deletions obtained (Male 3 cross C). **B**. Crossing scheme made to obtain heterozygous RACK1 mutants (mutation noted RACK1^{X}). **C**. Agarose gel after PCR made on individual males from the F1. The sequenced line is framed in red.

III. DISCUSSION

A. A role of PKC in RACK1-dependent selective translation?

RACK1 was first identified as an anchoring protein for activated PKC (Ron et al., 1994). Since then, it has been proposed that RACK1 links PKC and the ribosome. In mammalian cells, PKC stimulation leads to eIF6 phosphorylation, release, and subsequent joining of the two ribosomal subunits (Ceci et al., 2003). RACK1 interaction with eIF6 thus provides a physical link between PKC signaling and ribosome activation. Moreover, binding of PKCβII to RACK1 is important for PKC-mediated translational control (Grosso et al., 2008). This was confirmed *in vivo*, as MEFs derived from RACK1 heterozygous mutant mice have reduced PKC-stimulated translation activity in cell culture assays (Volta et al., 2013). All these data point to a role of RACK1 as a PKC platform at the ribosome, linking extracellular stimuli to translation. Unfortunately, we could not test the relevance of PKC interaction towards viral translation, since its binding site on RACK1 is still unknown.

B. How to separate between RACK1 function at the ribosome and in signaling?

RACK1 has previously been associated with a diversity of signaling pathways (Adams et al., 2011; Nielsen et al., 2017). Hence, the function of RACK1 in selective translation of mRNAs may be dependent on the signaling activity of its binding partners. Our *ex vivo* data do not support this hypothesis. However, we only tested cofactors for which the interacting site on RACK1 was mapped. This small list of proteins does not represent the plethora of RACK1 protein partners described. Of note, our study of RACK1 partners *ex vivo* in S2 cells did not identify PKC, FAK, or other signaling proteins reported to interact with RACK1 (see above Results Chapter II and Kuhn et al., 2017). However, we still cannot exclude that RACK1 has a role in signaling pathways and interact with its signaling partners in a transient interaction. Indeed, comparison of the phosphoproteome of WT and Asc1/RACK1 mutant *S. cerevisiae* showed that the phosphorylation of 120 sites in 90 proteins is dependent on Asc1p/RACK1 (Schmitt et al., 2017). Additionally, several subunits of eIF3 are

phosphorylated. Thus, it is possible that RACK1-associated kinases could regulate the function of eIF3 on the ribosome, regulating the initiation process (Siridechadilok et al., 2005). A way to decipher the mechanism of RACK1-dependent translation of viral RNAs would be to perform mass spectrometry analysis of endogenous RACK1 immunoprecipitates *in vivo*, in the course of an infection. The identification of RACK1 partners and/or PTMs should help in understanding how RACK1 is acting at the interface between signaling and translation.

However, some functions of RACK1 might be strictly dependent on its function at the ribosome. For instance, expression of WT RACK1 in Huh7 cells promotes resistance to apoptosis induced by doxorubicin (an anti-cancer drug used in chemotherapy) (Ruan et al., 2012). Expression of the ribosome-binding defective mutant had the opposite phenotype, as it increases the cell sensibility to this drug. The other mutants (Y302F, Y52F, and Y228F/Y246F) still promoted resistance of HCC cells like WT RACK1. As in our assay, it seems that resistance to apoptosis is due to the function of RACK1 at the ribosome, and not to its interaction with cofactors. However, similar to our experiments, this study only tested the effect of the interaction with a limited number of cofactors.

C. Mechanism by which the RACK1 knob mediates selective translation

Overall, our results suggest a role of the knob region of RACK1 in the selective translation of the 5'IRES of CrPV and DCV. Indeed, its complete deletion does not affect the integration of RACK1 to the ribosome, but affects 5'IRES translation in a similar way than a ribosomal mutant. We did not manage to narrow down the important residues, as single amino acid mutations in this region either did not impact the tested function of the protein or affected its expression. In particular, we highlighted the importance of the residue Thr279 in the stability of the protein. Indeed, both T279A and T279E mutants are unstable and degraded.

The knob region of RACK1 is of particular interest, as it has been shown to be phosphorylated by Poxviruses kinase and to favor viral RNA translation (Jha et al., 2017). In our experimental system, expression of the phosphomimics SPTS-EPEE, which favors Poxviruses translation, seemed to prevent CrPV 5'IRES translation. Thus, the knob region of RACK1 might play a role in viral translation

through virus-specific mechanisms. We suspect that some residues in the knob could be phosphorylated upon viral infection. Indeed, *Drosophila* RACK1 knob region (9 amino acids) contains two serines and one threonine, which are potential phosphorylation sites. Thus, our results suggest that the knob region of RACK1 is a platform for the recruitment to the ribosome of cofactors required for selective translation. Clearly, a more detailed analysis of the function of this region of RACK1 is warranted.

CHAPTER IV

RACK1 REGULATES GENE EXPRESSION IN RESPONSE TO STRESS

I. Introduction

In the last five years, RACK1 has been described as an host factor necessary for the replication of several human diseases-causing viruses such as HCV, VacV, DENV, ZIKV and WNV (Hafirassou et al., 2017; Jha et al., 2017; Majzoub et al., 2014). These results raise interest for the use of RACK1 as a HTA target for a broad range of viral infections. However, targeting a host protein might result in cellular toxicity, highlighting the importance of understanding the role of RACK1 in the cell biology in non-infected conditions.

Our *ex vivo* studies in *Drosophila* cells suggest that RACK1 is not required for cell viability in normal culture conditions (Majzoub et al., 2014). Furthermore, depletion of RACK1 *in vivo* only affects long-term survival in optimal conditions. However, RACK1 is necessary during the development of multicellular organisms such as mouse and *Drosophila* (Kadrmas et al., 2007; Volta et al., 2013). One obvious way to identify cellular mRNAs for which translation require RACK1 would be to study the precise role of RACK1 in development. However, this can be expected to be a complicated task, as RACK1 homozygous mutant flies are not viable and lethality could result from tissue-specific defects or occur with delayed kinetics following defective translation of one or a set of mRNAs. Reports published in the literature, mainly on yeasts, suggest a role for RACK1 in stress response. For example, in *S. pombe*, Cpc2/RACK1 is involved in the control of arsenite response (Sanchez-Marinas et al., 2018). Moreover, the cellular response against hydrogen peroxide stress is partially compromised in Cpc2/RACK1 depleted cells (Núñez et al.,

2009). In cultured human cells as well, RACK1 facilitates the activation of the MAPK pathway by X-rays or genotoxic drugs (Arimoto et al., 2008).

All these results made us wonder whether RACK1 may also be involved in stress response in a multicellular organism such as *Drosophila*. Indeed, the rapid response to stress would provide an interesting experimental system to uncover the RACK1-dependent cellular mRNAs with the aim of shedding light on translation-based mechanisms of adaptation to stress.

II. Results

A. RACK1 is required for viability after stress *in vivo* and *ex vivo*

To identify RACK1-dependent mRNAs, we looked for conditions in which RACK1 is required for cell viability. To this aim, we tested the response to ER and oxidative stress both *in vivo* and *ex vivo.* As RACK1 null mutations are lethal during development (Kadrmas et al., 2007), we used the inducible *Actin*Gal4/*Tubulin*Gal80^{TS} system that drives the expression of a transgene under the control of an upstream activating sequence (UAS) in the whole organism, upon temperature switch to 29ºC. Once adult flies hatched, we incubated them at 29°C for five days to drive the ubiquitous expression of shRNAs targeting either RACK1 (shRACK1) or mCherry (shmCherry) as a control. We previously showed that the RACK1 protein is knocked-down (KD) after five days at 29°C (Majzoub et al., 2014). We then fed the shmCherry and shRACK1 flies with a sucrose solution containing or not the tested chemical. Expression of RACK1 was still strongly reduced three days post exposure to the stress (**Figure 13A**). We monitored fly survival every day after exposure to 25mM or 50mM Dithiothreitol (DTT), an inducer of endoplasmic reticulum (ER) stress (**Figures 13B, 13C**). We also used paraquat, a well-known herbicide inducing an oxidative stress (**Figures 13D, 13E**) and tunicamycin, another inducer of ER stress (**Figures 13F, 13G**). After 7 days with the control regimen (sucrose only), both fly lines started to decline. When treated with the drugs, the survival of the flies was impaired in a dose-dependent manner. Interestingly, shRACK1 flies succumbed faster than the shmCherry control flies when exposed to DTT (25mM and 50mM), tunicamycin

(8µM) and paraquat (3mM and 4mM). These results suggest that RACK1 participates in stress responses *in vivo*.

In parallel, we tested the role of RACK1 in response to stress *ex vivo* using cell culture. We used a modified S2 cell line (S2_shRACK1) that stably expresses a shRNA targeting the 5'UTR of RACK1 mRNA expressed under the control of the metallothionein promoter (Majzoub et al., 2014). Treatment with 0.5mM $CuSO_4$ induced the expression of the shRACK1 and an efficient KD of RACK1 after five days compared to $CuSO_4$ treated S2 cells, as previously reported (**Figure 14A**). We then incubated both cell lines with normal medium, or medium containing 25mM DTT for one hour and monitored the cell viability during the following days. After two days of culture in non-stressed condition, 90% of the untreated cells were viable for both cell lines (**Figure 14B**). However, we observed an impaired viability of the S2_shRACK1 cells 48 hours after the ER stress compared with the control cells (**Figure 14C**). Similar results were obtained when cells were treated with 10mM hydrogen peroxide (H_2O_2) for one hour (**Figure 14D**). These data indicate that RACK1 is also required for stress response in tissue culture cells.

To test whether RACK1 is also required for cell viability upon stress in human cells, we used the Hap1 cell line and two derived KO lines (Jha et al., 2017). We confirmed by western-blot the loss of RACK1 expression in the two KO cell lines (**Figure 14E**). We then subjected these cells to medium containing 1mM H_2O_2 or not for one hour and monitored cell viability for two days. Treatment with control medium did not affect cell viability (**Figure 14F**). However, upon treatment with H_2O_2, we observed an impaired viability of both RACK1 E3A5 and E3A6 KO cell lines two days after the stress (60% and 40% of living cells respectively) (**Figure 14G**). These results indicate that RACK1 is required for stress response to oxidative stress in human Hap1 cells, as in *Drosophila*.

Overall, these data reveal that RACK1 is required for cell viability *in vivo* and *ex vivo*, in flies and humans. We hypothesized that this reflected the role of RACK1 in the translational regulation of mRNAs involved in stress response.

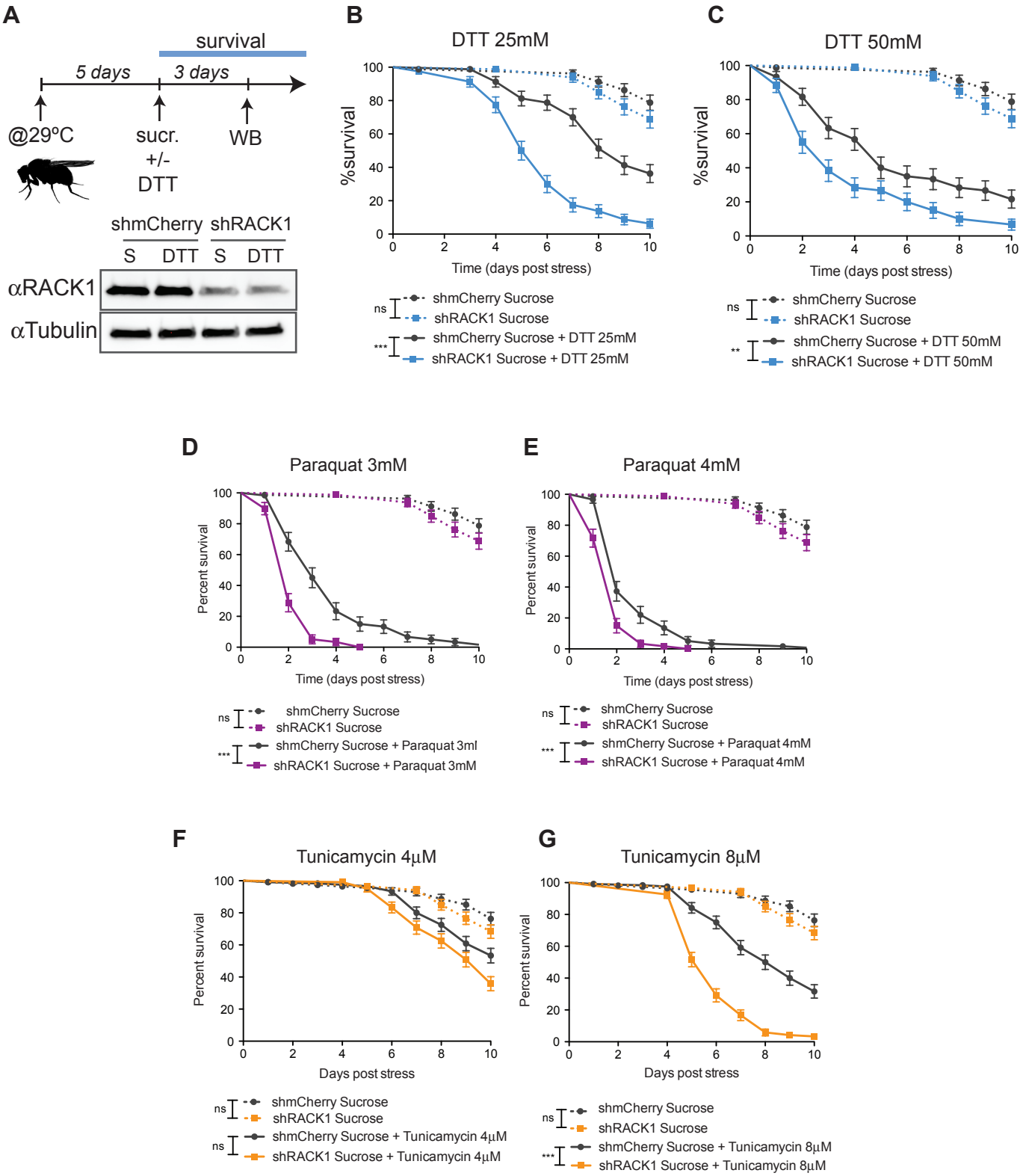

Figure 13: RACK1 is required for stress response in *Drosophila in vivo*. A. *Actin*Gal4;*Tubulin*Gal80^{TS} >UAS::shmCherry and >UAS::shRACK1 flies were raised for 5 days at 29ºC to induce shRNA expression. Flies were treated with sucrose supplemented or not with DTT and Western-blot (WB) was performed 3 days later to assess RACK1 KD efficiency. One blot representative of 2 independent experiments is presented. **B-C.** Survival of *Actin*Gal4;*Tubulin*Gal80^{TS}>UAS::shmCherry and >UAS::shRACK1 flies after ER stress induced by DTT feeding at 25mM (**B**) or 50mM (**C**). **D-E**. Survival of *Actin*Gal4;*Tubulin*Gal80^{TS} >UAS::shmCherry and >UAS::shRACK1 flies after oxidative stress induced by paraquat feeding at 3mM (**D**) or 4mM (**E**). **F-G**. Survival of *Actin*Gal4;*Tubulin*Gal80^{TS} >UAS::shmCherry and >UAS::shRACK1 flies after ER stress induced by tunicamycin feeding at 4µM (**F**) or 8µM (**G**). **B-G**. Fly survival was monitored every day and statistical analysis was performed using Log-rank (Mantel-Cox) Test. Data represent mean+SEM of 3 independent experiments (total of n=60 flies). ns: nonsignificant; *p<0.05; **p < 0.01; ***p<0.001.

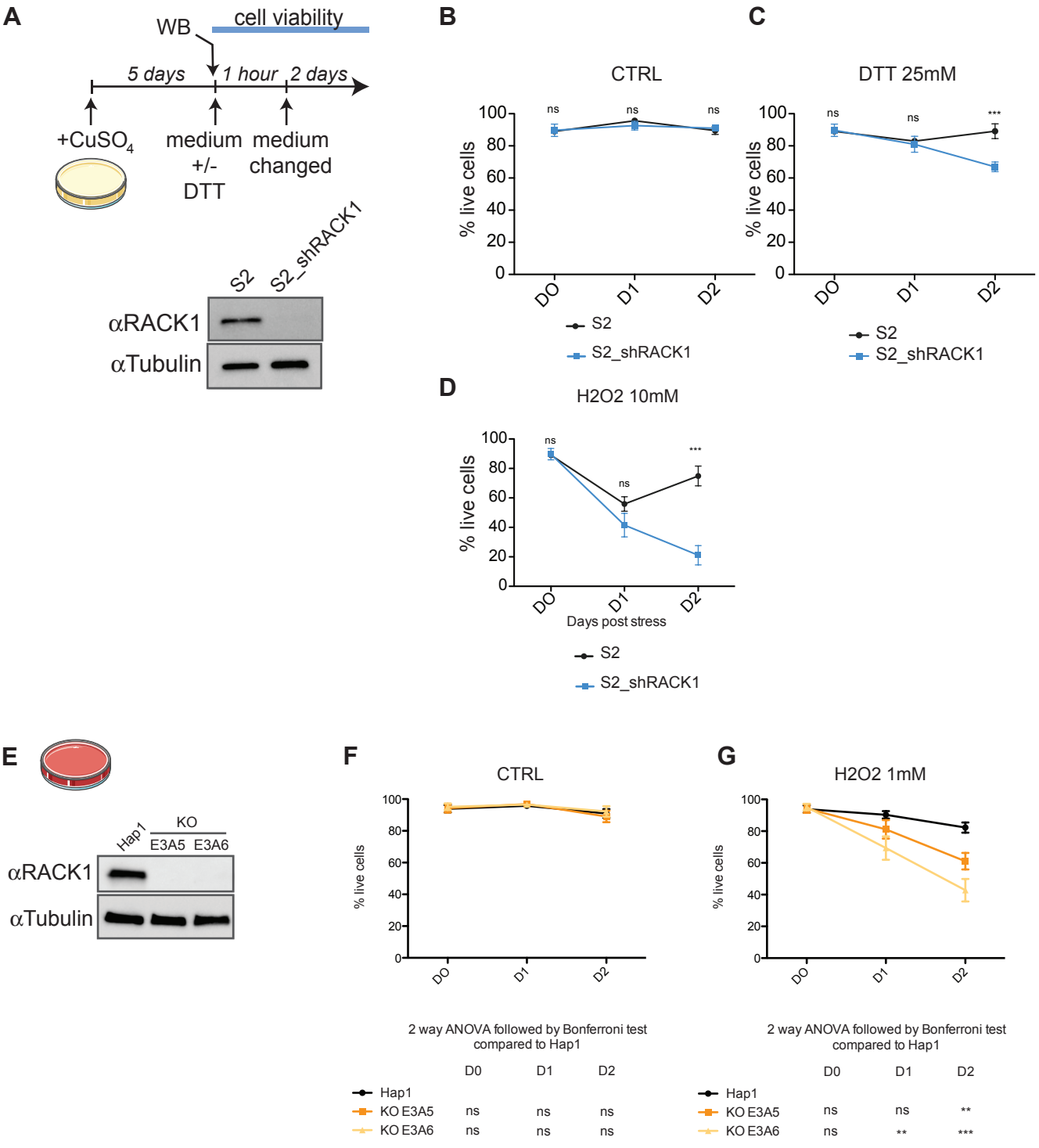

Figure 14: RACK1 is required for stress response in *Drosophila* and human cells. A. Western-blot (WB) of S2 and S2_shRACK1 cells after 5 days of CuSO4 treatment. One blot representative of 3 independent experiments is presented. **B-D**. Drosophila S2 cells or S2_shRACK1 cells were incubated with control culture medium (**B**), medium containing 25mM DTT (**C**) or medium containing 10mM H2O2 (**D**) for one hour. This medium was replaced by control medium and cell viability was monitored at day 0 (D0), day 1 (D1) and day 2 (D2) by Trypan blue. **E.** Western-blot showing RACK1 expression the Hap1 cell line and the two RACK1 KO cell lines. Data representative of two independent experiments. **F-G.** Hap1 parental cell line and two RACK1 KO cell lines were incubated with control medium (**F**) or medium containing 1mM H2O2 (**G**) for one hour. Cell viability was monitored at day 0 (D0), day 1 (D1) and day 2 (D2) by Trypan blue. **B-D, F-G.** Data represent mean+SEM of 3 independent experiments. Statistical analysis was performed using 2way ANOVA followed by Bonferroni's post test. ns: nonsignificant; *p<0.05; **p < 0.01; ***p<0.001.

B. Transcriptomic analysis reveals RACK1-dependent or stress-dependent genes

To identify mRNAs that may require RACK1 for their translation during stress, we performed polysome profiling in control shmCherry and in shRACK1 flies (**Figures 15A**). We chose the 25mM DTT treatment as a stress condition, and collected the flies at three days post treatment, when the stressed flies start to die. As a control, we also performed a transcriptome analysis of whole flies before fractionation, to verify global mRNA quantity. Principal component analysis (PCA) showed that triplicates of transcriptome samples were clustering according to the conditions (**Figure 15B**). We performed pairwise comparison of (i) shRACK1 *vs* shmCherry or (ii) DTT *vs* sucrose for all combinations of transcriptome to uncover genes which depend on RACK1 or that are regulated in response to stress respectively (**Figure 16A**). The sequencing of triplicates allowed assigning a *p*value to each fold change ratio, and we chose a twofold ratio (log2 fold change > 1 or < -1) with $p<0.05$ as a biological significance threshold.

We first analyzed the effect of RACK1 KD *in vivo* in both unstressed (Sucrose) and DTT stressed conditions (**Figure 16B, Table 1**). Of note, RACK1 mRNA was highly expressed *in vivo* and its level was reduced by two-fold in sucrose-treated shRACK1 flies compared to sucrose-treated shmCherry flies (**Figure 17**). In the absence of stress, 82 or 53 genes were respectively up- or down-regulated in shRACK1 flies. In the same way, 55 or 44 genes were respectively up- or down-regulated in stressed shRACK1 flies. In each case, around 30% of these genes were commonly regulated in both unstressed and stressed conditions. Gene ontology (GO) analysis in the different gene populations did not detect enrichment of any biological process. These results suggest that RACK1 can have an effect on mRNA transcription or stability.

We then analyzed the changes in mRNA levels in response to stress (**Figure 16C, Table 2**). In shmCherry flies, 60 or 112 genes were up- or down-regulated in DTT-treated conditions. In the absence of RACK1, 45 or 152 genes were respectively up- or down-regulated in DTT-treated conditions. We observed an overlap between DTT-dependent genes in both fly lines (between 25 and 28% of the genes). For instance, genes involved in lipid metabolic processes were repressed by DTT in both fly lines, suggesting that part of the lipid metabolism is shut down in

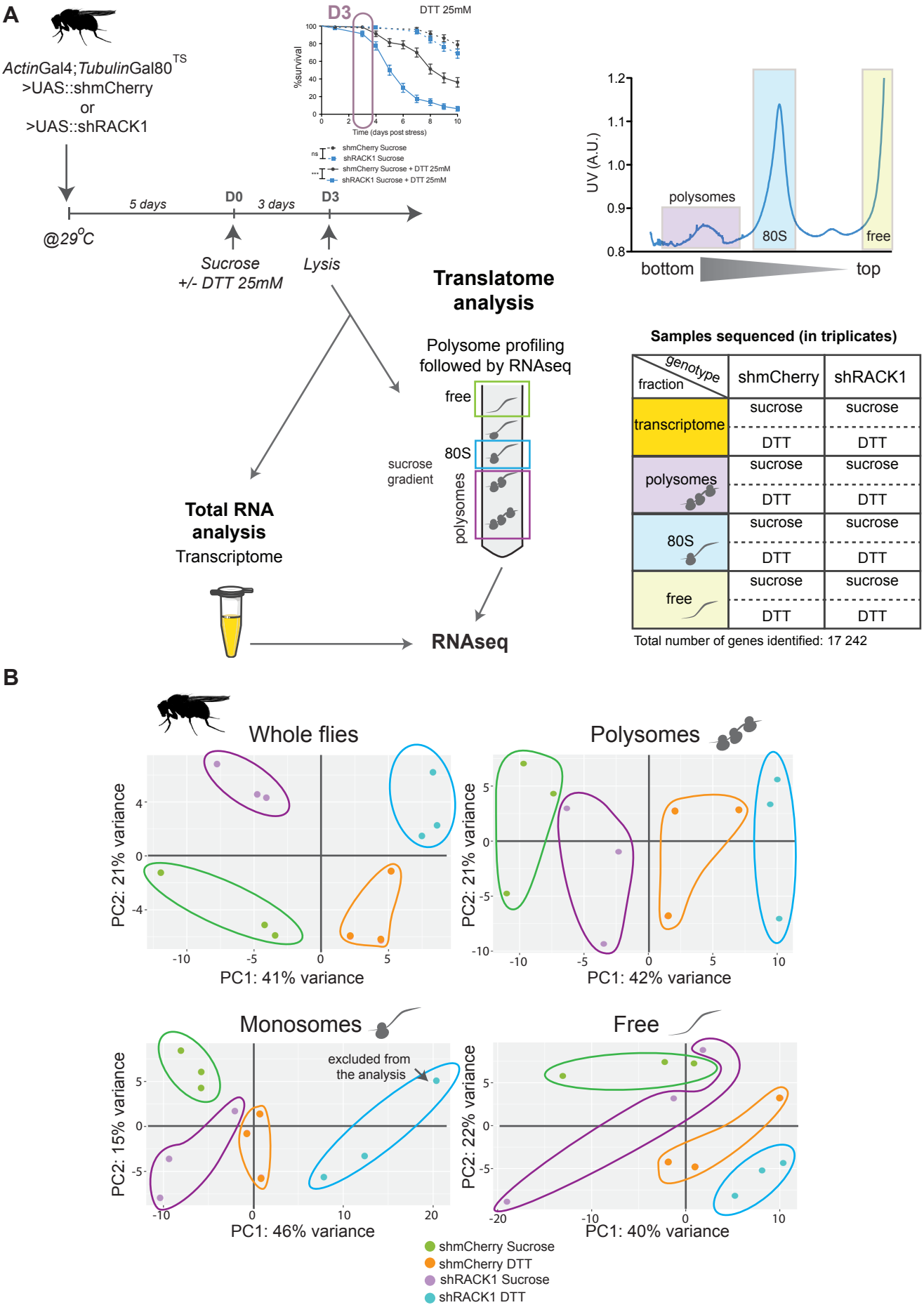

Figure 15: Polysome profiling followed by RNA sequencing. A. Experimental pipeline of RNA sequencing. *Actin*Gal4;*Tubulin*Gal80^{TS} >UAS::shmCherry and >UAS::shRACK1 flies were raised for 5 days at 29ºC to induce shRNA expression. Flies were treated with sucrose supplemented or not with 25mM DTT and whole fly lysates were prepared 3 days later for RNA sequencing. The colored areas of the absorbance profile at 254nm correspond to the fractions selected for subsequent RNA extraction and RNA sequencing.The list of the samples sequenced is indicated. **B**. Principal component analysis (PCA) plot of all the samples. Each dot corresponds to a replicate.

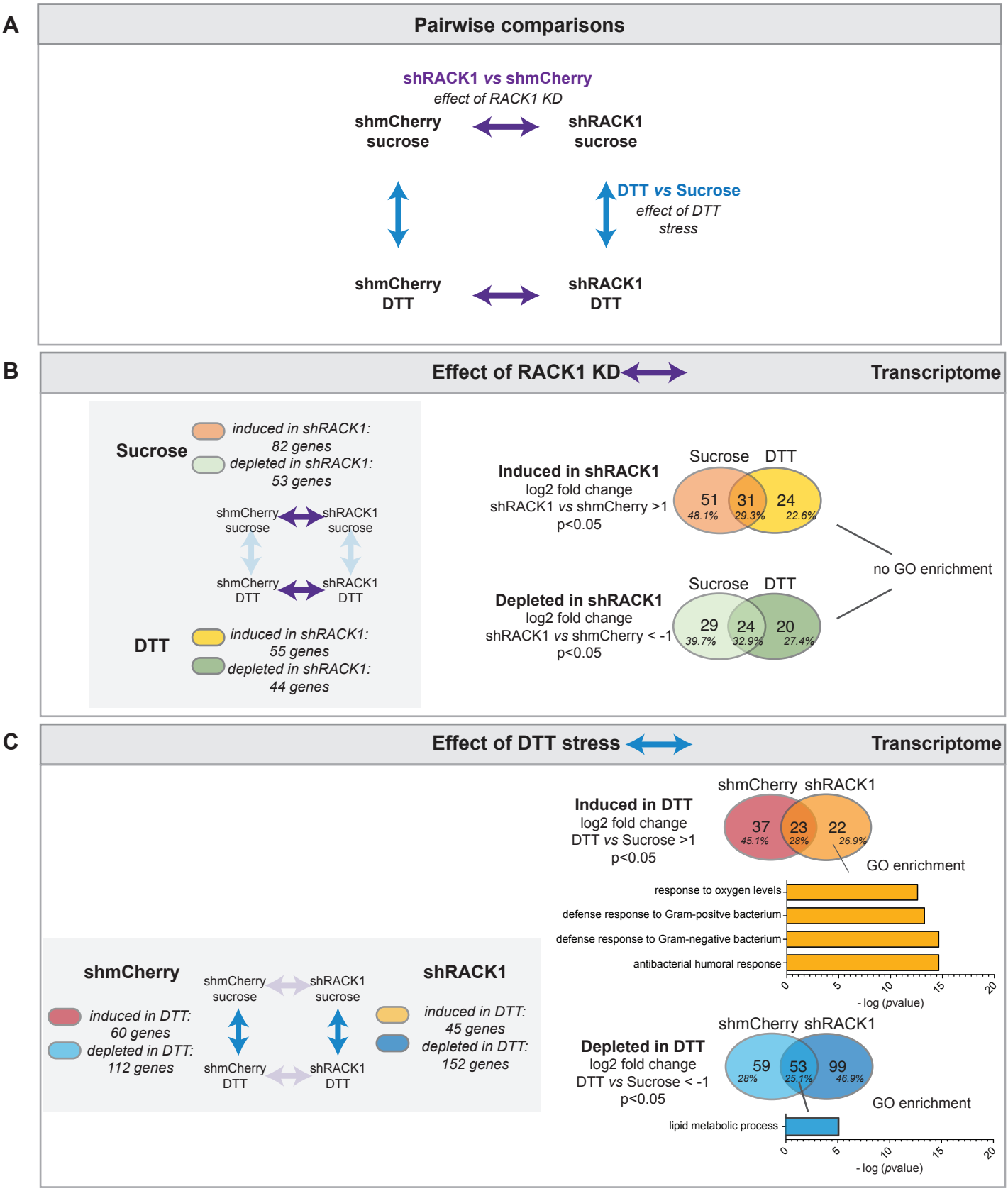

Figure 16: Transcriptome analysis identifies RACK1-dependent genes and DTT stress-dependent genes. A. Pairwise comparisons performed to assess the effect of RACK1 depletion (purple arrow: shRACK1 *vs* shmCherry) or the effect of the DTT treatment (blue arrow: DTT *vs* Sucrose). **B**. Analysis of the effect of RACK1 depletion (pairwise comparison shRACK1 *vs* shmCherry) in sucrose condition or DTT treated condition. Venn diagramm allowed to identify genes induced by RACK1 KD or depleted by RACK1 KD in sucrose only, DTT only, or in both conditions. Gene Ontology enrichment of Biological process was performed with *pantherdb.org*. **C**. Analysis of the effect of DTT treatment (pairwise comparison DTT*vs* Sucrose) in both fly genotypes. Venn diagramm allowed to identify genes induced or depleted by DTT stress in shmCherry flies only, shRACK1 flies only, or in both fly lines. Gene Ontology enrichment of Biological process was performed with *pantherdb.org*.

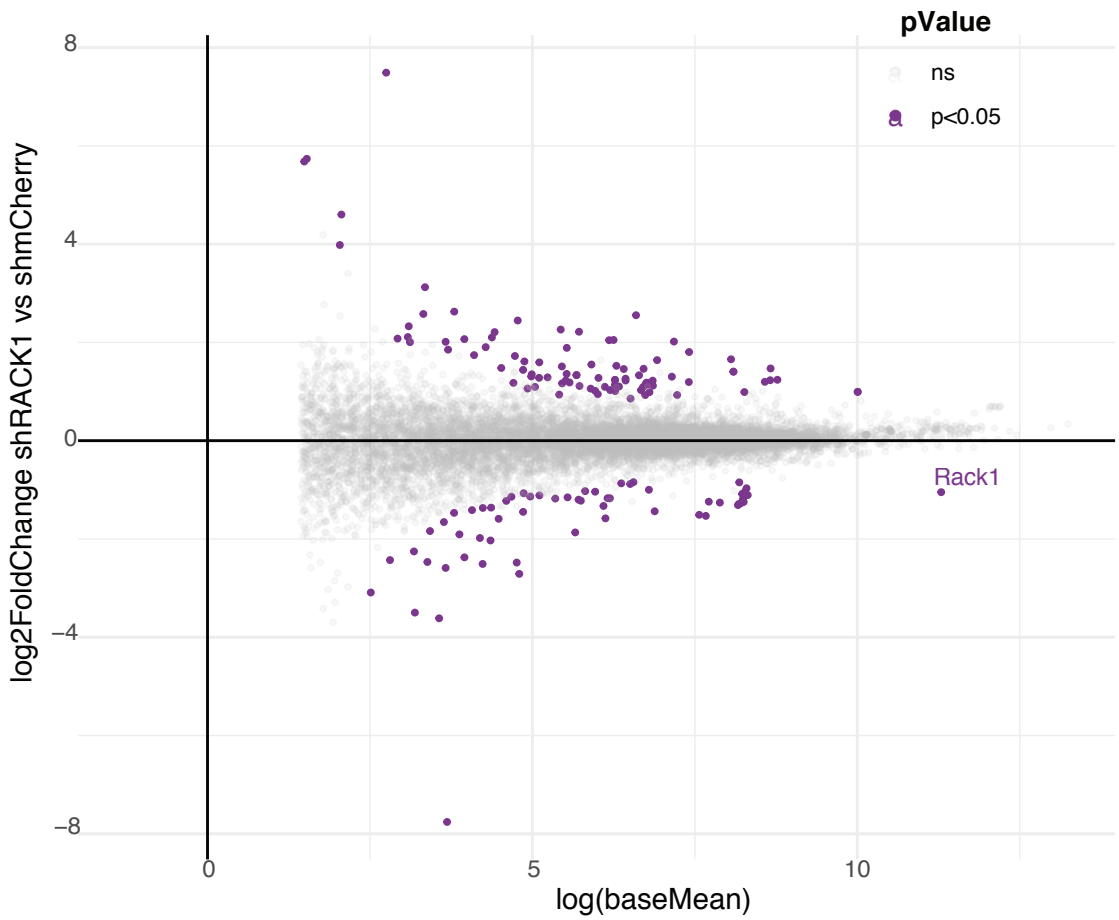

Figure 17: RACK1 mRNA level is decreased in shRACK1 flies. Scatterplot showing the genes upregulated in sucrose-treated shRACK1 flies (log2 fold change shRACK1 *vs* shmCherry >0) or downregulated in shRACK1 flies (log2 fold change shRACK1 *vs* shmCherry<0) in the input. Data are mean of triplicates and statistical analysis are performed on the triplicate values. The genes for which p<0.05 are depicted in purple.

response to ER stress in a RACK1-independent manner. Strikingly, many biological processes were enriched in the 22 genes up-regulated only in the shRACK1 flies. These biological processes displayed a very low *p*value, indicating a very robust enrichment in genes involved in immune response such as antibacterial humoral response. Of note, some genes classified as “response to oxygen levels” were also enriched only in the shRACK1 fractions but all of them were immune-related genes. These results suggest that RACK1 prevents the induction of mRNAs encoded by immune genes in response to an abiotic stress.

C. RACK1 represses the transcription of IMD target genes

We next looked at the 22 genes induced by DTT only in RACK1 silenced flies. Eleven of them are immune genes related to the *Drosophila* immune deficiency (IMD) pathway (**Figure 18A**). This pathway is induced following infection with gram-negative bacteria and leads to the expression of anti-microbial peptides (AMPs) such as Attacins (e.g. AttA), Diptericins (e.g. DptA) and Cecropins (e.g. CecC), mainly through the transcription factor Relish (Myllymäki et al., 2014). We confirmed that the AMPs and other IMD-regulated genes are upregulated by DTT in shRACK1 flies (**Figure 18B**). Of note, we also observed an increased expression of those genes in DTT-stressed shmCherry flies, although it was not statistically significant. Moreover, we also noted that AMPs expression is higher in stressed shRACK1 flies than in stressed shmCherry flies, although the difference is again not significant. This is explained by the increase in AMPs expression upon stress in the shmCherry controls. In S2 cells, AMPs were not regulated by DTT, whether RACK1 was silenced or not (**Figure 18C**). Strikingly however, we observed a significant upregulation of the IMD-regulated genes *DptA*, *Peptidoglycan recognition protein SB1* (*PGRP-SB1)*, *edin* and *Metchnikovin (Mtk)* when expression of RACK1 was silenced in control cells. Increased expression of *AttA* and *CecC* in the absence of RACK1 was also visible, but the difference was not statistically significant. We monitored the activity of the promoters of *DptA* and *Mtk* genes using luciferase reporters in both S2 and S2_shRACK1 cells and observed that the activity of the promoters reflected the accumulation of the corresponding mRNAs (**Figure 18D**). Overall, these unexpected results show that RACK1 represses the transcription of IMD target genes. *In vivo*, this repression is visible in DTT-treated conditions, whereas it is constitutive *ex vivo*.

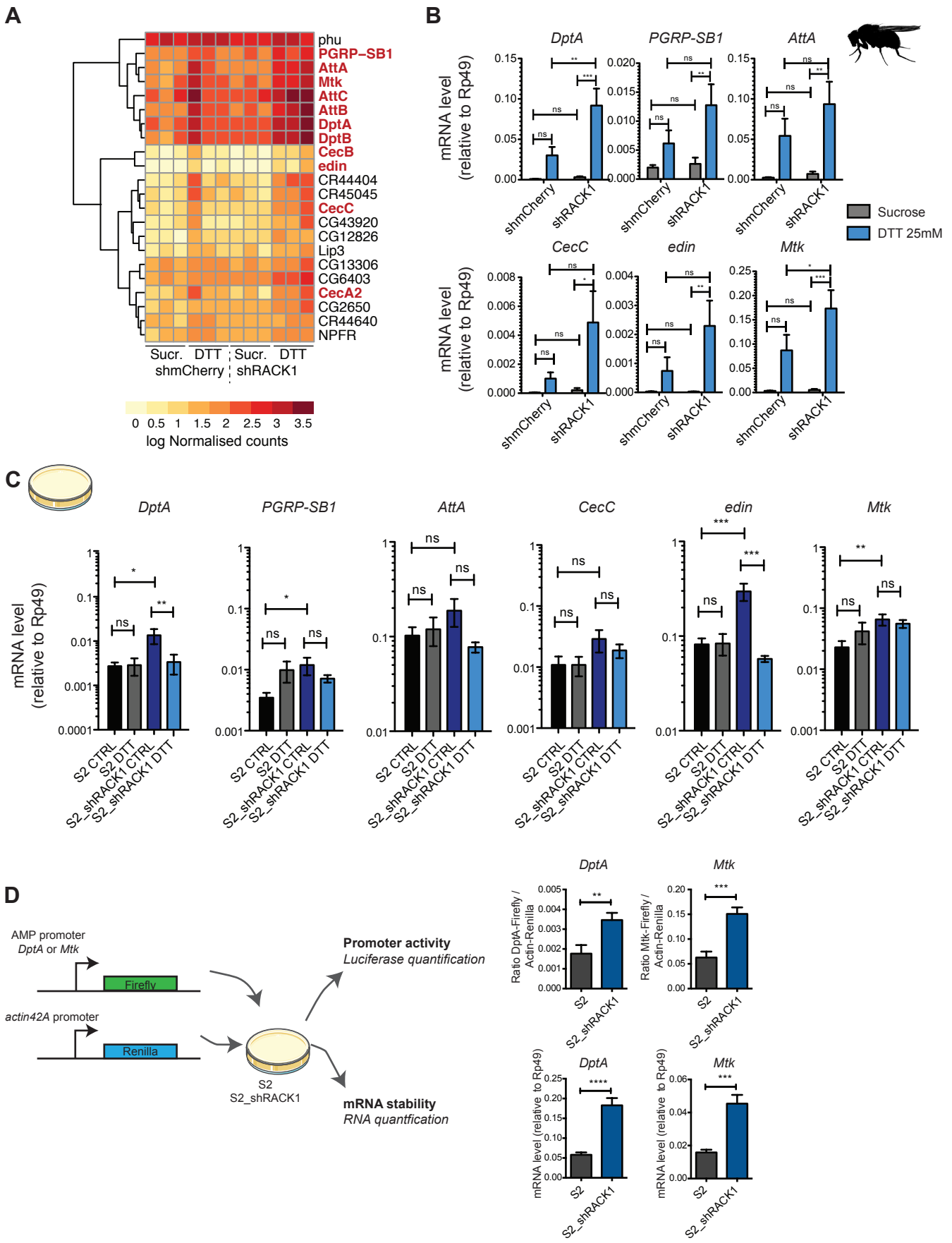

Figure 18: RACK1 inhibits AMPs RNA expression *in vivo* and *ex vivo*. A. Heatmap of normalised counts for the 22 genes specifically upregulated in the DTT-treated shRACK1 flies. In bold red font are indicated the genes belonging to the Drosophila IMD pathway. **B**. RT-qPCR confirmation in independent samples of the level of *DptA*, *PGRP-SB1*, *AttA*, *CecC*, *edin* and *Mtk* mRNAs in shmCherry and shRACK1 flies at 3 days post 25mM DTT treatment. **C**. RT-qPCR quantification of *DptA*, *PGRP-SB1*, *AttA*, *CecC*, *edin* and *Mtk* mRNAs in S2 and S2_shRACK1 cells one day after treatment with culture medium containing (DTT) or not (CTRL) 25mM DTT. **B-C.** Data represented are mean + SEM of 3 independent experiments. Statistics were performed using 2way ANOVA followed by Bonferroni post-test. **D**. Luciferase assay showing the activity of the Mtk and DptA promoters, together with the levels of endogenous *Mtk* and *DptA* mRNAs in S2 and S2_shRACK1 cells. Data represented are mean + SEM of 3 independent experiments. Statistics were performed using unpaired t-test with Welch correction. ns: nonsignificant; *p<0.05; **p < 0.01; ***p<0.001; ****p<0.0001.

D. RACK1 represses the translation of AMPs mRNAs through their 5'UTR

We wondered whether RACK1 was also involved in the selective translation of mRNAs during stress. We fractionated whole fly extracts from control shmCherry and shRACK1 flies, DTT-treated and untreated, and extracted RNAs from different sucrose gradient fractions, according to their translational status: polysomes (actively translated), monosomes (mRNAs in initiation and/or with short open reading frames) and free (untranslated) (**Figure 15A**). PCA of all the sequencing data showed that one of the triplicates from the monosomes fraction (shRACK1 DTT) did not cluster with the two other replicates. It was the source of many false positive candidates and was thus excluded from the analysis (**Figure 15B**).

We performed pairwise comparison of DTT *vs* sucrose for all fractions to uncover genes translationally deregulated by DTT stress in both fly lines. We identified genes enriched or depleted from polysomes, monosomes and free fraction in stressed condition (**Figure 19, Table 2**). Again, we found genes specifically modulated by DTT-stress in shmCherry or shRACK1 flies, as well as genes commonly regulated between the two fly lines. The genes depleted from polysomes of shmCherry flies upon DTT treatment were enriched in biological process related to vesicular trafficking (**Figure 19A**). Genes related to hexose metabolic process were enriched in both shmCherry and shRACK1 flies, suggesting that upregulation of this pathway is related to a stress response independent of RACK1. More strikingly, we observed a strong and consistent GO enrichment of immune-related genes in the polysomes, monosomes and free fractions of shRACK1 DTT-stressed flies (**Figures 19A, 19B, 19C**), similar to the enrichment we observed in the transcriptome data (**Figure 16**). These genes were again mainly AMPs from the IMD pathway (**Figures 20A, 20B**). This enrichment could reflect the increased total mRNA levels observed for these genes. Alternatively, RACK1 may also repress the translation of these mRNAs, resulting in an upregulation when RACK1 is depleted.

To distinguish between these possibilities, we monitored mRNA translation efficiency, using a cell culture model. We transfected mRNAs containing the 5'UTR or the IGR IRES of CrPV upstream of the Renilla luciferase into S2 and S2_shRACK1 cells. These mRNAs were capped with a non-functional G(5')ppp(5')A cap to avoid cap-dependent translation of the IRES constructs as well as 5'-3' mRNA

degradation. We tested the translational activity of the whole 5'IRES (709 nucleotides upstream of the AUG codon), the minimal 5'IRES (352 nucleotides upstream of the AUG codon) and the intergenic IRES (Gross et al., 2017). All CrPV reporter mRNAs were co-transfected with an mRNA containing the 5'UTR of the *actin42A* gene upstream of the Firefly luciferase to normalize the transfection efficiency. This mRNA was polyadeylated and capped with a functional m^7G anti-reverse cap analogue (ARCA). RACK1 depletion prevented the translation of both whole and minimal 5'IRES, whereas it had no effect on the IGR IRES translation (**Figure 20C**). As previous reports suggested an involvement of RACK1 in translation regulation through the 5'UTR (Rachfall et al., 2012; Ruan et al., 2012), we constructed reporter mRNAs containing the 5'UTR of DptA, Cecropin A1 (CecA1), Cecropin B (CecB) and Attacin C (AttC) upstream of the firefly luciferase. We also added reporter containing the 5'UTR of Poor imd response upon knock-in (Pirk), a negative regulator of the IMD pathway (Kleino et al., 2008) which was depleted from the polysome and monosomes of DTT-stressed shRACK1 flies. After addition of the m^7G ARCA cap and polyA tail, these mRNAs were transfected into S2 and S2_shRACK1 cells. An mRNA containing the 5'UTR of the gene *TNF associated factor 6* (*TRAF6)* was added as a negative control, as TRAF6 mRNAs expression was found to be stable in all the fractions recovered. These mRNAs were co-transfected with an mRNA containing the Renilla luciferase under the control of the 5'UTR of the gene *actin42A*, to normalize for transfection efficiency. Translation of the *AttC*, *CecB* and *DptA* reporter mRNAs significantly increased in S2_shRACK1 cells compared to the S2 control cell line, whereas translation of the *CecA1* and *TRAF6* reporter mRNAs did not (**Figure 20D**). Moreover, the 5'UTR of Pirk-RA isoform was not affected by RACK1 depletion. Unfortunately, the construct containing the 5'UTR of Pirk-RB isoform did not allow the detection of the Firefly luciferase. Thus, we cannot conclude yet whether Pirk-RB mRNA is translated in a RACK1-dependent way. Of note, we did not test mRNA stability of our constructs. Nevertheless, these results demonstrate that RACK1 represses the translation of *AttC*, *CecB* and *DptA* mRNAs through their 5'UTR *ex vivo*.

One key question emerging from these results is to uncover the *cis*-acting sequences/structures that drive RACK1-dependent selectivity. AMPs mRNAs have relatively short 5'UTRs (64nt for *AttC*, 44nt for *DptA*), compared to the average size of *Drosophila* 5'UTRs (around 217-260nt) (Celniker and Rubin, 2003). Using a bioinformatics analysis based on alternative start codon efficiency (Diaz de Arce et

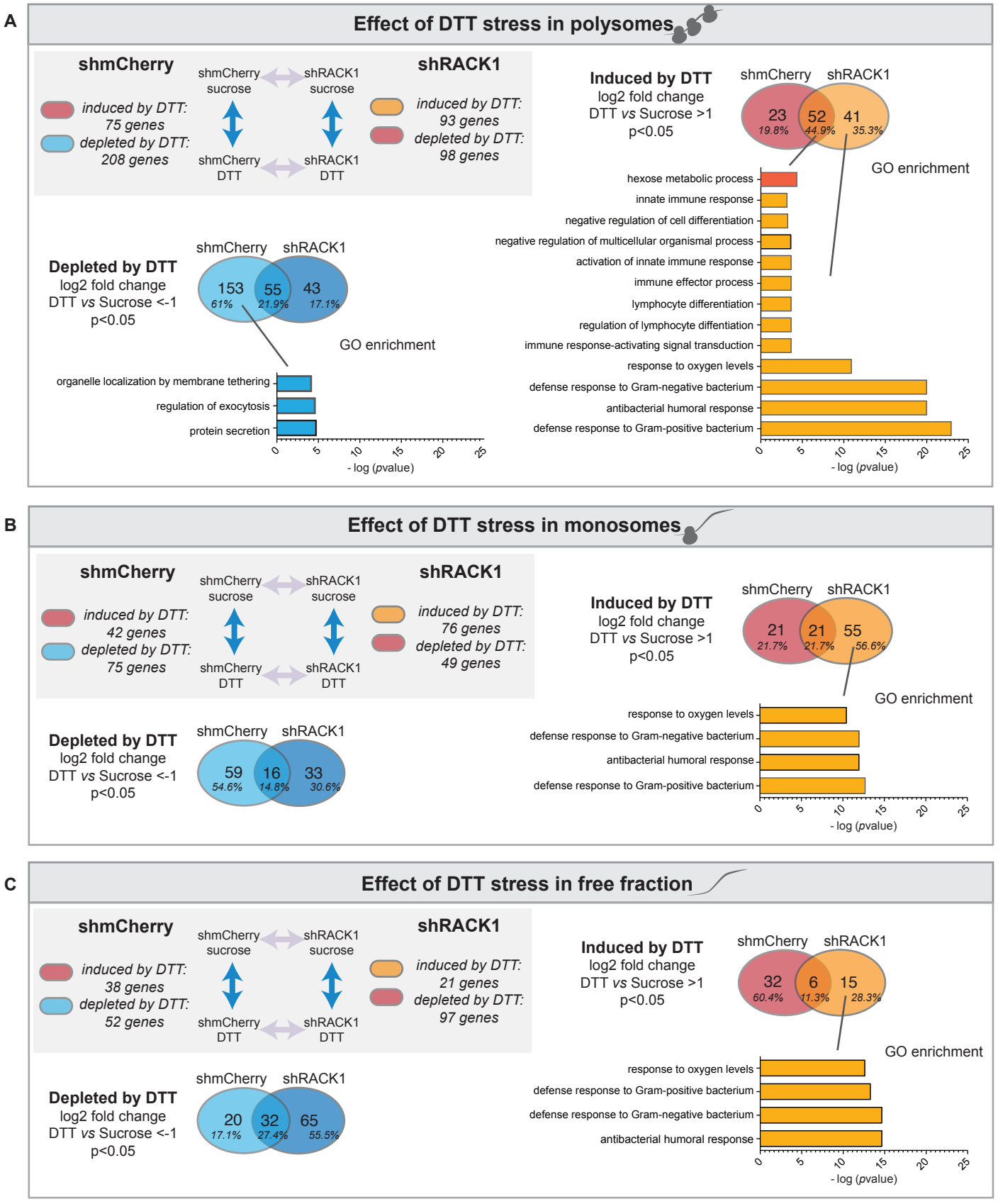

Figure 19: Polysome profiling followed by RNA sequencing identifies genes modulated by DTT treatment. Analysis of the effect of DTT treatment (pairwise comparison DTT*vs* Sucrose) in both fly genotypes for polysomes (**A**), monosomes (**B**) and free (**C**) fractions. Venn diagramm allowed to identify genes induced or depleted by DTT stress in shmCherry flies only, shRACK1 flies only, or in both fly lines. Gene Ontology enrichment of Biological process was performed with *pantherdb.org*.

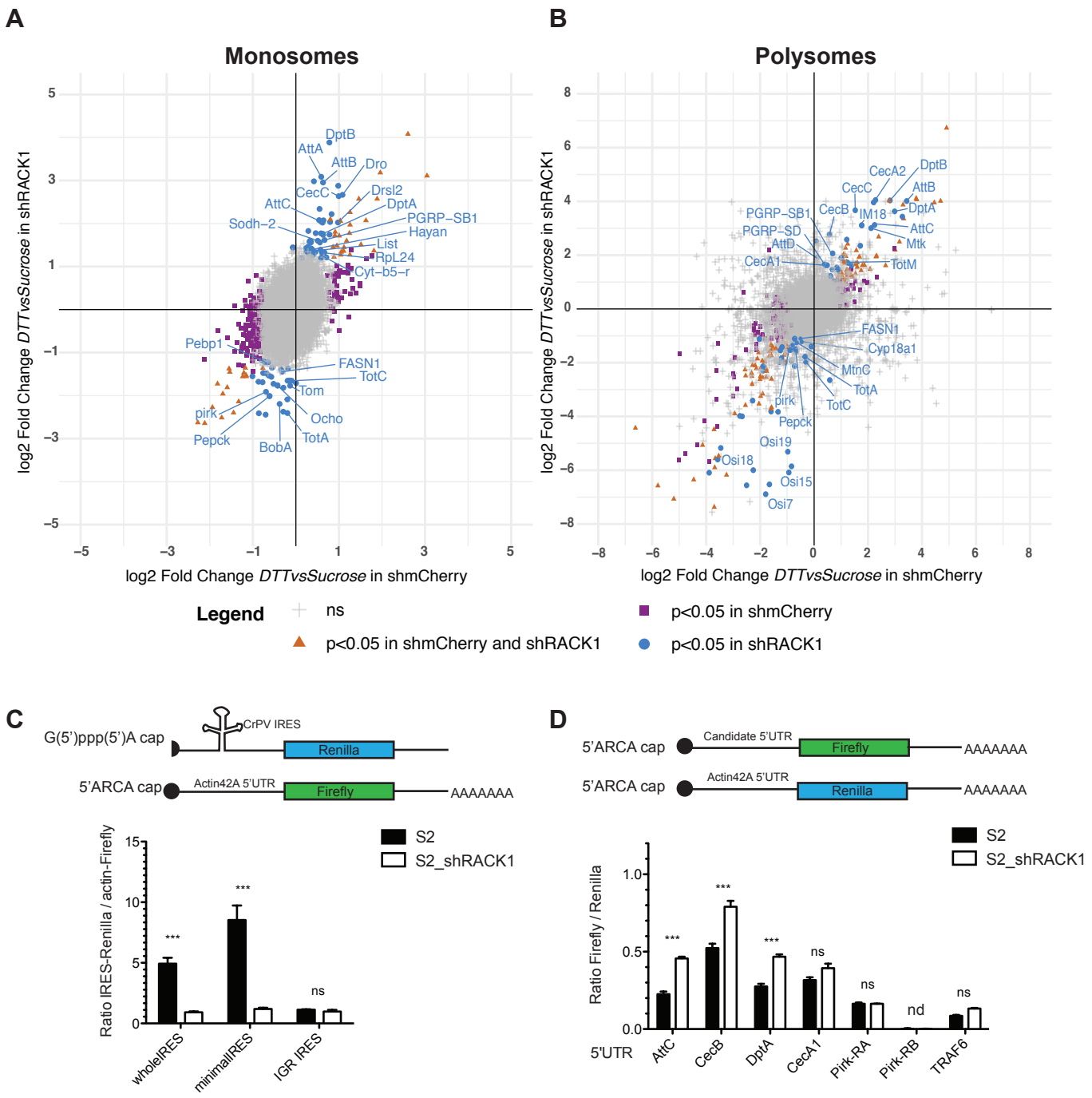

Figure 20: RACK1 prevents AMPs translation. A-B. Scatterplot showing the effect of DTT stress (log2 fold change between DTT and sucrose) in both shmCherry and shRACK1 fly lines. Blue dots indicate the genes significantly enriched/depleted from monosomes (**A**) or polysomes (**B**) of stressed shRACK1 flies. **C**. Functional control of the S2 and S2_shRACK1 cells. These cells were transfected with mRNA bearing a non-functional cap containing the full CrPV 5'IRES, the minimal CrPV 5'IRES or the CrPV IGR IRES driving Renilla luciferase translation. A capped actin-Firefly mRNA was co-transfected and the ratio of Renilla / Firefly is represented. **D**. mRNAs encoding the Firefly luciferase under the control of the indicated 5'UTR were transfected into S2 and S2_shRACK1 cells together with a 5'UTR(actin42A)-Renilla luciferase mRNA. Ratios of Firefly / Renilla values are normalised to the ratio of 5'UTR(actin42A)-Firefly/5'UTR(actin42A)Renilla for each cell line. (**C-D**) Data show mean+SEM of 3 independent experiments. Statistics were performed using 2way ANOVA followed by Bonferroni's post-test. ns: nonsignificant; *p<0.05; **p < 0.01; ***p<0.001; nd: not detected.

al., 2017), we did not find any enrichment in potential uORFs in RACK1-dependent 5'UTRs compared to the RACK1-independent 5'UTRs. Altogether, these results point to a role of RACK1 in the selective translation of some AMPs mRNAs and suggest the presence of a *cis*-acting element within their 5'UTR involved in this regulation.

E. Involvement of the IMD pathway in RACK1-dependent AMP expression and in stress survival

The upregulation of IMD-dependent genes when RACK1 is silenced raises the question whether it is dependent on the activation of the IMD pathway. We treated S2 and S2_shRACK1 cells with dsRNAs targeting the TF Relish (Rel) or its activating kinase Immune response-deficient 5 (Ird5), and checked AMPs expression (**Figure 21A**). *RACK1* mRNA was almost not detectable in S2_shRACK1 cells and both *Ird5* and *Rel* mRNAs were efficiently silenced upon treatment with the corresponding dsRNAs (**Figure 21B**). As expected, RACK1 KD led to an increased expression of *DptA*, *Mtk*, *edin* and *AttA* mRNAs. This induction was strongly reduced in Relish KD cells and to a lower extent in Ird5 KD cells. These results suggest that the RACK1-dependent overexpression of AMPs is mediated by the IMD pathway through the Relish TF. As overexpression of AMPs is known to be detrimental for fly survival (Katzenberger et al., 2015; Lamiable et al., 2016; Lin et al., 2018), these results suggest that the increased lethality of RACK1 silenced flies upon DTT treatment results from the deregulated expression of IMD target genes. To test if AMPs deregulation could explain the phenotype of shRACK1 flies, we fed control (w^{1118}) and Relish homozygous mutant flies (Rel^{E20}) with a sucrose solution containing or not 25mM DTT (**Figure 21C**). We monitored fly survival every day after exposure and observed an impaired survival of Relish mutant flies compared to the controls. Surprisingly, these data, which will need to be confirmed, suggest that the complete absence of AMPs is detrimental for survival.

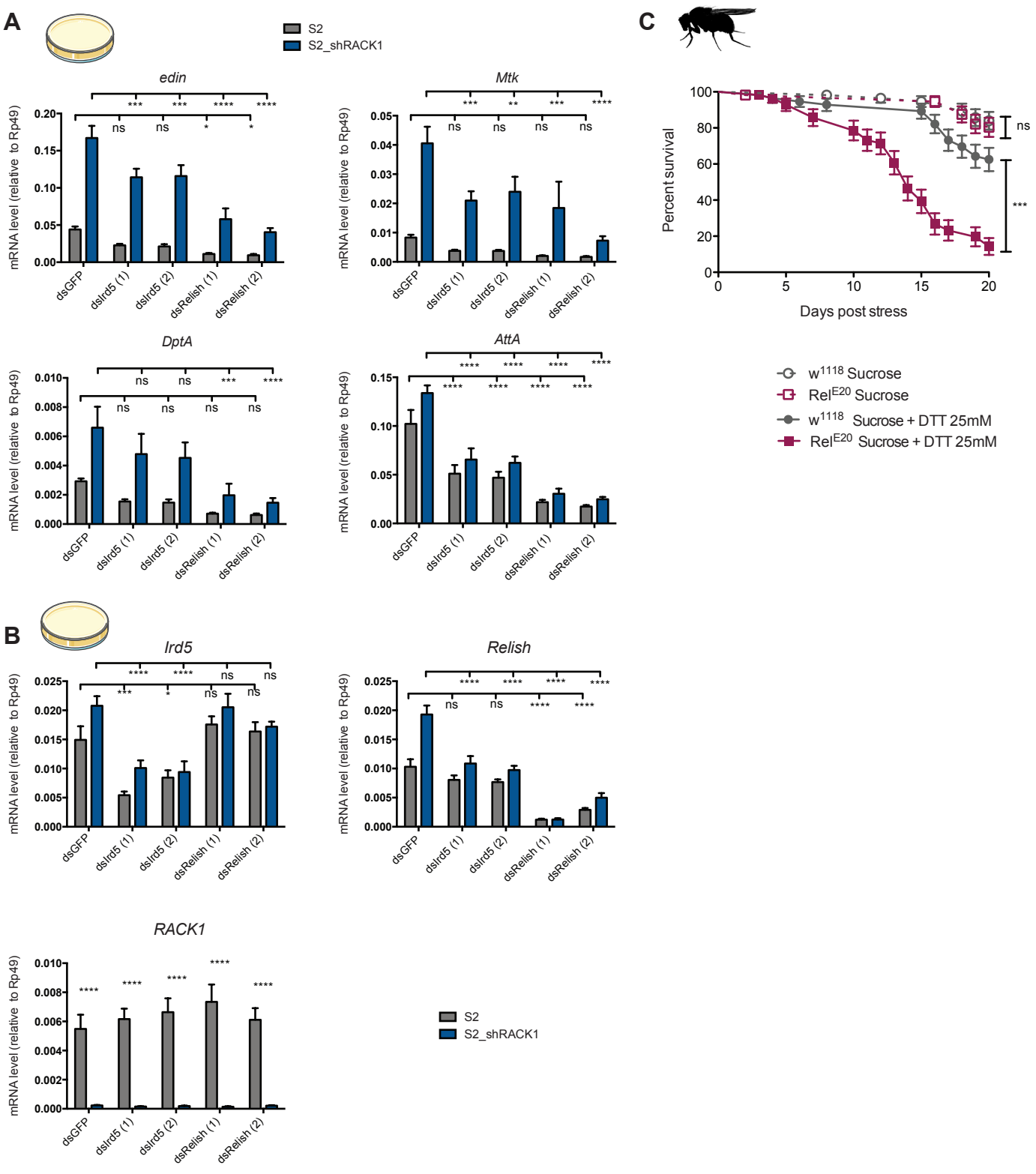

Figure 21: The IMD pathway is involved in stress response. A. S2 and S2_shRACK1 cells were transfected with dsRNAs targetting GFP, Ird5 or Rel and the expression of edin, Mtk, DptA and AttA was quantified by RT-qPCR. **B.** In parallel, KD efficiency was assessed by quantifying the expression of Ird5, Relish and RACK1 mRNA. **A-B**. Data show mean + SEM of 3 independent experiments. Statistics were performed using 2way ANOVA followed by Bonferroni's post-test. **C**. Survival of WT w^{1118} and Rel^{E20} flies after ER stress induced by DTT feeding at 25mM. Fly survival was monitored every day and statistical analysis was performed using Log-rank (Mantel-Cox) Test. Data represent mean+SEM of 3 independent experiments (total of n=60 flies). ns: nonsignificant; *p<0.05; **p < 0.01; ***p<0.001; ****p<0.0001.

F. Identification of a set of genes requiring RACK1 for translation

Our polysome profiling followed by RNA sequencing identified many mRNAs depleted from polysomes or monosomes in shRACK1 flies. Even if no GO enrichment other than vesicular trafficking-related genes was detected (**Figure 19**), it still remains that these RACK1-dependent mRNAs might play a role in stress response. Genes from the Osiris family (Osi7, Osi15, Osi19 and Osi18) were strongly depleted from polysomes of shRACK1 flies upon DTT stress (**Figures 20B, 22A**). These genes are conserved in insects but do not have any known function in *Drosophila* yet (FlyBase Curators et al., 2004; Shah et al., 2012). However, the common RACK1-dependent regulation of four genes of this family might reflect a functional role, which needs to be further studied

Moreover, the mRNAs for CG18814, a gene with unknown function potentially involved in oxidation-reduction process (FlyBase Curators et al., 2004), and Cytochrome P450-18a1 (Cyp18a1), an enzyme known to inactivate 20-hydroxyecdysone (Guittard et al., 2011), were also depleted from the polysomes of stressed RACK1-silenced flies (**Figure 22A**). Interestingly, the phenotype of Cyp18a1 mutant flies was reminiscent of the developmental phenotype of RACK1 mutant flies we observed (C. Meignin, unpublished). To test whether the impaired expression of the *CG18814* or *Cyp18a1* mRNAs in shRACK1 flies contributes to the lethality upon DTT stress, we used the *Actin*Gal4/*Tubulin*Gal80^{TS} system and UAS-shRNA transgenes targeting the two genes. We fed shmCherry, shRACK1, shCG18814 and shCyp18a1 flies with a sucrose solution containing or not 25mM DTT and monitored survival daily (**Figure 22B**). Upon sucrose regimen, we observed no difference in viability between all four fly lines. As expected, shRACK1 flies succumbed faster than the control shmCherry upon DTT treatment. Interestingly, the survival of Cyp18a1 silenced flies was also significantly affected by DTT stress, although these flies resisted longer than the RACK1 depleted ones. A trend for reduced survival was also observed for CG18814 silenced flies (**Figure 22B**). These results indicate that the loss of one RACK1-dependent gene is probably not sufficient to entirely recapitulate the phenotype of shRACK1 flies. Nevertheless, they suggest that the concomitant decreased translation of several mRNAs in RACK1-silenced flies might explain the lethality upon DTT stress.

We thus constructed reporter mRNAs containing the 5'UTR of the two isoforms of Cyp18a1, Cyp18a1-RA and Cyp18a1-RB, upstream of the firefly luciferase and tested their translation efficiency in our cell culture model (**Figure 22C**). The luciferase activity of both Cyp18a1-RA and Cyp18a1-RB 5'UTR reporters was barely detected. Nevertheless, we did not see a RACK1-dependency of these 5'UTRs. Further optimizations are required to confirm these results.

Altogether, these results show that many genes might be translated in a RACK1-dependent manner. These genes still need further characterization to understand the role of RACK1 in stress response.

III. Discussion

A. Comments on the polysome profiling followed by RNA sequencing

The two main techniques for the quantification of the translatome are polysome profiling and ribosome profiling. Historically, polysome profiling was aimed at analyzing the translation efficiency of individual genes, but its coupling to high-throughput sequencing made it a powerful tool to generate translatomes. Polysome profiling gives a direct view of ribosome density on each mRNAs by the separation of polysomal, monosomal and free mRNAs for instance. On the other hand, ribosome profiling results from an estimation of ribosome occupancy (ribosome footprints) relative to the total mRNA abundance. Nevertheless, this technique indicates the precise position of ribosome, allowing the identification of alternative initiation codons for instance (Ingolia, 2014; Jin and Xiao, 2018). In our case, we used polysome profiling because we wanted to see the difference in translation efficiency by a shift from polysome to monosomes or free fraction. However, we did not observe such shifts in our data. Nevertheless, we observed a shift from polysomes to monosomes for some genes, although we did not analyze it further yet. More bioinformatics analyses are required to dissect changes on translation efficiencies.

A

gene name	log2FC DTT vs Sucrose in shmCherry				log2FC DTT vs Sucrose in shRACK1			
	Transcriptome	Polysomes	Monosomes	Free	Transcriptome	Polysomes	Monosomes	Free
Osi7	ns	ns	ns	ns	ns	***	ns	ns
Osi15	ns	ns	ns	ns	ns	*	ns	ns
Osi19	ns	ns	ns	ns	ns	*	ns	ns
Osi18	ns	ns	ns	ns	ns	*	ns	ns
CG18814	ns	ns	ns	ns	ns	*	ns	ns
Cyp18a1	ns	ns	ns	ns	ns	*	ns	ns

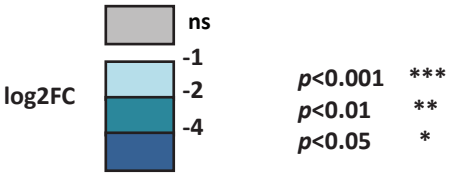

B

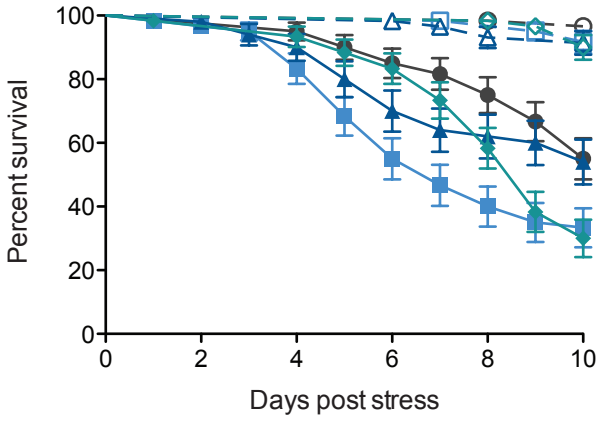

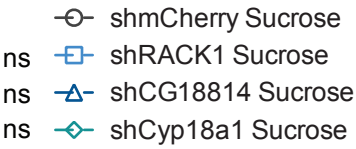

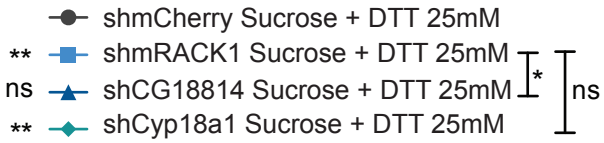

C

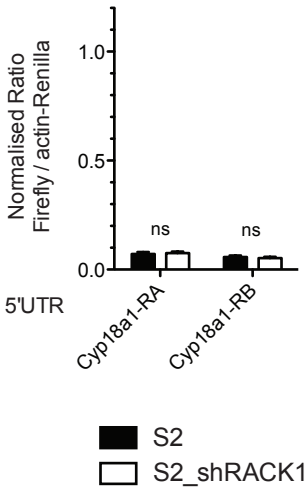

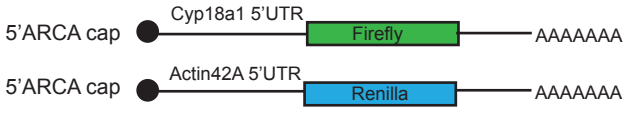

Figure 22: Identification of RACK1-dependent mRNAs. A. Heatmap showing the log2 Fold Change of DTT *vs* Sucrose obtained in the transcriptome and polysome profiling in all fractions for Osi7, Osi15, Osi19, Osi18, CG18814 and Cyp18a1. **B**. Survival of *Actin*Gal4;*Tubulin*Gal80^{TS}>UAS::shmCherry, >UAS::shRACK1, >UAS::shCG18814 and >UAS::shCyp18a1 flies after ER stress induced by DTT feeding at 25mM. Fly survival was monitored every day and statistical analysis was performed using Log-rank (Mantel-Cox) Test. Data represent mean+SEM of 3 independent experiments (total of n=60 flies). **C**. mRNAs encoding the Firefly luciferase under the control of the indicated 5'UTR were transfected into S2 and S2_shRACK1 cells together with a 5'UTR(actin42A)-Renilla luciferase mRNA. Ratios of Firefly / Renilla values are normalised to the ratio of 5'UTR(actin42A)-Firefly/5'UTR(actin42A)Renilla for each cell line. Data show mean+SEM of 3 independent experiments. Statistics were performed using 2way ANOVA followed by Bonferroni's post-test. ns: nonsignificant; *p<0.05; **p < 0.01; ***p<0.001. nd: not detected.

This method identified hundreds of mRNAs regulated by RACK1. We focused our attention on AMPs genes and some stress-related genes, but the study of many other genes would be relevant as well. For instance, we identified 23 genes enriched in the polysomes of DTT-stressed shmCherry flies only (**Figure 19A**). Translation of these genes might take part in the increased resistance to stress of the shmCherry flies compared to the shRACK1 flies. Of note, we found long non-coding RNAs (lncRNAs) in polysomes and monosomes fractions (e.g. CR45045 and CR44404). This suggests that the status of these RNAs as non-coding needs to be re-evaluated. In this aim, ORF prediction might be performed together with whole fly mass spectrometry to identify the corresponding peptide.

B. RACK1 is involved in transcription regulation of immune genes

We observed a clear and strong signature of IMD target genes in DTT stressed shRACK1 flies, at the level of transcription. One trivial explanation for this result may be a modification of the gut barrier permeability in RACK1 silenced flies. Indeed, as every animals, flies possess a gut microbiota composed among other of Gram-negative bacteria such as *Proteobacteria* (Broderick and Lemaitre, 2012). DTT feeding in these conditions would result in bacterial crossing of the barrier, leading to systemic infection and activation of the IMD pathway. While we cannot completely rule out such a scenario, we think it is unlikely since (i) we failed to detect increased gut permeability in RACK1 silenced flies and (ii) we also observed an induction of AMPs upon RACK1 silencing in our bacteria-free S2 cell culture model.

In *Drosophila*, we identified Pirk as a potential RACK1-dependent gene, both at the level of transcriptome and translatome (**Table 2**). Further experiments are required to confirm these results. For instance, we still need to confirm the decreased *Pirk* mRNA expression in DTT-stressed shRACK1 flies and in S2_shRACK1 cells. Expression of a WT RACK1 or a ribosome-binding defective mutant of RACK1 (e.g. R36D-K38E) in these cells should indicate whether this regulation of Pirk is dependent on translation or on an extra-ribosomal function of RACK1. Moreover, we did not see a RACK1-dependency of Pirk-RA translation in our S2 cell model, although we cannot exclude that Pirk-RB 5'UTR is RACK1-dependent. We might turn

to *in vitro* translation experiments to increase the luciferase signal we obtained from this reporter.

Additionally, we identified some AMPs (e.g. DptA and CecB) as being negatively regulated by RACK1, both at the level of transcriptome and translatome (**Table 2**). It was at first unexpected to observe a role for a ribosomal protein in the regulation of transcription of immune genes. Nevertheless, RACK1 has been shown to have an extra-ribosomal signaling function in immune pathways in mammals. Indeed, overexpression of RACK1 in HEK293T cells delays the expression of TNF-induced genes such as Interleukin 8 (IL-8) and TNFα (Yao et al., 2013). RACK1 interaction with IκB kinase (IKK) proteins delays the activation of the pathway. Similarly, RACK1 is a negative regulator of interferon (IFN)-β-luciferase reporter and KD of RACK1 increases *IFNβ1*, *Interferon stimulated gene 15* (*ISG15)* and *Regulated upon Activation, Normal T cell Expressed, and Secreted* (*RANTES)* mRNA levels induced by poly(I:C) or Sendai virus (Long et al., 2014). In the retinoic acid-inducible gene I (RIG-I) pathway, RACK1 interacts with Virus-induced signaling adapter (VISA) and prevent its association with TRAF proteins, impairing the activation of IFNβ promoter (Xie et al., 2019). These studies and our results point to a role of RACK1 as a negative regulator of immune pathways, in *Drosophila* and mammals.

C. Link between RACK1 and fly survival upon stress

In this study, we observed an impaired viability of RACK1 silenced flies compared to shmCherry control flies. In parallel, we identified mRNAs whose translation is blocked by RACK1 (e.g. AMPs such as *AttC* and *DptA*) or require RACK1 (e.g. stress-related genes such as *Cyp18a1* and *CG18814*). This raises two scenarios for the role of RACK1 in stress response.

(1) <u>In the case of genes translationally repressed by RACK1 (e.g. AMPs):</u>
DTT stress induces the expression of genes, which are harmful for the fly. The presence of RACK1 at the ribosome prevents the translation of these mRNAs. To verify that AMP expression contributes to the demise of the DTT stressed flies, we used Relish mutant flies, but we found that they succumb much more rapidly than the WT controls. This may be explained by the fact that Relish regulates a large number of genes

besides AMPs, some of which may participate in resistance to stress (De Gregorio et al., 2002). We now need to test *in vivo* whether the silencing of AMPs alone or in combination in shRACK1 flies is beneficial for survival. In the opposite, depletion of Pirk in shRACK1 flies should reduce even more the fly survival. This will give us a hint whether deregulated AMPs expression is the cause of the lethality of RACK1 depleted flies.

(2) In the case of genes which require RACK1 for their translation:
DTT stress induces the expression of genes beneficial for fly survival. The presence of RACK1 at the ribosome is required for the translation of these mRNAs. We showed that depletion of CG18814 and Cyp18a1 impairs fly survival upon treatment with DTT, albeit to a lower extent than depletion of RACK1. However, we did not confirm the RACK1-dependency of the 5'UTR of these mRNAs in our tissue culture assay. As with Pirk, we might have to turn to *in vitro* translation assays to increase the luciferase signal from the reporters. Moreover, we only tested two genes in our DTT-stress assay, but more genes were identified as RACK1-dependent upon stress and need further characterization (e.g. Osiris family members).

While we cannot with our present results rule out one of the two scenarios, we note that they are not mutually exclusive. Indeed, the conjunction of positive regulation of beneficial genes and negative regulation of harmful genes may explain the sensitivity of RACK1 silenced flies to stress.

D. Post-transcriptional regulation of immune genes

Our results suggest the existence of a post-transcriptional regulation of IMD-dependent genes. Activation of the UPR leads to nuclear factor-kappa B (NF-κB)-dependent transcription of immune genes and to the phosphorylation of eIF2α and subsequent cap-dependent translation shutdown (Frakes and Dillin, 2017). Interestingly, bacterial infection in *Drosophila* activates GCN2, and leads to the expression of 4E-BP and shut-down of cap-dependent translation (Vasudevan et al., 2017). Nevertheless, AMPs mRNAs such as *DptA* and *AttA* are still translated, in a cap-independent manner. As we showed that RACK1 represses the translation of

AMPs, we can speculate that RACK1 represses the cap-independent translation of these mRNAs (**Figure 23**). Of note, a similar mechanism of post-transcriptional regulation might exist in mammals, as a recent study identified cap-independent sequences in the 5'UTR of immune genes such as IL-6, IL-11 and IL-32 (Weingarten-Gabbay et al., 2016). Overall, it seems that when a cell encounters a stressor, the first step is to activate transcription of immune genes. In a second step, their translation is modulated to avoid harmful effect. Our results suggest that RACK1 might play a key role in this process, as a gatekeeper of immune genes expression.

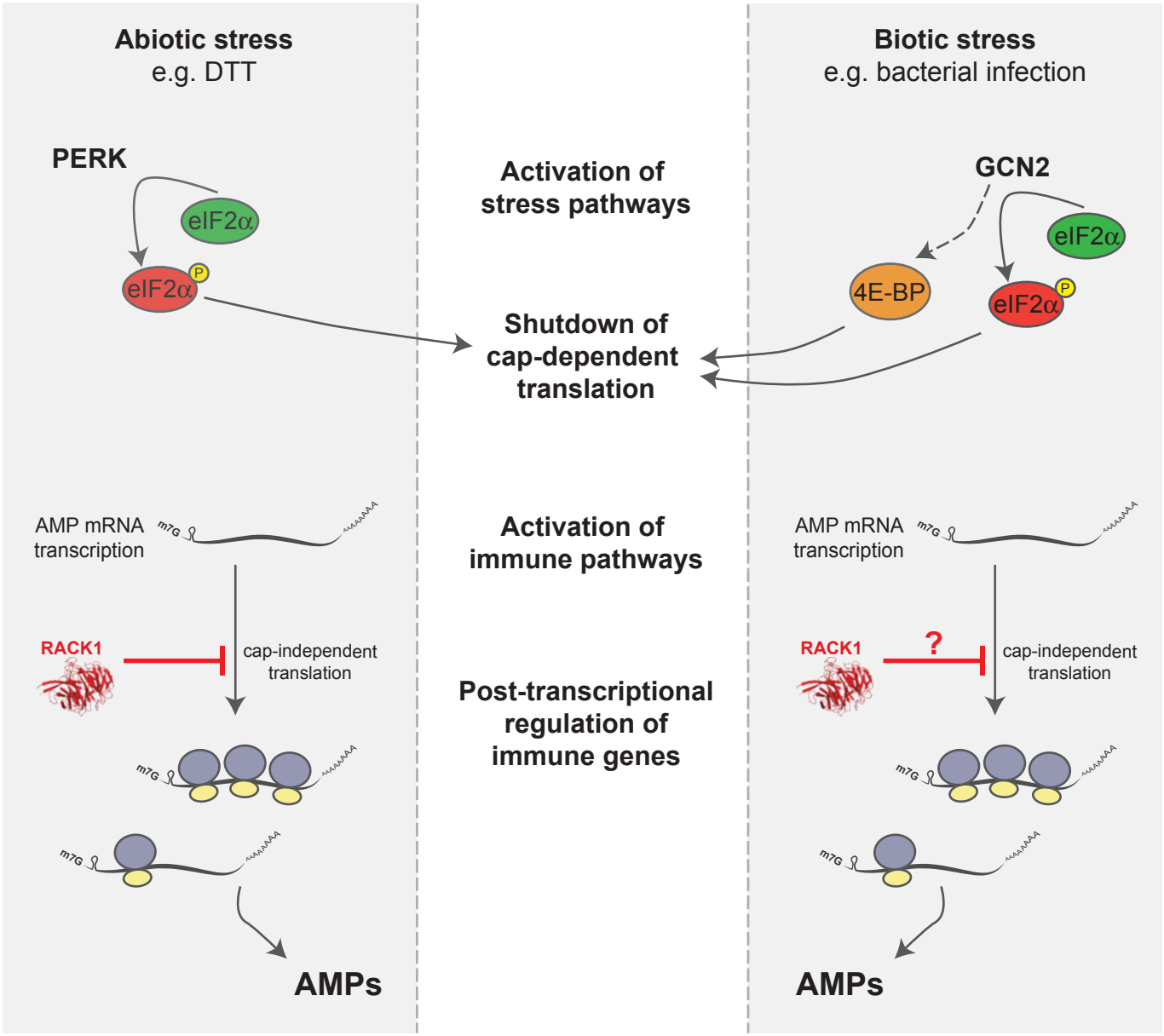

Figure 23: Post-transcriptional gene regulation in abiotic and biotic stresses. Both stresses activate PERK and GCN2, kinases from the integrated stress response pathway, leading to shutdown of cap-dependent translation. In parallel, both stresses activate the transcription of immune pathways and expression of AMPs mRNA. AMPs are translated by cap-independent mechanisms and their translation is blocked by RACK1.

Table 1

shRACK1 vs shmCherry **Transcriptome**
log2FC>1 or <-1 and p<0.05

Sucrose

UP			DOWN		
gene_name	log2FC_Sucrose	log2FC_DTT	gene_name	log2FC_Sucrose	log2FC_DTT
CR44316	*	ns	CR44319	**	ns
CG43742	*	ns	CR45174	*	ns
CG34211	****	ns	CR44284	*	ns
CG13947	****	ns	CR43839	***	ns
LysX	**	ns	CG3528	***	ns
GstD8	**	ns	Appl	***	ns
CG14695	**	ns	CG14763	***	ns
CR44767	*	ns	CG14205	**	ns
IM1	****	ns	CR44667	**	ns
CG6106	****	ns	CG40813	**	ns
IM4	****	ns	CG41562	**	ns
CG5791	****	ns	mwh	**	ns
CG15818	****	ns	CG10734	**	ns
CG33470	****	ns	Ir75d	**	ns
IMPPP	****	ns	teq	**	ns
CG15065	***	ns	CG11626	*	ns
IM23	***	ns	CR44112	*	ns
IM14	***	ns	CR44847	*	ns
IM3	***	ns	CG34279	*	ns
CG43156	**	ns	CG43318	*	ns
CG34040	**	ns	Vha16-5	*	ns
Cpr57A	**	ns	CR32658	*	ns
Obp57d	**	ns	CG18536	*	ns
CG3699	**	ns	CG18675	*	ns
CG34026	**	ns	CG42299	*	ns
CG16836	**	ns	CG14106	*	ns
CG10912	**	ns	CG8509	*	ns
CG44140	**	ns	CR43810	*	ns
CG44141	**	ns	eIF3g2	*	ns
CG34136	**	ns			
GstZ2	**	ns			
IM2	**	ns			
CG11878	**	ns			
CG31704	**	ns			
hgo	**	ns			
CG14499	*	ns			
Jon25Bi	*	ns			
CG13155	*	ns			
Drsl4	*	ns			
Cyp309a1	*	ns			
CG4363	*	ns			
CG14246	*	ns			
Fst	*	ns			
CG15210	*	ns			
CG15043	*	ns			
Cyp6d2	*	ns			
Obp57c	*	ns			
CG16713	*	ns			
CG43074	*	ns			
sPLA2	*	ns			
CG10910	*	ns			

DTT

UP			DOWN		
gene_name	log2FC_Sucrose	log2FC_DTT	gene_name	log2FC_Sucrose	log2FC_DTT
CG43355	ns	****	CR45449	ns	*
sala	ns	****	CG43773	ns	**
CG14529	ns	****	snoRNA:Or-CD2	ns	*
cn	ns	***	CR45330	ns	*
CR44897	ns	**	daw	ns	****
SPH93	ns	**	CG18446	ns	****
AttD	ns	*	MFS14	ns	****
CR43719	ns	*	Pebp1	ns	***
CR44396	ns	**	vri	ns	***
CR44827	ns	**	sug	ns	***
CG14963	ns	**	CR45604	ns	**
Spn88Eb	ns	**	Cyp28d2	ns	**
Faa	ns	**	CG3106	ns	**
CG43348	ns	**	CG3739	ns	**
CR43421	ns	*	CNT2	ns	**
CR46112	ns	*	Lip4	ns	**
Efhc1.2	ns	*	CG9505	ns	**
CG32302	ns	*	CG6295	ns	*
CG2650	ns	*	Cyp4d14	ns	*
dec-1	ns	*	CR44389	ns	*
CR43823	ns	*			
wbl	ns	*			
CG30110	ns	*			
Ance-4	ns	*			

Sucrose and DTT

UP			DOWN		
gene_name	log2FC_Sucrose	log2FC_DTT	gene_name	log2FC_Sucrose	log2FC_DTT
CR45259	****	***	Pp1-Y1	****	****
CR43409	*	*	CR43767	****	****
CR41443	****	****	l(2)03659	****	****
Acp54A1	****	****	CR44344	****	****
CR45923	****	****	sphinx	****	****
CG14500	****	****	CR45410	****	****
Mal-B1	****	****	hkb	****	***
CG12708	****	****	yellow-e2	****	**
CG33301	****	****	CR46007	**	*
CR44704	****	*	CR43433	****	****
CR43256	***	****	phr6-4	****	****
CG43403	*	***	CG7768	****	****
CR43399	*	**	eIF4E3	****	**
CG10918	*	*	Rack1	***	****
CR43969	*	*	Muc30E	***	*
CG18641	****	****	CR44370	***	*
CG11912	*	****	CG7295	***	*
CG10013	****	***	CG33267	***	*
Tsf1	****	*	Elp78C	***	*
CG15721	***	**	bab1	***	*
whe	***	*	bw	***	*
CG15646	**	****	Zmynd10	**	**
pyd3	**	****	CR32652	**	*
CG9344	**	**	CG15734	**	*
CG16762	**	*			
LysP	**	*			
CG9676	*	***			
GstD5	*	***			
CG14245	*	**			
CG6996	*	**			
Obp56g	*	**			

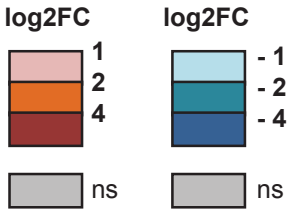

Table 1: Heatmap showing the log2 Fold change of shRACK1 *vs* shmCherry in all fractions. The color code correspond to the log2 Fold change (log2FC) value, and the statistical value is indicated. ****: p<0.0001; ***: p<0.001; **: p<0.01; *: p<0.05; ns: not significant.

Table 1

shRACK1 *vs* shmCherry
log2FC>1 or <-1 and p<0.05

POLYSOMES

Sucrose

UP			DOWN		
gene_name	log2FC_Sucrose	log2FC_DTT	gene_name	log2FC_Sucrose	log2FC_DTT
lncRNA:CR43409	****	ns	Pp1-Y1	****	ns
CG14695	****	ns	CG14635	****	ns
CG12766	***	ns	CG17917	*	ns
CG34040	**	ns	asRNA:CR45886	****	ns
CG10912	**	ns	yellow-e2	***	ns
CG15721	**	ns	lncRNA:CR44112	***	ns
CG34136	**	ns	CG42870	***	ns
Fst	**	ns	CG34279	***	ns
IM1	**	ns	lncRNA:CR43854	**	ns
Cyp309a1	**	ns	lncRNA:CR45410	**	ns
CG13947	**	ns	lncRNA:CR44344	**	ns
IMPPP	**	ns	lncRNA:CR42756	**	ns
CG33470	**	ns	CG45063	*	ns
CG18641	*	ns	CG14634	*	ns
CG12998	*	ns	CG3528	****	ns
Rchy1	*	ns	Zmynd10	****	ns
bbg	*	ns	CG14456	***	ns
Rdl	*	ns	Vha16-3	***	ns
CG13482	*	ns	lncRNA:CR44919	***	ns
IM23	*	ns	CG10822	***	ns
CG16727	*	ns	CG43296	***	ns
snoRNA:660	*	ns	CG41562	***	ns
CG10910	*	ns	CG15734	***	ns
CG34026	*	ns	CG1428	***	ns
CG11878	*	ns	Naa30B	***	ns
CG43273	*	ns	CG9308	***	ns
beat-Vb	*	ns	eIF4E3	***	ns
CG10911	*	ns	CG13426	**	ns
Tsf1	*	ns	BBS8	**	ns
corolla	*	ns	CG12506	**	ns
CG3726	*	ns	CG3927	**	ns
			CG40813	**	ns
			Rab9D	**	ns
			Rab9Fa	**	ns
			Vha16-5	**	ns
			Rab9E	**	ns
			CG9962	**	ns
			CG14106	**	ns
			lncRNA:CR43905	**	ns
			Rab9Db	**	ns
			yip3	**	ns
			CG34029	**	ns
			Cyp4d14	**	ns
			CG14763	**	ns
			lncRNA:CR45030	**	ns
			robl22E	**	ns
			Obp99b	**	ns
			HP6	**	ns
			Rpt4R	**	ns
			SkpD	**	ns
			Ssl	**	ns
			eIF3d2	**	ns
			CG43317	**	ns
			ND-49L	**	ns
			asRNA:CR45015	*	ns
			CG8117	*	ns
			Vha16-4	*	ns
			asRNA:CR45053	*	ns
			CG31928	*	ns
			CG34434	*	ns
			CG42580	*	ns
			Ib	*	ns
			CG17192	*	ns
			CG14219	*	ns
			CG34283	*	ns
			Pk34A	*	ns
			lncRNA:CR42696	*	ns
			Tsp42A	*	ns
			CG32110	*	ns
			CG13171	*	ns
			CG3491	*	ns
			lncRNA:CR44389	*	ns
			CG13829	*	ns
			lncRNA:CR45248	*	ns
			ND-51L1	*	ns
			CG42300	*	ns
			CG31848	*	ns
			CG17580	*	ns
			CG13723	*	ns
			CG43702	*	ns
			Atg8b	*	ns
			lncRNA:CR32658	*	ns
			Ir75d	*	ns
			cep290	*	ns
			CG13540	*	ns
			CG42299	*	ns
			CG7768	*	ns
			robl37BC	*	ns
			CG43922	*	ns
			lncRNA:CR43264	*	ns
			CG42810	*	ns
			CG43052	*	ns
			phu	*	ns
			CG8509	*	ns
			eIF3g2	*	ns
			CG13471	*	ns
			asRNA:CR45271	*	ns
			CG14684	*	ns
			CG14070	*	ns
			CG32812	*	ns
			d-cup	*	ns
			ATPsynGL	*	ns
			e(y)2b	*	ns
			CG33267	*	ns
			bab1	*	ns
			fan	*	ns
			CG32488	*	ns
			Eip78C	*	ns
			Appl	*	ns
			bw	*	ns

DTT

UP			DOWN		
gene_name	log2FC_Sucrose	log2FC_DTT	gene_name	log2FC_Sucrose	log2FC_DTT
SPH93	ns	***	Tom	ns	*
ppk13	ns	**	CG43773	ns	**
yellow-g2	ns	**	vri	ns	****
LysS	ns	*	Pebp1	ns	**
CG13311	ns	****	daw	ns	**
CG14963	ns	***	Npc1b	ns	*
LysP	ns	***	asRNA:CR45604	ns	*
Drsl3	ns	**	CG6295	ns	*
CG42782	ns	**	CG18446	ns	*
CG14245	ns	**	MFS14	ns	*
Cyp6a23	ns	**			
CG32302	ns	*			
Nepl17	ns	*			
Ag5r	ns	*			
Spn88Eb	ns	*			
MtnB	ns	*			
GstD5	ns	*			
CG17239	ns	*			
whe	ns	*			
CG16713	ns	*			
CG34284	ns	*			
sPLA2	ns	*			
CG14246	ns	*			

Sucrose and DTT

UP			DOWN		
gene_name	log2FC_Sucrose	log2FC_DTT	gene_name	log2FC_Sucrose	log2FC_DTT
lncRNA:CR45259	****	****	lncRNA:sphinx	****	****
CG3650	***	*	asRNA:CR43767	****	****
CG10013	****	**	l(2)03659	****	****
lncRNA:CR43256	****	***	CG7295	****	**
Mal-B1	****	****	asRNA:CR43433	****	*
CG13403	****	****	hkb	**	****
lncRNA:dntRL	****	***	CG13946	**	*
CG34038	*	***	phr6-4	****	***
CG10918	*	***	Rack1	****	***
CG14500	***	****	CG31275	**	*
CG33301	***	***	Cyp28d2	*	*
CG9676	***	*			
CG43403	**	****			
Acp54A1	**	****			
CG16762	**	**			
CG15818	**	*			
nAChRalpha3	**	*			
CG13810	*	***			
CG15646	*	**			
beat-Vb	*	*			
CG12708	*	*			

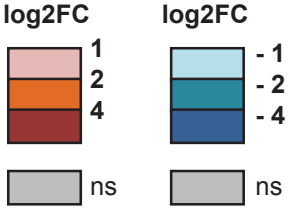

Table 1

shRACK1 *vs* shmCherry
log2FC>1 or <-1 and p<0.05

MONOSOMES

Sucrose

UP			DOWN		
gene_name	log2FC_Sucrose	log2FC_DTT	gene_name	log2FC_Sucrose	log2FC_DTT
CG34434	***	ns	lncRNA:CR45259	****	ns
BBS8	***	ns	CG14500	****	ns
CG10822	***	ns	CG15721	***	ns
lncRNA:CR44112	***	ns	lncRNA:CR44316	**	ns
Vha16-3	***	ns	CG42728	**	ns
CG14106	***	ns	CG34136	**	ns
ND-51L1	***	ns	CG34040	**	ns
Rack1	***	ns	CG10912	**	ns
lncRNA:CR43854	**	ns	CG34176	**	ns
lncRNA:CR43721	**	ns	LysP	**	ns
lncRNA:CR44789	**	ns	Ilp6	**	ns
CG13426	**	ns	IM4	*	ns
VhaAC39-2	**	ns	CG43074	*	ns
yip3	**	ns	CG43349	*	ns
CG3515	**	ns	GstZ2	*	ns
asRNA:CR45886	**	ns	CG18641	*	ns
betaNACtes4	**	ns	CG43295	*	ns
vanin-like	**	ns	Fst	*	ns
CG3528	**	ns	CG18628	*	ns
CG42870	*	ns	CG5011	*	ns
lncRNA:CR43940	*	ns	CG9344	*	ns
CG43308	*	ns	CG13428	*	ns
CG34279	*	ns			
CG17580	*	ns			
Best3	*	ns			
Vha16-5	*	ns			
lncRNA:CR44617	*	ns			
CG10748	*	ns			
Cyp4d14	*	ns			
lncRNA:CR42696	*	ns			
CG32320	*	ns			
CG14456	*	ns			
CG10993	*	ns			
Vha16-4	*	ns			
CG14763	*	ns			
asRNA:CR31912	*	ns			
lncRNA:CR43264	*	ns			
CG32639	*	ns			
ATPsynbetaL	*	ns			
phu	*	ns			
lncRNA:CR45248	*	ns			
rho-6	*	ns			
CG34283	*	ns			
CG1428	*	ns			
CG7573	*	ns			
CG10931	*	ns			
asRNA:CR45927	*	ns			
Rpt4R	*	ns			
Rab9E	*	ns			
ND-20L	*	ns			
CG32232	*	ns			
Rab9D	*	ns			
lncRNA:CR43763	*	ns			
CG9308	*	ns			
Zmynd10	*	ns			
G6P	*	ns			
asRNA:CR45271	*	ns			
CG2772	*	ns			
Ir75d	*	ns			
lncRNA:CR32658	*	ns			
Jheh3	*	ns			

DTT

UP			DOWN		
gene_name	log2FC_Sucrose	log2FC_DTT	gene_name	log2FC_Sucrose	log2FC_DTT
CG31275	ns	****	lncRNA:CR44298	ns	****
vri	ns	****	asRNA:CR44704	ns	****
Cyp28d2	ns	***	CG12708	ns	****
CG34173	ns	***	lncRNA:CR44557	ns	****
CG43638	ns	***	snRNA:U2:38ABa	ns	****
asRNA:CR44370	ns	***	CG30334	ns	****
CG7634	ns	***	CG34227	ns	****
janB	ns	***	CG3640	ns	****
TotA	ns	**	CG15067	ns	****
CG43673	ns	**	CG18107	ns	****
CG33285	ns	**	CG9691	ns	****
CG34287	ns	**	l(2)34Fc	ns	****
CG18536	ns	**	SPH93	ns	***
Naa30B	ns	**	CG6220	ns	***
CG34292	ns	**	CG10918	ns	***
Spag1	ns	**	snRNA:U2:38ABb	ns	***
CG31804	ns	**	snRNA:U2:14B	ns	***
Pebp1	ns	**	CG43403	ns	***
CG14926	ns	**	CG43236	ns	***
CG32371	ns	**	CG9650	ns	***
CG30039	ns	**	CG15646	ns	***
CG18446	ns	**	CG15065	ns	***
CG43773	ns	*	Drsl4	ns	***
Muc14A	ns	*	sick	ns	***
CG16995	ns	*	CG5791	ns	***
lncRNA:CR45279	ns	*	RNaseMRP:RNA	ns	***
CG6295	ns	*	CG16713	ns	***
daw	ns	*	IM23	ns	***
CG12402	ns	*	CG34250	ns	***
CG43800	ns	*	Nepl17	ns	**
CG31525	ns	*	snRNA:U2:34ABa	ns	**
Mdr50	ns	*	CG14795	ns	**
CG31230	ns	*	Alp11	ns	**
GstD10	ns	*	CG2650	ns	**
Uhg4	ns	*	Drsl3	ns	**
CG18132	ns	*	CG13641	ns	**
Ugt37A2	ns	*	lncRNA:CR43793	ns	**
alphaTub85E	ns	*	CG16837	ns	**
Myo28B1	ns	*	Obp56e	ns	**
CG31952	ns	*	CG43267	ns	**
CG14708	ns	*	CG32512	ns	**
CG11892	ns	*	CG6403	ns	**
CG31690	ns	*	Reg-2	ns	**
			NimB3	ns	**
			CG12310	ns	**
			CG3699	ns	**
			lncRNA:CR43411	ns	**
			CG42471	ns	**
			CG8369	ns	**
			CG13227	ns	*
			lncRNA:CR43486	ns	*
			snRNA:U2:34ABc	ns	*
			CG11912	ns	*
			snRNA:U2:34ABb	ns	*
			CecC	ns	*
			CG30178	ns	*
			lncRNA:CR44236	ns	*
			lncRNA:CR45256	ns	*
			DIP-beta	ns	*
			asRNA:CR46047	ns	*
			Spn88Eb	ns	*
			asRNA:CR44381	ns	*
			NimC4	ns	*
			Stacl	ns	*
			lncRNA:CR45631	ns	*
			Cp16	ns	*
			CG43061	ns	*
			CG43060	ns	*
			usp	ns	*
			CG43788	ns	*
			nAChRalpha5	ns	*
			CG17239	ns	*

Sucrose and DTT

UP			DOWN		
gene_name	log2FC_Sucrose	log2FC_DTT	gene_name	log2FC_Sucrose	log2FC_DTT
lncRNA:sphinx	****	****	lncRNA:CR43256	****	***
Pp1-Y1	****	****	Mal-B1	****	****
asRNA:CR43767	****	****	lncRNA:dntRL	****	***
l(2)03659	***	****	CG10013	***	***
asRNA:CR43433	***	***	CG34038	*	*
CG7295	***	***			
eIF4E3	***	**			
CG3927	***	*			
CG15734	***	*			
phr6-4	**	****			
lncRNA:CR45410	**	**			
eIF3d2	**	*			
CG7768	*	****			
lncRNA:CR44344	*	**			
lncRNA:CR45560	*	*			
CG41562	*	*			
CG40813	*	*			

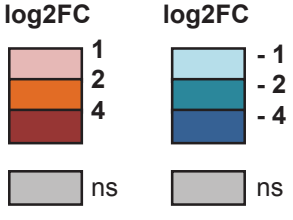

Table 1

shRACK1 *vs* shmCherry
log2FC>1 or <-1 and p<0.05

FREE

Sucrose

UP			DOWN		
gene_name	log2FC_Sucrose	log2FC_DTT	gene_name	log2FC_Sucrose	log2FC_DTT
lncRNA:CR46063	**	ns	lncRNA:CR45449	*	ns
CG34211	****	ns	lncRNA:CR45410	***	ns
snRNA:U2:38ABa	*	ns	yellow-e2	**	ns
snRNA:U2:38ABb	*	ns	lncRNA:CR43854	*	ns
snRNA:U2:14B	*	ns	CG13739	*	ns
IM1	*	ns			

DTT

UP			DOWN		
gene_name	log2FC_Sucrose	log2FC_DTT	gene_name	log2FC_Sucrose	log2FC_DTT
cn	ns	**	CG12057	ns	****
CG34038	ns	*	lncRNA:CR44389	ns	****
lncRNA:CR44199	ns	*	Pebp1	ns	****
LysS	ns	*	CG3106	ns	***
SPH93	ns	****	CG42828	ns	**
Acp54A1	ns	****	nompC	ns	*
lncRNA:CR43399	ns	***	Cpr65Ec	ns	*
lncRNA:CR43414	ns	***	CG44088	ns	*
Nlg4	ns	**	CG43773	ns	*
CG43814	ns	*	eIF4E3	ns	****
Cpr72Eb	ns	*	CG14763	ns	****
CG34273	ns	*	asRNA:CR43433	ns	***
lncRNA:CR43969	ns	*	Mipp1	ns	***
CG17075	ns	*	Cp15	ns	***
flz	ns	*	CG8834	ns	***
Efhc1.2	ns	*	Acbp5	ns	***
en	ns	*	Six4	ns	**
asRNA:CR44981	ns	*	PGRP-SC1a	ns	**
CG2650	ns	****	Rack1	ns	**
CG12708	ns	***	PGRP-SC1b	ns	**
lncRNA:CR46112	ns	**	asRNA:CR43430	ns	**
snoRNA:660	ns	**	daw	ns	**
lncRNA:CR44236	ns	**	asRNA:CR46101	ns	**
CG45770	ns	**	lncRNA:CR44324	ns	**
Mst77Y-7	ns	**	CG3739	ns	**
CG12448	ns	**	CG34279	ns	**
side-V	ns	**	CG18446	ns	**
Mst77Y-13	ns	**	CG15649	ns	**
Cyp6a23	ns	**	CG17124	ns	**
lncRNA:CR45448	ns	**	CG15734	ns	**
CG9344	ns	**	E(spl)mbeta-HLH	ns	*
CG11342	ns	**	CG31041	ns	*
Ac78C	ns	**	SP	ns	*
lncRNA:CR44360	ns	*	Mst57Db	ns	*
lncRNA:CR45286	ns	*	sug	ns	*
lncRNA:CR44710	ns	*	Nrk	ns	*
r-cup	ns	*	Tret1-1	ns	*
asRNA:CR31845	ns	*	CG4250	ns	*
dimm	ns	*	Zmynd10	ns	*
CG10912	ns	*	CG13171	ns	*
LysP	ns	*	CG13607	ns	*
CG44355	ns	*	MFS14	ns	*
lncRNA:CR44660	ns	*	lncRNA:CR43960	ns	*
CG43348	ns	*	Atg8b	ns	*
lncRNA:CR43486	ns	*	Mur2B	ns	*
DIP-beta	ns	*			
CG11630	ns	*			
CG15071	ns	*			
CG15484	ns	*			
CG6996	ns	*			
Uro	ns	*			
Nepl17	ns	*			
Mst77Y-9	ns	*			
CG13538	ns	*			
CG45765	ns	*			
CG45764	ns	*			
CG13021	ns	*			
CG43998	ns	*			
CG43999	ns	*			
CG45766	ns	*			
CG18063	ns	*			
Obp56g	ns	*			
dpr10	ns	*			
GstZ2	ns	*			

Sucrose and DTT

UP			DOWN		
gene_name	log2FC_Sucrose	log2FC_DTT	gene_name	log2FC_Sucrose	log2FC_DTT
lncRNA:CR45259	****	****	Pp1-Y1	****	****
lncRNA:CR44316	****	****	lncRNA:sphinx	****	****
lncRNA:CR43256	****	****	CG18536	****	****
CG10918	****	***	lncRNA:CR44344	***	****
CG33301	****	****	lncRNA:CR32658	***	****
CG14500	**	****	CG7768	***	**
CG11912	**	****	lncRNA:CR32652	**	****
Mal-B1	**	**	Obp99b	*	*
asRNA:CR44704	**	*			
lncRNA:CR41443	*	**			

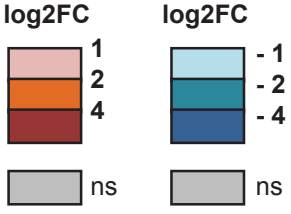

Table 2

DTT *vs* SUCROSE **Transcriptome**
log2FC>1 or <-1 and p<0.05

shRACK1

UP			DOWN		
gene_name	log2FC_shmCherry	log2FC_shRACK1	gene_name	log2FC_shmCherry	log2FC_shRACK1
CR44404	ns	****	Tom	ns	****
edin	ns	**	Brd	ns	***
AttA	ns	****	Ocho	ns	***
AttB	ns	****	CG13465	ns	***
CR45045	ns	****	CG13427	ns	**
AttC	ns	****	CG15731	ns	**
DptB	ns	****	Jon66Cii	ns	**
DptA	ns	****	CG13159	ns	**
CG43920	ns	***	CG4440	ns	*
CecC	ns	****	CG2962	ns	*
CecA2	ns	****	CG6295	ns	****
Mtk	ns	****	PGRP-SC1a	ns	****
CecB	ns	**	PGRP-SC1b	ns	****
CG12826	ns	**	TotX	ns	****
Lip3	ns	**	Drsl4	ns	****
phu	ns	****	CG32368	ns	****
PGRP-SB1	ns	**	Jon74E	ns	****
CG6403	ns	**	Obp56a	ns	****
CG13306	ns	**	CG45087	ns	****
NPFR	ns	*	Pepck	ns	****
CG2650	ns	*	Npc2e	ns	***
CR44640	ns	*	TotC	ns	***
			CG12998	ns	**
			Zip42C.2	ns	**
			Cpr60D	ns	**
			Cp7Fb	ns	*
			CR45330	ns	*
			lectin-37Da	ns	****
			CG34026	ns	****
			Jon65Ai	ns	****
			CG13607	ns	****
			thetaTry	ns	****
			MtnC	ns	****
			Cpr65Au	ns	****
			Cp15	ns	****
			pirk	ns	****
			Listericin	ns	****
			epsilonTry	ns	****
			CG5804	ns	****
			CG1648	ns	****
			mag	ns	***
			TotA	ns	***
			CG7203	ns	***
			Met75Ca	ns	***
			Met75Cb	ns	***
			CG8628	ns	***
			Jon99Ci	ns	***
			FASN1	ns	***
			CG5945	ns	***
			CG13360	ns	***
			CR43051	ns	***
			CR43432	ns	**
			CG43673	ns	**
			Jon99Fii	ns	**
			Dr	ns	**
			Jon99Fi	ns	**
			msopa	ns	**
			Mst57Db	ns	**
			Jon65Aiv	ns	**
			CG31313	ns	**
			Obp19d	ns	**
			CG31233	ns	**
			CG16749	ns	**
			sug	ns	**
			CG32633	ns	**
			dsb	ns	**
			CG10300	ns	*
			CR45601	ns	*
			CR44181	ns	*
			CG43251	ns	*
			betaTry	ns	*
			Jon99Ciii	ns	*
			CG14963	ns	*
			CG43319	ns	*
			Jon99Cii	ns	*
			Obp56e	ns	*
			CG10943	ns	*
			vri	ns	*
			Cp36	ns	*
			CG42481	ns	*
			CG11892	ns	*
			TpnC47D	ns	*
			CG43061	ns	*
			odd	ns	*
			snoRNA:CG43051-a	ns	*
			CG6125	ns	*
			CG42656	ns	*
			CG10657	ns	*
			CG14949	ns	*
			Cys	ns	*

shRACK1

DOWN		
gene_name	log2FC_shmCherry	log2FC_shRACK1
CG34291	ns	*
CG8773	ns	*
Tsf1	ns	*
CG42825	ns	*
CG17124	ns	*
CG5162	ns	*
Scp2	ns	*
Clect27	ns	*
CG15202	ns	*

shmCherry

UP			DOWN		
gene_name	log2FC_shmCherry	log2FC_shRACK1	gene_name	log2FC_shmCherry	log2FC_shRACK1
CG34211	***	ns	MFS1	**	ns
CG31089	**	ns	E(spl)mgamma-HLH	**	ns
CG33301	****	ns	E(spl)m5-HLH	*	ns
CG34040	****	ns	CG14110	*	ns
GstZ2	****	ns	E(spl)m4-BFM	***	ns
LManV	****	ns	CG10591	***	ns
CG11842	****	ns	Cyp6a16	**	ns
CG10513	****	ns	nerfin-1	*	ns
Cyp12a5	***	ns	CG13083	*	ns
CR45144	***	ns	CR30009	*	ns
CG13659	***	ns	ImpL1	*	ns
CG9498	***	ns	yellow-g2	*	ns
CG15784	***	ns	link	*	ns
IM3	***	ns	CG7804	***	ns
CG16836	***	ns	CG9259	***	ns
CG31975	**	ns	Pkd2	***	ns
ovm	**	ns	CG14500	**	ns
CG5724	**	ns	CG15570	**	ns
CG34316	**	ns	CG2861	**	ns
CG31272	**	ns	Rbp4	**	ns
Cyp9b2	**	ns	CG6675	**	ns
IM14	**	ns	CG4021	**	ns
CG14109	**	ns	sa	**	ns
CG6271	**	ns	Pk34A	*	ns
CG5999	*	ns	CG33290	*	ns
CR45813	*	ns	mira	*	ns
CG13325	*	ns	CG7991	*	ns
CR45875	*	ns	CG2663	*	ns
CG9312	*	ns	CG3123	*	ns
Cyp6t3	*	ns	Vha16-5	*	ns
CG1698	*	ns	Art2	*	ns
Cpr66D	*	ns	CG43167	*	ns
CG7142	*	ns	CG5681	*	ns
Ugt86Dd	*	ns	tbrd-3	*	ns
Mal-B1	*	ns	LS2	*	ns
Act88F	*	ns	CG42300	*	ns
MtnE	*	ns	Tsp42A	*	ns
			CG32259	*	ns
			B9d2	*	ns
			tctn	*	ns
			CG18258	*	ns
			CG3927	*	ns
			CG9701	*	ns
			CG5246	*	ns
			CG42299	*	ns
			blanks	*	ns
			CG18284	*	ns
			Acp26Aa	*	ns
			CG32568	*	ns
			CG30025	*	ns
			CG1428	*	ns
			CG10748	*	ns
			alphaTry	*	ns
			Vha16-2	*	ns
			CG30031	*	ns
			deltaTry	*	ns
			gammaTry	*	ns
			Muc30E	*	ns
			Ssl	*	ns

shRACK1 and shmCherry

UP			DOWN		
gene_name	log2FC_shmCherry	log2FC_shRACK1	gene_name	log2FC_shmCherry	log2FC_shRACK1
CG32284	****	****	Vm26Aa	****	****
CR44138	****	****	Vm34Ca	*	***
CG10814	**	****	BobA	*	***
Drsl3	**	****	CG12011	***	**
Dro	*	****	nw	**	**
CG13749	***	**	CG4830	**	*
Cyp6w1	****	****	CG6738	*	*
Mal-B2	****	****	Vm26Ab	****	****
Cyp28a5	****	****	CG17192	***	****
Gnmt	****	****	Jon66Ci	*	****
Cyp6a8	**	****	PPO1	****	****
TotM	*	***	Lsp1beta	****	****
CG34136	****	**	fit	****	****
CG13905	****	**	Obp99b	****	****
CG43348	***	**	CG12374	***	****
CG11425	***	**	CG12057	***	****
Cpr62Ba	**	**	CR43887	**	*
CG32198	*	**	CG6733	****	****
LManIII	****	*	Diedel3	****	****
CG17560	**	*	Def	**	****
CG33282	*	*	CG15353	**	****
CG45061	*	*	CG5770	**	****
CG13641	*	*	Obp99a	**	****
			PPO2	**	****
			Pebp1	*	****
			CG9184	**	**
			Npc1b	**	**
			dec-1	****	**
			Sfp24Ba	**	**
			CR45142	*	*
			Yp2	****	****
			CG16762	****	****
			Lsd-1	***	****
			CR45046	***	****
			CG5773	**	****
			Nplp3	*	****
			Acp54A1	****	***
			EbpII	****	***
			Sfp87B	****	***
			Lsp2	***	***
			Sfp24Bb	***	***
			CG5853	**	***
			CG8129	*	***
			Cp38	*	***
			CG15199	***	**
			CG14439	***	**
			CG42782	**	**
			CG7300	*	**
			Yp3	***	*
			Acp24A4	***	*
			Npc2d	*	*
			CG17637	*	*
			Cpr49Ab	*	*

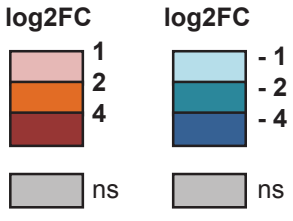

Table 2: Heatmap showing the log2 Fold change of DTT *vs* Sucrose in all fractions. The color code correspond to the log2 Fold change (log2FC) value, and the statistical value is indicated. ****: p<0.0001; ***: p<0.001; **: p<0.01; *: p<0.05; ns: not significant.

Table 2

DTT *vs* SUCROSE **POLYSOMES**
log2FC>1 or <-1 and p<0.05

shRACK1

UP			DOWN		
gene_name	log2FC_shmCherry	log2FC_shRACK1	gene_name	log2FC_shmCherry	log2FC_shRACK1
CG43920	ns	****	Tom	ns	****
DptB	ns	****	SNCF	ns	****
AttB	ns	****	CR45138	ns	***
CecA2	ns	****	Osi7	ns	***
CecC	ns	****	CG14317	ns	**
DptA	ns	****	Bsg25A	ns	**
CR45045	ns	****	Osi15	ns	*
AttC	ns	****	Osi19	ns	*
IM18	ns	****	Osi18	ns	*
CG10332	ns	****	CG2962	ns	*
Mtk	ns	****	CG13159	ns	*
CG43729	ns	****	CG10035	ns	****
PGRP-SB1	ns	****	CG31002	ns	**
CecB	ns	***	CG6034	ns	**
CG13227	ns	**	halo	ns	*
CG1273	ns	**	CG15731	ns	*
TotM	ns	****	Sfp79B	ns	*
PGRP-SD	ns	****	Lcp65Ag3	ns	*
Alp2	ns	****	CG18814	ns	*
AttD	ns	***	ppk20	ns	*
CG43403	ns	***	Obp56a	ns	****
CG13641	ns	***	CG15282	ns	***
CecA1	ns	**	TotC	ns	***
Cyp28a5	ns	**	Lsp2	ns	***
CG9312	ns	**	TotA	ns	***
CG5955	ns	**	Pepck	ns	***
Cyp12d1-d	ns	**	CG45087	ns	***
GstD5	ns	**	CG32368	ns	***
Cyp12d1-p	ns	**	mira	ns	**
CR44641	ns	*	Npc2e	ns	**
CG14291	ns	*	pirk	ns	**
CG34290	ns	*	CG13607	ns	**
CG43400	ns	*	CR45949	ns	*
CG17751	ns	*	CG43673	ns	*
CG2650	ns	*	CG1648	ns	*
CG6283	ns	*	CG5157	ns	*
CG14606	ns	*	MtnC	ns	*
CG15408	ns	*	Cyp18a1	ns	*
CG10592	ns	*	CG13155	ns	*
LManVI	ns	*	Cp15	ns	*
CG30022	ns	*	Jon65Aiv	ns	*
			FASN1	ns	*
			Ebp	ns	*

shmCherry

UP			DOWN		
gene_name	log2FC_shmCherry	log2FC_shRACK1	gene_name	log2FC_shmCherry	log2FC_shRACK1
CG43894	*	ns	CG9184	****	ns
mir-2494	*	ns	CG10591	**	ns
CG34040	****	ns	ImpE2	*	ns
CG15784	****	ns	nerfin-1	*	ns
Chchd2	****	ns	E(spl)mdelta-I	*	ns
CG5999	***	ns	Obp99b	****	ns
CR45144	***	ns	CG14500	****	ns
beat-Vb	***	ns	CR45945	***	ns
Cyp9b2	***	ns	CG7991	***	ns
CG33301	**	ns	Ilp4	**	ns
CG10912	**	ns	Vm32E	**	ns
bbg	**	ns	CG14756	**	ns
CG8745	**	ns	CG4702	**	ns
CG13309	**	ns	nw	**	ns
CG3726	**	ns	CG14110	*	ns
Cyp4p1	**	ns	MFS1	*	ns
CG13325	*	ns	ImpL1	*	ns
CG33093	*	ns	Vm26Ac	*	ns
CR45813	*	ns	Zip42C.2	*	ns
CG31778	*	ns	CG13801	*	ns
Act88F	*	ns	CR44817	*	ns
Fs	*	ns	CG7213	*	ns
Ugt86Dd	*	ns	link	*	ns
			CG43355	*	ns
			sala	*	ns
			Acp54A1	****	ns
			CG42782	****	ns
			CG2663	***	ns
			Rbp4	***	ns
			EbpII	***	ns
			Mst57Db	***	ns
			CG4891	***	ns
			CG13639	**	ns
			Cyp6a16	**	ns
			CG11269	**	ns
			CG9962	**	ns
			Acp98AB	**	ns
			Vha16-3	**	ns
			hog	**	ns
			CG7907	**	ns
			yip3	**	ns
			CG42852	**	ns
			CR43264	**	ns
			CG4563	**	ns
			CG1428	**	ns
			CG31848	**	ns
			CG42481	**	ns
			CG14070	**	ns
			CG43251	**	ns
			CG14841	**	ns
			Cyp4d14	**	ns
			CG5250	**	ns
			Acp24A4	**	ns
			CG9259	**	ns
			betaTry	**	ns
			CG4000	**	ns
			CG10748	**	ns
			CR43812	**	ns
			Vha100-3	**	ns
			CG12078	**	ns
			Twdlalpha	**	ns
			msopa	**	ns
			CG16762	**	ns
			CG32277	**	ns
			CG30431	**	ns
			Npc2h	**	ns
			CG13360	**	ns
			CR43637	**	ns
			phm	*	ns
			kmg	*	ns
			CG14635	*	ns
			CG8117	*	ns
			Cp16	*	ns
			CG42580	*	ns
			CR43239	*	ns
			Pk34A	*	ns
			CG42579	*	ns
			Rab9Fa	*	ns
			CR31429	*	ns
			Rab9E	*	ns
			Rab9D	*	ns
			CG31776	*	ns
			CG43980	*	ns
			Rab9Db	*	ns
			Cp18	*	ns
			CG33290	*	ns
			CG32833	*	ns
			ATPsynbetaL	*	ns

shmCherry

DOWN		
gene_name	log2FC_shmCherry	log2FC_shRACK1
brv3	*	ns
Cpr65Au	*	ns
CG34289	*	ns
Vha16-2	*	ns
CG41562	*	ns
CG40813	*	ns
CG14840	*	ns
CG15641	*	ns
svp	*	ns
CG5653	*	ns
CG17625	*	ns
CG31068	*	ns
Sfp60F	*	ns
CG10909	*	ns
G6P	*	ns
CG43292	*	ns
CG14456	*	ns
Vha16-5	*	ns
CG5246	*	ns
CR44389	*	ns
CG11630	*	ns
CG10459	*	ns
VhaPPA1-2	*	ns
Prosbeta2R2	*	ns
CG15450	*	ns
HP6	*	ns
CG16848	*	ns
Prosbeta4R1	*	ns
CG15357	*	ns
CG30184	*	ns
Acp53C14a	*	ns
Acp33A	*	ns

shmCherry

DOWN		
gene_name	log2FC_shmCherry	log2FC_shRACK1
CG10931	*	ns
CG3491	*	ns
betaNACtes6	*	ns
Cpr62Bb	*	ns
CG10300	*	ns
CG7227	*	ns
Sfp87B	*	ns
CG42300	*	ns
tbrd-3	*	ns
CG3927	*	ns
CG34434	*	ns
NetB	*	ns
CG12477	*	ns
RpL37b	*	ns
Tsp42A	*	ns
CG3515	*	ns
Npc2d	*	ns
CG34230	*	ns
VhaAC39-2	*	ns
CG32259	*	ns
CG11741	*	ns
Nplp3	*	ns
CR44269	*	ns
Acp53C14c	*	ns
CR45055	*	ns
Tim17b1	*	ns
CG14839	*	ns
CG17633	*	ns
CG31642	*	ns
CG16904	*	ns
Tsp33B	*	ns
CG17580	*	ns
TpnC47D	*	ns

shRACK1 and shmCherry

UP			DOWN		
gene_name	log2FC_shmCherry	log2FC_shRACK1	gene_name	log2FC_shmCherry	log2FC_shRACK1
edin	*	**	Brd	**	****
CR44138	****	****	Ocho	**	****
CG32284	****	****	Vm34Ca	*	****
Drsl3	****	****	CG12011	****	***
Dro	*	****	E(spl)m4-BFM	***	*
CR44404	*	****	CG4830	****	****
Lip3	****	****	CG13427	****	****
CG10814	**	****	BobA	*	****
Drsl2	**	****	CG13465	*	****
AttA	*	****	CG4440	*	****
CG31089	**	***	Vm26Aa	**	**
Cyp6w1	***	****	Cpr60D	****	****
CR44640	***	****	CG12374	****	****
CG6403	**	****	PPO1	****	****
Cyp6a8	*	****	PPO2	****	****
CG13905	****	****	fit	****	****
CG12826	**	**	Jon66Ci	***	****
CG13749	****	*	CG12998	**	****
CG34136	****	*	CG6738	*	****
CG43348	****	****	CG17192	**	**
CG11425	****	****	E(spl)mgamma-HLH	**	*
Gnmt	****	****	Jon66Cii	*	*
CG1698	*	***	CR43887	*	*
phu	*	****	CG6295	****	****
CG3285	*	****	Diedel3	****	****
CG9498	***	****	Def	****	****
MtnB	**	****	Lsp1beta	***	****
CG5697	**	****	Npc1b	***	****
CG45061	****	***	TotX	**	****
Cyp12a5	****	***	PGRP-SC1a	**	****
CG10513	****	***	PGRP-SC1b	**	****
CG31272	**	***	Vm26Ab	*	****
CG33282	*	***	CG42586	**	**
CG13324	*	***	CG31775	**	**
Mal-B2	****	**	dec-1	***	**
CG13659	****	**	Drsl4	****	*
CG2004	****	**	CR45046	****	****
LManIII	***	**	Lsd-1	****	****
Mal-B1	***	**	mag	***	****
CG31975	***	**	Pebp1	**	****
ovm	***	**	Jon74E	**	****
CG10477	**	**	CG6733	****	***
Fst	**	**	CG12057	***	***
LManV	****	*	Yp2	**	***
CG10383	****	*	Yp3	*	***
CG5724	***	*	Obp99a	****	**
CG11842	**	*	Cpr49Ab	****	**
Cht4	*	*	CG5773	**	**
NPFR	*	*	CG5770	*	**
CG34316	*	*	CG8129	*	**
CG17560	*	*	CG14439	****	*
CG15043	*	*	CG15199	****	*
			CG15353	**	*
			CG9701	**	*
			CG7300	*	*

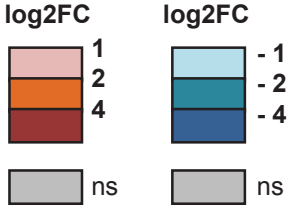

Table 2

DTT *vs* SUCROSE **MONOSOMES**

log2FC>1 or <-1 and p<0.05

shRACK1

UP			DOWN		
gene_name	log2FC_shmCherry	log2FC_shRACK1	gene_name	log2FC_shmCherry	log2FC_shRACK1
DptB	ns	****	CG6295	ns	****
AttA	ns	****	CG43673	ns	****
CG43920	ns	****	TotA	ns	****
AttB	ns	****	Vm34Ca	ns	****
CR44404	ns	****	Pepck	ns	****
Dro	ns	****	CG45087	ns	****
CecC	ns	****	BobA	ns	***
CG13227	ns	****	CG13465	ns	***
CR45045	ns	****	pirk	ns	***
CG13641	ns	****	Npc2e	ns	***
CG30334	ns	****	Jon74E	ns	***
RNaseMRP:RNA	ns	****	Tom	ns	**
AttC	ns	****	Pgcl	ns	**
CG2650	ns	****	CG43402	ns	**
CG3640	ns	****	CG15353	ns	**
Drsl2	ns	***	TotC	ns	**
phu	ns	****	FASN1	ns	**
CG6403	ns	****	CG13607	ns	**
CR43793	ns	***	Ocho	ns	*
Cpr62Ba	ns	***	CG10943	ns	*
snRNA:U11	ns	***	CG43773	ns	*
DptA	ns	***	CG5157	ns	*
PGRP-SB1	ns	***	CG5509	ns	*
Sodh-2	ns	***	SNCF	ns	*
Cyp6w1	ns	***	CG5770	ns	*
CG32599	ns	**	Spn28F	ns	*
CG34316	ns	**	msopa	ns	*
CG18107	ns	**	CG9568	ns	*
CG9993	ns	**	fln	ns	*
CR43683	ns	**	thetaTry	ns	*
7SLRNA:CR32864	ns	*	Jon65Aiv	ns	*
7SLRNA:CR42652	ns	*	Pebp1	ns	*
CG43236	ns	*	betaTry	ns	*
CG1698	ns	*			
CR44298	ns	*			
snRNA:U2:34ABa	ns	*			
CG11852	ns	*			
NimC4	ns	*			
Hayan	ns	*			
CG17999	ns	*			
List	ns	*			
CG1271	ns	*			
CR44784	ns	*			
nAChRalpha5	ns	*			
CG3285	ns	*			
RpL24	ns	*			
CG13133	ns	*			
CG14196	ns	*			
Cht8	ns	*			
CG15067	ns	*			
Cyt-b5-r	ns	*			
CG14292	ns	*			
CG7882	ns	*			
CG5955	ns	*			
CG3500	ns	*			

shmCherry

UP			DOWN		
gene_name	log2FC_shmCherry	log2FC_shRACK1	gene_name	log2FC_shmCherry	log2FC_shRACK1
CR44138	****	ns	CG12011	****	ns
CG13905	****	ns	CG10591	****	ns
Cyp12a5	****	ns	CG9184	****	ns
CG15784	****	ns	CG15199	****	ns
Cyp9b2	****	ns	Acp54A1	****	ns
CR44640	***	ns	PPO1	***	ns
CG34136	***	ns	CG31068	***	ns
CG13659	***	ns	CG6675	***	ns
CG34040	***	ns	Lsd-1	***	ns
CG45061	**	ns	CG6220	**	ns
CG13749	**	ns	CG7991	**	ns
CG34211	**	ns	Jon66Ci	**	ns
CG31089	**	ns	CG4830	**	ns
CR45813	**	ns	CR43494	**	ns
CG33301	**	ns	CR45945	**	ns
CG5724	**	ns	Best3	**	ns
CG8745	**	ns	TotX	**	ns
CG16836	**	ns	Lsp2	**	ns
CR45875	*	ns	CR43358	**	ns
CG31272	*	ns	Osi2	**	ns
GstD10	*	ns	Sfp87B	**	ns
			Brd	**	ns
			CG13829	**	ns
			CG31642	**	ns
			Tsp33B	**	ns
			CR31429	**	ns
			brv3	**	ns
			CG31465	**	ns
			CG30432	**	ns
			CG5653	**	ns
			Rtnl2	**	ns
			CG8219	**	ns
			betaNACtes1	*	ns
			CG9657	*	ns
			jb	*	ns
			CG6738	*	ns
			dec-1	*	ns
			CR44817	*	ns
			CG15056	*	ns
			Pk34A	*	ns
			CG3513	*	ns
			CG14111	*	ns
			Vha16-4	*	ns
			CG2663	*	ns
			CG18558	*	ns
			yellow-g2	*	ns
			PpD5	*	ns
			CG32259	*	ns
			Tsp42A	*	ns
			CG17637	*	ns
			CG4563	*	ns
			CG4702	*	ns
			Acp24A4	*	ns
			VhaAC39-2	*	ns
			CG14187	*	ns
			Obp99b	*	ns
			Yp3	*	ns
			CG10931	*	ns
			Npc1b	*	ns

shRACK1 and shmCherry

UP			DOWN		
gene_name	log2FC_shmCherry	log2FC_shRACK1	gene_name	log2FC_shmCherry	log2FC_shRACK1
Drsl3	****	****	Lsp1beta	****	****
CG32284	****	****	CG12374	****	****
CG10814	****	****	Diedel3	****	****
CG11425	****	****	Vm26Ab	***	****
Mtk	***	****	mag	***	****
CG43729	**	****	CG17192	****	***
IM18	*	****	fit	****	****
CG10332	*	****	CR45046	****	****
CecA2	****	***	CG6733	****	**
MtnB	****	****	PPO2	**	**
Mal-B2	****	***	CG13427	****	*
Gnmt	****	***	Yp2	****	*
CG17560	*	***	Def	***	*
CG2004	****	**	CG12057	**	*
Cyp6a8	**	**	Nplp3	**	*
CG9498	**	**	Cpr60D	**	*
CG31975	**	**			
ovm	**	**			
CG43348	****	*			
CG10513	**	*			
CG13324	**	*			

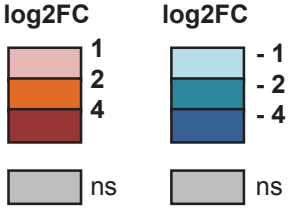

Table 2

DTT *vs* SUCROSE **FREE**
log2FC>1 or <-1 and p<0.05

shRACK1

UP			DOWN		
gene_name	log2FC_shmCherry	log2FC_shRACK1	gene_name	log2FC_shmCherry	log2FC_shRACK1
CR44404	ns	****	Jon66Cii	ns	****
CR45045	ns	****	BobA	ns	***
Dro	ns	****	Vm26Ac	ns	***
AttA	ns	****	CG13465	ns	**
DptB	ns	****	CR43887	ns	**
AttB	ns	****	SNCF	ns	*
AttC	ns	****	CG6295	ns	****
DptA	ns	****	Cp38	ns	****
CG43920	ns	***	PGRP-SC1a	ns	****
Drsl2	ns	**	PGRP-SC1b	ns	****
CecC	ns	*	Cpr60D	ns	****
Cyp6w1	ns	***	Npc2e	ns	****
Mtk	ns	*	Pebp1	ns	****
TotM	ns	*	Jon74E	ns	****
CG43729	ns	*	Def	ns	****
			PPO2	ns	****
			Obp56a	ns	****
			Cp15	ns	****
			CG5804	ns	****
			Cp36	ns	***
			Drsl4	ns	***
			TotX	ns	***
			Mst57Db	ns	***
			Cp18	ns	**
			Npc2d	ns	**
			Jon99Fii	ns	**
			CG13947	ns	**
			Cpr65Au	ns	**
			Obp99a	ns	**
			epsilonTry	ns	**
			Jon25Bi	ns	**
			betaTry	ns	**
			CR43358	ns	*
			Jon99Fi	ns	*
			Jon99Ciii	ns	*
			Jon99Cii	ns	*
			Jon65Ai	ns	*
			CG42782	ns	*
			CG13607	ns	***
			CG34026	ns	**
			Tsf1	ns	**
			Yp3	ns	**
			CG5773	ns	**
			TotC	ns	**
			Met75Cb	ns	*
			Met75Ca	ns	*
			Jon65Aiv	ns	*
			CG30025	ns	*
			CG4734	ns	*
			obst-A	ns	*
			CG30031	ns	*
			gammaTry	ns	*
			deltaTry	ns	*
			Listericin	ns	*
			alphaTry	ns	*
			CG7203	ns	*
			Pepck	ns	*
			CG45087	ns	*
			TotA	ns	*
			CR44389	ns	*
			CG42852	ns	*
			MtnC	ns	*
			CG16775	ns	*
			FASN1	ns	*
			Lsd-1	ns	*

shmCherry

UP			DOWN		
gene_name	log2FC_shmCherry	log2FC_shRACK1	gene_name	log2FC_shmCherry	log2FC_shRACK1
CG11425	**	ns	Vm26Aa	****	ns
CG13749	**	ns	Vm34Ca	*	ns
Cyp12a5	*	ns	CG12011	*	ns
CG34211	****	ns	CG13159	*	ns
CR45813	****	ns	Acp54A1	****	ns
CG13641	***	ns	dec-1	**	ns
CG45061	**	ns	CG10591	*	ns
CG34040	**	ns	CG6220	*	ns
CG13306	**	ns	Ca-beta	*	ns
CG15784	**	ns	CG5770	*	ns
CG34316	**	ns	CG33290	*	ns
CG6403	**	ns	CG43167	**	ns
Cpr62Ba	**	ns	CG32259	**	ns
CG10513	**	ns	CG40813	**	ns
CG8745	**	ns	CG41562	**	ns
CG2650	*	ns	aust	*	ns
MtnB	*	ns	CG30472	*	ns
CG32198	*	ns	svp	*	ns
CG33301	*	ns	CG42299	*	ns
CG31975	*	ns	CG13481	*	ns
ovm	*	ns			
CG13659	*	ns			
CG9498	*	ns			
Ugt86Dd	*	ns			
CG17560	*	ns			
CG14120	*	ns			
CG31272	*	ns			
CG14022	*	ns			
LManIII	*	ns			
CG2004	*	ns			
Cyp9b2	*	ns			
Cyp28a5	*	ns			

shRACK1 and shmCherry

UP			DOWN		
gene_name	log2FC_shmCherry	log2FC_shRACK1	gene_name	log2FC_shmCherry	log2FC_shRACK1
Drsl3	****	****	Tom	**	**
CG32284	****	****	Brd	**	*
CG10814	****	****	Jon66Ci	**	****
CR44138	***	****	CG17192	*	***
Gnmt	****	****	CG13427	*	***
Mal-B2	****	*	Zip42C.2	*	**
			CG10035	*	**
			Vm26Ab	****	****
			Lsp1beta	****	****
			CG12374	****	****
			fit	****	****
			CR45046	****	****
			Obp99b	****	****
			Sfp79B	**	****
			Diedel3	*	****
			CG12057	*	****
			mag	*	****
			Lsp2	**	***
			CR44942	****	**
			CG9184	**	**
			CR43494	*	*
			PPO1	*	****
			CG6733	**	****
			CG16762	**	**
			CR44672	**	*
			msopa	*	***
			CG15353	***	*
			Sfp24Bb	**	*
			Sfp87B	**	*
			Nplp3	**	*
			Yp2	*	*
			EbpII	*	*

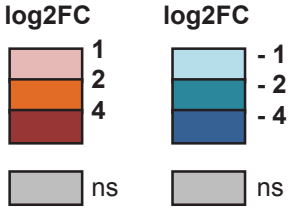

V. CONCLUDING REMARKS

Did we crack the RACK1-code?

This PhD work led to the characterization of the RACK1-dependent 5'IRES of CrPV as a class III IRES, similar to the 5'IRES of HCV. It also characterized RACK1 cofactors that may play a role in RACK1-mediated selectivity in the model organism *Drosophila melanogaster*. We uncovered the RACK1 knob region as an important region for viral IRES-dependent translation. Finally, we described a role for RACK1 in stress response and as a modulator of the expression of several genes, including genes from the *Drosophila* IMD pathway.

Overall, we made a step forward in deciphering the RACK1-code, but we still miss the mechanism by which this selectivity towards specific mRNAs is mediated. We showed that RACK1 has a dual role towards mRNA translation regulation. On one hand it favors viral IRES translation such as CrPV and HCV (Majzoub et al., 2014). On the other hand, it prevents translation of cellular AMP mRNAs (**Figure 24**). RACK1 position at the ribosome close to the mRNA exit channel opens intriguing possibilities for RACK1 as a translational selector. During scanning, the mRNA 5'UTR would come in close proximity to RACK1, and be blocked (in the case of AMPs mRNAs for instance) or not (in the case of viral IRES-dependent mRNAs). One intriguing possibility pertains to the role of the RACK1 knob in this selective translation. Indeed, we showed that the RACK1 knob is required for IRES-dependent translation of viruses, and its depletion does not impair RACK1 incorporation into the ribosome. It is tempting to speculate that this region would also play a role in the repression of AMPs translation. As mentioned above, the RACK1 knob has a high potential for PTMs. These PTMs could be different depending on the stressor (viral infection or ER stress), and lead to a switch of RACK1 from a translational enhancer to repressor respectively, possibly by the differential recruitment of proteins. This

hypothesis brings together both signaling and translation functions of RACK1, as RACK1 would be a stress sensor that impacts translation of specific mRNAs. In this regard, our RACK1 interactome study identified partners of RACK1, which did not play a role in viral translation, but which might be involved in the repression of AMPs translation (Kuhn et al., 2017). Of note, recent work assessed the ribo-interactome and revealed many ribosome-associated proteins with various functions, including viral IRES-dependent translation, RNA- and protein-modifying enzymes (Simsek et al., 2017). One intriguing possibility is that some of these interactions depend on RACK1.

Similarly, opposite outcomes regarding mRNA translation have been previously shown for the eIF3 initiation factor (Lee et al., 2015; Meyer et al., 2015). eIF3 binds to the 5'UTR of mRNAs and has opposed effects on mRNAs translation depending on the 5'UTR structure, cofactors or m^6A RNA modifications in the 5'UTR. It was shown that 12 of the 13 eIF3 subunits are recruited by the CrPV 5'IRES and that the eIF3j subunit is required for CrPV and HCV replication (Gross et al., 2017; Majzoub et al., 2014). Moreover, RACK1 associates with eIF3 subunits in yeast (Kouba et al., 2011) and is close to eIF3 in mammalian 43S pre-initiation complex (des Georges et al., 2015; Hashem et al., 2013). Thus, we can speculate that RACK1 and eIF3 act together in viral selective translation, and possibly in cellular mRNA selective translation as well.

The next step in deciphering the RACK1-code will be to identify the *cis*-acting sequences or mRNA structures that underlie this code. As RACK1 is conserved through evolution, we can suspect this RACK1-code to be conserved in mammals. It could be applied to human mRNAs in order to predict and test the effect of RACK1 targeting as an HTA. Indeed, the results presented in this manuscript show a role of RACK1 in cellular resistance to stress, and suggest an unforeseen role of RACK1 as a regulator of a pro-inflammatory pathway. This is reminiscent of the GAIT system, where expression of pro-inflammatory genes are regulated by a complex containing a ribosomal protein (RpL13/uL13) through a specific sequence in the 3'UTR (Rauscher and Ignatova, 2015).

RACK1 is stoichiometric in mESC (Shi et al., 2017), but its expression is deregulated in many cancers, including breast cancer (Collins et al., 2018). As eukaryotic cells possess between 1 and 10 million ribosomes (Shi et al., 2017), even a slight down-regulation of RACK1 expression can lead to a huge amount of

ribosomes depleted of RACK1. Thus, in the case of breast cancer, we can suspect that RACK1 down-regulation will have major impact on the cellular translatome, possibly associated with immune or pro-inflammatory genes being upregulated. A topic we did not discuss here is the extra-ribosomal activity of RPs (Warner and McIntosh, 2009). In yeast, nearly half of ASC1/RACK1 is not associated with ribosomes at the stationary phase. We suspect that the situation is different in multicellular organisms, as we never detected endogenous RACK1 in the free fractions in our polysome profiling experiments in *Drosophila*. Only when RACK1 was overexpressed did we detect a significant portion of RACK1 protein in the free fraction, which might also be the case in some cancers, such as HCC, where RACK1 expression is often up-regulated (Ruan et al., 2012). In these conditions, RACK1 might have extra-ribosomal functions, be sensed as a damage signal or bind to murine double minute 2 (MDM2) and modulate the p53 oncogene activity, like other RPs (Warner and McIntosh, 2009).

From this study, we can predict that the use of RACK1 as an HTA protein will cause side effects. In this regard, the unexpected discovery that RACK1 is a negative regulator of the expression of innate immunity genes represents an important step forward. It would thus be of the utmost interest to understand the duality of RACK1 function, in order to block its function as an activator of IRES-dependent translation, without affecting its role in the control of inflammation-like process. The RACK1-dependent genes identified in this work will provide useful tools to decipher the mechanisms by which RACK1 regulates gene expression. There is no doubt that this promiscuous little molecule will continue to raise interest in the coming years.

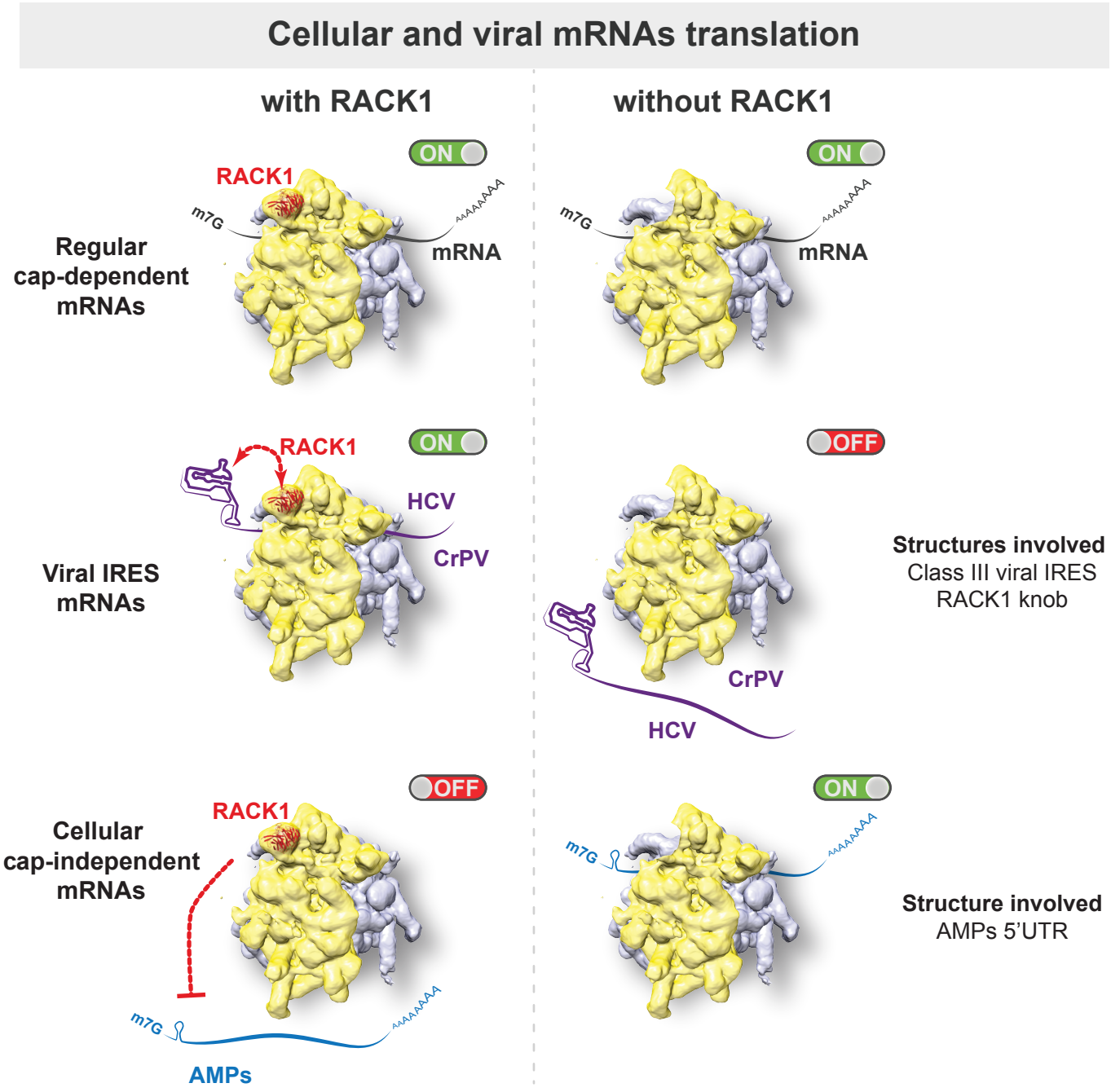

Figure 24: The dual role of RACK1 in viral and cellular mRNA translation. RACK1 has no effect on general cap-dependent translation. It favors the translation of viral IRESes such as CrPV, DCV and HCV through their 5'IRES. The knob region of RACK1 is involved in the selective translation of viruses. In the opposite, it represses cellular cap-independent translation of anti-microbial peptides (AMPs) through their 5'UTRs. Figure adapted from Majzoub *et al.*, 2014.

VI. MATERIALS & METHODS

Fly Breeding

Stocks used in the study

The Transgenic RNAi Project (TRiP) lines (shRACK1 [#34694], shmCherry [#35785], shCG18814 [#61975] and shCyp18a1 [#64923]) were obtained from the Bloomington Drosophila stock center, as well as the nanosCas9 (#54591) line. The drivers used were Actin5C-Gal4/CyO; Tub-Gal80^{TS}/Tub-Gal80^{TS}. Transgenic lines for expression of HA-RACK1 WT, modified versions of RACK1 or sgRNAs were inserted at attP2 sites (68A4 on 3L) (BestGene). *Relish^{E20}* (Hedengren et al., 1999) flies were used as mutant deficient for the IMD pathway, and were isogenized into the *w^{1118}* WT background. *w^{1118}* flies were used as controls for *Relish^{E20}* mutants. All flies used were Wolbachia-free.

Stress of flies

Males TRIP shRNA fly lines were crossed with Actin5C-Gal4/CyO, Actin5C-Gal4/CyO; Tub-Gal80^{TS}/Tub-Gal80^{TS} females and maintained at 18°C. 3 weeks later, the progeny of the desired genotype (Actin5C-Gal4/UAS-shRNA; Tub-Gal80^{TS}/3) was sorted according to wing phenotype and placed at 29°C to induce shRNA expression and subsequent knock-down. After 5 days, 10 males and 10 females from each genotype were put in tubes with Whatmann pad and 50mM sucrose solution supplemented or not with paraquat (Sigma), tunicamycin (Sigma) or DTT (Euromedex) at the indicated concentrations. 100mM sucrose solution was added daily and flies were kept at 29°C.

Cloning

sgRNA plasmid for in vivo transgenic line.

The sgRNAs were designed using the FlyRNAi website. Plasmid containing the 3 sgRNAs was generated following the protocol of Port and Bullock, 2016. Briefly, Gibson assembly was used to assemble polymerase chain reaction (PCR) products containing the sgRNAs sequences and the pCFD5 backbone plasmid.

RACK1 point mutations plasmids

Directed mutagenesis of RACK1 was performed directly on a Gateway entry plasmid containing the RACK1 sequence. DH5α bacteria were transformed using the $CaCl_2$ method (Maniatis et al., 1989) and grown in Luria Bertani (LB) medium containing 25µg/mL kanamycin. Plasmidic DNA was extracted using the IllustraTM plasmidPrep Mini Spin kit (GE Healthcare). After confirmation of the mutation by sequencing, the LR reaction was performed to transfer the RACK1 sequence into a S2 cell expression plasmid containing the actin promoter and a HA tag sequence or FLAG tag sequence either in N-terminal or C-terminal of the protein. LR reaction was also performed to transfer the RACK1 sequence into a fly expressing plasmid containing attR recombination sites, hsp70 promoter and a FLAG tag sequence in N-terminal of the protein. DH5α bacteria were transformed again and grown in LB containing 0.1mg/mL ampicillin. Plasmidic DNA was extracted using the QiaFilter Plasmid Midi kit (Qiagen) and correct insertion of the construct was checked by digestion with the restriction enzyme BamHI (Invitrogen).

Generation of 5'UTR candidates luciferase reporters

Sequences of 5'UTRs were downloaded from Flybase website. PCR amplification of 5'UTRs was performed using wild-type flies (Canton S) genomic DNA (for 5'UTRs without introns) or S2 cells cDNA (for 5'UTRs with introns) For Pirk-RB 5'UTR, the dsDNA was ordered from Intergrated DNA technologies website (gBlock). In parallel, luciferase (Firefly and Renilla) sequence was amplified from a luciferase-coding plasmid. PCR products were purified using QIAquick PCR purification kit (Qiagen) according to manufacturer's instructions. PCR primers were designed with the help of *nebuilder.neb.com* website. The pBluescript KS(-)plasmid (Agilent #212208) containing T7 promoter site was linearized using EcoICRI enzyme. Digested plasmid was purified by phenol/chloroform extraction. NEBuilder HIFI DNA assembly (NEB) was performed following manufacturer's instructions, allowing the assembly of backbone plasmid, candidate 5'UTR and Luciferase coding sequence. The obtained plasmids were digested with HincII enzyme to check for correct assembly and sequenced. All plasmids were linearized with SalI enzyme, which cuts 76nt after the STOP codon. Viral IRES DNA template was obtained by PCR amplification of plasmid vectors with primers containing the T7 promoter. Linearized DNA and PCR products were purified by phenol/chloroform method.

Functionally capped mRNAs were synthesized using HiScribe™ T7 ARCA mRNA Kit with tailing (NEB) following manufacturer's instructions. Viral IRES

constructs were in vitro transcribed using T7 HiScribe T7 High yield RNA synthesis kit (NEB) and capped with a non-functional G(5')ppp(5')A cap structure analog (NEB). After LiCl purification, mRNA integrity was checked on a TBE-Urea gel and quantified on Nanodrop One (Thermo).

dsRNA synthesis and purification

PCR amplification of S2 cells cDNA was performed followed by PCR purification using QIAquick PCR purification kit (Qiagen) according to manufacturer's instructions. *In vitro* transcription reaction was performed with the T7 Megascript kit (Thermo). After overnight incubation at 37°C, the reaction was stopped with 0.5M ammonium acetate. RNAs were extracted by adding an equal volume of phenol/chloroform (1:1). After centrifugation, the top aqueous phase was transferred to a new tube and dsRNAs were precipitated by adding isopropanol. After centrifugation, the pellet was washed with 70% ethanol, dried, and resuspended in water. dsRNAs were incubated at 65°C for 30 minutes and cooled down slowly at room temperature prior to quantification (Nanodrop One, Thermo).

Cell culture

Maintenance of S2, S2_shRACK1 and Hap1 cell lines

Schneider 2 (S2) cells were grown in Schneider medium (Biowest) complemented with 10% fetal bovine serum, 2mM glutamax, 100U/mL penicillin and 100µg/mL streptomycine (Life technologies). S2_shRACK1 cells are stably transfected under puromycin selection (1µg/mL) with a small hairpin RNA targetting the 5'UTR of RACK1 mRNA (shRACK1), expressed under the control of the metallothionein promoter. Treatment with 0.5mM $CuSO_4$ induces expression of the shRACK1 and efficient knock-down (KD) of RACK1 after five days (Majzoub et al., 2014).

Hap1 cells, and its derivatives RACK1 KO E3A5 (exon 3 sgRNA), RACK1 KO E3A6 (exon 3 sgRNA) and RACK1 WT rescue E2C5 (exon2 sgRNA expressing WT RACK1) were kindly provided by Gabriele Fuchs, University of Albany, USA. These cells were grown in Iscove's Modified Dulbecco's Media (IMDM) medium (Gibco) complemented with 10% fetal bovine serum, 2mM glutamax, 100U/mL penicilline and 100µg/mL streptomycine (Life technologies).

Cell stress

Five days after treatment with 0.5mM $CuSO_4$, 100 000 S2 and S2_shRACK1 cells per well were seeded into 96 well plate. Culture media was then replaced by Schneider medium containing $CuSO_4$, and H_2O_2 or DTT at the indicated concentrations. One hour after the stress, the medium was replaced by normal Schneider medium supplemented with $CuSO_4$.

For human cells, 25 000 Hap1 and WT rescue cells or 50 000 RACK1 KO E3A5 and E3A6 cells per well were seeded in 96 well plate. One or two days later, the medium was removed and replaced by IMDM medium containing the indicated concentration of H_2O_2 or DTT. One hour later, the culture medium was replaced.

Cell viability was assessed every day using Trypan blue (Invitrogen) and automatic cell count was performed using the Countess (Thermo).

DNA plasmids and dsRNA transfections

Plasmids coding for the Firefly luciferase under the control of the 5'IRES of CrPV as well as the actin-Renilla plasmid used are described in Majzoub *et al*., 2014. Plasmids coding for the Mtk (1528 nucleotides upstream of the AUG) and DptA (2204 nucleotides upstream of the 5'UTR and the 13 first nucleotides of the 5'UTR) promoters were derived from the pGL3 plasmid (Promega). For DptA-promoter plasmid expression, 10^{-6}M ecdysone (Sigma) was added 24 hours prior to cell collection and subsequent analysis.

Plasmid transfection was performed using the Effectene kit (Qiagen) following manufacturer's instructions on wells containing 100 000 cells (100ng DNA transfected) in 96 well plate or 500 000 (500ng DNA transfected) in 24 well plate. Alternatively, the calcium phosphate technique was used (Maniatis et al., 1989). Further analyses were performed 48 hours after transfection.

For infections, DCV and CrPV was used at a multiplicity of infection of 1 and 0.1 respectively for 16 hours and viral load was followed by qPCR.

For luciferase assay, cells were lysed and the luciferase activity was monitored according to the Dual-Luciferase® Reporter Assay kit (Promega).

mRNA Transfection in S2 cells

S2 and S2_shRACK1 cells were grown on medium containing 0.5mM $CuSO_4$ for five days. 50 000 cells per well were seeded in Schneider medium without serum complemented with $CuSO_4$. Two hours later, cells were transfected using 2µL

Lipofectamine messengerMax (Thermo) and 500ng mRNA per well, mixed in Schneider medium without serum. Two hours later, complete medium was added to the cells. Subsequent analysis by luciferase measurement was performed 24 hours later following the Dual-Luciferase® Reporter Assay kit (Promega) instructions.

dsRNA soaking in S2 cells

For dsRNA treatment, 50 000 cells were seeded in 24-well plate in 250µL serum-free media and incubated with 6µg dsRNA for 4 hours. Complete medium was the added. Five days later, cells were stimulated with heat-killed *E. coli* for 1, 2 or 4 hours.

Western blot

Protein lysates were run on 4-12% acrylamide gels (Biorad). Semi-dry transfert to nitrocellulose membrane was performed with Biorad TransBlot Turbo machine. Membranes were blocked with 5% non-fat dry milk in Tris-buffered saline (TBS)-Tween 0.05% one hour at room temperature (RT) and incubated overnight at 4°C with primary antibody in non-fat dry milk 2% TBS-Tween 0.05%. After washing, the secondary anti-Rabbit or anti-Mouse antibody fused to horseradish peroxidase (Abcam) was added to the membrane in non-fat dry milk 2% TBS-Tween 0.05% for one hour at RT. Membranes were washed and revealed with the enhanced chemiluminescence reagent (GE Healthcare).

Antibodies used and dilutions

Target	Reference	Origin	Dilution
hRACK1	Cell signaling technologies (D59D5)	Rabbit	1/1000
dRACK1	kindly provided by Berckerle lab	Rabbit	1/5000
Tubulin	Abcam (ab7291)	Mouse	1/5000
RpL10A	Abcam (ab55544)	Mouse	1/5000
RpS15	Abcam (ab157193)	Rabbit	1/10 000
Rabbit-HRP	Amersham (NA934)	Horse	1/10 000
Mouse-HRP	Amersham (NA931)	Sheep	1/10 000
Actin	Millipore (#MAB1501R)	Mouse	1/5000
FLAG tag	Sigma (F3165)	Mouse	1/5000
HA tag	Abcam (ab9110)	Rabbit	1/5000
HA-Peroxidase	Roche (3F10)	Rat	50U/mL

RNA extraction and quantitative RT-PCR

For infected cells, cell lysis, retrotranscription (RT) and quantitative PCR (qPCR) analysis were performed using the Cell-To-Ct kit (Ambion). Cells were washed in phosphate buffered saline, lysed in lysis buffer supplied by the manufacturer in the presence of DNAse I. Reverse transcription was performed on the lysate in SYBR RT buffer using the RT enzyme mix. Quantitative PCR was done using the SYBR Green power master mix and 0.5mM of forward and reverse primers.

10^6 cells or 6 flies per tube were lysed in 200µL or 350µL TRIzol RT (MRC) respectively together with 1/20 volume of Bromoanisole (MRC) added. After centrifugation, the top aqueous phase was recovered and precipitated with isopropanol. The pellet was washed with 70% ethanol, dried and resuspended in water. 1µg of RNA was used to perform reverse transcription with iScript cDNA synthesis kit (BioRad) or iScript gDNAclear cDNA synthesis kit (BioRad) following manufacturer's instructions. Quantitative PCR was done using the SYBR Green master mix (BioRad) and 0.5mM of forward and reverse primers. The qPCR cycle was the following: an initial denaturation of 15s at 98°C, followed by 35 cycles of 2s at 95°C and 30s at 60°C. The threshold cycle (Ct) of each sample is calculated by linear regression. Analysis is made by the ΔCt method using Rp49 as a reference gene: $2^{Ct(Rp49) - Ct(target)}$.

In vivo polysome profiling and bioinformatic analysis

Polysome profiling

100 Drosophila (50 males and 50 females) were collected in a tube and flash-frozen in liquid nitrogen. Lysis buffer containing 25mM Tris-HCl, 50 mM KCl, 5mM $MgCl_2$, 0.1% Triton X-100, 1mM dithiothreitol, 100µg/ml cycloheximide, protease inhibitor (Sigma) and 1U/µL RNAsin (Promega), adjusted at pH 7.4 was added and flies were smashed using Precellys Evolution and Cryolys (Bertin). Lysates were cleared by centrifugation several times for 10 minutes at 14 000 rpm at 4°C. After centrifugation, lysates were collected and put into 7%–47% sucrose gradients containing 25mM Tris-HCl pH7.4, 50mM KCl, 5mM $MgCl_2$, and 1mM dithiothreitol. Gradients and lysates were ultracentrifuged in a SW41 rotor for 2h30 at 37,000 rpm and fractions were collected and monitored using BioRad Econo UV monitor.

RNA purification and sequencing

Each selected sucrose fraction was incubated at 50°C for 30 minutes with 0.5% SDS and 200µg/mL proteinase K. RNAs were then extracted by adding an equal volume of TRIzol (Thermo) to the fractions. After 5 minutes incubation at room temperature, 200µL of chloroform per mL of TRIzol were added. After centrifugation, the top aqueous phase was collected and RNAs were precipitated by adding isopropanol and 20µg glycogen for pellet visualization. After centrifugation, pellets were washed in 70% ethanol, dried, dissolved in nuclease-free water and quantified by Nanodrop One (Thermo). To remove any phenol contamination, RNAs from sucrose samples were clean using NucAway kit (Thermo), following manufacturer's instructions. RNA integrity was subsequently checked for integrity by Bioanalyzer (Genomics agilent) and sent for sequencing at IGBMC sequencing platform (Strasbourg). There, 400ng (input, polysomes and free samples) or 1µg (monosomes) of RNA was used for library preparation with TruSeq Stranded mRNA Sample Preparation Kit (Illumina, Part Number RS-122-2101). Briefly, following purification with poly-T oligo attached magnetic beads, the mRNA was fragmented using divalent cations at 94°C for 2 minutes. The cleaved RNA fragments were copied into first strand cDNA using reverse transcriptase and random primers. Strand specificity was achieved by replacing dTTP with dUTP during second strand cDNA synthesis using DNA Polymerase I and RNase H. Following addition of a single 'A' base and subsequent ligation of the adapter on double stranded cDNA fragments, the products were purified and enriched with PCR (30 sec at 98°C; [10 sec at 98°C, 30 sec at 60°C, 30 sec at 72°C] x 12 cycles; 5 min at 72°C) to create the cDNA library. Surplus PCR primers were further removed by purification using AMPure XP beads (Beckman Coulter) and the final cDNA libraries were checked for quality and quantified using capillary electrophoresis. Libraries were sequenced in Illumina Hiseq 4000 and image analysis and base calling were performed using RTA 2.7.3 and bcl2fastq 2.17.1.14. Venn diagrams were generated using the jVenn Plug-in (Bardou et al., 2014). Gene ontology (GO) enrichment analysis was performed using PANTHER version 14.1 released 2019-03-12.

Protein purification

Proteins were purified directly from sucrose fractions by adding trichloroacetic acid up to 25% volume. After 30 minutes of precipitation, precipitates were centrifuged 15 minutes at 14 000 rpm at 4°C. Pellets were washed with 5mM HCl in acetone, then with pure acetone. Pellets were dried at RT and dissolved in protein

loading buffer containing NuPage LDS sample buffer (Thermo) and Reducing agent (Thermo) and boiled for 5 minutes at 95°C for subsequent analysis by western blot.

List of primers used, in 5'-3' orientation

Genotyping RACK1 (CRISPR/Cas9)

RACK1	Fw	CAAGATGTCCGAGACCCTGC
	Rv	GACGCCCGTTACAAAGGTCAG

Quantitative PCR

DCV	Fw	TCATCGGTATGCACATTGCT
	Rv	CGCATAACCATGCTCTTCTG
CrPV	Fw	GCTGAAACGTTCAACGCATA
	Rv	CCACTTGCTCCATTTGGTTT
DptA	Fw	GCGCAATCGCTTCTACTTTG
	Rv	CCTGAAGATTGAGTGGGTACTG
PGRP-SB1	Fw	AATCGCAAGAGCATTGGCATCGTC
	Rv	TTAGATCCTTGGCGTTCTGGAGCA
AttA	Fw	CTGGTCATGGTGCCTCTTT
	Rv	AGACCTTGGCATCCAGATTG
CecC	Fw	AAGCCGGTTGGCTGAAGAAACTTG
	Rv	GTTGCGCAATTCCCAGTCCTTGAA
edin	Fw	TCCTGCTGTCTGGTGACAAT
	Rv	CTGGAACTCCTCGGGATATG
Mtk	Fw	GCAACTTAATCTTGGAGCGATTT
	Rv	GGTCTTGGTTGGTTAGGATTGA
RACK1	Fw	AGACCCTGATCGTGTGGAAG
	Rv	TAGAGACGCTTCTGGGGGTA
imd	Fw	TCAGCGACCCAAACTACAATTC
	Rv	TTGTCTGGACGTTACTGAGAGT
RP49	Fw	GCCGCTTCAAGGGACAGTATCT
	Rv	AAACGCGGTTCTGCATGAG
Ird5	Fw	TTGCAGATGTTGATGTCAGCC
	Rv	CCTTTCTGCCTCTTCGATAGC
Relish	Fw	CCACCAATATGCCATTGTGTGCCA
	Rv	TTCCTCGACACAATTACGCTCCGT

Primers for dsRNA templates

RACK1	Fw	TAATACGACTCACTATAGGGAAGACCATCAAGCTGTGGAA
	Rv	TAATACGACTCACTATAGGGGCTCCTCAACGGTCTTCTTG
GFP	Fw	TAATACGACTCACTATAGGGAGACCTGAAGTTCATCTGCACCA

	Rv	TAATACGACTCACTATAGGGAAGTGGTTGTGGCGGATCTTGAAGT
Ird5 (1)	Fw	TAATACGACTCACTATAGGGACTGGAATGGACGAAAAGGAACTGT
	Rv	TAATACGACTCACTATAGGGCTTGTTAGCTGATCATAGGCAAAGG
Ird5 (2)	Fw	TAATACGACTCACTATAGGGCAAGCAAAGATTCCGTCCCGC
	Rv	TAATACGACTCACTATAGGGCCTCGCCCTCGTTATATAACTTG
Relish (1)	Fw	TAATACGACTCACTATAGGGCGCAAACTTATCGAGCACAAC
	Rv	TAATACGACTCACTATAGGGACCTGTATCGTCTGGATGGCC
Relish (2)	Fw	TAATACGACTCACTATAGGGCGGCGTTGCTAATGTCACCAG
	Rv	TAATACGACTCACTATAGGGAGGTTTTGGGCGTCCGCTTC

sgRNA cloning in pCFD5

PCR1	Fw	gcggcccgggttcgattcccggccgatgcaCCGACAACACCATCCGCGTCTGG GTTTTAGAGCTAGAAATAGCAAG
	Rv	CCGATAACCGTCAGATCGTGTCCTGCACCAGCCGGGAATCGAACCC
PCR2	Fw	GGACACGATCTGACGGTTATCGGGTTTTAGAGCTAGAAATAGCAAG
	Rv	attttaacttgctatttctagctctaaaacCCACCCGTCGCTTCGAGGGACAC TGCACCAGCCGGGAATCGAACCC

UNDERLINED : sgRNA guides
lowercase: Gibson homology sequence
UPPERCASE: gRNA core

RACK1 mutagenesis

R36D-K38E	Fw	CCATAATTTCGGCCTCCGATGACGAGACCCTGATCGTGTGG
	Rv	CCACACGATCAGGGTCTCGTCATCGGAGGCCGAAATTATGG
D108Y	Fw	CTTCGAGGGACACACTAAGTATGTTTTGTCGGTTGCCTTCT
	Rv	AGAAGGCAACCGACAAAACATACTTAGTGTGTCCCTCGAAG
T51A	Fw	CTGACCCGCGACGAGGACGCCAACTACGGCTACC
	Rv	GGTAGCCGTAGTTGGCGTCCTCGTCGCGGGTCAG
Y53F	Fw	CGACGAGGACACCAACTTCGGCTACCC
	Rv	GGGTAGCCGAAGTTGGTGTCCTCGTCG
Y303F	Fw	CTGTTCGCCGGCTTCTCCGACAACACC
	Rv	GGTGTTGTCGGAGAAGCCGGCGAACAG
Y247F	Fw	CGCCCAACCGCTTCTGGCTGTGCGT
	Rv	ACGCACAGCCAGAAGCGGTTGGGCG
Y229F	Fw	GACGGCAAGAACCTGTTCACTCTGGAGCACAAC
	Rv	GTTGTGCTCCAGAGTGAACAGGTTCTTGCCGTC
T279A	Fw	CCGAGGTCGTTTCGCCCGCGTCGAAGGCCGATCAG
	Rv	CTGATCGGCCTTCGACGCGGGCGAAACGACCTCGG
T279E	Fw	GCCCCGAGGTCGTTTCGCCCGAGTCGAAGGCCGATCAGCC
	Rv	GGCTGATCGGCCTTCGACTCGGGCGAAACGACCTCGGGGC
SPTS-EPEE	Fw	GAGCTGCGCCCCGAGGTCGTTGAGCCCGAGGAGAAGGCCGATCAGCCCC AGTG
	Rv	CACTGGGGCTGATCGGCCTTCTCCTCGGGCTCAACGACCTCGGGGCGCA GCTC
S280A	Fw	GAGGTCGTTTCGCCCACGGCGAAGGCCGATCAGCC

	Rv	GGCTGATCGGCCTTCGCCGTGGGCGAAACGACCTC
K281A	Fw	TTCGCCCACGTCGGCGGCCGATCAGCCC
	Rv	GGGCTGATCGGCCGCCGACGTGGGCGAA
D283A	Fw	GCCCACGTCGAAGGCCGCTCAGCCCCAGTGCCTG
	Rv	CAGGCACTGGGGCTGAGCGGCCTTCGACGTGGGC
Δknob	Fw	CTGCGCCCCGAGCAGCCCCAGTGC
	Rv	GCACTGGGGCTGCTCGGGGCGCAG

Generation of CrPV mRNA reporters

whole IRES	Fw	CAACAAATATTAATACGACTCACTATAGTTTAATAAGTGTTGTGCAG
	Rv	CTTATCATGTCTGCTCGAAG
minimal IRES	Fw	CAACAAATATTAATACGACTCACTATAGTTCGATACCAAGAGCTGGTG
	Rv	CTTATCATGTCTGCTCGAAG
IGR IRES	Fw	CAACAAATATTAATACGACTCACTATAGGCAAAAATGTGATCTTGCTTG
	Rv	CTTATCATGTCTGCTCGAAG

Generation of 5'UTR mRNA reporters

Pirk-RA-FF Luc	Fw	CACTATAGGGCGAATTGGAGGTTCAATAGCCAAAGTGC	Pirk-RA_5'UTR
	Rv	CTTCGGCCATTTTGGTGTGAATTACCGC	Pirk-RA_5'UTR
	Fw	TCACACCAAAATGGCCGAAGACGCCAAAAAC	Pirk-RA Luc
	Rv	CGGCCGCCACCGCGGTGGAGCAATTTGGACTTTCCGCCC	Bluescript-Luc
Pirk-RB-FF Luc	x	ordered from gBlock (IDT)	Pirk-RB 5'UTR
	Fw	TCACACCAAAATGGCCGAAGACGCCAAAAAC	Pirk-RB Luc
	Rv	CGGCCGCCACCGCGGTGGAGCAATTTGGACTTTCCGCCC	Bluescript-Luc
AttC-FF Luc	Fw	CACTATAGGGCGAATTGGAGATCGTCAGTCAACAGTCAG	AttC_5'UTR
	Rv	CTTCGGCCATCTTGCTGTATTAATCTCTTGATTTTC	AttC_5'UTR
	Fw	ATACAGCAAGATGGCCGAAGACGCCAAAAAC	AttC Luc
	Rv	CGGCCGCCACCGCGGTGGAGCAATTTGGACTTTCCGCCC	Bluescript-Luc
CecB-FF Luc	Fw	CACTATAGGGCGAATTGGAGCATCAGTCGCACAGTTCTC	CecB_5'UTR
	Rv	CTTCGGCCATGACGAGATTGTTGGCTTAC	CecB_5'UTR
	Fw	CAATCTCGTCATGGCCGAAGACGCCAAAAAC	CecB Luc
	Rv	CGGCCGCCACCGCGGTGGAGCAATTTGGACTTTCCGCCC	Bluescript-Luc
DptA-FF Luc	Fw	CACTATAGGGCGAATTGGAGGTATCAGTCAGCATATTCC	DptA_5'UTR
	Rv	CTTCGGCCATCTCAGTTGTTCTCAATTGAAG	DptA_5'UTR
	Fw	AACAACTGAGATGGCCGAAGACGCCAAAAAC	DptA Luc
	Rv	CGGCCGCCACCGCGGTGGAGCAATTTGGACTTTCCGCCC	Bluescript-Luc
CecA1-FF Luc	Fw	CACTATAGGGCGAATTGGAGCATCAGTCGCTCAGACCTC	CecA1_5'UTR
	Rv	CTTCGGCCATGGTGATATTTTCTTGATTTTTTCTTAGG	CecA1_5'UTR
	Fw	AAATATCACCATGGCCGAAGACGCCAAAAAC	CecA1 FFLuc
	Rv	CGGCCGCCACCGCGGTGGAGCAATTTGGACTTTCCGCCC	Bluescript-Luc
Cyp18a1-RA-FF Luc	Fw	CACTATAGGGCGAATTGGAGCGAGCCATTAGTCGAAAACTATAAACG	Cyp18a1-RA_5'UTR
	Rv	CTTCGGCCATGGCGGTGTAGCTGTAGCTG	Cyp18a1_5'UTR
	Fw	CTACACCGCCATGGCCGAAGACGCCAAAAAC	Cyp18a1 Luc
	Rv	CGGCCGCCACCGCGGTGGAGCAATTTGGACTTTCCGCCC	Bluescript-Luc

Cyp18a 1-RB-FF Luc	Fw	CACTATAGGGCGAATTGGAGTGCAGAGCTGCAGAGCTG	Cyp18a1-RB_5'UTR
	Rv	CTTCGGCCATGGCGGTGTAGCTGTAGCTG	Cyp18a1_5'UTR
	Fw	CTACACCGCCATGGCCGAAGACGCCAAAAAC	Cyp18a1 Luc
	Rv	CGGCCGCCACCGCGGTGGAGCAATTTGGACTTTCCGCCC	Bluescript-Luc
TRAF6-FF Luc	Fw	CACTATAGGGCGAATTGGAGCCAGTGTTGCACAATCCTCG	TRAF6_5'UTR
	Rv	CTTCGGCCATCTTGGCTGCTCCTCTGGC	TRAF6_5'UTR
	Fw	AGCAGCCAAGATGGCCGAAGACGCCAAAAAC	TRAF6 Luc
	Rv	CGGCCGCCACCGCGGTGGAGCAATTTGGACTTTCCGCCC	Bluescript-Luc
actin42a-FF Luc	Fw	CACTATAGGGCGAATTGGAGCCACTTTAACTCGAAAAAG	Act42A_5'UTR
	Rv	CTTCGGCCATTTTGTAGAAATTTTATTTGGATCTTTTATG	Act42A_5'UTR
	Fw	TTTCTACAAAATGGCCGAAGACGCCAAAAAC	Act42A Luc
	Rv	CGGCCGCCACCGCGGTGGAGCAATTTGGACTTTCCGCCC	Bluescript-Luc
actin42a-Rluc	Fw	CACTATAGGGCGAATTGGAGCCACTTTAACTCGAAAAAG	Act42A_5'UTR
	Rv	GAAAAGACATTTTGTAGAAATTTTATTTGGATCTTTTATG	Act42A_5'UTR
	Fw	TTTCTACAAAATGTCTTTTCAACAAACAAAC	Act42A RenLuc
	Rv	CGGCCGCCACCGCGGTGGAGTTATTGTTCATTTTTGAGAACTC	Bluescript RenLuc

VII. BIBLIOGRAPHY

Adams, D.R., Ron, D., and Kiely, P.A. (2011). RACK1, A multifaceted scaffolding protein: Structure and function. Cell Commun. Signal. *9*, 22.

Adivarahan, S., Livingston, N., Nicholson, B., Rahman, S., Wu, B., Rissland, O.S., and Zenklusen, D. (2018). Spatial Organization of Single mRNPs at Different Stages of the Gene Expression Pathway. Mol. Cell *72*, 727–738.e5.

Anders, M., Chelysheva, I., Goebel, I., Trenkner, T., Zhou, J., Mao, Y., Verzini, S., Qian, S.-B., and Ignatova, Z. (2018). Dynamic m6A methylation facilitates mRNA triaging to stress granules. Life Sci. Alliance *1*, e201800113.

Anger, A.M., Armache, J.-P., Berninghausen, O., Habeck, M., Subklewe, M., Wilson, D.N., and Beckmann, R. (2013). Structures of the human and Drosophila 80S ribosome. Nature *497*, 80.

Arimoto, K., Fukuda, H., Imajoh-Ohmi, S., Saito, H., and Takekawa, M. (2008). Formation of stress granules inhibits apoptosis by suppressing stress-responsive MAPK pathways. Nat. Cell Biol. *10*, 1324–1332.

Armistead, J., and Triggs-Raine, B. (2014). Diverse diseases from a ubiquitous process: The ribosomopathy paradox. FEBS Lett. *588*, 1491–1500.

Ban, N., Beckmann, R., Cate, J.H.D., Dinman, J.D., Dragon, F., Ellis, S.R., Lafontaine, D.L.J., Lindahl, L., Liljas, A., Lipton, J.M., et al. (2014). A new system for naming ribosomal proteins. Curr. Opin. Struct. Biol. *24*, 165–169.

Bardou, P., Mariette, J., Escudié, F., Djemiel, C., and Klopp, C. (2014). jvenn: an interactive Venn diagram viewer. BMC Bioinformatics *15*, 293.

Bévort, M., and Leffers, H. (2000). Down regulation of ribosomal protein mRNAs during neuronal differentiation of human NTERA2 cells. Differentiation *66*, 81–92.

Bhatt, A.P., Wong, J.P., Weinberg, M.S., Host, K.M., Giffin, L.C., Buijnink, J., van Dijk, E., Izumiya, Y., Kung, H., Temple, B.R.S., et al. (2016). A viral kinase mimics S6 kinase to enhance cell proliferation. Proc. Natl. Acad. Sci. *113*, 7876.

Bloomington Drosophila Stock Center An Introduction to Balancers.

Bou-Nader, C., Gordon, J.M., Henderson, F.E., and Zhang, J. (2019). The search for a PKR code — Differential regulation of Protein Kinase R activity by diverse RNA and protein regulators. RNA.

Brandman, O., and Hegde, R.S. (2016). Ribosome-associated protein quality control. Nat. Struct. Mol. Biol. *23*, 7–15.

Brina, D., Miluzio, A., Ricciardi, S., and Biffo, S. (2015). eIF6 anti-association activity is required for ribosome biogenesis, translational control and tumor progression. Transl. Cancer *1849*, 830–835.

Broderick, N.A., and Lemaitre, B. (2012). Gut-associated microbes of Drosophila melanogaster. Gut Microbes *3*, 307–321.

Ceci, M., Gaviraghi, C., Gorrini, C., Sala, L.A., Offenhäuser, N., Marchisio, P.C., and Biffo, S. (2003). Release of eIF6 (p27BBP) from the 60S subunit allows 80S ribosome assembly. Nature *426*, 579–584.

Celniker, S.E., and Rubin, G.M. (2003). The Drosophila Melanogaster Genome. Annu. Rev. Genomics Hum. Genet. *4*, 89–117.

Chang, Y., and Huh, W.-K. (2018). Ksp1-dependent phosphorylation of eIF4G modulates post-transcriptional regulation of specific mRNAs under glucose deprivation conditions. Nucleic Acids Res. *46*, 3047–3060.

Chang, B.Y., Chiang, M., and Cartwright, C.A. (2001). The Interaction of Src and RACK1 Is Enhanced by Activation of Protein Kinase C and Tyrosine Phosphorylation of RACK1. J. Biol. Chem. *276*, 20346–20356.

Chaudhuri, S., Vyas, K., Kapasi, P., Komar, A.A., Dinman, J.D., Barik, S., and Mazumder, B. (2007). Human ribosomal protein L13a is dispensable for canonical ribosome function but indispensable for efficient rRNA methylation. RNA *13*, 2224–2237.

Chou, A., Krukowski, K., Jopson, T., Zhu, P.J., Costa-Mattioli, M., Walter, P., and Rosi, S. (2017). Inhibition of the integrated stress response reverses cognitive deficits after traumatic brain injury. Proc. Natl. Acad. Sci. *114*, E6420.

Colina, R., Costa-Mattioli, M., Dowling, R.J.O., Jaramillo, M., Tai, L.-H., Breitbach, C.J., Martineau, Y., Larsson, O., Rong, L., Svitkin, Y.V., et al. (2008). Translational control of the innate immune response through IRF-7. Nature *452*, 323.

Collins, J.C., Ghalei, H., Doherty, J.R., Huang, H., Culver, R.N., and Karbstein, K. (2018). Ribosome biogenesis factor Ltv1 chaperones the assembly of the small subunit head. J. Cell Biol. *217*, 4141.

Corbett, A.H. (2018). Post-transcriptional regulation of gene expression and human disease. Cell Nucl. *52*, 96–104.

Coyle, S.M., Gilbert, W.V., and Doudna, J.A. (2009). Direct link between RACK1 function and localization at the ribosome in vivo. Mol. Cell. Biol. *29*, 1626–1634.

Dandekar, A., Mendez, R., and Zhang, K. (2015). Cross Talk Between ER Stress, Oxidative Stress, and Inflammation in Health and Disease. In Stress Responses: Methods and Protocols, C.M. Oslowski, ed. (New York, NY: Springer New York), pp. 205–214.

Darmanis, S., Gallant, C.J., Marinescu, V.D., Niklasson, M., Segerman, A., Flamourakis, G., Fredriksson, S., Assarsson, E., Lundberg, M., Nelander, S., et al. (2016). Simultaneous Multiplexed Measurement of RNA and Proteins in Single Cells. Cell Rep. *14*, 380–389.

De Gregorio, E., Spellman, P.T., Tzou, P., Rubin, G.M., and Lemaitre, B. (2002). The Toll and Imd pathways are the major regulators of the immune response in Drosophila. EMBO J. *21*, 2568–2579.

Diaz de Arce, A.J., Noderer, W.L., and Wang, C.L. (2017). Complete motif analysis of sequence requirements for translation initiation at non-AUG start codons. Nucleic Acids Res. *46*, 985–994.

Dinman, J.D. (2016). Pathways to Specialized Ribosomes: The Brussels Lecture. J. Mol. Biol. *428*, 2186–2194.

Dobrikov, M.I., Dobrikova, E.Y., and Gromeier, M. (2018a). Ribosomal RACK1:Protein Kinase C βII Phosphorylates Eukaryotic Initiation Factor 4G1 at S1093 To Modulate Cap-Dependent and -Independent Translation Initiation. Mol. Cell. Biol. *38*, e00304-18.

Dobrikov, M.I., Dobrikova, E.Y., and Gromeier, M. (2018b). Ribosomal RACK1:Protein Kinase C βII Modulates Intramolecular Interactions between Unstructured Regions of Eukaryotic Initiation Factor 4G (eIF4G) That Control eIF4E and eIF3 Binding. Mol. Cell. Biol. *38*, e00306-18.

Dowling, R.J.O., Topisirovic, I., Alain, T., Bidinosti, M., Fonseca, B.D., Petroulakis, E., Wang, X., Larsson, O., Selvaraj, A., Liu, Y., et al. (2010). mTORC1-Mediated Cell Proliferation, But Not Cell Growth, Controlled by the 4E-BPs. Science *328*, 1172.

Dresios, J., Panopoulos, P., and Synetos, D. (2006). Eukaryotic ribosomal proteins lacking a eubacterial counterpart: important players in ribosomal function. Mol. Microbiol. *59*, 1651–1663.

Dunn, J.G., Foo, C.K., Belletier, N.G., Gavis, E.R., and Weissman, J.S. (2013). Ribosome profiling reveals pervasive and regulated stop codon readthrough in Drosophila melanogaster. eLife *2*, e01179.

Erales, J., Marchand, V., Panthu, B., Gillot, S., Belin, S., Ghayad, S.E., Garcia, M., Laforêts, F., Marcel, V., Baudin-Baillieu, A., et al. (2017). Evidence for rRNA 2′-O-methylation plasticity: Control of intrinsic translational capabilities of human ribosomes. Proc. Natl. Acad. Sci. *114*, 12934.

Ferretti, M.B., Ghalei, H., Ward, E.A., Potts, E.L., and Karbstein, K. (2017). Rps26 directs mRNA-specific translation by recognition of Kozak sequence elements. Nat. Struct. Amp Mol. Biol. *24*, 700.

FlyBase Curators, Swiss-Prot Project Members, and InterPro Project Members (2004). Gene Ontology annotation in FlyBase through association of InterPro records with GO terms.

Frakes, A.E., and Dillin, A. (2017). The UPRER: Sensor and Coordinator of Organismal Homeostasis. Mol. Cell *66*, 761–771.

Fujii, K., Shi, Z., Zhulyn, O., Denans, N., and Barna, M. (2017). Pervasive translational regulation of the cell signalling circuitry underlies mammalian development. Nat. Commun. *8*, 14443.

Furic, L., Rong, L., Larsson, O., Koumakpayi, I.H., Yoshida, K., Brueschke, A., Petroulakis, E., Robichaud, N., Pollak, M., Gaboury, L.A., et al. (2010). eIF4E phosphorylation promotes tumorigenesis and is associated with prostate cancer progression. Proc. Natl. Acad. Sci. *107*, 14134.

Gallo, S., Ricciardi, S., Manfrini, N., Pesce, E., Oliveto, S., Calamita, P., Mancino, M., Maffioli, E., Moro, M., Crosti, M., et al. (2018). RACK1 Specifically Regulates Translation through Its Binding to Ribosomes. Mol. Cell. Biol. *38*, e00230-18.

Genuth, N.R., and Barna, M. (2018a). Heterogeneity and specialized functions of translation machinery: from genes to organisms. Nat. Rev. Genet. *19*, 431–452.

Genuth, N.R., and Barna, M. (2018b). The Discovery of Ribosome Heterogeneity and Its Implications for Gene Regulation and Organismal Life. Mol. Cell *71*, 364–374.

des Georges, A., Dhote, V., Kuhn, L., Hellen, C.U.T., Pestova, T.V., Frank, J., and Hashem, Y. (2015). Structure of mammalian eIF3 in the context of the 43S preinitiation complex. Nature *525*, 491.

Gerbasi, V.R., Weaver, C.M., Hill, S., Friedman, D.B., and Link, A.J. (2004). Yeast Asc1p and mammalian RACK1 are functionally orthologous core 40S ribosomal proteins that repress gene expression. Mol. Cell. Biol. *24*, 8276–8287.

Gibson, T.J. (2012). RACK1 research - ships passing in the night? FEBS Lett. *586*, 2787–2789.

Goldstein, D.S., and Kopin, I.J. (2007). Evolution of concepts of stress. Stress *10*, 109–120.

Gross, L., Vicens, Q., Einhorn, E., Noireterre, A., Schaeffer, L., Kuhn, L., Imler, J.-L., Eriani, G., Meignin, C., and Martin, F. (2017). The IRES 5′UTR of the dicistrovirus cricket paralysis virus is a type III IRES containing an essential pseudoknot structure. Nucleic Acids Res. *45*, 8993–9004.

Gross, L., Schaeffer, L., Alghoul, F., Hayek, H., Allmang, C., Eriani, G., and Martin, F. (2018). Tracking the m7G-cap during translation initiation by crosslinking methods. Anal. Transl. Mech. Modul. Gene Expr. *137*, 3–10.

Grosso, S., Volta, V., Sala, L.A., Vietri, M., Marchisio, P.C., Ron, D., and Biffo, S. (2008). PKCβII modulates translation independently from mTOR and through RACK1. Biochem. J. *415*, 77.

Guan, B.-J., van Hoef, V., Jobava, R., Elroy-Stein, O., Valasek, L.S., Cargnello, M., Gao, X.-H., Krokowski, D., Merrick, W.C., Kimball, S.R., et al. (2017). A Unique ISR Program Determines Cellular Responses to Chronic Stress. Mol. Cell *68*, 885–900.e6.

Guittard, E., Blais, C., Maria, A., Parvy, J.-P., Pasricha, S., Lumb, C., Lafont, R., Daborn, P.J., and Dauphin-Villemant, C. (2011). CYP18A1, a key enzyme of Drosophila steroid hormone inactivation, is essential for metamorphosis. Dev. Biol. *349*, 35–45.

Hafirassou, M.L., Meertens, L., Umaña-Diaz, C., Labeau, A., Dejarnac, O., Bonnet-Madin, L., Kümmerer, B.M., Delaugerre, C., Roingeard, P., Vidalain, P.-O., et al. (2017). A Global Interactome Map of the Dengue Virus NS1 Identifies Virus Restriction and Dependency Host Factors. Cell Rep. *21*, 3900–3913.

Halbeisen, R.E., and Gerber, A.P. (2009). Stress-dependent coordination of transcriptome and translatome in yeast. PLoS Biol. *7*, e1000105–e1000105.

Hashem, Y., des Georges, A., Dhote, V., Langlois, R., Liao, H.Y., Grassucci, R.A., Hellen, C.U.T., Pestova, T.V., and Frank, J. (2013). Structure of the mammalian ribosomal 43S preinitiation complex bound to the scanning factor DHX29. Cell *153*, 1108–1119.

Hedengren, M., BengtÅsling, Dushay, M.S., Ando, I., Ekengren, S., Wihlborg, M., and Hultmark, D. (1999). Relish, a Central Factor in the Control of Humoral but Not Cellular Immunity in Drosophila. Mol. Cell *4*, 827–837.

Hershey, J.W.B., Sonenberg, N., and Mathews, M.B. (2012). Principles of Translational Control: An Overview. Cold Spring Harb. Perspect. Biol. *4*.

Higgins, R., Gendron, J.M., Rising, L., Mak, R., Webb, K., Kaiser, S.E., Zuzow, N., Riviere, P., Yang, B., Fenech, E., et al. (2015). The Unfolded Protein Response Triggers Site-Specific Regulatory Ubiquitylation of 40S Ribosomal Proteins. Mol. Cell *59*, 35–49.

Hinnebusch, A.G., and Lorsch, J.R. (2012). The Mechanism of Eukaryotic Translation Initiation: New Insights and Challenges. Cold Spring Harb. Perspect. Biol. *4*.

Holcik, M., and Sonenberg, N. (2005). Translational control in stress and apoptosis. Nat. Rev. Mol. Cell Biol. *6*, 318.

Ikeuchi, K., and Inada, T. (2016). Ribosome-associated Asc1/RACK1 is required for endonucleolytic cleavage induced by stalled ribosome at the 3′ end of nonstop mRNA. Sci. Rep. *6*, 28234.

Imami, K., Milek, M., Bogdanow, B., Yasuda, T., Kastelic, N., Zauber, H., Ishihama, Y., Landthaler, M., and Selbach, M. (2018). Phosphorylation of the Ribosomal Protein RPL12/uL11 Affects Translation during Mitosis. Mol. Cell *72*, 84–98.e9.

Ingolia, N.T. (2014). Ribosome profiling: new views of translation, from single codons to genome scale. Nat. Rev. Genet. *15*, 205.

Jha, S., Rollins, M.G., Fuchs, G., Procter, D.J., Hall, E.A., Cozzolino, K., Sarnow, P., Savas, J.N., and Walsh, D. (2017). Trans-kingdom mimicry underlies ribosome customization by a poxvirus kinase. Nature *546*, 651–655.

Jin, H.Y., and Xiao, C. (2018). An Integrated Polysome Profiling and Ribosome Profiling Method to Investigate In Vivo Translatome. Methods Mol. Biol. Clifton NJ *1712*, 1–18.

Jovanovic, M., Rooney, M.S., Mertins, P., Przybylski, D., Chevrier, N., Satija, R., Rodriguez, E.H., Fields, A.P., Schwartz, S., Raychowdhury, R., et al. (2015). Dynamic profiling of the protein life cycle in response to pathogens. Science *347*, 1259038.

Kadrmas, J.L., Smith, M.A., Pronovost, S.M., and Beckerle, M.C. (2007). Characterization of RACK1 function in Drosophila development. Dev. Dyn. Off. Publ. Am. Assoc. Anat. *236*, 2207–2215.

Karamyshev, A.L., and Karamysheva, Z.N. (2018). Lost in Translation: Ribosome-Associated mRNA and Protein Quality Controls. Front. Genet. *9*, 431–431.

Katzenberger, R.J., Chtarbanova, S., Rimkus, S.A., Fischer, J.A., Kaur, G., Seppala, J.M., Swanson, L.C., Zajac, J.E., Ganetzky, B., and Wassarman, D.A. (2015). Death following traumatic brain injury in Drosophila is associated with intestinal barrier dysfunction. eLife *4*, e04790.

Kaufmann, S.H.E., Dorhoi, A., Hotchkiss, R.S., and Bartenschlager, R. (2017). Host-directed therapies for bacterial and viral infections. Nat. Rev. Drug Discov. *17*, 35.

Kiely, P.A., Baillie, G.S., Lynch, M.J., Houslay, M.D., and O'Connor, R. (2008). Tyrosine 302 in RACK1 Is Essential for Insulin-like Growth Factor-I-mediated Competitive Binding of PP2A and β1 Integrin and for Tumor Cell Proliferation and Migration. J. Biol. Chem. *283*, 22952–22961.

Kiely, P.A., Baillie, G.S., Barrett, R., Buckley, D.A., Adams, D.R., Houslay, M.D., and O'Connor, R. (2009). Phosphorylation of RACK1 on Tyrosine 52 by c-Abl Is Required for Insulin-like Growth Factor I-mediated Regulation of Focal Adhesion Kinase. J. Biol. Chem. *284*, 20263–20274.

Kim, M.-S., Pinto, S.M., Getnet, D., Nirujogi, R.S., Manda, S.S., Chaerkady, R., Madugundu, A.K., Kelkar, D.S., Isserlin, R., Jain, S., et al. (2014). A draft map of the human proteome. Nature *509*, 575.

Kleino, A., Myllymäki, H., Kallio, J., Vanha-aho, L.-M., Oksanen, K., Ulvila, J., Hultmark, D., Valanne, S., and Rämet, M. (2008). Pirk Is a Negative Regulator of the Drosophila Imd Pathway. J. Immunol. *180*, 5413.

Komili, S., Farny, N.G., Roth, F.P., and Silver, P.A. (2007). Functional Specificity among Ribosomal Proteins Regulates Gene Expression. Cell *131*, 557–571.

Kondrashov, N., Pusic, A., Stumpf, C.R., Shimizu, K., Hsieh, A.C., Xue, S., Ishijima, J., Shiroishi, T., and Barna, M. (2011). Ribosome-Mediated Specificity in Hox mRNA Translation and Vertebrate Tissue Patterning. Cell *145*, 383–397.

Kouba, T., Rutkai, E., Karaskova, M., and Valasek, L.S. (2011). The eIF3c/NIP1 PCI domain interacts with RNA and RACK1/ASC1 and promotes assembly of translation preinitiation complexes. Nucleic Acids Res. *40*, 2683–2699.

Kuhn, L., Majzoub, K., Einhorn, E., Chicher, J., Pompon, J., Imler, J.-L., Hammann, P., and Meignin, C. (2017). Definition of a RACK1 Interaction Network in Drosophila melanogaster Using SWATH-MS. G3 GenesGenomesGenetics.

Kuroha, K., Akamatsu, M., Dimitrova, L., Ito, T., Kato, Y., Shirahige, K., and Inada, T. (2010). Receptor for activated C kinase 1 stimulates nascent polypeptide-dependent translation arrest. EMBO Rep. *11*, 956.

Lam, Y.W., Evans, V.C., Heesom, K.J., Lamond, A.I., and Matthews, D.A. (2010). Proteomics analysis of the nucleolus in adenovirus-infected cells. Mol. Cell. Proteomics MCP *9*, 117–130.

Lamiable, O., Kellenberger, C., Kemp, C., Troxler, L., Pelte, N., Boutros, M., Marques, J.T., Daeffler, L., Hoffmann, J.A., Roussel, A., et al. (2016). Cytokine Diedel and a viral homologue suppress the IMD pathway in Drosophila. Proc. Natl. Acad. Sci. *113*, 698.

Landry, D.M., Hertz, M.I., and Thompson, S.R. (2009). RPS25 is essential for translation initiation by the Dicistroviridae and hepatitis C viral IRESs. Genes Dev. *23*, 2753–2764.

Lee, A.S.-Y., Burdeinick-Kerr, R., and Whelan, S.P.J. (2013). A ribosome-specialized translation initiation pathway is required for cap-dependent translation of vesicular stomatitis virus mRNAs. Proc. Natl. Acad. Sci. *110*, 324.

Lee, A.S.Y., Kranzusch, P.J., and Cate, J.H.D. (2015). eIF3 targets cell-proliferation messenger RNAs for translational activation or repression. Nature *522*, 111.

Lee, K.-M., Chen, C.-J., and Shih, S.-R. (2017). Regulation Mechanisms of Viral IRES-Driven Translation. Trends Microbiol. *25*, 546–561.

Li, J.-J., and Xie, D. (2015). RACK1, a versatile hub in cancer. Oncogene *34*, 1890–1898.

Li, J.J., Bickel, P.J., and Biggin, M.D. (2014). System wide analyses have underestimated protein abundances and the importance of transcription in mammals. PeerJ *2*, e270–e270.

Lin, Y.-R., Parikh, H., and Park, Y. (2018). Stress resistance and lifespan enhanced by downregulation of antimicrobial peptide genes in the Imd pathway. Aging *10*, 622–631.

Liu, Y., Beyer, A., and Aebersold, R. (2016). On the Dependency of Cellular Protein Levels on mRNA Abundance. Cell *165*, 535–550.

Long, L., Deng, Y., Yao, F., Guan, D., Feng, Y., Jiang, H., Li, X., Hu, P., Lu, X., Wang, H., et al. (2014). Recruitment of Phosphatase PP2A by RACK1 Adaptor Protein Deactivates Transcription Factor IRF3 and Limits Type I Interferon Signaling. Immunity *40*, 515–529.

Majzoub, K., Hafirassou, M.L., Meignin, C., Goto, A., Marzi, S., Fedorova, A., Verdier, Y., Vinh, J., Hoffmann, J.A., Martin, F., et al. (2014). RACK1 controls IRES-mediated translation of viruses. Cell *159*, 1086–1095.

Maniatis, T., Sambrook, J., and Fritsch, E.F. (1989). Molecular Cloning: A Laboratory Manual (Cold Spring Harbor Laboratory Press).

Martin, I., Kim, J.W., Lee, B.D., Kang, H.C., Xu, J.-C., Jia, H., Stankowski, J., Kim, M.-S., Zhong, J., Kumar, M., et al. (2014). Ribosomal Protein s15 Phosphorylation Mediates LRRK2 Neurodegeneration in Parkinson's Disease. Cell *157*, 472–485.

Martínez, A., Sesé, M., Losa, J.H., Robichaud, N., Sonenberg, N., Aasen, T., and Ramón y Cajal, S. (2015). Phosphorylation of eIF4E Confers Resistance to Cellular Stress and DNA-Damaging Agents through an Interaction with 4E-T: A Rationale for Novel Therapeutic Approaches. PLOS ONE *10*, e0123352.

Marygold, S.J., Roote, J., Reuter, G., Lambertsson, A., Ashburner, M., Millburn, G.H., Harrison, P.M., Yu, Z., Kenmochi, N., Kaufman, T.C., et al. (2007). The ribosomal protein genes and Minute loci of Drosophila melanogaster. Genome Biol. *8*, R216–R216.

Mauro, V.P., and Edelman, G.M. (2007). The Ribosome Filter Redux. Cell Cycle *6*, 2246–2251.

Mazumder, B., Sampath, P., Seshadri, V., Maitra, R.K., DiCorleto, P.E., and Fox, P.L. (2003). Regulated Release of L13a from the 60S Ribosomal Subunit as A Mechanism of Transcript-Specific Translational Control. Cell *115*, 187–198.

McCahill, A., Warwicker, J., Bolger, G.B., Houslay, M.D., and Yarwood, S.J. (2002). The RACK1 Scaffold Protein: A Dynamic Cog in Cell Response Mechanisms. Mol. Pharmacol. *62*, 1261–1273.

McCann, K.L., and Baserga, S.J. (2013). Mysterious Ribosomopathies. Science *341*, 849.

Meyer, K.D., Patil, D.P., Zhou, J., Zinoviev, A., Skabkin, M.A., Elemento, O., Pestova, T.V., Qian, S.-B., and Jaffrey, S.R. (2015). 5′ UTR m6A Promotes Cap-Independent Translation. Cell *163*, 999–1010.

Meyuhas, O. (2015). Chapter Two - Ribosomal Protein S6 Phosphorylation: Four Decades of Research. In International Review of Cell and Molecular Biology, K.W. Jeon, ed. (Academic Press), pp. 41–73.

Mills, E.W., and Green, R. (2017). Ribosomopathies: There's strength in numbers. Science *358*, eaan2755.

Mussabekova, A., Daeffler, L., and Imler, J.-L. (2017). Innate and intrinsic antiviral immunity in Drosophila. Cell. Mol. Life Sci. CMLS *74*, 2039–2054.

Myllymäki, H., Valanne, S., and Rämet, M. (2014). The Drosophila Imd Signaling Pathway. J. Immunol. *192*, 3455.

Nielsen, M.H., Flygaard, R.K., and Jenner, L.B. (2017). Structural analysis of ribosomal RACK1 and its role in translational control. Cell. Signal. *35*, 272–281.

Nilsson, J., Sengupta, J., Frank, J., and Nissen, P. (2004). Regulation of eukaryotic translation by the RACK1 protein: a platform for signalling molecules on the ribosome. EMBO Rep. *5*, 1137–1141.

Núñez, A., Franco, A., Madrid, M., Soto, T., Vicente, J., Gacto, M., and Cansado, J. (2009). Role for RACK1 orthologue Cpc2 in the modulation of stress response in fission yeast. Mol. Biol. Cell *20*, 3996–4009.

Ohn, T., Kedersha, N., Hickman, T., Tisdale, S., and Anderson, P. (2008). A functional RNAi screen links O-GlcNAc modification of ribosomal proteins to stress granule and processing body assembly. Nat. Cell Biol. *10*, 1224–1231.

Pakos-Zebrucka, K., Koryga, I., Mnich, K., Ljujic, M., Samali, A., and Gorman, A.M. (2016). The integrated stress response. EMBO Rep. *17*, 1374.

Parks, M.M., Kurylo, C.M., Dass, R.A., Bojmar, L., Lyden, D., Vincent, C.T., and Blanchard, S.C. (2018). Variant ribosomal RNA alleles are conserved and exhibit tissue-specific expression. Sci. Adv. *4*, eaao0665-eaao0665.

Piccirillo, C.A., Bjur, E., Topisirovic, I., Sonenberg, N., and Larsson, O. (2014). Translational control of immune responses: from transcripts to translatomes. Nat. Immunol. *15*, 503.

Plank, T.-D.M., and Kieft, J.S. (2012). The structures of nonprotein-coding RNAs that drive internal ribosome entry site function. Wiley Interdiscip. Rev. RNA *3*, 195–212.

Port, F., and Bullock, S.L. (2016). Augmenting CRISPR applications in Drosophila with tRNA-flanked sgRNAs. Nat. Methods *13*, 852.

Prlić, A., Bradley, A.R., Duarte, J.M., Rose, P.W., Rose, A.S., and Valasatava, Y. (2018). NGL viewer: web-based molecular graphics for large complexes. Bioinformatics *34*, 3755–3758.

Rabouw, H.H., Langereis, M.A., Knaap, R.C.M., Dalebout, T.J., Canton, J., Sola, I., Enjuanes, L., Bredenbeek, P.J., Kikkert, M., de Groot, R.J., et al. (2016). Middle East Respiratory Coronavirus Accessory Protein 4a Inhibits PKR-Mediated Antiviral Stress Responses. PLOS Pathog. *12*, e1005982.

Rachfall, N., Schmitt, K., Bandau, S., Smolinski, N., Ehrenreich, A., Valerius, O., and Braus, G.H. (2012). RACK1/Asc1p, a ribosomal node in cellular signaling. Mol. Cell. Proteomics MCP.

Ramagopal, S., and Ennis, H.L. (1981). Regulation of synthesis of cell-specific ribosomal proteins during differentiation of Dictyostelium discoideum. Proc. Natl. Acad. Sci. U. S. A. *78*, 3083–3087.

Raught, B., Peiretti, F., Gingras, A., Livingstone, M., Shahbazian, D., Mayeur, G.L., Polakiewicz, R.D., Sonenberg, N., and Hershey, J.W. (2004). Phosphorylation of eucaryotic translation initiation factor 4B Ser422 is modulated by S6 kinases. EMBO J. *23*, 1761.

Rauscher, R., and Ignatova, Z. (2015). Tuning innate immunity by translation. Biochem. Soc. Trans. *43*, 1247.

Robichaud, N., Hsu, B.E., Istomine, R., Alvarez, F., Blagih, J., Ma, E.H., Morales, S.V., Dai, D.L., Li, G., Souleimanova, M., et al. (2018). Translational control in the tumor microenvironment promotes lung metastasis: Phosphorylation of eIF4E in neutrophils. Proc. Natl. Acad. Sci. *115*, E2202.

Rodrigues, L.O.C.P., Graça, R.S.F., and Carneiro, L.A.M. (2018). Integrated Stress Responses to Bacterial Pathogenesis Patterns. Front. Immunol. *9*, 1306.

Ron, D., Chen, C.H., Caldwell, J., Jamieson, L., Orr, E., and Mochly-Rosen, D. (1994). Cloning of an intracellular receptor for protein kinase C: a homolog of the beta subunit of G proteins. Proc. Natl. Acad. Sci. U. S. A. *91*, 839–843.

Roth, H., Magg, V., Uch, F., Mutz, P., Klein, P., Haneke, K., Lohmann, V., Bartenschlager, R., Fackler, O.T., Locker, N., et al. (2017). Flavivirus Infection Uncouples Translation Suppression from Cellular Stress Responses. mBio *8*, e02150-16.

Roundtree, I.A., Evans, M.E., Pan, T., and He, C. (2017). Dynamic RNA Modifications in Gene Expression Regulation. Cell *169*, 1187–1200.

Ruan, Y., Sun, L., Hao, Y., Wang, L., Xu, J., Zhang, W., Xie, J., Guo, L., Zhou, L., Yun, X., et al. (2012). Ribosomal RACK1 promotes chemoresistance and growth in human hepatocellular carcinoma. J. Clin. Invest. *122*, 2554–2566.

Rubio, C.A., Weisburd, B., Holderfield, M., Arias, C., Fang, E., DeRisi, J.L., and Fanidi, A. (2014). Transcriptome-wide characterization of the eIF4A signature highlights plasticity in translation regulation. Genome Biol. *15*, 476–476.

Sanchez-Marinas, M., Gimenez-Zaragoza, D., Martin-Ramos, E., Llanes, J., Cansado, J., Pujol, M.J., Bachs, O., and Aligue, R. (2018). Cmk2 kinase is essential for survival in arsenite by modulating translation together with RACK1 orthologue Cpc2 in Schizosaccharomyces pombe. Free Radic. Biol. Med. *129*, 116–126.

Saxton, R.A., and Sabatini, D.M. (2017). mTOR Signaling in Growth, Metabolism, and Disease. Cell *168*, 960–976.

Schmitt, K., Smolinski, N., Neumann, P., Schmaul, S., Hofer-Pretz, V., Braus, G.H., and Valerius, O. (2017). Asc1p/RACK1 Connects Ribosomes to Eukaryotic Phosphosignaling. Mol. Cell. Biol. *37*, e00279-16.

Schwanhausser, B., Busse, D., Li, N., Dittmar, G., Schuchhardt, J., Wolf, J., Chen, W., and Selbach, M. (2011). Global quantification of mammalian gene expression control. Nature *473*, 337–342.

Selye, H. (1936). A Syndrome produced by Diverse Nocuous Agents. Nature *138*, 32–32.

Sengupta, J., Nilsson, J., Gursky, R., Spahn, C.M.T., Nissen, P., and Frank, J. (2004). Identification of the versatile scaffold protein RACK1 on the eukaryotic ribosome by cryo-EM. Nat. Struct. Amp Mol. Biol. *11*, 957.

Shah, N., Dorer, D.R., Moriyama, E.N., and Christensen, A.C. (2012). Evolution of a large, conserved, and syntenic gene family in insects. G3 Genes - Genomes - Genet. *2*, 313–319.

Shahbazian, D., Roux, P.P., Mieulet, V., Cohen, M.S., Raught, B., Taunton, J., Hershey, J.W., Blenis, J., Pende, M., and Sonenberg, N. (2006). The mTOR/PI3K and MAPK pathways converge on eIF4B to control its phosphorylation and activity. EMBO J. *25*, 2781.

Shahbazian, D., Parsyan, A., Petroulakis, E., Topisirovic, I., Martineau, Y., Gibbs, B.F., Svitkin, Y., and Sonenberg, N. (2010). Control of cell survival and proliferation by mammalian eukaryotic initiation factor 4B. Mol. Cell. Biol. *30*, 1478–1485.

Shi, Z., and Barna, M. (2015). Translating the Genome in Time and Space: Specialized Ribosomes, RNA Regulons, and RNA-Binding Proteins. Annu. Rev. Cell Dev. Biol. *31*, 31–54.

Shi, Z., Fujii, K., Kovary, K.M., Genuth, N.R., Röst, H.L., Teruel, M.N., and Barna, M. (2017). Heterogeneous Ribosomes Preferentially Translate Distinct Subpools of mRNAs Genome-wide. Mol. Cell *67*, 71–83.e7.

Shor, B., Calaycay, J., Rushbrook, J., and McLeod, M. (2003). Cpc2/RACK1 Is a Ribosome-associated Protein That Promotes Efficient Translation in Schizosaccharomyces pombe. J. Biol. Chem. *278*, 49119–49128.

Shveygert, M., Kaiser, C., Bradrick, S.S., and Gromeier, M. (2010). Regulation of eukaryotic initiation factor 4E (eIF4E) phosphorylation by mitogen-activated protein kinase occurs through modulation of Mnk1-eIF4G interaction. Mol. Cell. Biol. *30*, 5160–5167.

Silva, G.M., Finley, D., and Vogel, C. (2015). K63 polyubiquitination is a new modulator of the oxidative stress response. Nat. Struct. Amp Mol. Biol. *22*, 116.

Simsek, D., and Barna, M. (2017). An emerging role for the ribosome as a nexus for post-translational modifications. Curr. Opin. Cell Biol. *45*, 92–101.

Simsek, D., Tiu, G.C., Flynn, R.A., Byeon, G.W., Leppek, K., Xu, A.F., Chang, H.Y., and Barna, M. (2017). The Mammalian Ribo-interactome Reveals Ribosome Functional Diversity and Heterogeneity. Cell *169*, 1051–1065.e18.

Siridechadilok, B., Fraser, C.S., Hall, R.J., Doudna, J.A., and Nogales, E. (2005). Structural Roles for Human Translation Factor eIF3 in Initiation of Protein Synthesis. Science *310*, 1513.

Slavov, N., Semrau, S., Airoldi, E., Budnik, B., and van Oudenaarden, A. (2015). Differential Stoichiometry among Core Ribosomal Proteins. Cell Rep. *13*, 865–873.

Smith, R.W.P., Anderson, R.C., Larralde, O., Smith, J.W.S., Gorgoni, B., Richardson, W.A., Malik, P., Graham, S.V., and Gray, N.K. (2017). Viral and cellular mRNA-specific activators harness PABP and eIF4G to promote translation initiation downstream of cap binding. Proc. Natl. Acad. Sci. U. S. A. *114*, 6310–6315.

Spence, J., Gali, R.R., Dittmar, G., Sherman, F., Karin, M., and Finley, D. (2000). Cell Cycle–Regulated Modification of the Ribosome by a Variant Multiubiquitin Chain. Cell *102*, 67–76.

Starck, S.R., Tsai, J.C., Chen, K., Shodiya, M., Wang, L., Yahiro, K., Martins-Green, M., Shastri, N., and Walter, P. (2016). Translation from the 5′ untranslated region shapes the integrated stress response. Science *351*, aad3867.

Stumpf, C.R., and Ruggero, D. (2011). The cancerous translation apparatus. Curr. Opin. Genet. Dev. *21*, 474–483.

Sundaramoorthy, E., Leonard, M., Mak, R., Liao, J., Fulzele, A., and Bennett, E.J. (2017). ZNF598 and RACK1 Regulate Mammalian Ribosome-Associated Quality Control Function by Mediating Regulatory 40S Ribosomal Ubiquitylation. Mol. Cell *65*, 751–760.e4.

Szabo, S., Tache, Y., and Somogyi, A. (2012). The legacy of Hans Selye and the origins of stress research: A retrospective 75 years after his landmark brief “Letter” to the Editor# of Nature. Stress *15*, 472–478.

Taniuchi, S., Miyake, M., Tsugawa, K., Oyadomari, M., and Oyadomari, S. (2016). Integrated stress response of vertebrates is regulated by four eIF2α kinases. Sci. Rep. *6*, 32886.

Thompson, M.K., Rojas-Duran, M.F., Gangaramani, P., and Gilbert, W.V. (2016). The ribosomal protein Asc1/RACK1 is required for efficient translation of short mRNAs. eLife *5*, e11154.

Truitt, M.L., Conn, C.S., Shi, Z., Pang, X., Tokuyasu, T., Coady, A.M., Seo, Y., Barna, M., and Ruggero, D. (2015). Differential Requirements for eIF4E Dose in Normal Development and Cancer. Cell *162*, 59–71.

Vasudevan, D., Clark, N.K., Sam, J., Cotham, V.C., Ueberheide, B., Marr, M.T., and Ryoo, H.D. (2017). The GCN2-ATF4 Signaling Pathway Induces 4E-BP to Bias Translation and Boost Antimicrobial Peptide Synthesis in Response to Bacterial Infection. Cell Rep. *21*, 2039–2047.

Vogel, C., and Marcotte, E.M. (2012). Insights into the regulation of protein abundance from proteomic and transcriptomic analyses. Nat. Rev. Genet. *13*, 227.

Volta, V., Beugnet, A., Gallo, S., Magri, L., Brina, D., Pesce, E., Calamita, P., Sanvito, F., and Biffo, S. (2013). RACK1 depletion in a mouse model causes lethality, pigmentation deficits and reduction in protein synthesis efficiency. Cell. Mol. Life Sci. CMLS *70*, 1439–1450.

Walter, P., and Ron, D. (2011). The Unfolded Protein Response: From Stress Pathway to Homeostatic Regulation. Science *334*, 1081.

Warner, J.R., and McIntosh, K.B. (2009). How Common Are Extraribosomal Functions of Ribosomal Proteins? Mol. Cell *34*, 3–11.

Waskiewicz, A.J., Flynn, A., Proud, C.G., and Cooper, J.A. (1997). Mitogen-activated protein kinases activate the serine/threonine kinases Mnk1 and Mnk2. EMBO J. *16*, 1909–1920.

Wei, J., Kishton, R.J., Angel, M., Conn, C.S., Dalla-Venezia, N., Marcel, V., Vincent, A., Catez, F., Ferré, S., Ayadi, L., et al. (2019). Ribosomal Proteins Regulate MHC Class I Peptide Generation for Immunosurveillance. Mol. Cell *73*, 1162–1173.e5.

Weingarten-Gabbay, S., Elias-Kirma, S., Nir, R., Gritsenko, A.A., Stern-Ginossar, N., Yakhini, Z., Weinberger, A., and Segal, E. (2016). Systematic discovery of cap-independent translation sequences in human and viral genomes. Science *351*.

Wilson, D.N., and Doudna Cate, J.H. (2012). The Structure and Function of the Eukaryotic Ribosome. Cold Spring Harb. Perspect. Biol. *4*.

Wolf, A.S., and Grayhack, E.J. (2015). Asc1, homolog of human RACK1, prevents frameshifting in yeast by ribosomes stalled at CGA codon repeats. RNA *21*, 935–945.

Xie, T., Chen, T., Li, C., Wang, W., Cao, L., Rao, H., Yang, Q., Shu, H.-B., and Xu, L.-G. (2019). RACK1 attenuates RLR antiviral signaling by targeting VISA-TRAF complexes. Biochem. Biophys. Res. Commun. *508*, 667–674.

Xue, S., and Barna, M. (2012). Specialized ribosomes: a new frontier in gene regulation and organismal biology. Nat. Rev. Mol. Cell Biol. *13*, 355.

Xue, S., Tian, S., Fujii, K., Kladwang, W., Das, R., and Barna, M. (2015). RNA regulons in Hox 5' UTRs confer ribosome specificity to gene regulation. Nature *517*, 33–38.

Yao, F., Long, L.-Y., Deng, Y.-Z., Feng, Y.-Y., Ying, G.-Y., Bao, W.-D., Li, G., Guan, D.-X., Zhu, Y.-Q., Li, J.-J., et al. (2013). RACK1 modulates NF-κB activation by interfering with the interaction between TRAF2 and the IKK complex. Cell Res. *24*, 359.

Young, S.K., and Wek, R.C. (2016). Upstream Open Reading Frames Differentially Regulate Gene-specific Translation in the Integrated Stress Response. J. Biol. Chem. *291*, 16927–16935.

Zhao, Y., Wang, Q., Qiu, G., Zhou, S., Jing, Z., Wang, J., Wang, W., Cao, J., Han, K., Cheng, Q., et al. (2015). RACK1 Promotes Autophagy by Enhancing the Atg14L-Beclin 1-Vps34-Vps15 Complex Formation upon Phosphorylation by AMPK. Cell Rep. *13*, 1407–1417.

Zhou, J., Wan, J., Shu, X.E., Mao, Y., Liu, X.-M., Yuan, X., Zhang, X., Hess, M.E., Brüning, J.C., and Qian, S.-B. (2018). N6-Methyladenosine Guides mRNA Alternative Translation during Integrated Stress Response. Mol. Cell *69*, 636–647.e7.

VIII. ANNEX

Insect Immunity: From Systemic to Chemosensory Organs Protection

Chapter 9
Insect Immunity: From Systemic to Chemosensory Organs Protection

Evelyne Einhorn and Jean-Luc Imler

Abstract Insects are confronted to a wide range of infectious microorganisms. Tissues in direct contact with the environment, such as olfactory organs, are particularly exposed to pathogens. We review here the immune mechanisms operating in insects to control infections. Experiments conducted on the model organism *Drosophila melanogaster* (fruit fly) have provided genetic evidence that insects rely on both cellular and humoral mechanisms to control infections. Once epithelial barriers have been breached, circulating or membrane-associated innate immunity receptors trigger signaling in the fat body and lead to secretion of high concentrations of antimicrobial peptides active on fungi and bacteria in the hemolymph. This induced response involves the evolutionarily conserved Toll and immune deficiency (IMD) signaling pathways, which promote nuclear translocation of transcription factors of the NF-κB family. In addition, different subsets of differentiated blood cells or hemocytes can neutralize bacteria, fungi or parasites by phagocytosis, production of microbicidal compounds, or encapsulation. An alternative to mount costly immune responses is to sense pathogens through chemosensory cues and avoid them. Interestingly, some families of molecules, including the Toll receptors, participate in both olfaction and immunity.

E. Einhorn
CNRS-UPR9022, Institut de Biologie Moléculaire et Cellulaire, Strasbourg, France
e-mail: evelyne.einhorn@etu.unistra.fr

J.-L. Imler (✉)
CNRS-UPR9022, Institut de Biologie Moléculaire et Cellulaire, Strasbourg, France

Faculté des Sciences de la Vie, Université de Strasbourg, Strasbourg, France
e-mail: jl.imler@unistra.fr

J.-F. Picimbon (ed.), *Olfactory Concepts of Insect Control - Alternative to Insecticides*, https://doi.org/10.1007/978-3-030-05165-5_9

1 Introduction

Insects represent by far the largest class of multicellular organisms, both in terms of number of species (corresponding to more than half of the animal species documented) and number of individuals (Misof et al. 2014). They also exhibit a fantastic variation of morphologies, which make them a fascinating group to study.

Insects have colonized all terrestrial biotopes and are exposed to all kind of infectious agents, raising the question of how they defend themselves (see Chaps. 1, 2, 3, 4, 5, and 6, volume 1). There are several specific reasons to be interested in host-pathogen interactions in insects. First, infection of insects can cause important economic losses (e.g. flacherie or pébrine disease of silkworms; contribution to colony-collapse disorder in honey-bees) (also see Chaps. 1, 2, and 3, volume 1). Second, hematophagous insects such as *Aedes* or *Anopheles* mosquitoes can transmit viral (caused by so-called arthropod-borne viruses or arboviruses, e.g. dengue, yellow fever, West-Nile virus) or parasitic (e.g. malaria) diseases to mammalian hosts (see Chap. 1, volume 1). Third, microbial pathogens (e.g. baculoviruses) can be used as biological control agents against insect pests, which necessitates some knowledge of the host response to these microorganisms (see Chap. 4, volume 1).

To these, we may add a fourth and last reason, which is that the fruit fly *Drosophila melanogaster* is a valuable model organism used in the biomedical field to decipher complex issues in biology, including immunology (Fernández-Hernández et al. 2016).

Whereas the immune system of vertebrates is composed of two arms, innate and adaptive immunity, invertebrates and insects in particular only rely on innate immunity to counter infections. Innate immunity, which senses infection through preformed receptors, rapidly reacts to the invasion of microorganisms and triggers the production of antimicrobial compounds (Fig. 9.1) (Hoffmann et al. 1999). We present below the main mechanisms involved in insect immunity, which bear many similarities with mammalian innate immunity, betraying common phylogenetic origins (Hoffmann 2003).

Emphasis is placed on the *Drosophila* model, which has provided strong genetic evidence for involvement of several pathways in insect immunity. We first present the systemic humoral response and its regulation, which bears several interesting similarities with the induction of inflammation in vertebrates. We then highlight how two cell intrinsic mechanisms, RNA interference and apoptosis, participate in the control of viral infections. The insect immune system also encompasses a cellular arm, and we present the different population of hemocytes present in the blood and associated with tissues, and discuss their contribution to host defense. Finally, we turn to immunity at barrier epithelia, before closing the chapter with the particular case of chemosensory organs.

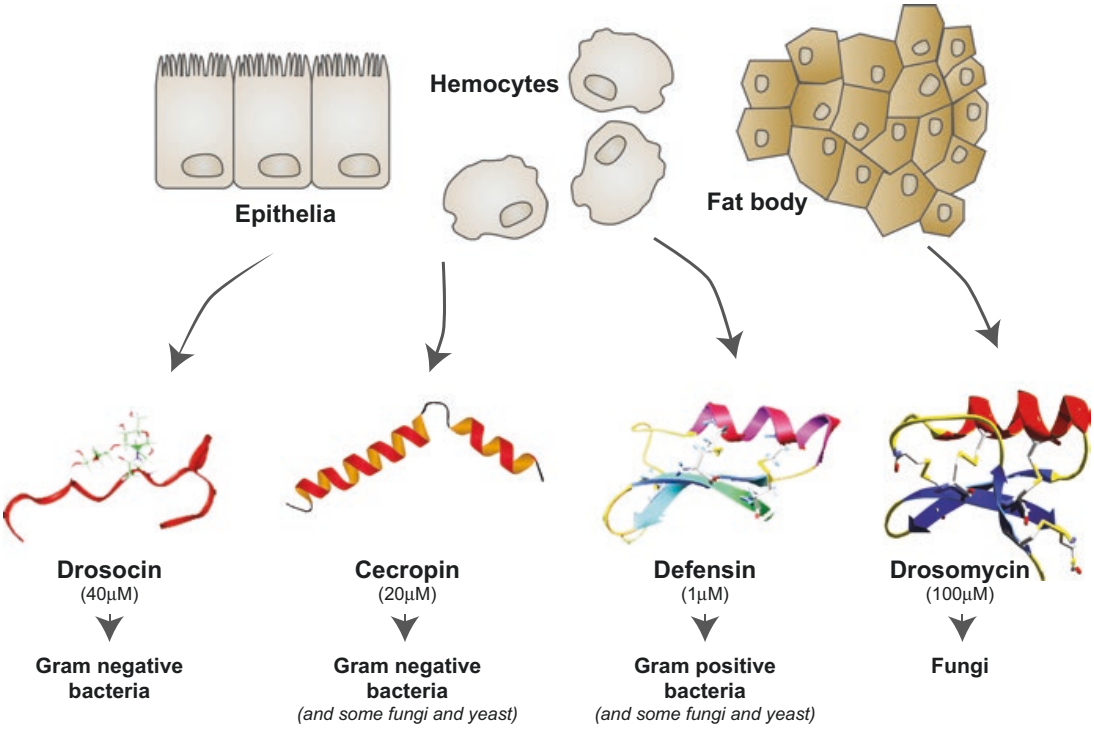

Fig. 9.1 The insect humoral response to microbial infections. Representative examples of antimicrobial peptides are shown with their microbial targets. Their concentration in the hemolymph of immune challenged *Drosophila* is indicated in parenthesis. These peptides are secreted by the fat body, but also plasmatocytes and surface epithelia

2 The Systemic Humoral Response to Infection by Bacteria, Fungi and Protozoa

2.1 A Battery of Secreted Antimicrobial Peptides Contribute to Humoral Immunity

One hallmark of the immune response of insects is the secretion in the hemolymph of a cocktail of small (<10 kDa for most of them), cationic antimicrobial peptides (AMPs).

These peptides, which participate in host defense in all metazoa, but also in plants, were initially discovered in an insect, the moth *Hyalophora cecropia* (Steiner et al. 1981). AMPs belong to different structural families and are active in micromolar concentrations against a broad range of microbes, with some specificity. They act on the microbial cell wall, although some have intracellular targets (Imler and Bulet 2005) (see Fig. 9.1).

The most commonly found AMPs in insects are the α-helical Cecropins, which are mainly active against a range of Gram-negative bacteria, and the disulphide-bridged Defensins, mostly active against Gram-positive bacteria (Boman et al. 1991; Hoffmann and Hetru 1992; Vilmos and Kurucz 1998). Besides these, each insect expresses a specific repertoire of AMPs (Koehbach 2017). One AMP specific to *D. melanogaster* is the antifungal peptide Drosomycin, which turned out to be an important marker of the immune response for the deciphering of the pathways leading to AMP expression (Zhang and Zhu 2009).

2.2 *Evolutionarily Conserved Signaling Pathways Control AMP Expression*

AMPs are induced upon infection, and are secreted in the hemolymph, where their combined concentration can reach 300 μM in the fruit fly *D. melanogaster*. The transcriptional induction of the genes encoding AMPs is mediated by factors of the NF-κB family, which in mammals play important roles in the induction of inflammation and immunity (Hoffmann et al. 1999). These transcription factors are retained in the cytosol of non-infected cells by ankyrin-repeat containing inhibitors of the IκB family. In response to an immune challenge, they rapidly translocate to the nucleus. Two pathways, named Toll and IMD, regulate AMP expression in insects, through activation of different members of the NF-κB family (Ferrandon et al. 2007) (Fig. 9.2).

The Toll pathway, named after the transmembrane receptor Toll, is involved in the humoral response to fungi and Gram-positive bacteria (Valanne et al. 2011). It is activated by a neurotrophin-like cytokine, Spaetzle, which is expressed as an inactive precursor unable to bind Toll (Weber et al. 2003). Infection by fungi or Gram-positive bacteria triggers a proteolytic cascade that culminates in the activation of the serine protease Spaetzle Processing Enzyme (SPE) and generates an active Toll ligand (Jang et al. 2006). Activation of Toll triggers intracytoplasmic signaling through the death domain (DD) adapter proteins DmMyD88 and Tube. This leads to activation of the serine/threonine kinase Pelle through specific homotypic DD-DD interaction (Sun et al. 2004). Pelle phosphorylates the IκB-like molecule Cactus, triggering its degradation by the proteasome. This releases the NF-κB transcription factor DIF, which translocates to the nucleus and activates expression of genes encoding AMPs such as antifungal peptide *drosomycin* (Rutschmann et al. 2000; Daigneault et al. 2013).

The IMD pathway, named after the *Drosophila* gene *immune deficiency* (*imd*), mediates inducible expression of antibacterial peptides (e.g. Diptericin, Drosocin) in response to infection by Gram-negative bacteria (Georgel et al. 2001). The pathway is activated by receptors of the PGRP family (see below) and involves the DD adapter proteins IMD and dFADD, and the caspase DREDD (Naitza et al. 2002). One target of DREDD is IMD itself. The new N-terminus of IMD then recruits the

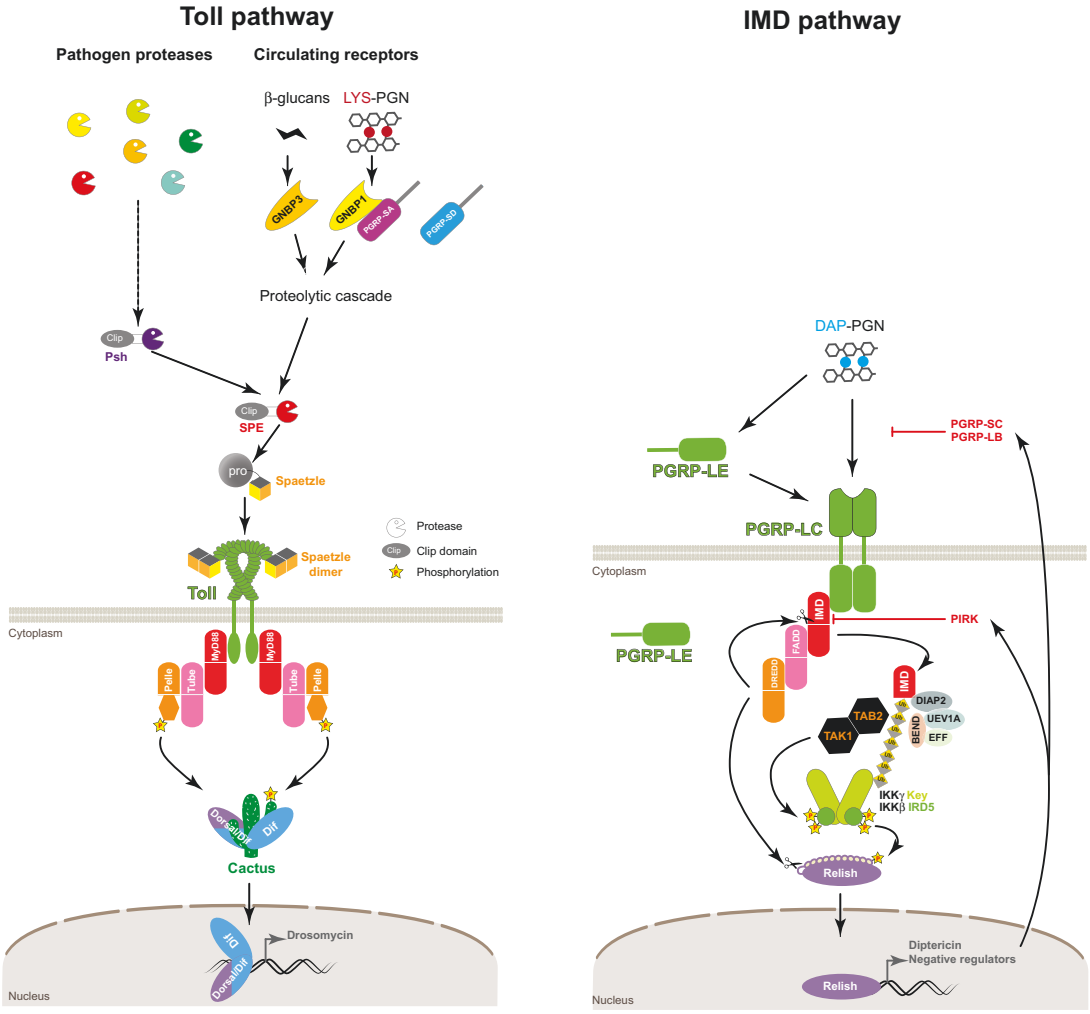

Fig. 9.2 Overview of the *Drosophila* Toll and IMD pathways. The Toll pathway is activated by a proteolytically processed form of the cytokine Spaetzle. Proteolytic cascades upstream of Spaetzle are induced upon sensing of ß-glucans or lysine-type peptidoglycan (derived respectively from the cell wall of fungi and most Gram positive bacteria) by circulating PRRs, or upon detection of abnormal proteolytic activity associated with infection. Activation of Toll leads to nuclear translocation of the NF-κB transcription factor Dif and/or Dorsal, which promote expression of AMPs such as Drosomycin. The IMD pathway is activated by members of the PGRP family that sense DAP-type peptidoglycan found in the cell wall of Gram-negative bacteria. It activates the NF-κB transcription factor Relish, which controls genes encoding AMPs (e.g. Diptericin) or negative regulators of the pathway (e.g. Pirk, PGRP-SC and PGRP-LB)

complex TAB2/TAK1, promoting the activation of the serine/threonine kinase TAK1 (Paquette et al. 2010). TAK1, together with the E3 ubiquitin ligase Uev1A/Ubc13, then activates the IκB kinase (IKK) complex formed by the kinase DmIKKβ and its regulatory subunit DmIKKγ. DmIKKβ subsequently phosphorylates the NF-κB protein Relish, thus promoting its cleavage by DREDD (Stoven et al. 2003). The 110 kDa Relish contains an N-terminal inhibitory ankyrin-repeat domain, which restrains the transcription factor to the cytosol. Proteolytic cleavage by DREDD releases the active domain of Relish, which is then free to translocate to the

nucleus, to trigger expression of antibacterial peptides genes, e.g. *diptericin* and/or *drosocin* (Stoven et al. 2003).

Interestingly, both the Toll and IMD pathways are evolutionarily ancient, and bear striking similarities with the mammalian Toll-like receptor (TLR)/interleukin-1 receptor (IL-1R) and Tumor necrosis factor receptor (TNF-R) pathways, respectively. The genetic characterization of these pathways in the *Drosophila* model organism was instrumental in revealing the interplay of molecules involved, and in particular played a decisive role in revealing the importance of TLRs in mammalian innate immunity (Hoffmann 2003).

2.3 Non-self and Danger Signals Trigger Humoral Immunity

In spite of the similarities mentioned above, the sensing of microorganisms upstream of the Toll and IMD pathways exhibit some differences with mammals.

Activation of innate immunity involves receptors commonly known as pattern-recognition receptors (PRRs), which recognize molecular motifs, or "patterns", shared by large groups of microorganisms and essential for their biology (e.g. lipopolysaccharide found in the cell wall of all Gram-negative bacteria, double-stranded RNA generated during viral replication), but absent from the host (Medzhitov and Janeway 2002). Whereas TLRs represent a major family of PRRs in vertebrates, Tolls in insects function as cytokine receptors or adhesion molecules (McIlroy et al. 2013; Paré et al. 2014). Recognition of microbial infection is mediated by receptors that belong to two other families of PRRs, the peptidoglycan (PGN) recognition proteins (PGRPs) and the β-glucan binding proteins (GNBPs) (Ferrandon et al. 2007). Initially identified in the silkworm moth *Bombyx mori*, these molecules were genetically characterized in *Drosophila* (Yoshida et al. 1986; Choe et al. 2002; Gottar et al. 2002, 2006).

The IMD pathway in flies is activated by a characteristic feature of PGN from Gram-negative bacteria (shared by Gram-positive bacilli), namely the presence of a diaminopimelic acid (DAP) residue at the third position in the four amino-acid peptide bridge between the chains of glycans (Kaneko et al. 2006). Two negatively charged groups of DAP form a strong electrostatic interaction with an Arginine residue in a specific pocket in the transmembrane receptor PGRP-LC, thus triggering signaling (Chang et al. 2005). A second member of the PGRP family in flies, PGRP-LE, exists as either a secreted isoform that facilitates interaction between PGN and PGRP-LC, or an intracellular isoform that senses PGN from intracellular bacteria (Steiner 2004; Royet et al. 2011). Of note, this cytosolic receptor also triggers a cell intrinsic response to infection, namely autophagy (Yano et al. 2008). Therefore, the IMD pathway is activated by PRRs that directly sense PGN from infecting bacteria.

By contrast, in the Toll pathway, recognition occurs upstream of Toll, and is mediated by circulating PRRs. In the case of many important Gram-positive bacteria, a Lysine residue replaces the DAP in the peptide stem of PGN, and this differ-

ence is sensed by PGRP-SA, with a contribution from PGRP-SD. Thus, a subtle difference in the structure of PGN between Gram-negative and Gram-positive bacteria is responsible for the activation of either the IMD or the Toll pathway, respectively (Steiner 2004; Royet et al. 2011). Recognition of fungi, on the other hand, involves a PRR from a different family, GNBP3, which binds β1-3-glucans (Gottar et al. 2006).

A second member of the GNBP family, GNBP1, participates to the sensing of Gram-positive bacteria, together with PGRP-SA (Gobert et al. 2003). Thus, GNBPs are not restricted to the sensing of fungal components. The PRRs acting upstream of Toll activate proteolytic cascades that culminate in the production of an endogenous ligand for the Toll receptor (Ferrandon et al. 2007).

Besides PGRPs and GNBPs, the Toll pathway can also be activated by the sensing of abnormal proteolytic activity in the hemolymph. This is mediated by the circulating zymogene Persephone, which can be activated by fungal or bacterial proteases (Gottar et al. 2006; El Chamy et al. 2008; Issa et al. 2018). These proteases are often used to penetrate the insect cuticle, and as such are important virulence factors, which can be sensed by Persephone. Upon activation, this serine protease activates a proteolytic cascade leading to processing of the Spaetzle precursor (Levashina et al. 1999; Ligoxygakis et al. 2002).

2.4 Complement Factors Contribute to Anti-parasitic Immunity

A family of secreted complement-like factors known as TEPs (thioester containing proteins) participates in host-defense in insects.

In vertebrates, the TEP family includes not only the protease inhibitors α_2-macroglobulins, but also the complement factors C3, C4 and C5 (Nonaka 2000; Shokal and Eleftherianos 2017).

Initially identified as immune-induced genes in *Drosophila*, the TEPs have been best characterized in the mosquito *Anopheles*, which transmit the malaria parasite to mammals (Levashina et al. 2001; Blandin and Levashina 2004). Out of the 19 TEPs identified in the genome of *Anopheles gambiae*, TEP1 is an extremely polymorphic gene that encodes for an acute phase secreted protein, which binds to the surface of bacteria and parasites. It promotes phagocytosis of bacteria and killing of parasites at the ookinete stage (Blandin et al. 2004; Obbard et al. 2008). Polymorphism in the gene encoding TEP1 explains a substantial part of the variability in transmission of *Plasmodium* parasites observed between *A. gambiae* individuals (Blandin et al. 2009). Interestingly, TEP1 bears similarities to the mammalian complement factor C3, both at the structural and functional levels (Baxter et al. 2007; Fraiture et al. 2009). In particular, two leucine-rich repeat proteins, APL1 and LRIM1, function like complement control proteins, preventing TEP1 from binding to self-tissues in the absence of infection.

2.5 *RNAi and Apoptosis: Two Cell Intrinsic Mechanisms of Antiviral Immunity*

Viruses represent a special challenge for multicellular organisms. Indeed, their small size, their great diverse shape, very robust replicable structure and simplicity of organization offer limited options for sensing and neutralization by the immune system. In addition, they replicate in the cytoplasm or nucleus on infected cells, which blurs the distinction between self and non-self. Finally, their error prone polymerases allow them to evolve rapidly, facilitating evasion from antiviral immune defenses (see Chap. 10 about evolution of chemosensory proteins).

RNA interference (RNAi) provides insects with a powerful mechanism of antiviral defense. It involves RNA targeting enzymes from two families, the Dicers and the Argonautes (AGOs) (Fig. 9.3).

RNAi was first identified as a potent antiviral defense mechanism in plants (Ding 2010). More recently, RNAi was also found to play an important role in the control

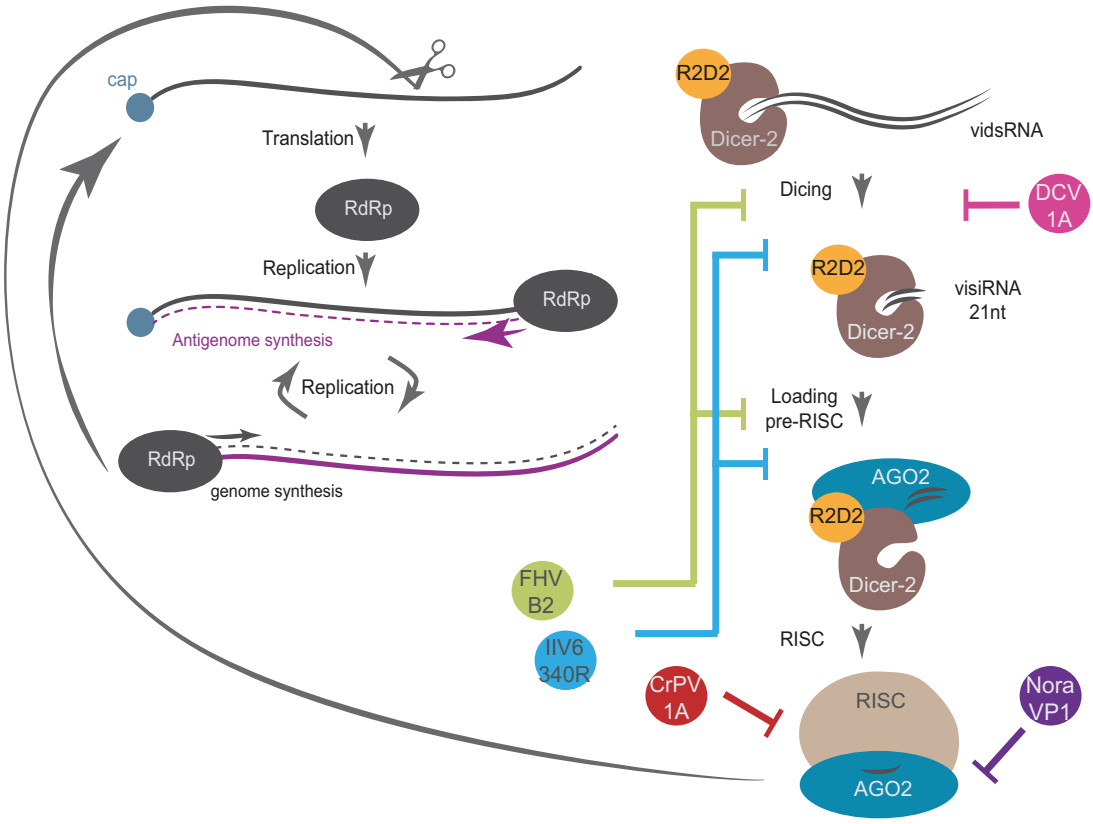

Fig. 9.3 The antiviral small interfering RNA (siRNA) pathway. Upon infection by a positive strand RNA virus, translation of the viral RNA dependent-RNA polymerase (RdRP) leads to initiation of replication. The resulting double-strand RNA (dsRNA) is sensed by the RNAseIII enzyme Dicer-2 (Dcr-2) and cleaved into virus-derived siRNAs duplexes. Upon loading onto Argonaute 2 (AGO2), one strand of the duplex is discarded and the remaining strand will guide the nuclease AGO2 and the RNA induced silencing complex (RISC) towards viral RNAs. Many insect viruses express suppressors that antagonize the siRNA pathway at different levels

of viral infection in insects (Aliyari and Ding 2009), eventually providing a new area of research for insect control (see also Chap. 5, volume 1).

Central to the RNAi mechanism are the enzymes of the AGO family, which mediate highly specific neutralization of target RNA molecules (Herzog and Ameres 2015). The specificity of AGO enzymes is achieved by their association with small RNAs, which guide them towards RNA molecules with complementary sequences. Three RNAi pathways, involving different members of the AGO family, have been defined in insects: (i) the small interfering (si)RNA pathway involves AGO-2, and is activated by double stranded (ds)RNA. siRNAs are produced by the RNaseIII enzyme Dicer-2, which forms a complex with the dsRNA binding protein (dsRBP) protein R2D2 (Paro et al. 2015); (ii) the micro (mi)RNA pathway involves AGO-1, Dicer-1 and its dsRBD co-factor Loquacious, and modulates expression of insect genes, in particular during tissue development (Carthew et al. 2017); (iii) finally, the piRNA pathway involves the other AGO proteins (Piwi, Aubergine and AGO3 in *Drosophila*).

Piwi-associated RNAs (piRNAs) are involved in the control of mobile genetic elements, including the retrovirus gypsy, in the germ line of *Drosophila* (Siomi et al. 2010). Virus-derived piRNAs are also generated in infected insect cell lines as found in *Drosophila* and mosquitoes. However, the piRNA pathway does not appear to participate in antiviral host defense at least in the fruit fly *Drosophila* (Petit et al. 2016). It is still unclear whether it participates in the control of viral infections in mosquitoes (Morazzani et al. 2012; Vodovar et al. 2012; Léger et al. 2013).

Demonstration of the critical role of the siRNA pathway in antiviral immunity in insects relies on three lines of evidence: first, genetic data indicating that siRNA pathway mutants (*Dicer-2*, *r2d2* or *AGO2*) are hypersensitive to RNA virus infections, and contain increased viral load (Galiana-Arnoux et al. 2006; van Rij et al. 2006; Wang et al. 2006); second, siRNAs of viral origin can be detected in infected cells or insects from a variety of species (Aliyari et al. 2008; Aguiar et al. 2015); and third, viral suppressors of RNAi (VSRs), which counteract the immune defense of the fly, have been identified in several insect viruses (van Rij et al. 2006).

RNA interference provides a highly specific and even adaptive mechanism to degrade viral nucleic acids in infected cells. Indeed, the sensing by Dicer-2 of a molecular pattern characteristic of viral infection, double stranded RNA, triggers the production of guide siRNAs for AGO2, thus programming it to specifically neutralize viral RNAs (Kemp and Imler 2009). RNAi is a cell autonomous process in *Drosophila* (Roignant et al. 2003), although in the context of infectious viral dsRNA released upon cell lysis can be taken up by non infected cells and trigger the antiviral siRNA pathway (Saleh et al. 2009). In addition, viral dsRNA and siRNAs can be shared between cells by cytoplasmic bridges (Karlikow et al. 2016). Besides RNAi, apoptosis is another cell intrinsic mechanism of antiviral defense operating in insects (Clem 2015; Nainu et al. 2015) (see also Chap. 5, volume 1).

3 Cellular Responses to Infections

3.1 Differentiation of Hemocytes in Insects

Hematopoiesis in insects occurs during embryogenesis and in larvae. It originates from the head mesoderm in embryos, and from a specific hematopoietic organ, the lymph gland, in larvae.

This gland is composed of two primary lobes, located on the sides of the aorta, which grow and form more posterior secondary lobes. While the secondary lobes contain only frequently dividing precursors called prohemocytes (small rounded cells [4–6 μm diameter] with a high nucleocytoplasmic ratio), the primary lobe can be differentiated in three zones. The medullatory zone composed of prohemocytes; the cortical zone composed of differentiating hemocytes; and a group of 20–30 cells at the posterior end of each lobe forming the posterior signaling center (PSC). The PSC plays a key regulatory role in third instar larvae, maintaining the balance between multipotent prohemocytes in the medullary zone and controlling hemocyte differentiation (Krzemień et al. 2007; Mandal et al. 2007). Interestingly, odorant receptors activation contributes to blood progenitors maintenance in *Drosophila* (Shim et al. 2013).

Several kinds of hemocytes have been described in insects and, because of the great diversity of insects and the important variability of histological features of the cells within one insect, it is difficult to provide a unified view of the different types of blood cells. Nevertheless, based on morphological and functional characteristics, it appears that insects contain a few blood cell types, which bear resemblance to cells of the myeloid lineage in vertebrates. They include the macrophage-like plasmatocytes and other non-phagocytic cells, which seem to be characteristic of particular groups of insects (e.g. crystal cells and lamellocytes in *Drosophila*) (Fig. 9.4).

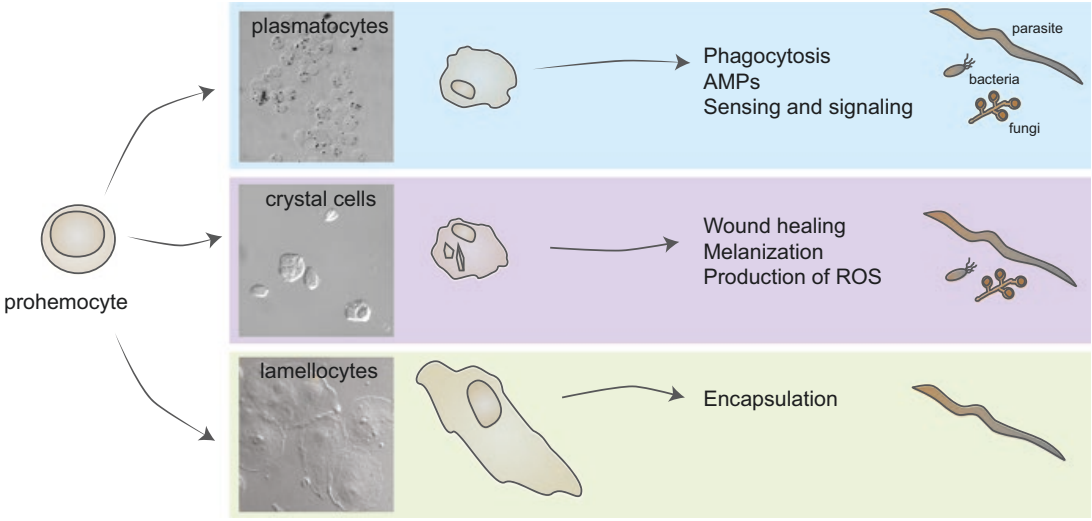

Fig. 9.4 Cellular immunity in the fruit fly *Drosophila melanogaster*. Differentiation of prohemocytes generates three types of hemocytes, which contribute by different mechanisms to host defense. (See paragraph 3.1)

Regulation of hemocyte differentiation involves evolutionarily conserved transcription factors also participating in hematopoiesis in mammals (e.g. Runx, GATA, STAT families). In addition to the larval lymph gland, hemocytes are found in circulation or in sessile patches of cells accumulating in various locations of the body (Lanot et al. 2001; Hillyer 2016).

3.2 Plasmatocytes Phagocytose Microbes and Dead Cells

Plasmatocytes form the majority of differentiated blood cells (90–95% of hemocytes in *Drosophila* larvae). They are relatively round cells, with diameter of 8–10 μm, which display phagocytic activity. Accordingly, their cytoplasm is rich in endoplasmic reticulum and lysosomes.

In some conditions, these cells exhibit pseudopod-like extensions (e.g. at the onset of metamorphosis), suggesting that the podocytes described in some insects may represent a specialized subtype of plasmatocytes. Commonly referred to as macrophages, plasmatocytes engulf and degrade dead cells, debris and invading pathogens. They also produce antimicrobial peptides in response to infection and participate to tissue remodeling through the secretion of extracellular matrix proteins (see Fig. 9.4). Phagocytosis involves several types of receptors, including the CD36 scavenger receptor homologue Croquemort for the removal of apoptotic cells and the EGF domain protein Eater (Franc et al. 1999; Kocks et al. 2005).

3.3 Phenoloxydases Catalyze the Production of Melanin and Toxic Microbicidal By-Products

Crystal cells (5% of larval hemocytes in *Drosophila*) are round cells with a 10–12 μm diameter and characteristic paracrystalline cytoplasmic inclusions. They are not involved in phagocytosis, but play a key role in melanization, participating to host defense and wound healing.

The crystal cell inclusions consist of massive amounts of components of the melanization enzymatic cascade, such as the prophenolxydase enzyme (PPO; Lu et al. 2014). A poorly characterized serine protease cascade converts the prophenoloxydase zymogen into active phenoloxydase. This oxydo-reductase then catalyzes the oxidation of phenols to quinones, which then polymerize into melanin. In the process, microbicidal reactive oxygen species such as hydrogen peroxide and nitric oxyde are generated. Insects express a varying number of PPOs. In *Drosophila*, two of the three PPOs, PPO1 and PPO2 are expressed in crystal cells (the third member of the family, PPO3, is expressed in lamellocytes). They contribute to the resistance to bacterial and fungal infections, but also to large parasites, in conjunction with lamellocytes (Binggeli et al. 2014).

3.4 Lamellocytes Encapsulate Large Parasites

Lamellocytes are large (15–40 μm diameter) flat adherent cells, which encapsulate and neutralize objects too large to be phagocytosed by plasmatocytes (see Fig. 9.4).

Interestingly, these cells can only be seen in parasitized larvae, indicating that their differentiation represents a dedicated immune response. Parasitization occurs frequently in nature when Hymenopteran wasps such as *Leptopilina* lay their eggs in larvae (Colinet et al. 2013). Detection of the egg, or of any object, even artificial, too large to be phagocytosed by plasmatocytes generates a signal that triggers a differentiation program in the PSC of the lymph gland, leading to the production and release of lamellocytes. These cells then adhere tightly to the foreign object and surround it to form a capsule. Crystal cells are subsequently recruited and melanization of the capsule participates in the containment and killing of the parasite.

In addition to these cell-mediated immune functions, hemocytes also participate in humoral response through production of AMPs and secretion in the hemolymph.

4 Immunity at Barrier Epithelia

In insects, as in many other organisms, surface epithelia represent a first barrier to infection. Surface epithelia are sites of major physiological functions involving exchange with the external environment, such as nutrient absorption, gas exchange, water conservation and reproduction. As a consequence, these cells are largely exposed to microorganisms (see Chap. 4, volume 1).

Host-defense in epithelia is mediated by both physical and chemical barriers.

4.1 Secreted Chitin-Based Matrices Form an Efficient Physical Barrier

One hallmark of insects is the presence of an exoskeleton, the cuticle, which forms an efficient physical barrier against infection but also as insecticide (Balabanidou et al. 2018) (see Chap. 3, volume 1).

The cuticle is composed of layers of chitin, a long chain polymer of N-acetylglucosamine secreted by the ectodermal epithelium, which can be cross-linked with proteins to increase rigidity and resistance. This protective layer also covers the tracheal tubes, which allow oxygen to diffuse to tissues. Only the thinner subbranches, the tracheolae, which ultimately bring oxygen directly to cells, are devoid of cuticle. In the digestive tract, the foregut and hindgut are lined by impermeable cuticle, but not the midgut, where food absorption occurs. However, the epithelial cells of the midgut are protected from the external environment by a peritrophic

matrix, lining the gut epithelium and isolating it from the food bolus. Composed of chitin and glycoproteins, the peritrophic matrix is produced continuously or upon ingestion of a meal (depending on the type of insects) by a specialized organ at the entry of the midgut, the cardia. It prevents direct contact of microbes with midgut epithelial cells and limits the action of microbial toxins produced in the gut, in a manner similar to mucous secretions in the mammalian gut (Kuraishi et al. 2011; Xuan et al. 2015; Liu et al. 2017).

These chitin-based barriers can be breached by injuries or pathogen-secreted enzymes. This leads to activation of chemical barriers, a second layer of defense in epithelia.

4.2 Chemical Barriers to Infection in Epithelia

The *Drosophila* digestive tract produces two different types of antimicrobial effectors, reactive oxygen species (ROS) and AMPs, which function in a complementary and probably synergistic manner to control infections.

In the digestive tract of dipteran insects microbicidal ROS are produced by the dual oxidase (DUOX) enzyme, which is also known to be essential to avoid eggshell dessication (Dias et al. 2013). This member of the NADPH oxidase family is expressed at a basal level in the gut, killing dietary yeasts but sparing the microbiota (Bae et al. 2010). Upon gut infection, it is strongly induced, leading to the destruction of many microbes. Induction of DUOX is mediated by the nucleotide uracil released by infecting bacteria. Uracil is thought to be sensed by an unidentified G-protein coupled receptor, signaling through the protein Gαq and the phospholipase C (PLC) β (Lee et al. 2013).

Another chemical barrier to infection operating in the digestive tract, but also in other epithelia is the production of AMPs. Initially characterized for their role in the systemic humoral response (see above), AMPs are also expressed in epithelia from the digestive tract, the respiratory tract, the excretory system or the reproductive tract. AMPs are expressed in a tissue-specific manner in epithelia, either constitutively or in response to local activation of the IMD signaling pathway (Tzou et al. 2000).

5 Immunity in Chemosensory Organs

5.1 Chemosensory Organs Are Permanently in Contact with the Environment

In insects, sensing of the environment occurs through specialized organs like antennae and maxillary palps (see Chaps. 1, 2, 3, 4, 5, 6, 7, 8, this chapter and counterparts 10, 11, 12 in this volume). An opening in the cuticule at the level of these

structures allows permanent exchanges with the environment. Therefore, chemosensory organs may represent a crucial portal of entry through which specific microorganisms and/or pathogens enter a susceptible insect host to cause disease or infection (see Chap. 4, volume 1).

Olfactory sensilla possess a discontinuous cuticule containing pores that range from 10 to 25 nm, followed by a pore kettle of 10–20 nm diameter (Cribb and Merritt 2013). Hence, even the smallest viruses, which have a diameter of *ca.* 30 nm, cannot pass through these pores. Below the cuticle, intercellular septate junctions form a second barrier compromising the spreading of infectious microorganisms (e.g. Bonnay et al. 2013). These natural barriers, however, may not be sufficient to prevent infection by bacterial microorganisms that can secrete specific chitinolytic enzymes (or chitinases; Patil et al. 2000). In addition, pathogens can access chemosensory organs through other routes, as suggested by the recent identification of a viral nucleocapsid in the antenna of *Rhodnius prolixus* (Oliveira et al. 2017).

Just like the rest of the insect body, antennae contain hemolymph within an antennal vessel. In Cockroaches (*blattidae*), this vessel contains hemocytes (Pass 1985), which may participate in host defense in the antennae. This is, however, not relevant for all insects, since the diameter of the antennal vessel is too small to allow circulation of hemocytes (e.g. 1–2 μm), as found for instance in mosquitoes (Boppana and Hillyer 2014).

5.2 Constitutive Expression of AMPs in Chemosensory Organs

Expression of AMPs largely contributes to the protection of chemosensory organs against microbial infection. In the fall armyworm *Spodoptera frugiperda*, antennae and maxillary palps strongly express AMPs. Most strikingly, Cecropin and Defensin peptides are expressed at higher levels in unchallenged antennae and maxillary palps than in the fat body after bacterial infection (Legeai et al. 2014). In the silkworm moth *B. mori*, antennae also express immune-related genes such as phenoloxidase, a member of the Toll receptor family and the immune-induced gene Hdd13 (Zhao et al. 2015). Of note, this expression of AMP might be regulated, as *Drosophila* antennae express Dnr1, a negative regulator of the IMD pathway that blocks Dredd activity (Foley and O'Farrell 2004; Anholt and Williams 2010).

Interestingly, the expression of immune genes in chemosensory organs appears to differ between social casts in the leaf-cutting ant *Atta vollenweideri*. Indeed, analysis of the antennal transcriptome of different social casts revealed a higher expression of most immune genes in antennae from queens compared to males and workers. In addition, differences in the sets of immune genes expressed were observed between workers and queens (e.g. hymenoptaecin expressed in the former and defensin in the latter) (Koch et al. 2013).

5.3 *Induction of Pherokines (CSP-Like) Upon Microbial Challenge*

Besides AMPs, many other protein families are up-regulated in the insect body in response to bacterial infection (Irving et al. 2001; De Gregorio et al. 2002). Interestingly, these include molecules related to the insect chemosensory protein family (see Chaps. 6 and 10). The most striking examples are pherokine-2 and -3, which are related to OS-D/A10, a secreted factor highly expressed not only in olfactory organs but throughout the whole insect body (Fig. 9.5) (Picimbon et al. 2000a, b,

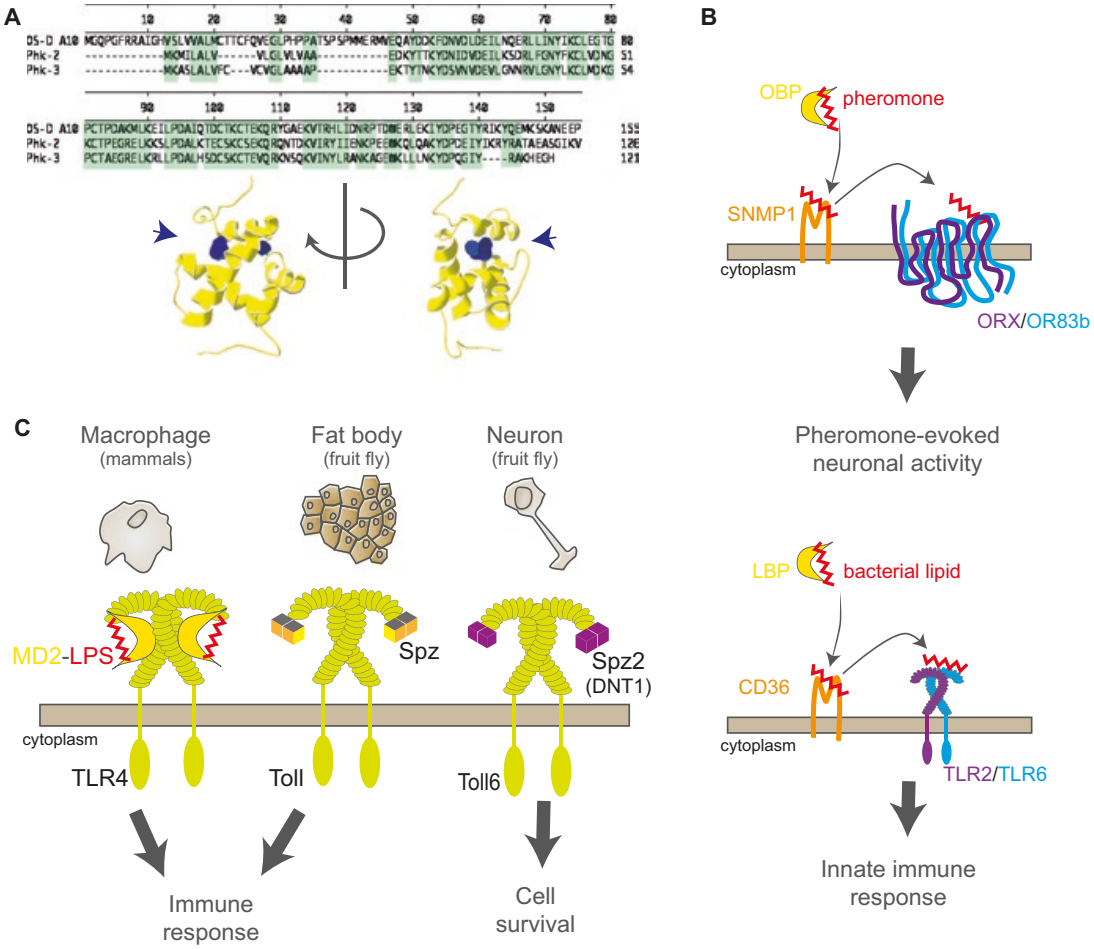

Fig. 9.5 Shared molecular mechanisms of immunity and olfaction. (**a**) Sequence alignment of *D. melanogaster* OS-D/A10, and its paralogs Pherokine-2 and -3, which are induced by infection. A model for the 3D structure of OS-D/A10 is shown at the bottom (Swissmodel; see Chaps. 6 and 10). The hydrophobic binding pocket (arrowhead) is highlighted in blue. (**b**) Involvement of CD36-related receptors in the transfer of hydrophobic ligands to signaling transmembrane receptors in the olfactory system and in the immunological system (Adapted from Benton et al. 2007). (**c**) Function of Toll receptors in the immune and nervous systems of insects. Whereas mammalian TLRs directly sense microbial ligands, as shown for TLR4 recognizing lipopolysaccharides (LPS) bound to the lipid-binding protein MD2, Toll receptors from insects are activated by neurotrophin-related cytokines

2001; Picimbon 2003). Secretion of the 13 kDa Phk-2 protein in the hemolymph is induced specifically in response to infection with DCV, whereas expression of the mRNA encoding Phk3 is induced by bacterial and fungal infection (Sabatier et al. 2003). Unfortunately, the function of these *Drosophila* molecules remains unknown. However, studies in other insects such as the whitefly *Bemisia tabaci,* the silkworm moth *B. mori* and the red flour beetle *Tribolium castaneum* strongly point to the involvement of the chemosensory protein family in insect defense (Xuan et al. 2015; Liu et al. 2014, 2016, 2017).

Other "olfactory" binding protein families are possibly involved in the insect response to chemical/viral infection (Xuan et al. 2015). For example, a transcriptomic analysis revealed an enrichment of pheromone binding proteins in hemocytes from *Aedes aegypti*, the mosquito vector of dengue, chikungunya or zika viruses (Bartholomay et al. 2004). In addition, two putative odor binding proteins (OBPs; see Chaps. 6, 7, 8, 10, 11, 12 and this chapter), OBP10 and OBP22 are up-regulated in the salivary glands of *A. aegypti* upon infection by dengue virus (Sim et al. 2012). Interestingly, silencing of these two genes impaired the efficiency of blood feeding. Regulation of chemosensory proteins by infection was also reported in another mosquito, the malaria vector *A. gambiae,* Indeed, the genes annotated as *obp4*, *7* and *obpd-2 (obp domain 2)* are upregulated following infection with the fungus *Beauveria bassiana*, whereas *obpd-1* (obp *domain 1)* is downregulated upon infection with *Salmonella typhimurium* (Aguilar et al. 2005).

In the silkworm *B. mori*, CSP11 was among the 50 genes induced by *B. bassiana* infection (Hou et al. 2013). It was also among the 17 CSP genes upregulated by insecticide (Xuan et al. 2015). Finally, studies in yet another insect, honeybees, point to a role for olfaction in induction of a hygienic behavior leading to a better ability to remove brood infested with *Varroa destructor.* Indeed, transcriptomic analysis of honeybees exposed to this ectoparasite showed that tolerant bees mainly differ from the others by a higher expression of genes regulating olfaction (Navajas et al. 2008) (see Chap. 6, volume1).

5.4 Biological Significance of the Immune Induction of OBP/CSP Molecules

Induction of chemosensory proteins (CSPs) and odor binding proteins (OBPs) in response to infection could reflect behavioral modifications participating in the resistance to infection. Indeed, although immunity represents a crucial aspect of resistance to infection, induction of an immune response is metabolically costly (Lazzaro 2015) and can have deleterious side effects (Cao et al. 2013). Avoiding infection by sensing contaminated food sources represents an interesting alternative for all animals, including insects. This is particularly relevant for insects like the

fruit fly *D. melanogaster*, which is known to feed on decaying/fermenting microbe-rich organic matter (Petkau et al. 2016).

Recent studies exploiting the *Drosophila* genetics toolbox emphasize the importance of gustatory and olfactory circuits in pathogen avoidance. For example, flies can taste the presence of bacterial LPS through gustatory neurons expressing Gr66a receptors. The subsequent activation of the chemosensory cation channel DTRP1 triggers a strong aversive response monitored in both feeding and egg laying assays (Soldano et al. 2016). Fruit flies can also distinguish food sources covered with toxic microbes. This is mediated by the microbial odorant geosmin (trans-1,10-dimethyl-trans-9-decalol), which alerts sensory neurons expressing the olfactory receptor OR56a and averts the fly to unsuitable feeding and breeding sites (Stensmyr et al. 2012) (see Chap. 4). Also in support for a role of CSPs/OBPs in behavioral modifications associated with infection, flies are more sexually attracted to individual fed on the same diet and this appears to depend on the composition of the gut microbiota. In particular, the symbiontic bacteria *Lactobacillus plantarum* affects the levels of cuticular hydrocarbon sex pheromones (Sharon et al. 2010; Venu et al. 2014). The mechanism by which this occurs is unknown, but could involve transmission of information through a cytokine participating in the innate immune response (Ringo et al. 2011). Indeed, a connection between immune stimulation and modulation of social interaction was reported in honeybee (Richard et al. 2008).

Alternatively, upregulation of OBP/CSP-related proteins may reflect functions other than olfaction as strongly emphasized by Xuan et al. (2015). Indeed, many chemosensory or odorant binding related proteins were annotated on the sole basis of their tissue specific expression in olfactory tissues or sequence homology to known proteins, and their names may not reflect their real function (Picimbon 2014). Indeed, a shared characteristic of the olfactory and immune systems is the need for soluble carriers of hydrophobic moieties to be delivered at plasma membrane receptors (e.g. pattern recognition receptors or odorant receptors) (Fig. 9.5). As an example, the protein RYA3, which is expressed exclusively in the rat olfactory mucosae, exhibits significant sequence homology to the LPS-binding protein, which transports LPS in the serum (Dear et al. 1991). Thus, an intriguing possibility is that some odorant-like binding proteins participate in tissue-specific defense mechanisms in olfactory organs, rather than olfaction per se. This is strongly supported by the existence of CSPs (and OBPs) in bacterial species such as *Acinetobacter baumannii* (Liu and Picimbon 2017). A second intriguing example was recently provided by the demonstration that OBP6 from tsetse flies activates a transcriptional program leading to differentiation of crystal cells and increased melanotic immune response. Of note, Obp28a, the orthologue of OBP6 in *Drosophila*, induces a similar response in fruit flies. Therefore, it appears that one OBP regulated by gut microbiota plays a conserved role in cellular immunity in dipteran insects (Benoit et al. 2017). This is reminiscent of the connection between olfactory stimulation and maintenance of a pool of progenitor blood cells in *Drosophila* larvae (Shim et al. 2013).

5.5 *Receptors Shared Between Immunity and Chemosensory Pathways*

Interestingly, some receptors activating innate immunity also have a role in olfaction. For example, CD36-related receptor participate in immunity and pheromone detection in *Drosophila* (Benton et al. 2007).

Several proteins from this family function in the immune system of animals as scavenger receptors recognizing lipids derived from bacteria. In flies, one family member, Peste, mediates uptake of mycobacteria by phagocytes (Philips et al. 2005). In addition, three other CD36-like receptors, CG10345, CG31741 and Croquemort mediate phagocytosis of Leishmania parasites, resulting in decreased parasite burden in flies (Okuda et al. 2016).

Of note, the latter of these receptors, Croquemort, also participates in the uptake and disposal of apoptotic cells (Franc et al. 1999). Sensory neurone membrane protein 1 (SNMP1) also belongs to the CD36 family. It is expressed in a population of olfactory sensory neurons where it is required for activation of odorant receptors by lipid-derived pheromone ligands (Rogers et al. 1997; see Chap. 4). Thus, CD36 receptors appear to participate in a common function in olfaction and innate immunity, coupling sensing of hydrophobic, lipid-derived ligands to activation of signaling transmembrane receptors (Benton et al. 2007; Gomez-Diaz et al. 2016) (see Fig. 9.5).

Toll receptors represent another example of a family whose members function in both immune system and nervous system, in particular olfaction. Toll receptors participate in host defense in both mammals and insects, albeit by different means. Indeed, whereas mammalian TLRs function as PRRs, directly interacting with microbial ligands (Lu and Sun 2012), *Drosophila* Toll function as receptor for the cytokine Spaetzle (Weber et al. 2003) (see Fig. 9.5). This dichotomy is supported by phylogenetic analysis, which reveals that insect Tolls and mammalian TLRs evolved independently (Imler and Zheng 2004).

Interestingly, it is becoming apparent that several *Drosophila* Toll receptors function in the nervous system and can affect olfaction. The *Drosophila* genome encodes a family of six neurotrophin-like ligands including Spaetzle. Some of them have been shown to promote cell survival in the central nervous system and to influence motor exon targeting (Zhu et al. 2008). Toll 6/7/8 function as receptors for these neurotrophins (McIlroy et al. 2013; Ballard et al. 2014) (see Fig. 9.5). Thus, a subset of Toll receptors actively participates in the development of the nervous system in *Drosophila*.

Interestingly, Toll6 and Toll7 also instruct wiring specificity in the *Drosophila* olfactory circuit (see Chaps. 1, 2, and 3). Toll2 and Toll8 could participate in the establishment of wiring specificities in other parts of the nervous system (Ward et al. 2015). Interestingly, a cell adhesion role for Toll receptors has also been reported during embryogenesis in the fly (Paré et al. 2014). In addition, Toll6 and Toll7 are known to promote microtubule dynamics in motoneurons through a non-canonical pathway, thus enabling rapid activity-dependent structural plasticity.

There is no indication at this stage that the involvement of Toll receptors in these neuronal functions impacts the resistance to infections. Interestingly, however, in another model organism, the nematode *Caenorhabditis elegans*, the only Toll receptor encoded by the genome, Tol-1, promotes the development of neurons that are required for sensory detection on bacterial microbes (Pradel et al. 2007; Brandt and Ringstad 2015), providing a connection between the function of Toll receptor in chemosensory neurons and infection.

References

Aguiar ERGR, Olmo RP, Paro S, Ferreira FV, de Faria IJ d S, Todjro YMH, Lobo FP, Kroon EG, Meignin C, Gatherer D, Imler JL, Marques JT (2015) Sequence-independent characterization of viruses based on the pattern of viral small RNAs produced by the host. Nucleic Acids Res 43:6191–6206

Aguilar R, Jedlicka AE, Mintz M, Mahairaki V, Scott AL, Dimopoulos G (2005) Global gene expression analysis of *Anopheles gambiae* responses to microbial challenge. Insect Biochem Mol Biol 35:709–719

Aliyari R, Ding SW (2009) RNA-based viral immunity initiated by the Dicer family of host immune receptors. Immunol Rev 227:176–188

Aliyari R, Wu Q, Li HW, Wang XH, Li F, Green LD, Han CS, Li WX, Ding SW (2008) Mechanism of induction and suppression of antiviral immunity directed by virus-derived small RNAs in *Drosophila*. Cell Host Microbe 4:387–397

Anholt RRH, Williams TI (2010) The soluble proteome of the *Drosophila* antenna. Chem Senses 35:21–30

Bae YS, Choi MK, Lee WJ (2010) Dual oxidase in mucosal immunity and host-microbe homeostasis. Trends Immunol 31:278–287

Balabanidou V, Grigoraki L, Vontas J (2018) Insect cuticle: a critical determinant of insecticide resistance. Curr Opin Insect Sci 27:68–74

Ballard SL, Miller DL, Ganetzky B (2014) Retrograde neurotrophin signaling through Tollo regulates synaptic growth in *Drosophila*. J Cell Biol 204:1157–1172

Bartholomay LC, Cho WL, Rocheleau TA, Boyle JP, Beck ET, Fuchs JF, Liss P, Rusch M, Butler KM, Wu RCC, Lin SP, Kuo HY, Tsao IY, Huang CY, Liu TT, Hsiao KJ, Tsai SF, Yang UC, Nappi AJ, Perna NT, Chen CC, Christensen BM (2004) Description of the transcriptomes of immune response-activated hemocytes from the mosquito vectors *Aedes aegypti* and *Armigeres subalbatus*. Infect Immun 72:4114–4126

Baxter RHG, Chang CI, Chelliah Y, Blandin S, Levashina EA, Deisenhofer J (2007) Structural basis for conserved complement factor-like function in the antimalarial protein TEP1. Proc Natl Acad Sci U S A 104:11615–11620

Benoit JB, Vigneron A, Broderick NA, Wu Y, Sun JS, Carlson JR, Aksoy S, Weiss BL (2017) Symbiont-induced odorant binding proteins mediate insect host hematopoiesis. eLife 6:e19535

Benton R, Vannice KS, Vosshall LB (2007) An essential role for a CD36-related receptor in pheromone detection in *Drosophila*. Nature 450:289–293

Binggeli O, Neyen C, Poidevin M, Lemaitre B (2014) Prophenoloxidase activation is required for survival to microbial infections in *Drosophila*. PLoS Pathog 10:e1004067

Blandin S, Levashina EA (2004) Thioester-containing proteins and insect immunity. Mol Immunol 40:903–908

Blandin S, Shiao SH, Moita LF, Janse CJ, Waters AP, Kafatos FC, Levashina EA (2004) Complement-like protein TEP1 is a determinant of vectorial capacity in the malaria vector *Anopheles gambiae*. Cell 116:661–670

Blandin SA, Wang-Sattler R, Lamacchia M, Gagneur J, Lycett G, Ning Y, Levashina EA, Steinmetz LM (2009) Dissecting the genetic basis of resistance to malaria parasites in *Anopheles gambiae*. Science 326:147–150

Boman HG, Faye I, Gudmundsson GH, Lee JY, Lidholm DQ (1991) Cell-free immunity in *Cecropia*. A model system for antibacterial proteins. Eur J Biochem 201:23–31

Bonnay F, Cohen-Berros E, Hoffmann M, Kim SY, Boulianne GL, Hoffmann JA, Matt N, Reichhart JM (2013) Big bang gene modulates gut immune tolerance in *Drosophila*. Proc Natl Acad Sci U S A 110:2957–2962

Boppana S, Hillyer JF (2014) Hemolymph circulation in insect sensory appendages: functional mechanics of antennal accessory pulsatile organs (auxiliary hearts) in the mosquito *Anopheles gambiae*. J Exp Biol 217:3006–3014

Brandt JP, Ringstad N (2015) Toll-like receptor signaling promotes development and function of sensory neurons required for a *C. elegans* pathogen-avoidance behavior. Curr Biol 25:2228–2237

Cao Y, Chtarbanova S, Petersen AJ, Ganetzky B (2013) Dnr1 mutations cause neurodegeneration in *Drosophila* by activating the innate immune response in the brain. Proc Natl Acad Sci U S A 110:E1752–E1760

Carthew RW, Agbu P, Giri R (2017) MicroRNA function in *Drosophila melanogaster*. Semin Cell Dev Biol 65:29–37

Chang CI, Ihara K, Chelliah Y, Mengin-Lecreulx D, Wakatsuki S, Deisenhofer J (2005) Structure of the ectodomain of *Drosophila* peptidoglycan-recognition protein LCa suggests a molecular mechanism for pattern recognition. Proc Natl Acad Sci U S A 102:10279–10284

Choe KM, Werner T, Stöven S, Hultmark D, Anderson KV (2002) Requirement for a peptidoglycan recognition protein (PGRP) in Relish activation and antibacterial immune responses in *Drosophila*. Science 296:359–362

Clem RJ (2015) Viral IAPs, then and now. Semin Cell Dev Biol 39:72–79

Colinet D, Deleury E, Anselme C, Cazes D, Poulain J, Azema-Dossat C, Belghazi M, Gatti JL, Poirie M (2013) Extensive inter- and intraspecific venom variation in closely related parasites targeting the same host: the case of Leptopilina parasitoids of *Drosophila*. Insect Biochem Mol Biol 43:601–611

Cribb BW, Merritt DJ (2013) Chemoreception. In: Chapman RF, Simpson SJ, Douglas AE (eds) The insects: structure and function, vol 5. Cambridge University Press, Cambridge, pp 771–791

Daigneault J, Klemetsaune L, Wasserman SA (2013) The IRAK homolog Pelle is the functional counterpart of IκB kinase in the *Drosophila* Toll pathway. PLoS One 8:e75150

De Gregorio E, Spellman PT, Tzou P, Rubin GM, Lemaitre B (2002) The Toll and Imd pathways are the major regulators of the immune response in *Drosophila*. EMBO J 21:2568–2579

Dear TN, Boehm T, Keverne EB, Rabbitts TH (1991) Novel genes for potential ligand-binding proteins in subregions of the olfactory mucosa. EMBO J 10:2813–2819

Dias FA, Gandara ACP, Queiroz-Barros FG, Oliveira RLL, Sorgine MHF, Braz GRC, Oliveira PL (2013) Ovarian dual oxidase (Duox) activity is essential for insect eggshell hardening and waterproofing. J Biol Chem 288:35058–35067

Ding SW (2010) RNA-based antiviral immunity. Nat Rev Immunol 10:632–644

El Chamy L, Leclerc V, Caldelari I, Reichhart JM (2008) Sensing of "danger signals" and pathogen-associated molecular patterns defines binary signaling pathways "upstream" of Toll. Nat Immunol 9:1165–1170

Fernández-Hernández I, Scheenaard E, Pollarolo G, Gonzalez C (2016) The translational relevance of *Drosophila* in drug discovery. EMBO Rep 17:471–472

Ferrandon D, Imler JL, Hetru C, Hoffmann JA (2007) The *Drosophila* systemic immune response: sensing and signalling during bacterial and fungal infections. Nat Rev Immunol 7:862–874

Foley E, O'Farrell PH (2004) Functional dissection of an innate immune response by a genome-wide RNAi screen. PLoS Biol 2:e203

Fraiture M, Baxter RHG, Steinert S, Chelliah Y, Frolet C, Quispe-Tintaya W, Hoffmann JA, Blandin SA, Levashina EA (2009) Two mosquito LRR proteins function as complement control factors in the TEP1-mediated killing of *Plasmodium*. Cell Host Microbe 5:273–284

Franc NC, Heitzler P, Ezekowitz RA, White K (1999) Requirement for croquemort in phagocytosis of apoptotic cells in *Drosophila*. Science 284:1991–1994

Galiana-Arnoux D, Dostert C, Schneemann A, Hoffmann JA, Imler JL (2006) Essential function in vivo for Dicer-2 in host defense against RNA viruses in *drosophila*. Nat Immunol 7:590–597

Georgel P, Naitza S, Kappler C, Ferrandon D, Zachary D, Swimmer C, Kopczynski C, Duyk G, Reichhart JM, Hoffmann JA (2001) *Drosophila* immune deficiency (IMD) is a death domain protein that activates antibacterial defense and can promote apoptosis. Dev Cell 1:503–514

Gobert V, Gottar M, Matskevich AA, Rutschmann S, Royet J, Belvin M, Hoffmann JA, Ferrandon D (2003) Dual activation of the *Drosophila* toll pathway by two pattern recognition receptors. Science 302:2126–2130

Gomez-Diaz C, Bargeton B, Abuin L, Bukar N, Reina JH, Bartoi T, Graf M, Ong H, Ulbrich MH, Masson JF, Benton R (2016) A CD36 ectodomain mediates insect pheromone detection via a putative tunnelling mechanism. Nat Commun 7:11866

Gottar M, Gobert V, Michel T, Belvin M, Duyk G, Hoffmann JA, Ferrandon D, Royet J (2002) The *Drosophila* immune response against Gram-negative bacteria is mediated by a peptidoglycan recognition protein. Nature 416:640–644

Gottar M, Gobert V, Matskevich AA, Reichhart JM, Wang C, Butt TM, Belvin M, Hoffmann JA, Ferrandon D (2006) Dual detection of fungal infections in *Drosophila* via recognition of glucans and sensing of virulence factors. Cell 127:1425–1437

Herzog VA, Ameres SL (2015) Approaching the golden fleece a molecule at a time: biophysical insights into argonaute-instructed nucleic acid interactions. Mol Cell 59:4–7

Hillyer JF (2016) Insect immunology and hematopoiesis. Dev Comp Immunol 58:102–118

Hoffmann JA (2003) The immune response of *Drosophila*. Nature 426:33–38

Hoffmann JA, Hetru C (1992) Insect defensins: inducible antibacterial peptides. Immunol Today 13:411–415

Hoffmann JA, Kafatos FC, Janeway CA, Ezekowitz RA (1999) Phylogenetic perspectives in innate immunity. Science 284:1313–1318

Hou CX, Qin GX, Liu T, Mei XL, Li B, Shen ZY, Guo XJ (2013) Differentially expressed genes in the cuticle and hemolymph of the silkworm, *Bombyx mori*, injected with the fungus *Beauveria bassiana*. J Insect Sci 13:138

Imler JL, Bulet P (2005) Antimicrobial peptides in *Drosophila*: structures, activities and gene regulation. Chem Immunol Allergy 86:1–21

Imler JL, Zheng L (2004) Biology of Toll receptors: lessons from insects and mammals. J Leukoc Biol 75:18–26

Irving P, Troxler L, Heuer TS, Belvin M, Kopczynski C, Reichhart JM, Hoffmann JA, Hetru C (2001) A genome-wide analysis of immune responses in *Drosophila*. Proc Natl Acad Sci U S A 98:15119–15124

Issa N, Guillaumot N, Lauret E, Matt N, Schaeffer-Reiss C, Van Dorsselaer A, Reichhart JM, Veillard F (2018) The circulating protease Persephone is an immune sensor for microbial proteolytic activities upstream of the *Drosophila* Toll pathway. Mol Cell 69:539–550

Jang IH, Chosa N, Kim SH, Nam HJ, Lemaitre B, Ochiai M, Kambris Z, Brun S, Hashimoto C, Ashida M, Brey PT, Lee WJ (2006) A Spätzle-processing enzyme required for toll signaling activation in *Drosophila* innate immunity. Dev Cell 10:45–55

Kaneko T, Yano T, Aggarwal K, Lim JH, Ueda K, Oshima Y, Peach C, Erturk-Hasdemir D, Goldman WE, Oh BH, Kurata S, Silverman N (2006) PGRP-LC and PGRP-LE have essential yet distinct functions in the drosophila immune response to monomeric DAP-type peptidoglycan. Nat Immunol 7:715–723

Karlikow M, Goic B, Mongelli V, Salles A, Schmitt C, Bonne I, Zurzolo C, Saleh MC (2016) *Drosophila* cells use nanotube-like structures to transfer dsRNA and RNAi machinery between cells. Sci Rep 6:27085

Kemp C, Imler JL (2009) Antiviral immunity in *drosophila*. Curr Opin Immunol 21:3–9

Koch SI, Groh K, Vogel H, Hansson BS, Kleineidam CJ, Grosse-Wilde E (2013) Caste-specific expression patterns of immune response and chemosensory related genes in the leaf-cutting ant, *Atta vollenweideri*. PLoS One 8:e81518

Kocks C, Cho JH, Nehme N, Ulvila J, Pearson AM, Meister M, Strom C, Conto SL, Hetru C, Stuart LM, Stehle T, Hoffmann JA, Reichhart JM, Ferrandon D, Rämet M, Ezekowitz RAB (2005) Eater, a transmembrane protein mediating phagocytosis of bacterial pathogens in *Drosophila*. Cell 123:335–346

Koehbach J (2017) Structure-activity relationships of insect defensins. Front Chem 5:45. https://doi.org/10.3389/fchem.2017.00045

Krzemień J, Dubois L, Makki R, Meister M, Vincent A, Crozatier M (2007) Control of blood cell homeostasis in *Drosophila* larvae by the posterior signalling centre. Nature 446:325–328

Kuraishi T, Binggeli O, Opota O, Buchon N, Lemaitre B (2011) Genetic evidence for a protective role of the peritrophic matrix against intestinal bacterial infection in *Drosophila melanogaster*. Proc Natl Acad Sci U S A 108:15966–15971

Lanot R, Zachary D, Holder F, Meister M (2001) Postembryonic hematopoiesis in *Drosophila*. Dev Biol 230:243–257

Lazzaro BP (2015) Adenosine signaling and the energetic costs of induced immunity. PLoS Biol 13:e1002136

Lee KA, Kim SH, Kim EK, Ha EM, You H, Kim B, Kim MJ, Kwon Y, Ryu JH, Lee WJ (2013) Bacterial-derived uracil as a modulator of mucosal immunity and gut-microbe homeostasis in *Drosophila*. Cell 153:797–811

Legeai F, Gimenez S, Duvic B, Escoubas JM, Gosselin Grenet AS, Blanc F, Cousserans F, Séninet I, Bretaudeau A, Mutuel D, Girard PA, Monsempes C, Magdelenat G, Hilliou F, Feyereisen R, Ogliastro M, Volkoff AN, Jacquin-Joly E, d'Alencon E, Nègre N, Fournier P (2014) Establishment and analysis of a reference transcriptome for *Spodoptera frugiperda*. BMC Genomics 15:704

Léger P, Lara E, Jagla B, Sismeiro O, Mansuroglu Z, Coppée JY, Bonnefoy E, Bouloy M (2013) Dicer-2- and Piwi-mediated RNA interference in Rift Valley fever virus-infected mosquito cells. J Virol 87:1631–1648

Levashina EA, Langley E, Green C, Gubb D, Ashburner M, Hoffmann JA, Reichhart JM (1999) Constitutive activation of toll-mediated antifungal defense in serpin-deficient *Drosophila*. Science 285:1917–1919

Levashina EA, Moita LF, Blandin S, Vriend G, Lagueux M, Kafatos FC (2001) Conserved role of a complement-like protein in phagocytosis revealed by dsRNA knockout in cultured cells of the mosquito, *Anopheles gambiae*. Cell 104:709–718

Ligoxygakis P, Pelte N, Hoffmann JA, Reichhart JM (2002) Activation of *Drosophila* Toll during fungal infection by a blood serine protease. Science 297:114–116

Liu GX, Picimbon JF (2017) Bacterial origin of chemosensory odor-binding proteins. Gene Transl Bioinform 3:e1548

Liu GX, Xuan N, Chu D, Xie HY, Fan ZX, Bi YP, Picimbon JF, Li YF, Qin YC, Zhong ST, Gao ZL, Pan WL, Wang GY, Rajashekar B (2014) Biotype expression and insecticide response of *Bemisia tabaci* chemosensory protein-1. Arch Insect Biochem Physiol 85:137–151

Liu GX, Ma HM, Xie YN, Xuan N, Xia G, Fan ZX, Rajashekar B, Arnaud P, Offmann B, Picimbon JF (2016) Biotype characterization, developmental profiling, insecticide response and binding property of *Bemisia tabaci* chemosensory proteins: role of CSP in insect defense. PLoS One 11:e0154706

Liu GX, Arnaud P, Offmann B, Picimbon JF (2017) Genotyping and bio-sensing chemosensory proteins in insects. Sensors 17:1801

Lu J, Sun PD (2012) The structure of the TLR5-flagellin complex: a new mode of pathogen detection, conserved receptor dimerization for signaling. Sci Signal 5:pe11

Lu A, Zhang Q, Zhang J, Yang B, Wu K, Xie W, Luan YX, Ling E (2014) Insect prophenoloxidase: the view beyond immunity. Front Physiol 5:252

Mandal L, Martinez-Agosto JA, Evans CJ, Hartenstein V, Banerjee U (2007) A Hedgehog- and Antennapedia-dependent niche maintains *Drosophila* haematopoietic precursors. Nature 446:320–324

McIlroy G, Foldi I, Aurikko J, Wentzell JS, Lim MA, Fenton JC, Gay NJ, Hidalgo A (2013) Toll-6 and Toll-7 function as neurotrophin receptors in the *Drosophila melanogaster* CNS. Nat Neurosci 16:1248–1256

Medzhitov R, Janeway CA (2002) Decoding the patterns of self and nonself by the innate immune system. Science 296:298–300

Misof B et al (2014) Phylogenomics resolves the timing and pattern of insect evolution. Science 346:763–767

Morazzani EM, Wiley MR, Murreddu MG, Adelman ZN, Myles KM (2012) Production of virus-derived ping-pong-dependent piRNA-like small RNAs in the mosquito soma. PLoS Pathog 8:e1002470

Nainu F, Tanaka Y, Shiratsuchi A, Nakanishi Y (2015) Protection of insects against viral infection by apoptosis-dependent phagocytosis. J Immunol Baltim Md 1950 195:5696–5706

Naitza S, Rossé C, Kappler C, Georgel P, Belvin M, Gubb D, Camonis J, Hoffmann JA, Reichhart JM (2002) The *Drosophila* immune defense against gram-negative infection requires the death protein dFADD. Immunity 17:575–581

Navajas M, Migeon A, Alaux C, Martin-Magniette M, Robinson G, Evans J, Cros-Arteil S, Crauser D, Le Conte Y (2008) Differential gene expression of the honey bee *Apis mellifera* associated with Varroa destructor infection. BMC Genomics 9:301

Nonaka M (2000) Evolution of the complement system. Curr Top Microbiol Immunol 248:37–50

Obbard DJ, Callister DM, Jiggins FM, Soares DC, Yan G, Little TJ (2008) The evolution of TEP1, an exceptionally polymorphic immunity gene in *Anopheles gambiae*. BMC Evol Biol 8:274

Okuda K, Tong M, Dempsey B, Moore KJ, Gazzinelli RT, Silverman N (2016) *Leishmania amazonensis* engages CD36 to drive parasitophorous vacuole maturation. PLoS Pathog 12:e1005669

Oliveira DS, Brito NF, Nogueira FCS, Moreira MF, Leal WS, Soares MR, Melo ACA (2017) Proteomic analysis of the kissing bug Rhodnius prolixus antenna. J Insect Physiol 100:108–118

Paquette N, Broemer M, Aggarwal K, Chen L, Husson M, Ertürk-Hasdemir D, Reichhart JM, Meier P, Silverman N (2010) Caspase-mediated cleavage, IAP binding, and ubiquitination: linking three mechanisms crucial for *Drosophila* NF-kappaB signaling. Mol Cell 37:172–182

Paré AC, Vichas A, Fincher CT, Mirman Z, Farrell DL, Mainieri A, Zallen JA (2014) A positional Toll receptor code directs convergent extension in *Drosophila*. Nature 515:523–527

Paro S, Imler JL, Meignin C (2015) Sensing viral RNAs by Dicer/RIG-I like ATPases across species. Curr Opin Immunol 32:106–113

Pass G (1985) Gross and fine structure of the antennal circulatory organ in cockroaches (Blattodea, Insecta). J Morphol 185:255–268

Patil RS, Ghomade V, Deshpande MV (2000) Chitinolytic enzymes: an exploration. Enzym Microb Technol 26:473–483

Petit M, Mongelli V, Frangeul L, Blanc H, Jiggins F, Saleh MC (2016) piRNA pathway is not required for antiviral defense in *Drosophila melanogaster*. Proc Natl Acad Sci U S A 113:E4218–E4227

Petkau K, Fast D, Duggal A, Foley E (2016) Comparative evaluation of the genomes of three common *Drosophila*-associated bacteria. Biol Open 5:1305–1316

Philips JA, Rubin EJ, Perrimon N (2005) *Drosophila* RNAi screen reveals CD36 family member required for mycobacterial infection. Science 309:1251–1253

Picimbon JF (2003) Biochemistry and evolution of CSP and OBP proteins. In: Blomquist GJ, Vogt RG (eds) Insect pheromone biochemistry and molecular biology-The biosynthesis and detection of pheromones and plant volatiles. Elsevier Academic Press, London, pp 539–566

Picimbon JF (2014) Renaming *Bombyx mori* chemosensory proteins. Int J Bioorg Chem Mol Biol 2e:1–4

Picimbon JF, Dietrich K, Breer H, Krieger J (2000a) Chemosensory proteins of *Locusta migratoria* (Orthoptera: Acrididae). Insect Biochem Mol Biol 30:233–241

Picimbon JF, Dietrich K, Angeli S, Scaloni A, Krieger J, Breer H, Pelosi P (2000b) Purification and molecular cloning of chemosensory proteins from *Bombyx mori*. Arch Insect Biochem Physiol 44:120–129

Picimbon JF, Dietrich K, Krieger J, Breer H (2001) Identity and expression pattern of chemosensory proteins in *Heliothis virescens* (Lepidoptera, Noctuidae). Insect Biochem Mol Biol 31:1173–1181

Pradel E, Zhang Y, Pujol N, Matsuyama T, Bargmann CI, Ewbank JJ (2007) Detection and avoidance of a natural product from the pathogenic bacterium *Serratia marcescens* by *Caenorhabditis elegans*. Proc Natl Acad Sci U S A 104:2295–2300

Richard FJ, Aubert A, Grozinger CM (2008) Modulation of social interactions by immune stimulation in honey bee, *Apis mellifera*, workers. BMC Biol 6:50

Ringo J, Sharon G, Segal D (2011) Bacteria-induced sexual isolation in *Drosophila*. Fly (Austin) 5:310–315

Rogers ME, Sun M, Lerner MR, Vogt RG (1997) Snmp-1, a novel membrane protein of olfactory neurons of the silk moth *Antheraea polyphemus* with homology to the CD36 family of membrane proteins. J Biol Chem 272:14792–14799

Roignant JY, Carré C, Mugat B, Szymczak D, Lepesant JA, Antoniewski C (2003) Absence of transitive and systemic pathways allows cell-specific and isoform-specific RNAi in *Drosophila*. RNA N Y N 9:299–308

Royet J, Gupta D, Dziarski R (2011) Peptidoglycan recognition proteins: modulators of the microbiome and inflammation. Nat Rev Immunol 11:837–851

Rutschmann S, Jung AC, Hetru C, Reichhart JM, Hoffmann JA, Ferrandon D (2000) The Rel protein DIF mediates the antifungal but not the antibacterial host defense in *Drosophila*. Immunity 12:569–580

Sabatier L, Jouanguy E, Dostert C, Zachary D, Dimarcq JL, Bulet P, Imler JL (2003) Pherokine-2 and -3: two *Drosophila* molecules related to pheromone/odor-binding proteins induced by viral and bacterial infections. Eur J Biochem FEBS 270:3398–3407

Saleh MC, Tassetto M, van Rij RP, Goic B, Gausson V, Berry B, Jacquier C, Antoniewski C, Andino R (2009) Antiviral immunity in *Drosophila* requires systemic RNA interference spread. Nature 458:346–350

Sharon G, Segal D, Ringo JM, Hefetz A, Zilber-Rosenberg I, Rosenberg E (2010) Commensal bacteria play a role in mating preference of *Drosophila melanogaster*. Proc Natl Acad Sci U S A 107:20051–20056

Shim J, Mukherjee T, Mondal BC, Liu T, Young GC, Wijewarnasuriya DP, Banerjee U (2013) Olfactory control of blood progenitor maintenance. Cell 155:1141–1153

Shokal U, Eleftherianos I (2017) Evolution and function of thioester-containing proteins and the complement system in the innate immune response. Front Immunol 8:759

Sim S, Ramirez JL, Dimopoulos G (2012) Dengue virus infection of the *Aedes aegypti* salivary gland and chemosensory apparatus induces genes that modulate infection and blood-feeding behavior. PLoS Pathog 8:e1002631

Siomi MC, Miyoshi T, Siomi H (2010) piRNA-mediated silencing in *Drosophila* germlines. Semin Cell Dev Biol 21:754–759

Soldano A, Alpizar YA, Boonen B, Franco L, López-Requena A, Liu G, Mora N, Yaksi E, Voets T, Vennekens R, Hassan BA, Talavera K (2016) Gustatory-mediated avoidance of bacterial lipopolysaccharides via TRPA1 activation in *Drosophila*. eLife 5:e13133

Steiner H (2004) Peptidoglycan recognition proteins: on and off switches for innate immunity. Immunol Rev 198:83–96

Steiner H, Hultmark D, Engström A, Bennich H, Boman HG (1981) Sequence and specificity of two antibacterial proteins involved in insect immunity. Nature 292:246–248

Stensmyr MC, Dweck HKM, Farhan A, Ibba I, Strutz A, Mukunda L, Linz J, Grabe V, Steck K, Lavista-Llanos S, Wicher D, Sachse S, Knaden M, Becher PG, Seki Y, Hansson BS (2012) A conserved dedicated olfactory circuit for detecting harmful microbes in *Drosophila*. Cell 151:1345–1357

Stoven S, Silverman N, Junell A, Hedengren-Olcott M, Erturk D, Engstrom Y, Maniatis T, Hultmark D (2003) Caspase-mediated processing of the *Drosophila* NF-kappaB factor Relish. Proc Natl Acad Sci U S A 100:5991–5996

Sun H, Towb P, Chiem DN, Foster BA, Wasserman SA (2004) Regulated assembly of the Toll signaling complex drives *Drosophila* dorsoventral patterning. EMBO J 23:100–110

Tzou P, Ohresser S, Ferrandon D, Capovilla M, Reichhart JM, Lemaitre B, Hoffmann JA, Imler JL (2000) Tissue-specific inducible expression of antimicrobial peptide genes in *Drosophila* surface epithelia. Immunity 13:737–748

Valanne S, Wang JH, Rämet M (2011) The *Drosophila* Toll signaling pathway. J Immunol 186:649–656

van Rij RP, Saleh MC, Berry B, Foo C, Houk A, Antoniewski C, Andino R (2006) The RNA silencing endonuclease Argonaute 2 mediates specific antiviral immunity in *Drosophila melanogaster*. Genes Dev 20:2985–2995

Venu I, Durisko Z, Xu J, Dukas R (2014) Social attraction mediated by fruit flies' microbiome. J Exp Biol 217:1346–1352

Vilmos P, Kurucz E (1998) Insect immunity: evolutionary roots of the mammalian innate immune system. Immunol Lett 62:59–66

Vodovar N, Bronkhorst AW, van Cleef KWR, Miesen P, Blanc H, van Rij RP, Saleh MC (2012) Arbovirus-derived piRNAs exhibit a ping-pong signature in mosquito cells. PLoS One 7:e30861

Wang XH, Aliyari R, Li WX, Li HW, Kim K, Carthew R, Atkinson P, Ding SW (2006) RNA interference directs innate immunity against viruses in adult *Drosophila*. Science 312:452–454

Ward A, Hong W, Favaloro V, Luo L (2015) Toll receptors instruct axon and dendrite targeting and participate in synaptic partner matching in a *Drosophila* olfactory circuit. Neuron 85:1013–1028

Weber ANR, Tauszig-Delamasure S, Hoffmann JA, Lelièvre E, Gascan H, Ray KP, Morse MA, Imler JL, Gay NJ (2003) Binding of the *Drosophila* cytokine Spätzle to Toll is direct and establishes signaling. Nat Immunol 4:794–800

Xuan N, Guo X, Xie HY, Lou QN, Bo LX, Liu GX, Picimbon JF (2015) Increased expression of CSP and CYP genes in adult silkworm females exposed to avermectins. Insect Sci 22:203–219

Yano T, Mita S, Ohmori H, Oshima Y, Fujimoto Y, Ueda R, Takada H, Goldman WE, Fukase K, Silverman N, Yoshimori T, Kurata S (2008) Autophagic control of listeria through intracellular innate immune recognition in *Drosophila*. Nat Immunol 9:908–916

Yoshida H, Ochiai M, Ashida M (1986) Beta-1,3-glucan receptor and peptidoglycan receptor are present as separate entities within insect prophenoloxidase activating system. Biochem Biophys Res Commun 141:1177–1184

Zhang ZT, Zhu SY (2009) Drosomycin, an essential component of antifungal defence in *Drosophila*. Insect Mol Biol 18:549–556

Zhao Y, Li H, Miao X (2015) Proteomic analysis of silkworm antennae. J Chem Ecol 41:1037–1042

Zhu B, Pennack JA, McQuilton P, Forero MG, Mizuguchi K, Sutcliffe B, Gu CJ, Fenton JC, Hidalgo A (2008) *Drosophila* neurotrophins reveal a common mechanism for nervous system formation. PLoS Biol 6:e284

Résumé en français

I. Introduction

L'expression génique est un processus hautement régulé. Depuis la découverte de l'opéron lactose chez les bactéries (Jacob et Monod, 1961), d'importants progrès ont été réalisés dans la compréhension de la régulation de l'expression des gènes au niveau de la transcription. En revanche, le ribosome était principalement considéré comme une machine moléculaire complexe composée de protéines ribosomales (RP) et d'ARN (ARNr) impliqué dans la traduction des protéines mais dépourvu de capacité de régulation intrinsèque. Des études comparatives ont montré que les transcriptomes et les protéomes cellulaires présentent très peu de corrélation, soulignant l'importance majeure de la traduction dans la régulation de l'expression des gènes (Schwanhausser et al., 2011). Peu à peu, il est devenu évident que le ribosome lui-même joue un rôle majeur dans la régulation de la traduction. En effet, certaines RP sont maintenant décrites comme des facteurs régulant la traduction sélective d'un sous-ensemble d'ARNm. Les souris hémizygotes pour gène codant RpL38 présentent des défauts tissus-spécifiques au cours du développement. Ce phénotype résulte de la traduction altérée d'un sous-ensemble d'ARNm *homéobox* (*hox*) (Kondrashov et al., 2011). Des résultats récents indiquent que RpL38 intervient dans la traduction du gène *hox* par le biais de régulons d'ARN dans la région 5' non traduite de l'ARNm (5'UTR) (Xue et al., 2015). De plus, il est devenu évident que même dans un type de cellule, tous les ribosomes n'ont pas le même contenu de RP. Cette hétérogénéité du ribosome lui-même conduit à une traduction sélective (Genuth et Barna, 2018; Shi et al., 2017).

Certains ARNm contiennent des sites d'entrée internes du ribosome (IRES), dont l'initiation de la traduction est effectuée indépendamment de la coiffe en 5'. Initialement caractérisés chez les virus, les éléments IRES contournent certains des facteurs d'initiation, permettant ainsi la traduction virale lorsque la traduction cellulaire est arrêtée. En conséquence, les virus détournent les ribosomes de la cellule hôte pour leur traduction (Simoes et Sarnow, 1991). RpS25, une protéine de la petite sous-unité du ribosome, est nécessaire à la traduction dépendante de l'IRES du virus de la paralysie de Cricket (CrPV) et du virus de l'hépatite C (HCV). La présence de RpS25 au niveau du ribosome est nécessaire à la traduction de ces ARNm viraux, mais pas à la traduction générale (Landry et al., 2009). Par conséquent, l'image du ribosome eucaryote évolue et celui-ci est de plus en plus considéré comme une machine dynamique dotée de capacités de régulation et capable de filtrer la traduction d'ARNm spécifiques, sur la base d'un «code ribosome» (Mauro et Edelman, 2007). ; Shi et Barna, 2015; Topisirovic et Sonenberg, 2011).

Le laboratoire dans lequel j'effectue ma thèse a identifié la protéine RACK1 (Receptor for activated PKC 1) de la petite sous-unité du ribosome comme étant nécessaire à la traduction de virus à IRES (Site d'entrée interne du ribosome) comme le CrPV (Cricket Paralysis Virus) ou le virus de l'hépatite C (Majzoub et al., 2014). Initialement identifiée comme protéine d'ancrage à la PKC (protéine kinase C) activée, RACK1 a par la suite été impliquée dans de nombreuses voies de signalisation. De plus, de par sa localisation au ribosome, RACK1 est un candidat idéal pour intégrer les signaux provenant de différentes voies de signalisation et orchestrer une réponse traductionnelle. Cependant, aucune étude n'a été réalisée à ce jour pour étudier le lien entre les fonctions de traduction et de signalisation de RACK1.

Mon objectif est de déchiffrer le mécanisme par lequel RACK1 intervient dans la traduction sélective d'ARNm et de comprendre comment l'interaction avec les molécules de signalisation module cette activité.

II. Résultats

A. Caractérisation de RACK1 et d'un IRES viral dépendant de RACK1

Pour comprendre le rôle de RACK1 dans la traduction, j'ai participé à deux projets destinés à (1) définir l'intéractome de RACK1 et (2) caractériser l'IRES en 5' RACK1-dépendant du virus CrPV.

1. Définition d'un interactome de RACK1

Des résultats préliminaires du laboratoire ont identifié 52 protéines interagissant avec RACK1 par spectrométrie de masse, y compris plusieurs molécules impliquées dans la traduction (composants structuraux du ribosome, facteurs régulant l'initiation ou l'élongation de la traduction et les protéines de liaison à l'ARN). J'ai réalisé un criblage par ARN interférence en cellules S2 de drosophile et montré que parmi ces 52 partenaires, 10 sont des facteurs antiviraux et que seul Lark (RBM4 chez les mammifères) est un facteur proviral comme RACK1 **(Figure 1A)**. Cependant, bien que la déplétion de Lark empêche la réplication du virus CrPV, celle-ci n'affecte pas la traduction de l'IRES en 5' du CrPV **(Figures 1B-D)**. La protéine Lark favorise la réplication du virus CrPV par un mécanisme différent de RACK1. Ces résultats ont été publiés en 2017.

2. Caractérisation de l'IRES en 5' de CrPV

Le génome du virus CrPV contient deux IRES, mais seule la traduction de l'IRES en 5' (5'IRES) est dépendante de RACK1. Contrairement à l'IRES intergénique, le 5'IRES reste largement inexploré. L'objectif du projet était d'approfondir la compréhension du mécanisme de traduction du 5'IRES. L'analyse par spectrométrie de masse a révélé que le 5'IRES recrute le facteur d'initiation eIF3,

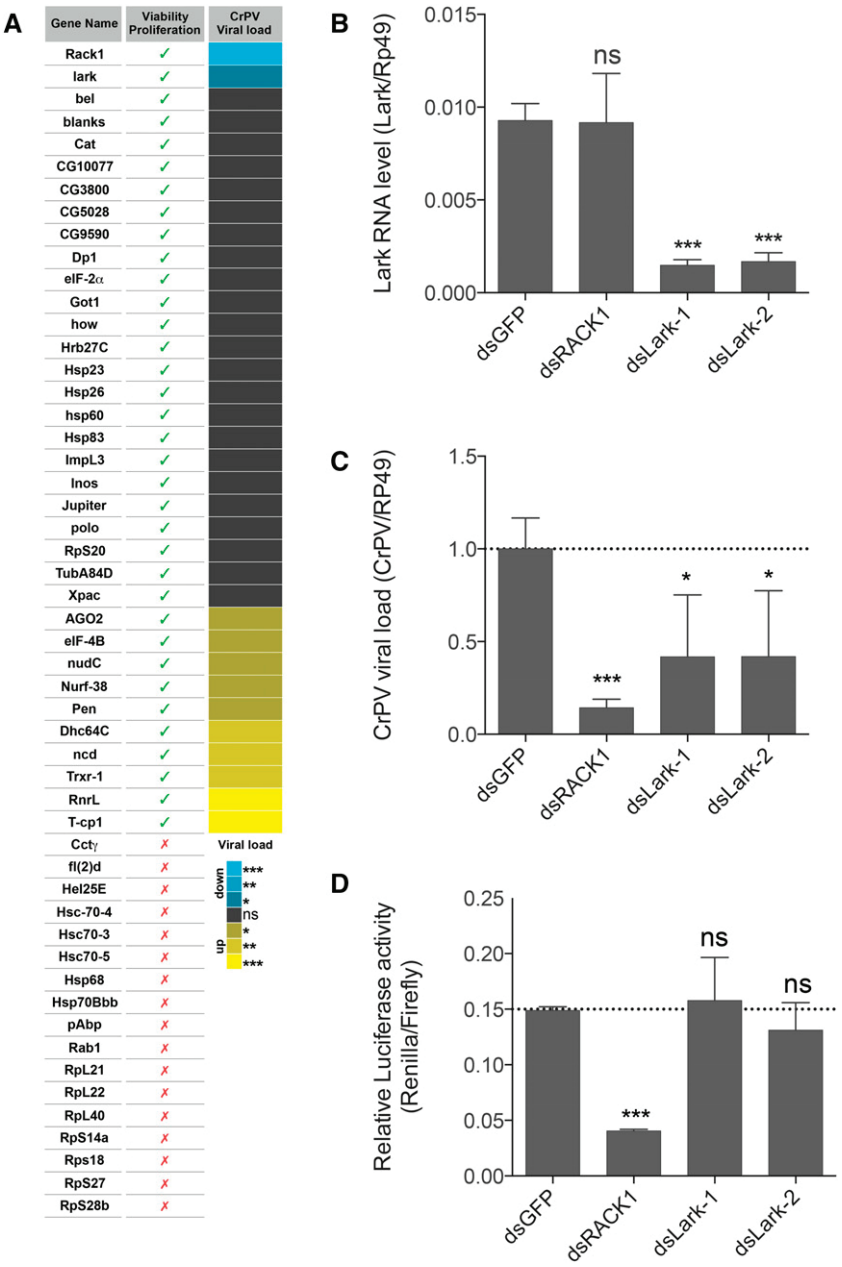

Figure 1: Caractérisation fonctionnelle des 52 partenaires de RACK1. A. Effet de l'inhibition de l'expression génique des 52 gènes sur la viabilité des cellules et la réplication de CrPV. La charge virale n'a été mesurée que sur les cellules dont la viabilité n'était pas affectée par l'inhibition de l'expression génique. **B.** L'incubation de cellules S2 avec deux ARN bouble brin (dsRNA) dirigés contre le gène Lark induit une inhibition efficace de l'expression du gène. **C**. L'inhibition de l'expression du gène Lark empêche la réplication de CrPV, de façon similaire à RACK1. **D**. L'inhibition de l'expression du gène Lark n'a pas d'effet sur la traduction de l'IRES en 5' de CrPV, par opposition à RACK1. L'analyse statistique est effectuée par *t*-test de Student; ns: non significatif; *p<0.05; **p < 0.01; ***p<0.001.

ce qui confirme son appartenance à la classe d'éléments de classe III de type IRES (comme le HCV). Des études structurelles ont montré que le 5'IRES contient une structure pseudo-noeud essentielle au bon repliement et au bon recrutement des ribosomes. J'ai testé l'importance de l'intégrité de cette structure pseudo-noeud *ex vivo* en générant des mutations ponctuelles dans cette structure **(Figure 2A)**. L'efficacité de la traduction de ces mutants a ensuite été évaluée par dosage de la luciférase en culture cellulaire **(Figure 2B)**. J'ai également montré que, bien que le pseudo-noeud soit essentiel pour l'activité 5'IRES, il n'est pas nécessaire pour le recrutement d'eIF3b **(Figure 3C)**. Ces résultats ont été publiés en 2017.

B. Caractérisation fonctionnelle des modifications post-traductionnelles de RACK1 *ex vivo* et *in vivo*

Pour comprendre le lien entre les fonctions de traduction et de signalisation de RACK1 décrites dans la littérature, j'ai généré plusieurs versions mutantes de RACK1. Certaines sont défectives pour l'interaction de RACK1 avec le ribosome ou des protéines de signalisation, d'autres portent des mutations localisées dans une protubérance de RACK1 située à l'interface entre le ribosome et le cytosol appelée « knob » (bouton). Ces constructions ont été testées en cellules S2 pour leur capacité à permettre la traduction du 5'IRES de CrPV **(Figure 3)**. La présence de RACK1 au ribosome est nécessaire pour la traduction de l'IRES, tandis que l'interaction avec les protéines de signalisation testée n'est pas nécessaire. De façon intéressante, l'expression de la protéine ribosomale RACK1 délétée du « knob » ne permet pas la traduction du 5' IRES.

L'étude de drosophiles sauvages et mutées pour RACK1 a montré que la protéine RACK1 est requise pendant le développement. Cependant, les mécanismes moléculaires impliqués sont inconnus. Il a été montré au laboratoire que l'expression d'un transgène exprimant une version sauvage de RACK1, mais pas un mutant défectif pour son association aux ribosomes permet un sauvetage de ce phénotype développemental.

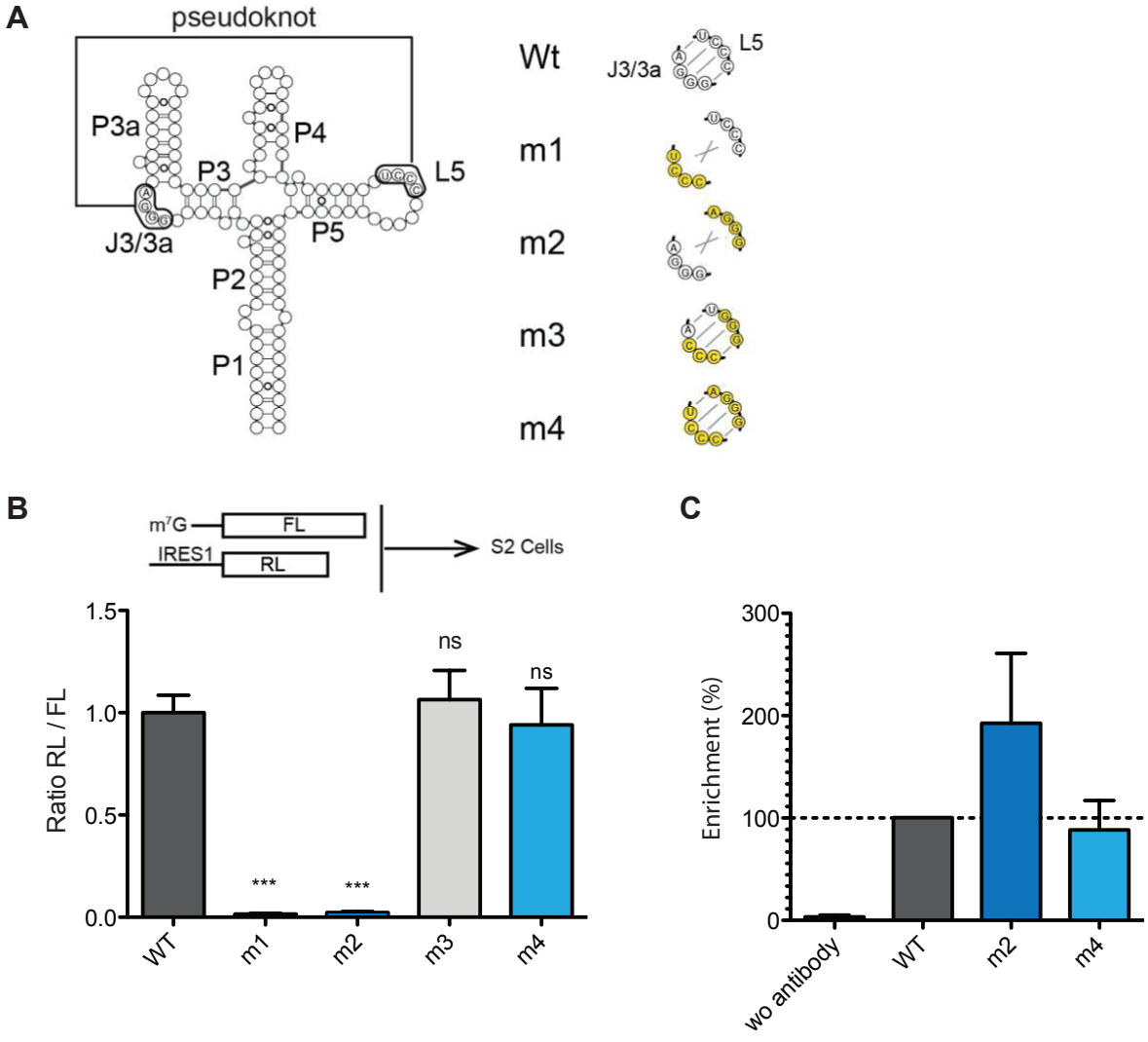

Figure 2: Le pseudo-noeud est nécessaire pour la traduction de CrPV, mais pas pour le recrutement de eIF3b. A. Structure du pseudo-noeud de l'IRES en 5' de CrPV et les mutants générés. **B.** Traduction *ex vivo* des rapporteurs luciférase après transfection en cellules S2. L'analyse statistique est effectuée par *t*-test de Student; ns: non significatif; *p<0.05; **p < 0.01; ***p<0.001. **C**. Immunoprécipitation par l'anticorps anti-eIF3b des ARN générés par les versions WT, mut2 et mut4 et quantification par RT-qPCR. L'enrichissement représente le ratio immunoprécipitation / input.

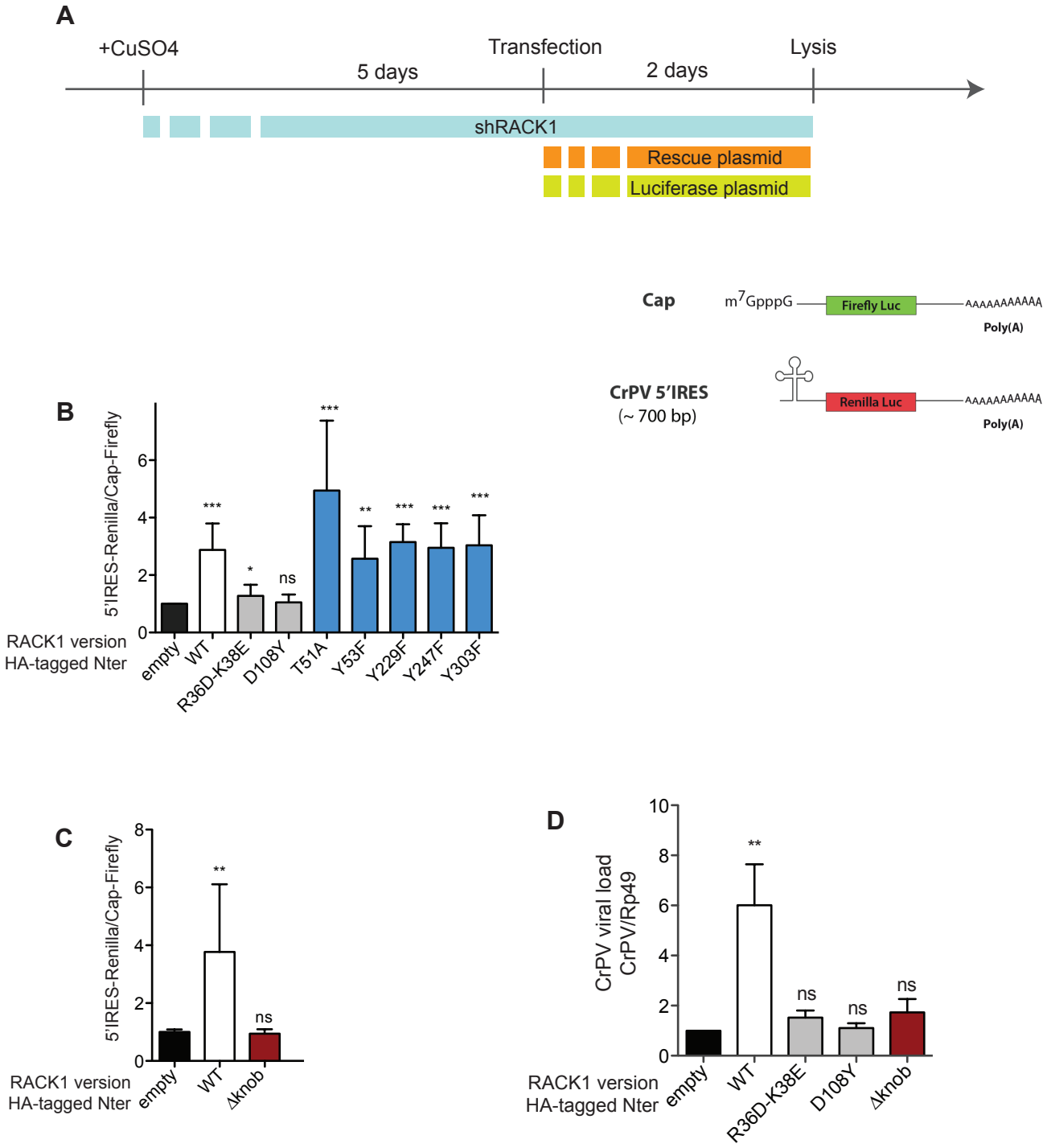

Figure 3: Activité de l'IRES 5' de CrPV dans des cellules S2 exprimant différentes versions de RACK1. A. Condition expérimentale. Des cellules S2 exprimant un shARN contre RACK1 ont été complémentées avec différentes versions de RACK1, ainsi que des rapporteurs coiffe-firefly et 5'IRES-Renilla. **B**. Mesure de l'activité de l'IRES 5' de CrPV après expression de versions de RACK1 étiquetées en N-terminal. Les versions utilisées sont les versions sauvages (blanc), les versions ne pouvant interagir avec le ribosome (gris), ou avec différents partenaires de voies de signalisation (bleu). **C**. Mesure de l'activité de l'IRES 5' de CrPV après expression de versions de RACK1 étiquetées en N-terminal. Les versions utilisées sont les versions sauvages (blanc) ou déplétées de la région du knob (rouge). **C**. Les cellules complémentées avec les versions sauvages de RACK1 (blanc), les versions ne pouvant interagir avec le ribosome (gris), déplétées de la région du knob (rouge) ont été infectées avec CrPV et la charge virale a été mesurée par RT-qPCR. L'analyse statistique est effectuée par *t*-test de Student avec correction de Welch; ns: non significatif; *p<0.05; **p < 0.01; ***p<0.001. Les graphiques montrent la moyenne et l'erreur standard de la moyenne de n=3 expériences.

C. RACK1 et la traduction sélective en réponse au stress

1. RACK1 est nécessaire pour la réponse au stress

Afin d'identifier les ARNm dont la traduction dépend de RACK1, j'ai recherché des conditions dans lesquelles RACK1 est nécessaire à la viabilité *ex vivo* et *in vivo*. J'ai testé plusieurs types de stress (exposition au paraquat, au peroxyde d'hydrogène [H_2O_2], à la tunicamycine, et au dithiothréitol [DTT]) et observé une contribution significative et reproductible de RACK1 dans la récupération des cellules S2 de drosophile après un stress dû à l'H_2O_2 et au DTT. Ces résultats ont été confirmés pour l'H_2O_2 en cellules humaines. J'ai mené une expérience similaire *in vivo* et montré que les drosophiles déplétées de RACK1 avec un shARN (shRACK1) succombent plus rapidement que les drosophiles témoins shContrôle (shmCherry) lorsqu'elles sont exposées au paraquat, au DTT et à la tunicamycine **(Figure 4)**. Ce résultat indique que RACK1 est nécessaire à la réponse au stress *ex vivo* et *in vivo*, potentiellement en régulant la traduction des ARNm impliqués dans la réponse au stress.

2. Identification des ARNm dépendant de RACK1

L'étape suivante consiste à identifier les ARNm dépendant de RACK1 en réponse au stress. J'ai utilisé la condition de stress au DTT *in vivo* pour effectuer une approche de séquençage des ARNm. Pour ce faire, des lysats de drosophile ont été séparés sur des gradients de sucrose par ultracentrifugation. Ceci permet de discriminer entre les ARNm fortement traduits (polysomes), les ARNm en initiation ou à court cadre de lecture (monosomes) et les ARNm non traduits (libres). J'ai aussi utilisé des lysats totaux de drosophiles sans séparation sur gradient de sucrose afin de déterminer le niveau d'expression des ARNm en réponse au stress. Après extraction des ARN de ces fractions, les échantillons ont été envoyés pour séquençage.

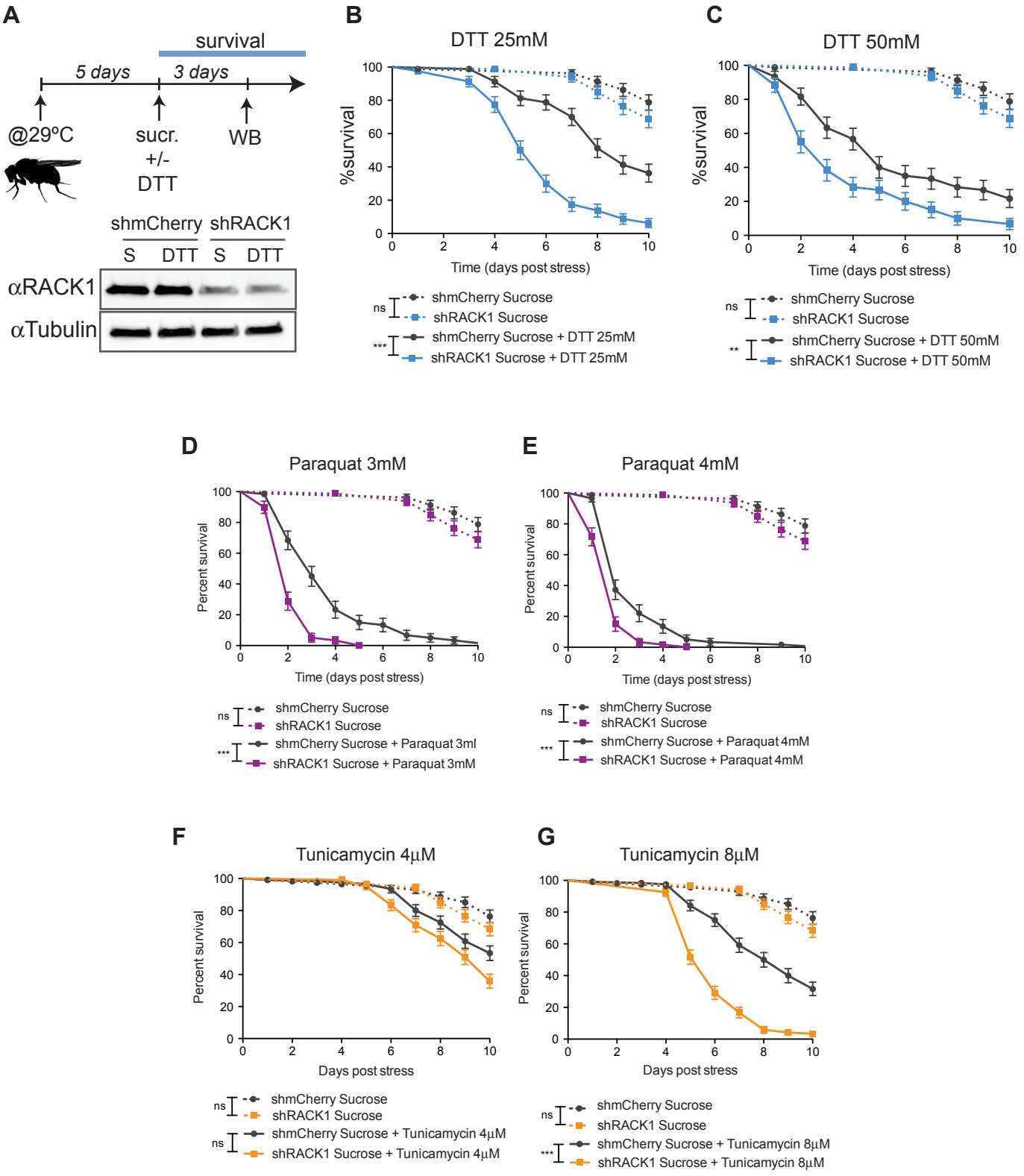

Figure 4: RACK1 est nécessaire à la réponse au stress chez la Drosophile *in vivo*. A. Des drosophiles *Actine*Gal4;*Tubuline*Gal80^{TS}>UAS::shmCherry et >UAS::shRACK1 ont été exposées à une température de 29ºC pendant 5 jours pour induire l'expression du shARN. Les drosophiles ont été traitées avec une solution de sucrose supplémentée ou non de DTT. Un western-blot a été effectué 3 jours pous tard pour mesurer l'efficacité de knock-down. **B-C.** Survie des drosophiles *Actine*Gal4;*Tubuline*Gal80^{TS} >UAS::shmCherry et >UAS::shRACK1 après stress du réticulum endoplasmique par ingestion de DTT à 25mM (**B**) ou 50mM (**C**). **D-E**. Survie des drosophiles *Actine*Gal4;*Tubuline*Gal80^{TS} >UAS::shmCherry et >UAS::shRACK1 après un stress oxidatif induit par ingestion de paraquat à 3mM (**D**) ou 4mM (**E**). **F-G**. Survie des drosophiles *Actine*Gal4;*Tubuline*Gal80^{TS}>UAS::shmCherry et >UAS::shRACK1 après stress du réticulum endoplasmique par ingestion de tunicamycine à 4µM (**F**) or 8µM (**G**). **B-G**. L'analyse statistique est effectuée par test Log-rank (Mantel-Cox) Test. ns: non significatif; *p<0.05; **p < 0.01; ***p<0.001.

L'analyse des extraits totaux a montré que 376 gènes ont une expression dérégulée dans les drosophiles shContrôle et/ou shRACK1. Seuls 22 gènes sont plus exprimés spécifiquement dans les drosophiles shRACK1 stressées. La moitié de ces gènes sont reliés à la voie antibactérienne IMD. Cette voie est homologue à la voie pro-inflammatoire TNF-R des mammifères et régule l'expression de peptides antimicrobiens (AMPs) en réponse à des infections bactériennes de type Gram négatif **(Figure 5)**. Ces résultats suggèrent un rôle de RACK1 dans l'expression de gènes immuns.

L'analyse du traductome a aussi montré des ARNm qui sont différentiellement représentés dans les polysomes et/ou les monosomes des drosophiles shRACK1 stressées. Ces ARNm codent principalement pour des protéines de fonction inconnue, mais j'ai sélectionné quelques candidats dont la traduction est dépendante de RACK1 comme preuve de principe. J'ai ainsi pu montrer que la traduction des AMPs via leur 5'UTR est réprimée par RACK1 **(Figure 6)**.

III. Conclusion

J'ai participé pendant ma thèse à la caractérisation fonctionnelle de l'IRES 5' du virus CrPV et à l'analyse de l'interactome de RACK1. Les deux projets ont tous les deux donné lieu à des publications. J'ai établi un modèle expérimental permettant d'étudier le lien entre les fonctions de signalisation et de traduction de RACK1, et montré que le « knob » est une région importante de RACK1 pour la traduction du 5'IRES de CrPV. De plus, j'ai identifié par séquençage des ARNm dont la traduction est dépendante de RACK1 et je les ai validés fonctionnellement.

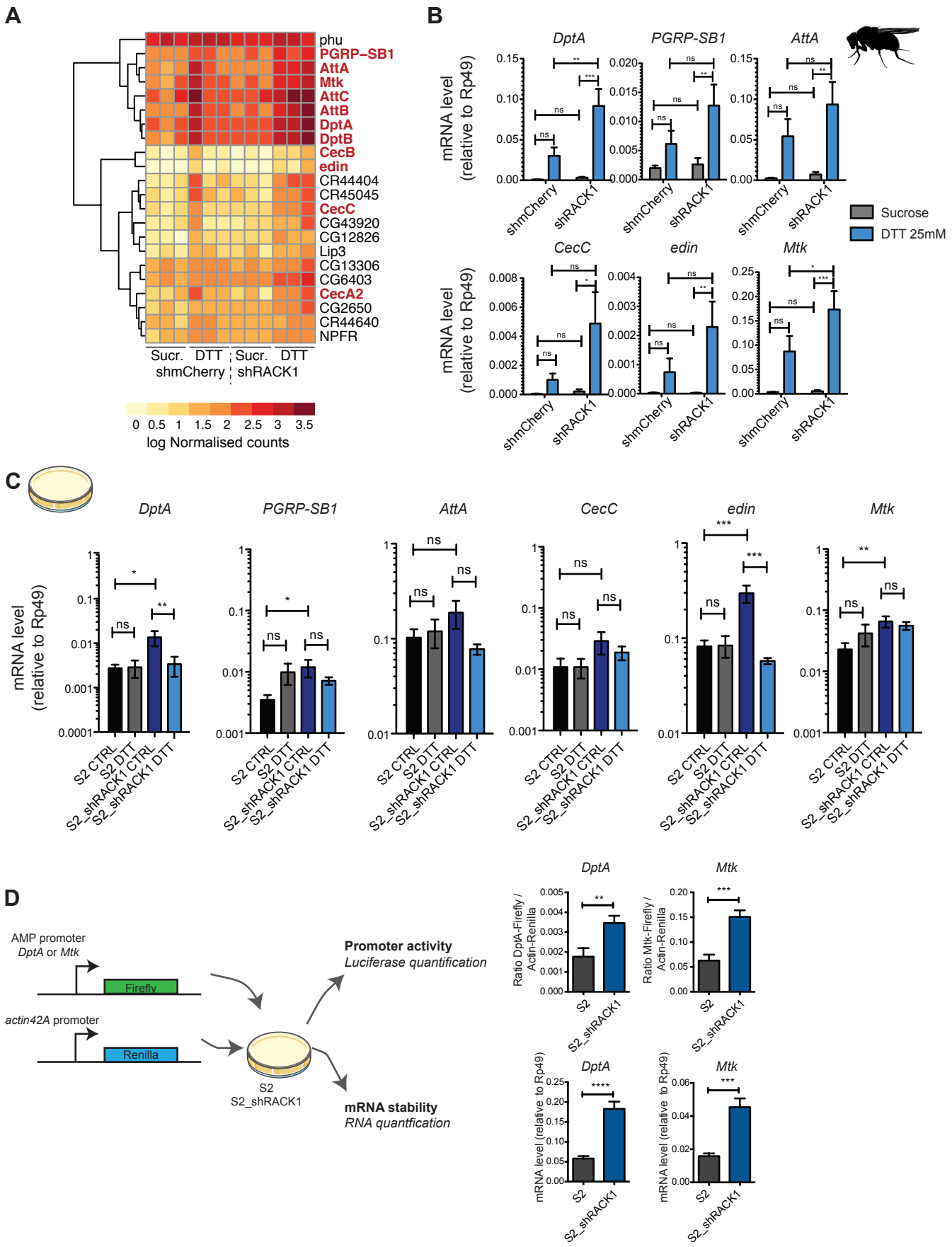

Figure 5: RACK1 inhibe l'expression des AMP *in vivo* et *ex vivo*. A. Heatmap du nombre de reads normalisé pour les 22 gènes spécifiquement induit dans les drosophiles shRACK1 traitées au DTT. Les gènes appartenant à la voie IMD sont indiqués en police rouge et en gras. **B**. Quantification par RT-qPCR des ARNm de *DptA*, *PGRP-SB1*, *AttA*, *CecC*, *edin* et *Mtk* dans les drosophiles shmCherry et shRACK1 à 3 jours post traitement à 25mM de DTT. **C**. Quantification par RT-qPCR des ARNm de *DptA*, *PGRP-SB1*, *AttA*, *CecC*, *edin* et *Mtk* dans les cellules S2 and S2_shRACK1 un jour après traitement des cellules avec du milieu de culture contenant du DTT à 25mM ou non (CTRL). L'analyse statistique est effectuée par 2way ANOVA suivi d'un post-test de Bonferroni. **D**. Essai luciférase montrant l'activité des promoteurs de la Mtk et de la DptA, ainsi que le niveau endogène des ARNm codant pour *DptA* et *Mtk*. L'analyse statistique est effectuée par *t*-test de Student avec correction de Welch; ns: non significatif; *p<0.05; **p < 0.01; ***p<0.001.

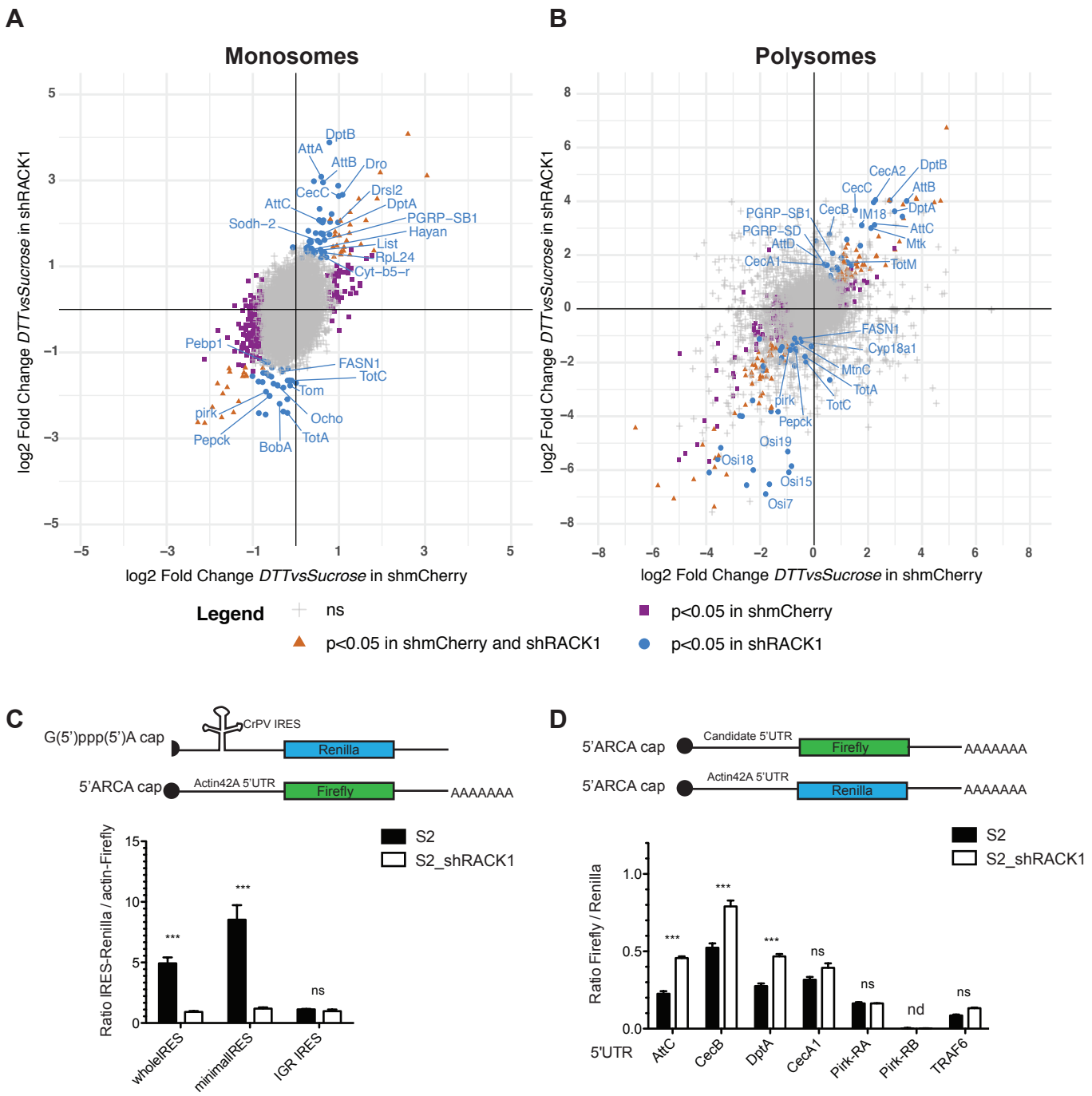

Figure 20: RACK1 empêche la traduction des AMPs. A-B. Nuage de points représentant l'effet du stress au DTT chez les drosophiles contrôles (shmCherry) et shRACK1. Les points bleus indiquent les gènes enrichis ou déplétés de façon significative dans les monosomes (**A**) ou les polysomes (**B**) des drosophiles shRACK1 stressées. **C**. Contrôle fonctionnel des cellules S2 et cellules S2_shRACK1. Ces cellules ont été transfectées avec un ARNm contenant l'IRES 5' de CrPV, l'IRES 5' minimal de CrPV, ou l'IGR IRES de CrPV permettant l'expression de la Renilla. Ces ARNm possèdent une coiffe non-fonctionnelle. Un ARNm coiffé fonctionnellement contenant le 5'UTR de l'actine permettant l'expression de la Firefly a été co-transfecté. Le ratio Renilla/Firefly est représenté. **D**. Des ARNm codant la Firefly sous le contrôle des 5'UTR indiqués ont été transfectés dans des cellules S2 ou S2_shRACK1 avec un ARNm contenant le 5'UTR de l'actine permettant l'expression de la Renilla. Ces ARNm ont été coiffés avec une coiffe fonctionnelle. Le ratio Firefly/Renilla est représenté. (**C-D**) L'analyse statistique est effectuée par 2way ANOVA suivi d'un post-test de Bonferroni; ns: non significatif; *p<0.05; **p < 0.01; ***p<0.001.

Evelyne EINHORN

Rôle de la protéine ribosomale RACK1 dans la régulation de la traduction

Résumé

RACK1 (Receptor for activated protein C kinase 1) est une protéine ribosomale associée à de nombreuses voies de signalisation. RACK1 est nécessaire à la traduction sélective de virus contenant des sites d'entrée interne du ribosome (IRES). En outre, l'expression de RACK1 est nécessaire au cours du développement, suggérant que ce facteur participe à la traduction de certains ARNm cellulaires.

Dans le but de mieux comprendre la fonction de RACK1 chez la drosophile, j'ai au cours de ma thèse caractérisé l'interactome de RACK1 et un IRES viral régulé par ce facteur. J'ai également essayé d'établir un lien entre signalisation cellulaire et traduction, et montré que la région du knob est importante pour la fonction de RACK1 au ribosome. Enfin, j'ai établi que RACK1 est nécessaire à la réponse à des stress abiotiques, et identifié les gènes cellulaires régulés par RACK1 dans ce contexte. J'ai en particulier découvert que RACK1 était un régulateur négatif de l'expression de plusieurs gènes de l'immunité innée. Mes résultats suggèrent que RACK1 joue un rôle pivot au sein du ribosome, régulant la traduction de façon positive ou négative selon l'ARNm et le contexte cellulaire.

Mots clés : RACK1 – IRES – traduction sélective – stress – *Drosophila melanogaster*.

Résumé en anglais

RACK1 (Receptor for activated protein C kinase 1) is a ribosomal protein associated to many signaling pathways. RACK1 is required for the selective translation of viruses containing internal ribosome entry sites (IRES). In addition, expression of RACK1 is necessary during development, suggesting that it regulates the translation of cellular mRNAs.

In order to better understand the function of RACK1 in *Drosophila*, I have participated in the characterization of the RACK1 interactome and of a RACK1-dependent viral IRES. I have also attempted to establish a connection between the function of RACK1 in signaling and in translation, and I have shown that the knob domain of RACK1 is important for IRES-dependent translation. Finally, I have established that RACK1 is required for the response to abiotic stresses, and I have identified cellular genes regulated by RACK1 in this context. In particular, I discovered that RACK1 is a negative regulator of several innate immunity genes. My results suggest that RACK1 plays a pivotal role within the ribosome, regulating translation positively or negatively in an mRNA- and possibly context-specific manner.

Keywords: RACK1 – IRES – selective translation – stress – *Drosophila melanogaster*.